Title
Changes in the functional organization of the cerebral cortex of adult primates following improvements in performance of a tactile discrimination task

Author
Recanzone, Gregg H.

Publication Date
1990

Peer reviewed|Thesis/dissertation

Changes in the Functional Organization of the Cerebral Cortex of Adult Primates Following Improvements in Performance of a Tactile Discrimination Task

by

Gregg H. Recanzone

DISSERTATION

Submitted in partial satisfaction of the requirements for the degree of

DOCTOR OF PHILOSOPHY

in

NEUROSCIENCE

in the

GRADUATE DIVISION

of the

UNIVERSITY OF CALIFORNIA

San Francisco

ACKNOWLEDGMENTS

This work was accomplished with the help of many individuals to whom I am grateful. Foremost is Michael Merzenich who was an inspiring mentor and whose intellect and personality have shaped much of my thinking of the brain and how it functions. My collaborators included Christoph Schreiner, to whom I am indebted to for his insight and knowledge that made possible the third and prehaps most interesting section of this thesis, and introduced to me to how temporal processing of neurons could be coding temporal phenomenon, and William Jenkins, without whom the behavioral part of this thesis would never have been attempted, and who collected much of the data during these long experiments, and Gary Hradek, whose imagination and sense of humor kept my spirits up and kept the monkeys learning during the months of behavioral training.

My other collaborators include Kamil Grajski, Brett Peterson and Hubert Dinse, who mapped receptive fields, and Terry Allard and Randy Nudo for their helpful comments and criticisms during the development of the experimental protocol.

I would like to thank my thesis committe members, Peter Ralston, who was the idealized version of a thesis committe chariman from a graduate student point of view, Michael Stryker, whose input led to much of the analysis of the receptive field data that resulted in a much better understanding of this data, and Gordon Shaw, whose enthusiasm never waivered throughout these experiments. I would also like to thank Steve Lisberger, who was the original chairman, who provided guidance at the initial half of this project.

Finally, I would like to thank my friends from the Coleman Laboratory Thomas Chimento, Mitchell Sutter Russel Snyder, Patricia Leake, Julie Mendelson, Keith Grasse and Dan Goldreich. I would especially like to thank Sonya Gettner for her love, insights and support as well as Susan Burton, and most of all my thanks to my parents, who have always stood behind me.

The concepts and ideas described in this thesis were inspired by the work of Vernon B. Mountcastle and his collaborators over two decades ago, and I am grateful to this superb scientist for pioneering the path that I have followed.

ABSTRACT

Changes in the Functional Organization of the Cerebral Cortex of Adult Primates Following Improvements in Performance of a Tactile Discrimination Task.

By Gregg H. Recanzone

The effects of discrimination training and the resulting increase in perceptual acuity with training were studied in primary somatosensory cortex of adult primates. Adult owl monkeys were trained in a tactile frequency discrimination task for 30-131 days. The area of skin stimulated was restricted to an invariant location on a single digit no greater than 3.5 mm in diameter. Four of five studied monkeys showed an improvement of discrimination performance for stimuli presented to the trained skin region when compared to the corresponding skin region of an adjacent digit. A second set of monkeys were trained to receive the same tactile stimulation in a passive manner. The cortical representations of the trained hand and of the opposite, untrained hand in somatosensory cortical areas 3a and 3b were determined electrophysiologically by multiple microelectrode penetration "mapping" experiments. In every case the area of representation of the trained skin in areas 3a and 3b increased in monkeys that had behavioral improvements in performance. This representation was accompanied by an increase in receptive field size and an increase in receptive field overlap. The temporal response properties of these neurons were enhanced to fire at only a restricted portion of the stimulus cycle in trained monkeys. This temporal enhancement of neuronal firing in area 3b was sufficient to account for the improvement in discrimination performance.

Table of Contents

List of Tables

List of Figures

INTRODUCTION

All vertebrate species have the ability to acquire new skills and behaviors throughout life. Many behaviors are learned early and are continuously modified as the individual animal grows and as the environment demands. Other behaviors are acquired and subsequently lost, and still others are acquired and remain stable for years or decades. A central question in neurobiology is how the central nervous system can provide a substrate for the continuous ability to refine formerly acquired behaviors and to learn new behaviors throughout life. "Learning" to the neurobiologist has a variety of meanings. For the purposes of this thesis, learning is functionally defined as the improvement in performance that results from the repetition of a specific sensory or motor task. Learning as defined by other criteria is beyond the scope of this work (see Thompson et al 1988; Byrne et al 1987 for reviews).

Improvement in performance with training depends on an intact representation of the appropriate sensory and/or motor modality within the central nervous system. This type of learning has been observed in virtually all sensory modalities and applies to a wide variety of motor behaviors (for reviews see James 1890; Gibson 1953; Anderson 1980; Singley and Anderson 1989) leading to the early conclusion that an alteration of the distributed "excitability" of the cerebral cortex could account for the phenomenon (James 1890). Sherrington and colleagues provided the first experimental evidence that the cerebral cortex could be functionally reorganized in the adult mammal. They investigated the organization of the motor cortex of monkeys and great apes by electrical stimulation of the cortical surface. This stimulation resulted in an alteration of the movement "map" in the motor cortex (Graham Brown and

Sherrington 1911; see also Graham Brown 1915). The concept of "the mutability of the cortical point" was raised by Sherrington and colleagues (Graham Brown and Sherrington 1912) and hypothesized by them to underlie the acquisition of motor skill. Experiments conducted within the past fifteen years provide unequivocal evidence that the distributed response properties of cortical neurons in the adult cerebral cortex are mutable (see Kaas et al 1983; Merzenich et al 1988, 1991 for reviews). The demonstrated 'plasticity' in the functional organization of the cerebral cortex potentially reveals the neurophysiological basis of learning. The majority of these plasticity studies have been conducted in the primary somatosensory cortex (SI) of adult mammals. This sensory system has been investigated in the experimental work presented in this thesis. The following discussion is a brief review of the anatomical connections and physiological responses of the primate SI cortical fields, and summarizes some of the experimental evidence from this system that indicates that the plasticity of cortical representational topographies could potentially account for improvements in sensory/perceptual performance with training.

Primate SI

The complete topographic organization of SI was described physiologically for the human by Penfield and colleagues (Penfield and Boldrey 1937; see also Penfield and Rasmussen 1950). They described the contralateral body surface as being represented along the medial-lateral axis of the post-central gyrus and that certain body surfaces, particularly the hand and lips in the human, occupied greater areas than did functionally less important skin surfaces. Marshall and colleagues (Marshall et al 1937, 1941; Woolsey et al 1942), and later Mountcastle and Powell (Mountcastle and Powell 1959; Powell and

Mountcastle 1959b) extended these studies in the macaque monkey, demonstrating that 1) The overall topographic organization of SI in the monkey and human were similar. 2) The cortex is columnarly organized, such that all radially oriented neurons spanning the cortical layers have nearly identical receptive field centers. And 3) Representations of the submodalities of touch and of kinesthesis were segregated to some extent within and between the four cytoarchitectonic areas of the SI cortex. Merzenich and Kaas mapped the cortical somatosensory representations in detail in the species investigated in this thesis work, the New World owl monkey (genus *Aotus*). They described two complete cutaneous representations of the body roughly oriented as mirror images, one each in areas 3b and 1 (Merzenich et al 1978). They concluded that there are four distinct body representations in primate SI: areas 3b and 1 are responsive to cutaneous inputs, and areas 3a and 2 are responsive to non-cutaneous inputs (Merzenich et al 1978; Kaas et al 1979). A complete body representation has subsequently been documented in area 2 in macaque monkeys (Pons et al 1985).

Area 3b

Area 3b is considered to be a true granular cortical field (a koniocortex) as it has a thinned layer V-VI, fused layers II and IIIa, a distinct layer IV and less dense layer V (Brodmann 1905; Powell and Mountcastle 1959a; see Jones 1975a, b for an extensive anatomical description of SI cortical fields in New World monkey). It is bounded by area 1 caudally and by area 3a rostrally. Area 3b receives its main inputs from the ventrobasal thalamus (Clark and Powell 1953; Jones 1975a; Jones et al 1982a, b; Lin et al 1978), and sends projections to each of the three other anterior parietal somatosensory areas (areas 3a, 1

and 2) as well as to SII and the more posterior parietal cortex (see Shanks et al 1985b).

Area 3b is driven by stimulation of the peripheral receptors innervated by large-diameter axons (Aß fibers). Area 3b neurons have small, cutaneous receptive fields on the contralateral body surface (Mountcastle and Powell 1959; Merzenich et al 1978; Kaas et al 1979). Ablation of this cortical area results in a permanent deficit in the ability to tactually discriminate shape, size, frequency of vibration, and texture (Cole and Gless 1954; Semmes et al 1972, 1974; Randolph and Semmes 1974; LaMotte and Mountcastle 1979; Carlson 1981). A small percentage of neurons in this area have also been shown to be responsive to noxious inputs and to temperature (Kenshalo et al 1983, 1988). Area 3b is considered to be a primary somatosensory processing area, termed "SI proper" by Merzenich and colleagues (Merzenich et al 1978). Although its functional roles are incompletely defined, the functional organization, hierarchical projections and the cortical lesion studies indicate that it is involved in the encoding and processing of most aspects of tactile perception.

Area 3a

Area 3a is located immediately rostral to area 3b and caudal to 'primary' motor cortex, area 4. The cytoarchitectonic border between areas 3a and 3b is marked by a reduction of layers III-IV in area 3a, by a reduction in the small pyramidal cell density in layer III, by an overall thickening of the cellular layers, and by larger pyramidal cells in layer V (Brodmann 1905; Vogt and Vogt 1919; Kreig 1954; Powell and Mountcastle 1959a). Area 3a receives it's main thalamic input from the "shell" region of the ventroposterior nucleus of the thalamus (Clark and Powell 1953; Lin et al 1979; Friedman and Jones 1981;

Cusick and Gould 1990). There may be some overlap of the neurons in the ventrobasal thalamus that project to the two areas, but this has not yet been unequivocally demonstrated (see Cusick and Gould 1990).

Physiologically, area 3a neurons are most directly excited by stimulation of the Ia muscle spindle afferents (Phillips et al 1971; Lucier et al 1975; Heath et al 1976). Receptive fields of these neurons are usually classified as "deep", as they respond specifically to pressure on muscles, to muscle stretching, or to movement of the joints, all of which excite the Ia afferent muscle stretch receptors. Electrophysiological recordings have revealed sub-threshold responses of area 3a neurons from cutaneous receptors (Zarzecki et al 1982, 1983), and cutaneous receptive fields are occasionally defined within this field (see Kaas et al 1979; Cusick et al. 1989). There are also small patches of cortex in area 3a which are labeled by 2-DG uptake following cutaneous stimulation of the skin (Juliano and Whitsel 1987). The topographic organization of muscle and joint stimulation in area 3a roughly mirrors the cutaneous body surface representation recorded in area 3b.

Topographic organization of the body surface representation in area 3b

Extensive microelectrode mapping experiments have been conducted to define the functional representation of the body surface in SI in detail (owl and squirrel monkey: Merzenich et al 1978, 1987; Kaas et al 1979; Sur et al 1980, 1982, 1984; macaque: Nelson et al.1980; Pons et al 1987; *Saguinus*: Carlson et al 1986; cebus monkey: Carlson et al 1982; marmoset: Krubitzer et al 1990; slow loris: Krishnamurti et al 1976). In these experiments, small clusters of neurons in the middle cortical layers are typically recorded at several hundred locations. Given the columnar organization of the cerebral cortex, defining

receptive fields in the middle layers provides an accurate estimate of the receptive field throughout the cortical layers (see Sur et al 1985). The low-amplitude stimuli used in these mapping studies have been punctate, usually delivered by a fine tipped, hand-held probe. This stimulus activates the large diameter primary afferents that subserve the sensation of light touch and flutter-vibration, but not nociception, muscle movement or joint movement. The area of skin stimulated in this way that excites the neurons at a given cortical location is defined as the "receptive field" for that location. By relating the receptive field sizes and locations to the cortical locations from which they were recorded, in experiments in which several hundred cortical locations were sampled, several principles of the functional organization of area 3b have been derived.

Overlap Rule; Representational Discontinuities

In the cortical map of a normal animal, the extent to which receptive fields overlap between two cortical locations is roughly inversely related to the distance between them (overlap $\propto$ 1 / cortical distance). The distance at which the overlap drops to zero has been measured as approximately 400-600 μm in the squirrel and owl monkey regardless of the skin region represented (Sur et al 1981; Merzenich et al 1983a, 1984). Several discontinuities are recorded in the body surface representation, and in these specific instances the overlap 'rule' is broken. In the hand representation there are discontinuities between the representations of individual digits, between the representations of the hand and face, between the representations of the hand and wrist, and between the representations of the hairy and glabrous skin. All of these discontinuities are sharp. Cortical locations separated by as little as 100μm across these functional boundaries commonly have completely non-overlapping receptive fields.

Inverse Rule

The average receptive field size representing a given skin surface is roughly inversely related to the area of representation of that skin surface. In the hand representation, the distal phalanges of the digits have the largest cortical representation of any digit segment, and the receptive fields on this digit segment are usually the smallest. Similarly, the cortical representation of the palmar pads is relatively small, and the receptive fields on the palm are correspondingly larger. The relationship between the receptive field overlap with the cortical distance between two locations is maintained across the cortical representation, even though receptive fields on the distal segment of the digits may be only a fraction of the size of the receptive fields located on the more proximal limb surfaces and trunk.

Normal variability

The details of the hand representation vary among individual animals. The main features of the map are similar across individuals, i.e. the digits are usually represented with digit 5 (little finger) represented most medially and digit 1 (thumb) represented most laterally, the distal tips are usually represented rostrally, the palm caudally, and the hairy skin is represented in 'islands' throughout the glabrous representation. However, the fine details of these representations are widely variable among individual owl and squirrel monkeys. Merzenich et al (1984, 1987) found that the locations of the borders between digits, the absolute sizes of each digit representation, and the locations of the hairy skin representations, among other map features, were not the same among individual monkeys. A similar result was later found in macaque monkeys (Pons et al 1987), and can also be observed - although this

issue was not specifically addressed in published reports - in the normal mapping data derived in other primates (see references cited above). This variability could be the result of genetic or epigenetic differences in the anatomical connections created during development. An alternative explanation, as Merzenich and colleagues have suggested, is that these topographic 'maps' do not only reflect the anatomical input to the cortical neurons, but are also refined in detail by the stimulation of the skin. The differences in representation could then be the result of the idiosyncratic differences between the individual monkey's use of its hand. The latter possibility predicts that the details of cortical topographic representations are modifiable throughout life (see Edelman 1978, 1987; Merzenich et al 1988, 1991).

EVIDENCE OF PLASTICITY IN THE TOPOGRAPHIC ORGANIZATION OF SI

Several studies have addressed the plasticity of the topographic representation in the cortex following alteration of the peripheral input. These experimental manipulations have included deafferentation, surgical fusion of digits (syndactyly), neurovascular island transfer, and behaviorally controlled differential stimulation (see Merzenich et al 1988, 1990 for review). The results of these experiments show that the details of the topographic representation of the hand are alterable in the adult owl monkey. The representation of a given digit border can be shifted six to eight hundred microns following nerve transection or digit amputation (Merzenich et al 1983a, b, 1984). The area 3b representation of a small skin surface that was repeatedly stimulated in a behaviorally controlled paradigm can increase 3-5 fold (Jenkins et al 1990). The sharp discontinuity in the cortical representation of two adjacent digits was eliminated by the surgical fusion of the two digits (Allard et al 1991). This

reorganization was shown to take place centrally rather than by sprouting of sensory afferents in the periphery.

Cortical reorganization following deafferentation has also been reported in the cat (Franck 1980; Kalaska and Pomeranz 1982), rat (Wall et al 1984), raccoon (Rasmusson 1982; Kelehan and Deutch 1986), and flying fox (Calford and Tweedale 1988). The phenomenon is not restricted to SI, as cortical topographic reorganization following deprivation of the normal input has also been demonstrated in the primate second somatosensory cortex (Pons et al 1988), in rat motor cortex (Sanes et al 1990), in guinea pig primary auditory cortex (Robertson and Irvine 1989) and in cat visual cortex (Kaas et al 1990).

In every case of cortical reorganization produced by peripheral stimulation or surgery in the owl monkey, the internal topography, receptive field overlap, and magnification function are roughly maintained. The cortical area that formerly represented an amputated digit represents the adjacent digits topographically. Receptive field sizes are smaller in the cortical area of representation that increased in extent after the experimental manipulation. These consistent findings have been cited as evidence that the observed reorganization is the result of normal, dynamic processes that shape the functional organization of the cortex throughout life (see Merzenich 1988, 1990). One prediction of this theory is that changes in topography would result by changes in the animal's behavior.

The demonstration that cortical topographies are alterable in the adult raises the issue of the perceptual consequences of the reorganization. One possible example is the phenomenon of 'telescoping phantom limbs' and an

increase in tactile acuity of the stump skin of human amputees (see Henderson and Smyth 1949; Teuber et al 1949; Cronholm 1951). The 'phantom' is the sensation that the amputated limb still exists. The phantom is virtually always present immediately after the amputation and gradually disappears over many weeks to months, although in some patients it persists indefinitely. In most cases, the phantom "telescopes", i.e., the amputated arm is perceived to shorten, resulting in the illusion that the phantom hand approaches the stump (Henderson and Smyth 1949). Psychophysical tests of two-point discrimination, absolute location, and intensity thresholds all show increased acuity over the stump skin when compared to the homologous skin of the contralateral arm, or of normal individuals (Teuber et al 1949; Haber 1958). These clinical and quantitative psychophysical observations are consistent with a conservation of the representation of the missing limb in the cortex; the 'telescoping' is due to the occupation of the proximal limb representation by the representation of the stump skin. The increased representation of the stump skin can then explain the increased acuity over this area. This explanation was recognized by both Teuber and Haber (cited above; see also Merzenich et al 1984). A potentially confounding factor is the regeneration of the cut peripheral nerves into the stump skin. The data available indicate that the regenerating nerves are limited in extent, and those that do successfully reinnervate the skin do so in random fashion. While the potentially increased innervation density over this skin region could account for the increased acuity, the randomized reinnervation should not result in the percept of a complete, normally formed phantom limb.

A second issue relating to the perceptual consequences of cortical reorganization is the effective stimulation necessary to evoke reorganization. The vast majority of plasticity experiments have been conducted by altering the

peripheral input in some manner, then allowing the animal to recover for several weeks or months before the cortical organization was defined. The animal's use of the altered skin surface was not systematically documented, and it was assumed that the animal 'self-rehabilitated' during the period between the manipulation and the final experiment. Studies in the human literature suggest that the active participation of the patient facilitates the recovery following injury to the nervous system (see Wade et al 1985; Wagenaar et al 1990). If the cortical reorganization does in fact confer correlated changes in perceptual acuity, the question is raised as to whether selectively attending to the alteration-producing stimuli is necessary for the cortical reorganization.

These issues have been addressed directly by asking the questions: 1) Is the topographic representation of the hand in cortical areas 3a and 3b of an adult primate altered as a result of the animal's learning a perceptual task through repetition? 2) Does the behavioral relevance of a stimulus influence the changes that occur in the cortex?

Psychophysical capacities and neurophysiological properties of the somatosensory system

Several investigators have studied the responses of the primary afferents to specific tactile stimuli in order to define the specific input available to the CNS. In some studies the neural responses were related to known psychophysical detection and discrimination thresholds in humans or monkeys. These studies have provided clear evidence that tactile stimulation is parcelled into several parallel submodal inputs based on the class of the receptor in the skin. The

neurons processing information in each of these parallel channels are largely segregated up to at least area 3b (see Dykes 1983 for review). The threshold for activation of the SA (slowly-adapting) or RA (rapidly-adapting) peripheral mechanoreceptors closely matches the threshold for detecting a stimulus (Johannson and Vallbo 1979; see also Torebjork et al 1980, 1987). The SA afferents code the most refined spatial and pressure information (Johnson and Phillips 1981; Phillips and Johnson 1981; Torebjork et al 1987), the RA afferents are best suited to process temporal information at 'flutter' frequencies ranging over 10-50 Hz (Talbot et al. 1968; Mountcastle et al 1972) and the Pacinian afferents encode 'vibration' frequencies (>50 Hz), as well as texture (Talbot et al 1968; Mountcastle et al 1972; Lamb 1983).

Mountcastle and colleagues have specifically studied the peripheral and central neural responses to tactile stimulation in the flutter frequency range (see Mountcastle et al 1969, 1990; LaMotte and Mountcastle 1975, 1979). These studies have revealed possible neural correlates of tactile frequency detection and discrimination. The rapidly-adapting primary afferents innervating the Meissner's corpuscles in the glabrous skin were the most likely to code the frequency of the stimulus in the range of 10-50 Hz (Talbot et al 1968). The amplitude of a tactile stimulus that corresponded to the psychophysically defined detection threshold was the same as the threshold amplitude for single neurons in SI (Mountcastle et al 1969). A range of stimulus amplitudes intervened in which detection was accurate, yet below threshold for discrimination. This amplitude range was termed the 'atonal interval' (LaMotte and Mountcastle 1975). Finally, the amplitude thresholds at which frequency discriminations could be made approximately corresponded to the amplitudes at which single cortical neurons fired at least one action potential for every

stimulus cycle. Increasing the amplitude further did not significantly affect the subject's ability to discriminate the frequency of the stimulus.

These studies led to three important conclusions: 1) The tactile frequency discrimination of humans and macaque monkeys were roughly equivalent. 2) Single cortical neurons in SI could fire action potentials at every stimulus cycle for frequencies in the flutter range (10-50 Hz). 3) The stimulus intensities at which SI neurons would respond by cycle-for-cycle firing occurred at the stimulus intensities at which the frequency of the stimulus could be discriminated.

The analysis of the cycle-for-cycle response, or entrainment, of cortical neurons in the macaque were compared to the behavioral data derived in a well trained human subject (Mountcastle et al 1969). The human observer showed a slightly better performance than was predicted by the SI neuronal response in the macaque. The responses of SI neurons and the behavioral performance of the same animal were compared directly in a more recent study (Mountcastle et al 1990). The response of SI neurons was sharply entrained to the frequency of a sinusoidal stimulus presented to the center of the receptive field, but no data on the prediction of the behavioral data by the neuronal response was presented.

The results described for frequency discrimination in the macaque suggest that neuronal responses in SI are sufficient to account for the frequency discrimination performance. It was of interest to know if the discrimination performance to stimulation of a small skin location would improve if the discrimination task was practiced at that particular location over several

thousand trials. If improvement in performance, defined by a smaller increase in frequency that can be detected as different, does occur selectively for the "trained" skin, the neural responses to stimulation of the trained skin could be compared to those of an analogous area of skin that was not trained, and that therefore had a higher discrimination threshold.

If SI neuronal responses can account for tactile discrimination performance, these differences in discriminability should be represented by a specific difference of the spatial and/or temporal response properties of neurons representing the stimulus presented to the trained vs. untrained skin surface.

To test this hypothesis a behavioral procedure was developed in which adult owl monkeys were trained to discriminate the frequency of a test stimulus when compared to a standard stimulus of 20Hz. Stimuli were presented to a small, invariant skin location. The behavioral performance of these animals was defined over a period of several weeks, and once the performance had improved the topographic representation of the stimulated hand in areas 3a and 3b was determined. The opposite, untrained hand was similarly mapped and used as a control. The cortical representation of stimulated skin was compared to that of the skin on adjacent, non-stimulated digits, as well as to the control hemisphere. The specific question was: Is the cortical representation of this limited skin area altered as a result of this behavioral training?

At most cortical locations studied in the mapping process the neural responses to tactile stimulation at the same frequencies that were used in the behavioral task were recorded. Responses to stimulation of the trained skin used in the behavior were then compared to responses to the same stimuli

presented to corresponding but unpracticed skin on the adjacent digit. The specific question was: Can the temporal structure of the responses of SI neurons account for the animal's ability to discriminate the frequency of a tactile stimulus?

To control for the effects of stimulation alone, a second set of monkeys were trained to attend to an auditory stimulus while receiving tactile stimulation identical to that presented to the experimental animals. These "passive-stimulation" control monkeys were not required to discriminate the tactile stimulus and presumably did not attend to this stimulus. The specific question was: Is stimulation alone sufficient to drive the changes in the cerebral cortex, or must the animal subject be actively discriminating the stimulus for these changes to occur?

METHODS

Animals

Feral adult owl monkeys of both sexes were used in all experiments. Animals were judged to be adults by their body weight and overall appearance. They were individually caged with free access to water and were maintained on a reverse 12 hour light/dark cycle with the lights coming on at 7:00 p.m. Care was take to ensure that the animals were in good general health throughout the course of the study.

Psychophysics

The psychophysical training and testing protocol is described in detail in Appendix I. Briefly, animals were trained to discriminate the frequency of a sinusoidal tactile stimulus presented to a restricted skin region of a single digit. The skin region comprised less than a single phalanx of a single digit. The animal initiated a trial by placing its hand onto a hand mold, through which the tactile stimulus was presented. The animal maintained contact throughout repeated presentations of a 20 Hz stimulus (S1). These stimuli were 650 msec in duration with a 650 msec interstimulus-interval. The animal was required to break contact with the hand mold when the frequency of the tactile stimulus was greater than 20Hz (S2). The S2 was randomly presented in the second to sixth stimulus presentation (bin). Correct responses were rewarded with a 45mg food pellet, incorrect responses to the 20 Hz stimulus (False-positives) or failures to respond to the S2 (Miss) were penalized with 1-5 sec time-outs. Animals were tested 6 days a week and received 500-700 trials/day (1500-2100 stimulus bursts/day). Six to ten S2 frequencies, one of which was always near enough to the S1 to be below threshold (see below), were presented on

20-50 trials/session. In a few sessions for each animal the tactile stimulator was positioned to contact the corresponding skin surface on the digit adjacent to that which was usually trained. The threshold was then measured for this digit. Once the behavioral performance was stable on the trained digit, the animal was prepared for the electrophysiological study conducted the following day.

Passive-stimulation Paradigm

A second set of animals were trained on an auditory frequency discrimination paradigm. These animals were required to make the same hand-mold contact as the tactile discrimination animals. The same tactile stimuli were presented to these animals, but the bin in which the tactile S2 frequency was presented was randomized. Auditory stimuli were presented as tone pairs of either equal (S1|S1) or unequal (S1|S2) frequency. The S1 auditory frequency was constant for each animal. These animals were required to actively discriminate between the auditory stimuli while receiving the tactile stimuli in a passive manner.

The auditory discrimination animals were trained over a period of time similar to the tactile discrimination monkeys, and were tactually stimulated for a similar number of stimulus presentations. The tactile stimulus in these animals was a series of 650 msec periods of sinusoidal stimulation, as with the tactile animals. A tactile stimulus frequency greater than 20 Hz was presented, at most, only one time in any trial. 20 Hz stimuli were presented alone on 5-15% of the trials, depending on the animal's False-positive rate. The tactile S2 frequency could occur in time bin 1, which never happened in the tactile discrimination task, and it could also occur during the S2 auditory stimulus. Thus, the tactile stimulus was randomly presented and in no way predicted the

time for a correct response to the auditory stimuli. The absolute number and duration of stimuli presented to the skin in both paradigms were equivalent.

Following a short period of training, these animals adopted a stereotypic hand placement. Analysis of videotaped sessions with the camera mounted directly above the hand mold was done to address the variability of the hand placement, and thus the stimulus probe location. The position of each knuckle was marked on an acetate overlay on the video monitor for 500-1000 trials over the course of several sessions for each animal. The absolute range of knuckle position on the stimulated digit was measured as a radius of less than 0.75 mm. This corresponds to a total area of skin stimulated by the stimulus probe throughout the training period to not exceed 3.5 mm in diameter.

Electrophysiology

The primary goal of the electrophysiological study was to define the cortical representation of the hand surface in cortical áreas 3a and 3b in both hemispheres. These electrophysiological maps were derived in one continuous experiment conducted at the end of the psychophysical training period. The hemisphere contralateral to either the trained hand in experimental animals or the stimulated hand in passive-stimulation control animals was studied first. The control hemisphere, ipslateral to the trained hand, was studied as time permitted. In some cases only a partial map of the control hemisphere was possible. Two of the passive-stimulation control animals (P-2 and P-3) were only partially mapped on the hemisphere contralateral to the stimulated digit. The area 3a and 3b maps in these two cases included the entire representation of the stimulated digit (D3) and the adjacent digit (D4). These animals were investigated in auditory cortical areas as part of a second study.

Anesthesia was induced with a halothane: oxygen: nitrous oxide mixture (3.0%:5.0%:1.5%). The femoral vein was cannulated. The gaseous anesthetic was withdrawn and Sodium Pentobarbital given i.v. as needed to maintain a surgical level of anesthesia. Lactated Ringer's solution with 5% Dextrose was continuously infused i.v. (2-5 ml/hr) throughout the course of the experiment. Animals gave no sign of discomfort or reflexive responses throughout the experiment. Atropine sulfate (0.1 mg/12 hrs) and penicillin G (30,000 units/24 hrs) were given i.m. Body temperature was maintained at 37° C with a thermostatically controlled heating blanket. Heart rate and respiration rate were monitored. Blood pressure, pulse, and hydration level could be estimated by the cortical vasculature viewed at 40X magnification, and skin turgidity of the hand. The bladder was evacuated at regular intervals. These animals were anesthetized for up to 56 hours and every effort was made to maintain a constant physiological state.

The head was stabilized in a stereotaxic apparatus. A craniotomy exposed the relevant cortical area. The dura was resected and a silicon oil well was constructed. The cortical vasculature was imaged by either a photograph or a video-computer image. This image was magnified 40X. Similar imaging with less magnification was done for the hand surfaces to be investigated.

Microelectrodes were either glass micropipettes filled with 3.6M KCl solution (beveled tip; diameter 28-22μm) or parylene-coated tungsten-iridium electrodes. In either case impedances measured 1-3 MΩ at 1 kHz. All microelectrode penetrations were parallel and roughly perpendicular to the cortical surface, and the insertion points were marked on the image of the

cortical surface with reference to the vasculature. All data were collected at a depth of 700-950 μm below the cortical surface. Multi-unit recordings were amplified and displayed using conventional methods.

Cortical receptive fields were defined using opaque fine-tipped (diameter approx. 0.5mm) glass probes to depress the skin. The stimulus amplitude used was sufficient to cause just-visible skin indentation was was constant for all studied monkeys (see Merzenich et al 1978, 1983a, 1984). Receptive field boundaries were reproduced on the image of the hand surface, and qualitative descriptions were documented.

Peri-stimulus time histograms were collected at many cortical locations. The hand was stabilized in a plasticene mold, glabrous skin facing upward. The tactile stimulator was placed on a marked location corresponding to the skin location stimulated in the behavioral apparatus or to the corresponding location on the adjacent digit. The probe was the same as that used in the behavioral experiment. The initial contact force was uniform (5-10 g) for each stimulation for each animal on both digits and matched the force used by that animal in the behavioral apparatus.

The tactile stimulus was a 350-650 msec period of sinusoidal stimulation at a given frequency. This stimulus was presented for 10 repetitions. Each repetition was separated in time by 1 sec. Each frequency was tested sequentially using these same time parameters. The tested frequencies always included 20, 21, 22, 24 and 26 Hz. The window discriminator was set to include all waveforms with an amplitude greater than 2X the spike-free neural noise level. This eliminated all low amplitude, "hash" responses from analysis and

only included waveforms that were characteristic of single neurons in both shape and time. These accepted waveforms (usually 2-5 single units) were continuously inspected visually.

Near the end of each experiment electrolytic lesions were made at selected locations within the studied area by passing 10 μA of DC current for 10-20 sec. In addition, Indian Ink marks were made at four locations marking the widest boundaries of the investigated region. 1 ml of Heparin Sulfate was given i.v., then the animal was perfused intracardially with 37°C saline followed by one of three fixatives in phosphate buffer: 10% formalin, 1.0% paraformaldehyde, or 1.0% paraformaldehyde and 0.5% glutaraldehyde. Brains were then removed and prepared for histology. Frozen sections were cut in the parasagital plane and stained with cresyl violet.

Data Analysis

Psychophysics

Thresholds were derived from each session in which two criteria were met; 1) The overall False-positive rate was below 15% and 2) There were at least 20 stimulus presentations of an S2 frequency below the 50% performance level. In these sessions, the performance was defined as

$$S-((1-H)*S)$$

where

$$H = \#Hits/(\#Hits+\#Misses)$$

S = (#safe periods with no response / #safe periods presented).

This adjusted performance function takes into account small variations in the False-Positive rate over a number of sessions (see Appendix I for more details). Threshold is then defined as the frequency with a 50% performance value. The difference between this frequency and the S1 (20 Hz) frequency is defined as the delta frequency (Δf). This value was usually interpolated by defining the straight line between the two S2 values bracketing the 50% performance line (i.e. performances of 40% and 60%).

The value d' was determined by subtracting the z-score of (1-False-positive rate) from the z-score of (1-Hit rate). We did not systematically vary the False-positive and hit ratios so ROC curves were not generated.

Map reconstructions:

All map reconstructions were done on a Macintosh II computer. Electrode penetration locations were either reproduced by optical scanning of the brain photograph or were taken directly into the computer during the experiment (see above). To determine the boundaries of the representations of digit segments, lines were drawn midway between cortical locations representing adjacent segments. The physiological boundary between areas 3a and 3b was determined as bisecting the two cortical locations in the A-P axis in which the more caudal one had a cutaneous response and the next rostral location had either 1) a non-cutaneous (deep) response 2) a significantly (>2X) larger receptive field than those locations caudal to it or 3) a reversal in the topographic location of the receptive field.

Receptive field analysis

Receptive field areas were measured on the Macintosh II using the software Canvas. The receptive field location was defined as the receptive field center, as estimated by eye. Most receptive fields were elliptical in shape and thus this procedure was adequate. Receptive fields which included multiple digits were not assigned a specific digit location.

Receptive field overlap was taken by selecting a subset of receptive fields as 'standards'. All receptive fields on the same digit, their center located within the central 1/3 of the digit, were then compared to each standard. These 'standard' receptive fields were randomly selected to provide a reasonable sample of locations throughout the cortical representation of the digit. Overlap was defined as (the area common to both receptive fields) divided by (the area of the standard receptive field). This procedure was repeated for each (2-8) standard receptive field.

Statistical analysis

All statistical analysis was done using Statview 512+. The specific statistical tests are described where appropriate in the Results. P values <0.01 were taken as significant. Correlations were done using a r.m.s. best fit line to the data.

Analysis of temporal responses

Quantitative analysis of the PSTHs included total spikes, peristimulus time histograms, and period histograms. PSTHs were constructed by the cumulative count of accepted waveforms that occurred in a 350 msec period beginning at the stimulus onset for each of the ten repetitions of a given stimulus frequency.

Binwidth was 75 μsec. Cycle histograms were constructed by adding all spikes which occurred at the same time relative to the stimulus cycle. The first cycle commonly evoked a large onset response and was therefore eliminated from this analysis. Binwidth was 500/ (period length of the stimulus) i. e. 100 μsec for 20 Hz.

Measures of phase-locking were taken as vector strengths. Vector strength was calculated from the cycle histograms by defining a vector at each time period with the amplitude equal to the total spikes at that time, and the phase equal to the phase of the stimulus. These vectors were then summed and the resultant vector was normalized by dividing by the total number of spikes. This measure varies from 0 (spikes occurring randomly in relation to the stimulus) to 1 (all spikes occur at the same time in relation to the stimulus).

Population Histograms

Population peri-stimulus time histograms were derived by summing the response to 350 msec of the stimulus for every cortical location in which the vector strength of the response at that location exceeded 0.5. The response was binned in 2 msec time bins. Population cycle histograms were derived by summing the cycle histograms determined at each cortical location. This procedure is shown for two frequencies, 20 and 26 Hz, in Figure 1. Spikes were summed in 200μsec bins. The resulting cycle histogram represents the average response of the neurons to each cycle of the stimulus frequency

In order to estimate the separation of the response between cycles in time, population cycle histograms were also constructed using two cycles of the stimulus (2-cycle histograms; Figure 1, bottom). In this procedure, all cycles

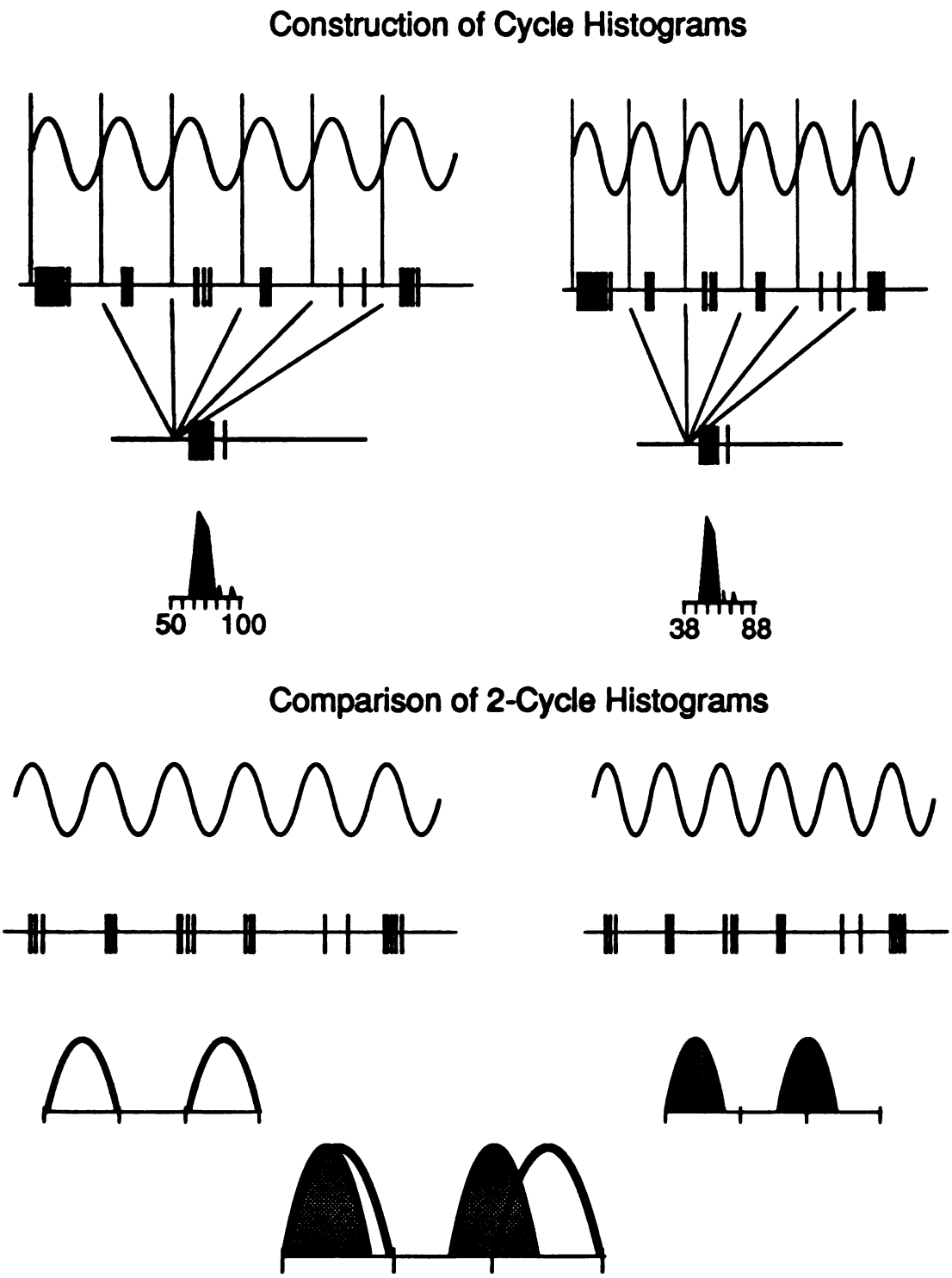

Figure 1. Method of constructing cycle histograms (top) and two-cycle histograms (bottom) from the neural data collected in these experiments. Two cycle histograms are shown as schematics in the lower figure. Comparisons were made between the second cycle of the two-cycle histograms. See text for details.

contribute to each of the two cycles of the histogram, except for the first (onset) cycle, which only contributes to the first of the two cycles. The response was plotted using real time (msec) on the x-axis as opposed to time relative to the stimulus cycle (radians) as is more commonly done. The resulting histograms then represent an estimate of the average response between two stimulus cycles in real time and a direct comparison of the temporal distribution of action potentials between two stimulus frequencies.

Estimates of overlap between the responses of two different frequencies were done by superimposing the 2-cycle histograms of the responses to the 20 Hz frequency with the responses to each of the four S2 frequencies (21, 22, 24 and 26 Hz). The first cycle in the histograms were aligned and the distribution of the action potentials in the second cycle were compared. Comparison of the second cycles is thus a comparison of the real time interval between the bursts of action potentials seen in the raw data. The total number of spikes in the S2 histogram occurring during the presentation of the second stimulus that did not overlap with the response in the 20Hz histogram was divided by the total number of spikes in the S2 histogram occurring during the presentation of the second stimulus. This value is thus a measure of the response at the S2 stimulus that is different from the response at the 20 Hz stimulus. This value, which ranges from 0 to 1.0, was then multiplied by 100 to give a percent value (0-100%).

RESULTS

The results of this study will be presented in three sections. The first describes the results of the psychophysical experiments. The second section describes the results from the electrophysiological mapping of cortical areas 3b and 3a in the behaviorally trained and control animals. The third section quantitatively describes some response properties of neurons in SI to the presentation of a tactile stimulus to the skin trained in the behavioral task and to the homologous skin on an untrained digit.

PSYCHOPHYSICS

Thresholds

Five monkeys were trained on the tactile discrimination task. Thresholds were determined for 30-131 sessions in these animals. Four animals ultimately achieved frequency discrimination thresholds on the trained digit of 2-3 Hz relative to the 20 Hz standard (range 1.95-2.69 Hz). Frequency discrimination thresholds for stimuli presented to the untrained, adjacent digit had a higher threshold in each of these four cases (see Table 2). Three other animals were trained on the auditory discrimination paradigm. These animals were trained for an equivalent number of sessions (64, 118, and 105 for P-1, P-2 and P-3).

Improvement in Performance

Four of the five animals studied on the tactile frequency discrimination paradigm showed a clear improvement in performance with training. Thresholds were taken at three different stages of training and are shown in

Table 1. Summary of the Thresholds Defined on the Trained Digit

Monkey	Initial Training Sessions	Middle Training Sessions	Final Training Sessions	Total Number of Training Sessions
E1	6.43 ± 0.17	3.89 ± 0.21	1.95 ± 0.25	58
E2	9.85 ± 1.64	3.79 ± 0.14	2.22 ± 0.14	131
E3	6.68 ± 0.57	4.68 ± 0.21	2.69 ± 0.24	110
E4	7.28 ± 2.28	5.74 ± 0.84	7.84 ± 5.5	80
E5	7.04 ± 0.45	3.11 ± 1.74	2.20 ± 0.71	30
Mean	7.46 ± 1.38	3.87 ± 0.64	2.26 ± 0.31	

Thresholds are taken as the mean and standard deviations for three consecutive days of training.
Initial Training Sessions are the first three consecutive days of training in which thresholds were derived.
Middle Training Sessions are the three sessions beginning at the midpoint of the total days of training.
Final Training Sessions are the final three sessions of the training period for that monkey, shown in the last column.
Mean was calculated from the three threshold values for each monkey . Case Case E4 was omitted from calculation of the mean for the Middle and Final training sessions.

Table 1. The initial stage was defined as the first three consecutive sessions in which thresholds were obtained. The final stage was defined as the last three consecutive sessions, and the middle stage was the three sessions at the midpoint between these two extremes. In four of these five monkeys (all monkeys except E4) the thresholds progressively decreased over these three stages of training. The difference between the initial stage and middle stage, as well as between the middle stage and final stage, were statistically significant ($P<0.01$; paired t-test). All monkeys had similar thresholds over these three periods of training even though the durations of training ranged over 21-131 consecutive days. The mean initial threshold for all monkeys was 7.46 Hz. The mean middle threshold for all monkeys except E4 was 3.87Hz, which represents 48% of the initial threshold. Monkey E4 is omitted from the calculation of the mean for the middle and final threshold values as this monkey did not show a significant improvement in performance by any measure (see below). Finally, the mean final threshold was calculated at 2.34, which represents a 40% improvement with respect to the middle threshold and a 69% improvement with respect to the threshold defined in the initial stages of training.

The performance at the discrimination task did not improve linearly with training, as the improvements were very rapid in the initial stages of training and then progressed at a more gradual rate. Figure 2 shows the threshold, defined as the difference in frequency (delta frequency; Δf) at which the animal performed at 50% correct, plotted as a function of consecutive days since the first thresholds were derived for each animal. This measure was taken as every animal has a small number of sessions in which thresholds could not be derived because either the False-Positive rate was greater than

Figure 2

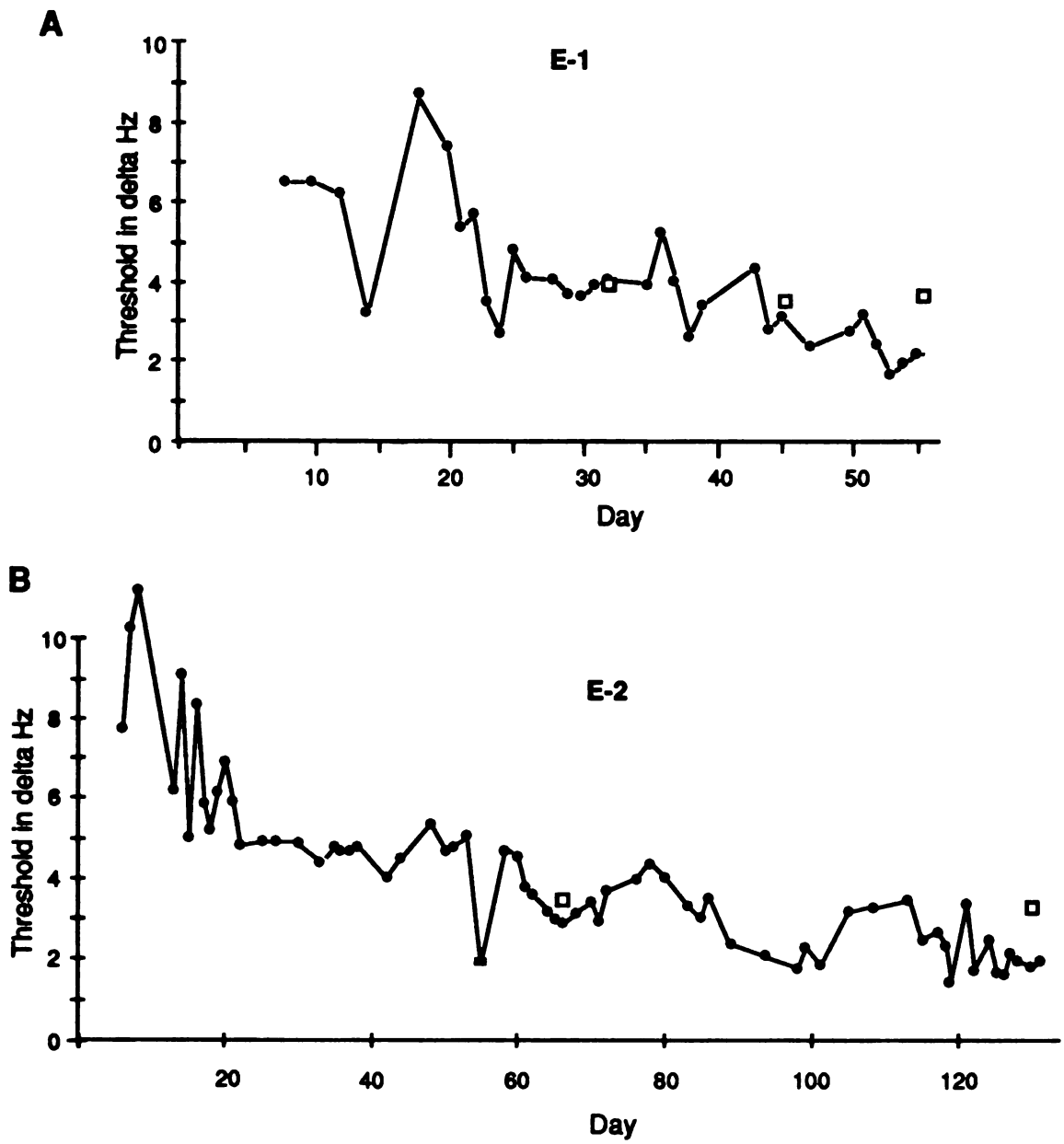
A
E-1
Threshold in delta Hz
0
2
4
6
8
10
10
20
30
40
50
Day
B
E-2
Threshold in delta Hz
0
2
4
6
8
10
20
40
60
80
100
120
Day

Figure 2

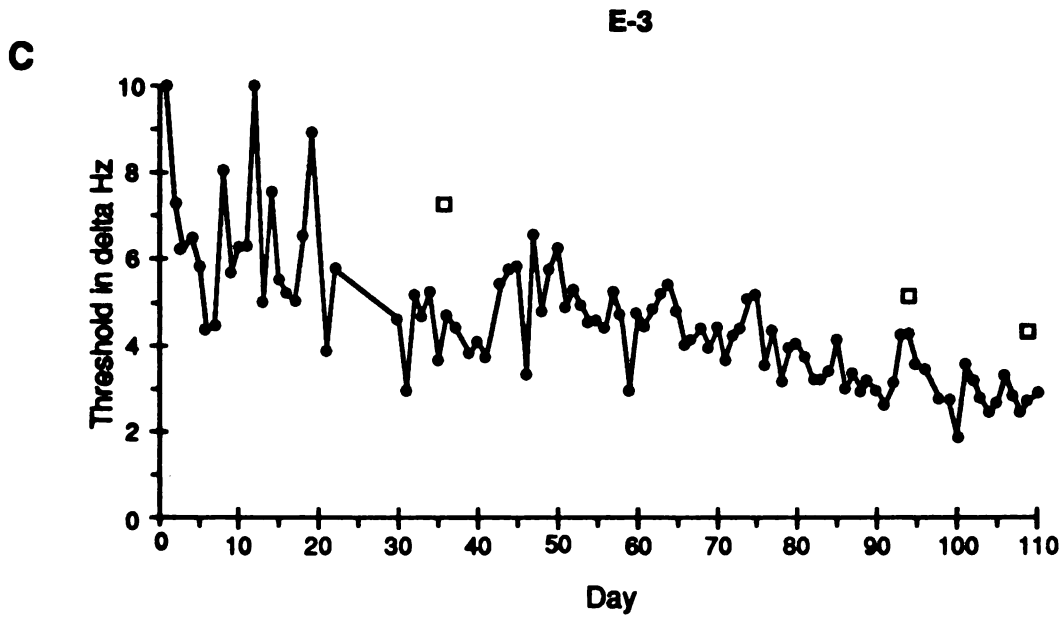
C
E-3
Threshold in delta Hz
0
2
4
6
8
10
0
10
20
30
40
50
60
70
80
90
100
110
Day

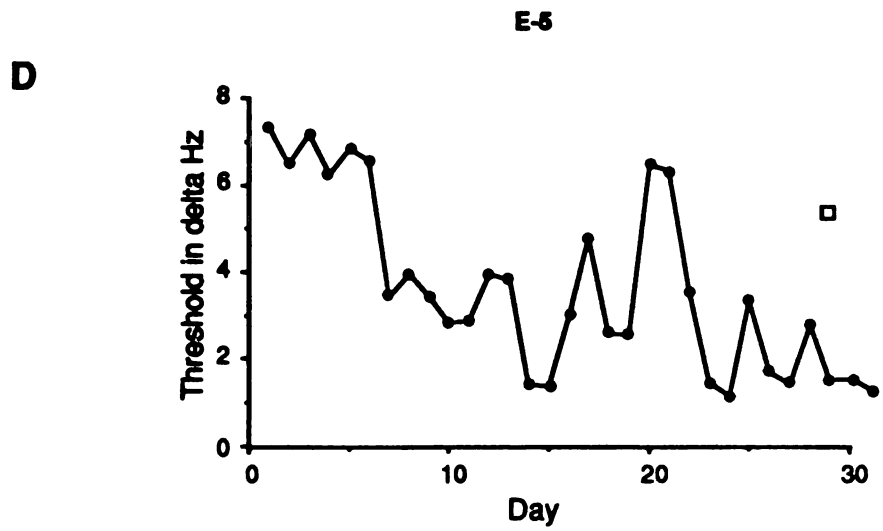
D
E-5
Threshold in delta Hz
0
2
4
6
8
0
10
20
30
Day

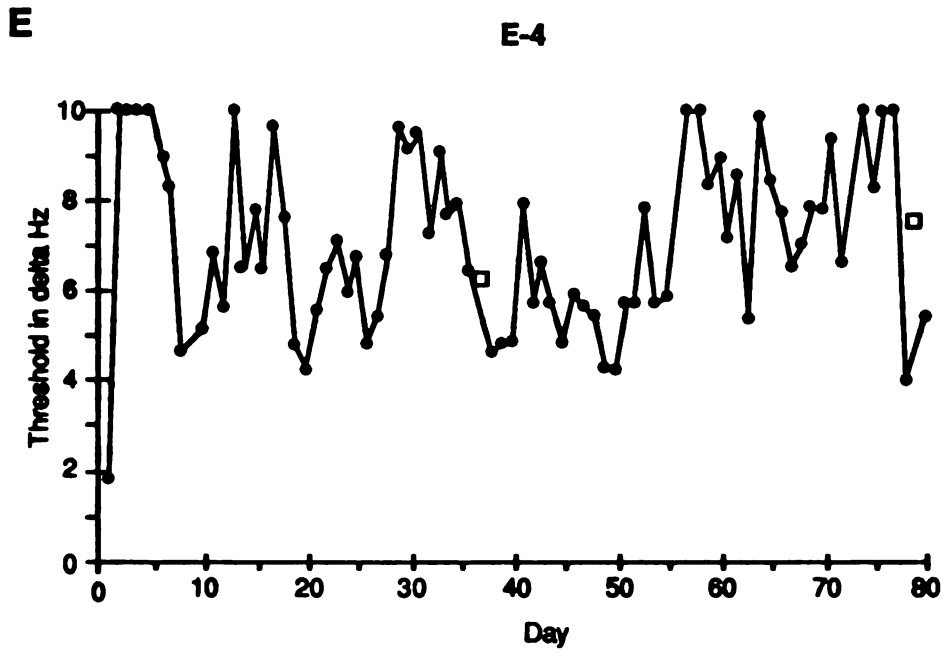

FIGURE 2. Improvements in performance plotted as a function of consecutive days of training. Day 1 is taken as the first training day a delta frequency was presented in which the performance was below 50%. Filled circles denote thresholds determined on the trained digit, open squares denote thresholds determined on the adjacent, untrained digit. The comparison frequency was 20Hz in this and all following figures. Bold type letter-number combinations refer to the individual monkey.

15% or there were not at least 20 presentations of an S2 stimulus below threshold. Data from these sessions are not plotted even though the animal performed several hundred trials. All monkeys were trained on at least six of every seven consecutive days.

The improvement in performance was rapid over the first 10-20 sessions. This time period shows the most variation in threshold between consecutive days (i. e. animal E-3, Figure 2C). The rate of improvement was more gradual over the next several weeks to months. This period usually had a smaller variation of the measured threshold between sessions, and the performance approached an asymptotic level. An exception was seen in one animal (Animal E-4, Figure 2E). This animal never consistently resolved the smaller delta frequencies which led to a large variability in threshold measurements throughout training.

In Figure 3 the psychometric functions for 5 different sessions taken throughout the course of training in a representative monkey are shown in Parts A-E, with these functions shown together in F for direct comparison. The performance at high frequencies (greater than 28Hz) improved to nearly perfect levels, with less variability between frequencies. The discrimination performance at frequencies closer to threshold, however, revealed a progressive improvement. For example, the improvement at Δfs of 6 and 8 Hz is greater than at 5 Hz between sessions 3 and 48 (see Figure 3F). The improvement at Δfs of 4 Hz and 5 Hz is greater than for 3 Hz between sessions 48 and 74, similarly the improvement at Δfs of 3 Hz is greater than the improvement at 1 Hz and 2 Hz between sessions 74 and 120. Psychometric

FIGURE 3 Representative performance functions taken during five different training sessions in one representative animal (E-3). The performance at each S2 frequency is plotted on the y-axis (see *Methods* and *Appendix I*). The delta frequency, defined as the difference in frequency between the S2 and the 20 Hz comparison, is plotted on the x-axis. The dashed line is drawn through a performance of 50%, which was considered threshold. Parts A-E are taken from different training sessions. Part F is a composite of parts A-E.

Figure 3

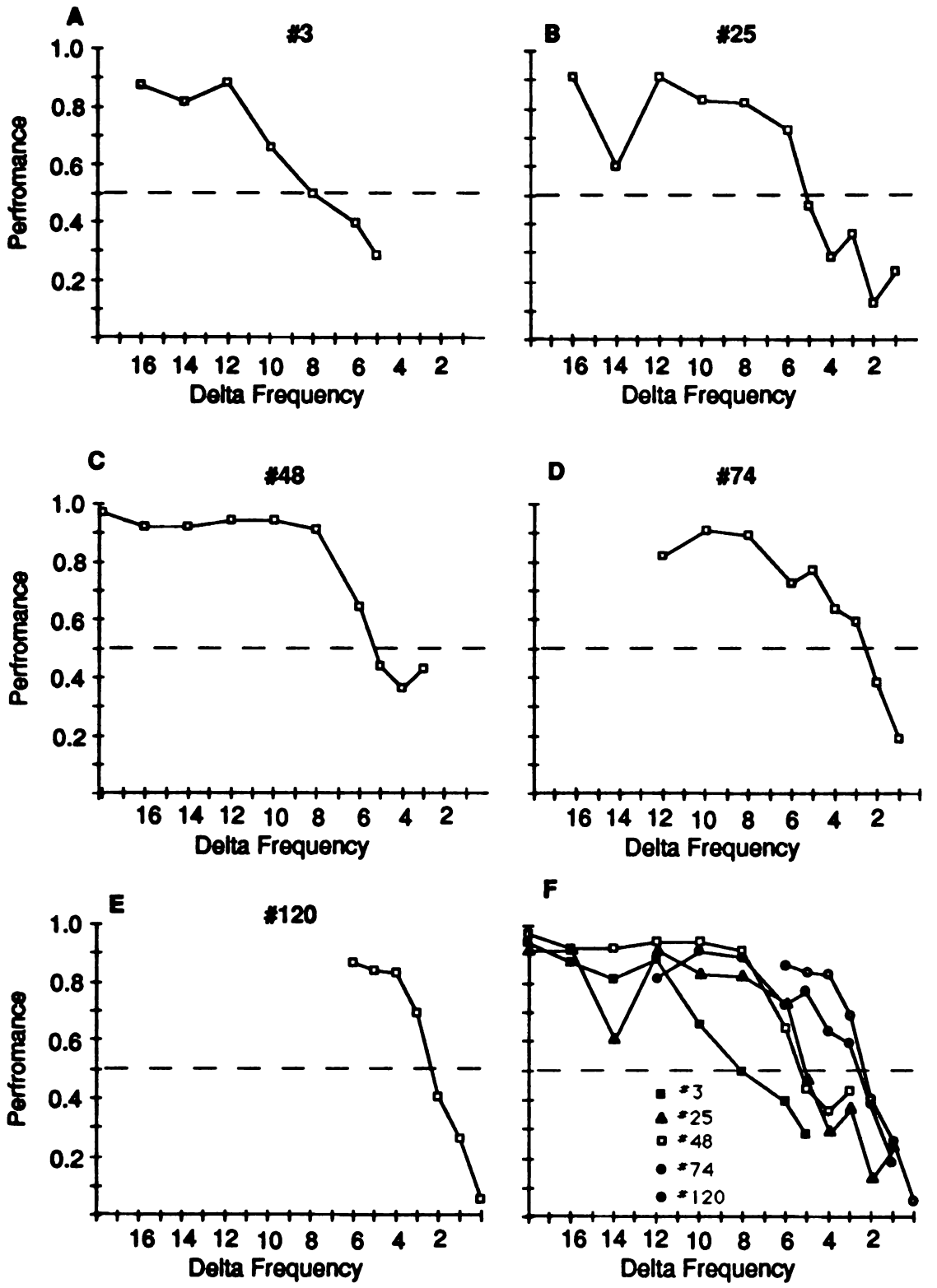
A
#3
B
#25
C
#48
D
#74
E
#120
F
Perfromance
1.0
0.8
0.6
0.4
0.2
16 14 12 10 8 6 4 2
Delta Frequency
#3
#25
#48
#74
#120

functions shifted to the left and steepened during the course of training.

The progressive improvement in discrimination performance is shown by plotting the performance at a particular frequency across sessions (Figure 4). This representative animal first improved at 30 Hz on session 2 (Figure 4A); at 26 Hz the performance improved above 50 % after 48 sessions (Figure 4B); at 24 Hz the performance improved on session 79 (Figure 4C). This animal (E-3) never consistently performed above 50% at at 22 Hz (Figure 4D). A similar progression in discrimination learning was seen for each of the three other cases in which performance substantially improved.

Thresholds on the adjacent digit

In each animal, an adjacent digit was tested using the same behavioral paradigm (open symbols, Figure 2) in two or three single sessions. Frequency discrimination thresholds for stimuli presented on the adjacent digit were in every case greater than the thresholds determined on the preceding and following sessions for stimuli presented to the adjacent trained digit (Table 2).

The performance functions for both digits are shown for each session in which the adjacent digit was tested in a representative example in Figure 5. In each case the performance function of the trained digit is plotted with the performance function of the untrained digit on the next day. Discrimination on the trained digit was consistently better than on the untrained digit for all but the highest frequency differences.

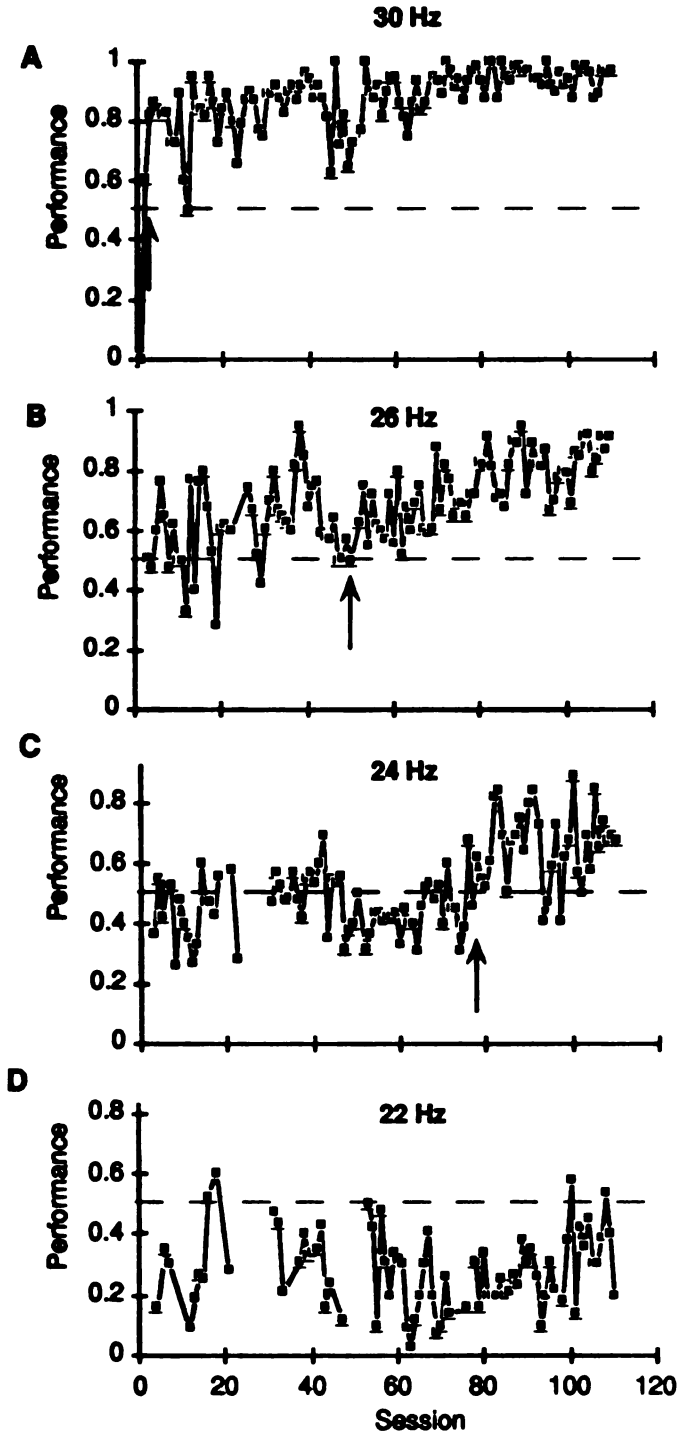

Figure 4. The corrected performance at a given frequency plotted as a function of consecutive days for a representative monkey. The dashed line is drawn through a performance of 50% (threshold). The arrow indicates the first session in which the discrimination of this frequency from the 20 Hz standard was maintained above threshold. All data is from monkey E-3.

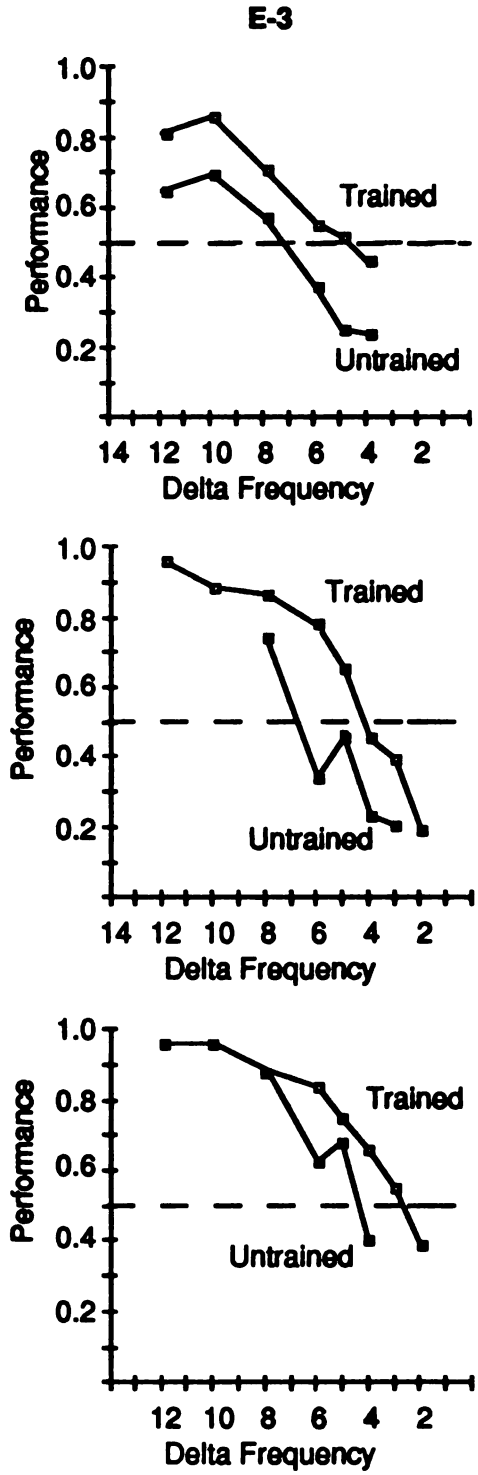

Figure 5. Performance functions derived from animal E-3 from both the trained digit (open squares) and the adjacent, untrained digit (filled squares). Conventions as in figure 3.

There appeared to be modest improvements with training conferred on the adjacent digit. The rate of improvement on the adjacent, untrained digit was less than that of the trained digit, and the threshold defined on the adjacent digit was always lower than the threshold defined on over the initial stage of training on the trained digit. Table 2 shows all thresholds defined on the adjacent digit, and the mean thresholds defined on the trained digit over three sessions at the same stage in training. Monkey E-1 showed a decrease of threshold on the trained digit of 30% between sessions 44 and 55, while the adjacent digit threshold actually slightly increased. Monkey E-2 had a decrease in threshold of 44% between sessions 65 and 128 on the trained digit, and only 22% on the adjacent digit over the same period. Finally, monkey E-3 had a decrease in threshold of 34% between sessions 93 and 109 on the trained digit, and only 16% on the adjacent digit. By the final stage in training, the difference in the measured threshold between the trained and adjacent digit was greater than two standard deviations of the mean threshold on the last three sessions on the trained digit in all cases except E-4. It should be noted that the false-positive rate when the animal performed the task when stimulated on the adjacent digit was approximately equal to the false-positive rate when the animal was stimulated on the trained digit.

The performance functions in Figure 6 illustrate some of the results from the one monkey that did not improve in performance with training (E-4, Figure 2E). This animal would consistently make correct responses for large frequency differences (12-20 Hz), but the behavior degenerated to a guessing strategy once the task became more difficult. The thresholds remained very variable between sessions and were unreliable. Representative examples of the performance functions of this animal over time are shown in Figure 6A.

Table 2. Thresholds on the Trained Digit and an Adjacent, Untrained Digit

Monkey	Session Number	Trained Digit Threshold	Adjacent Digit Threshold	Adjacent / Trained
E1	30	3.89 ± 0.21	4.75	1.22
	44	2.79 ± 0.38	3.50	1.25
	55	1.95 ± 0.25	3.75	1.92
E2	65	3.94 ± 0.73	3.96	1.01
	128	2.22 ± 0.14	3.10	1.40
E3	35	4.28 ± 0.53	7.24	1.69
	93	4.06 ± 0.41	5.17	1.27
	109	2.69 ± 0.21	4.34	1.61
E4	37	5.24 ± 0.97	8.55	1.63
	78	7.85 ± 5.5	7.67	0.98

Thresholds on the trained digit are taken as the mean and standard deviations of three consecutive sessions beginning on the session indicated (Session Number).
Thresholds on the Adjacent Digit are taken in a single session (Session Number)
Adjacent / Trained: ratio of the threshold derived on the adjacent digit divided by the mean threshold derived on the Trained Digit. Ratios taken for the final training sessions are underlined.

The performance at frequencies below 25Hz never improved above threshold (dashed line), even though this animal had a similar number of training sessions compared to successfully trained animals (see Table 1). The performance at large Δfs, 8 Hz and 10 Hz, was improved and the animal performed well at these high frequencies.

In contrast to other trained monkeys, this animal's performance functions did not change in slope, but appeared to shift along the y-axis. The only apparent improvement over time was for 26 Hz between sessions 34 and 58. The performance on the adjacent digit was tested on day #37 (Figure 6B) and was clearly worse in performance than was the trained digit.

Analysis by the Theory of Signal Detection

The results expressed by simply plotting the threshold defined for each session as a function of training suggests an improvement in the frequency discrimination ability of that specific skin region. Signal Detection Theory (Green and Swets, 1966) models a subjects' performance as setting a criteria level between two partially overlapping distributions; a hypothetical "signal" distribution and a "signal-plus-noise" distribution. The model assumes that these two distributions are Gaussian in shape and have equal variance. The difference between the two peaks in these distributions are expressed in units of variance as the value d', where d' values of 0 represent complete overlap, and d' values of 3 or greater represent no overlap. d' values of 1 (one standard deviation separation) are generally taken as threshold.

Signal detection theory can account for improvements in performance in two ways: 1) The monkey could change it's criteria so that it makes more 'Hits',

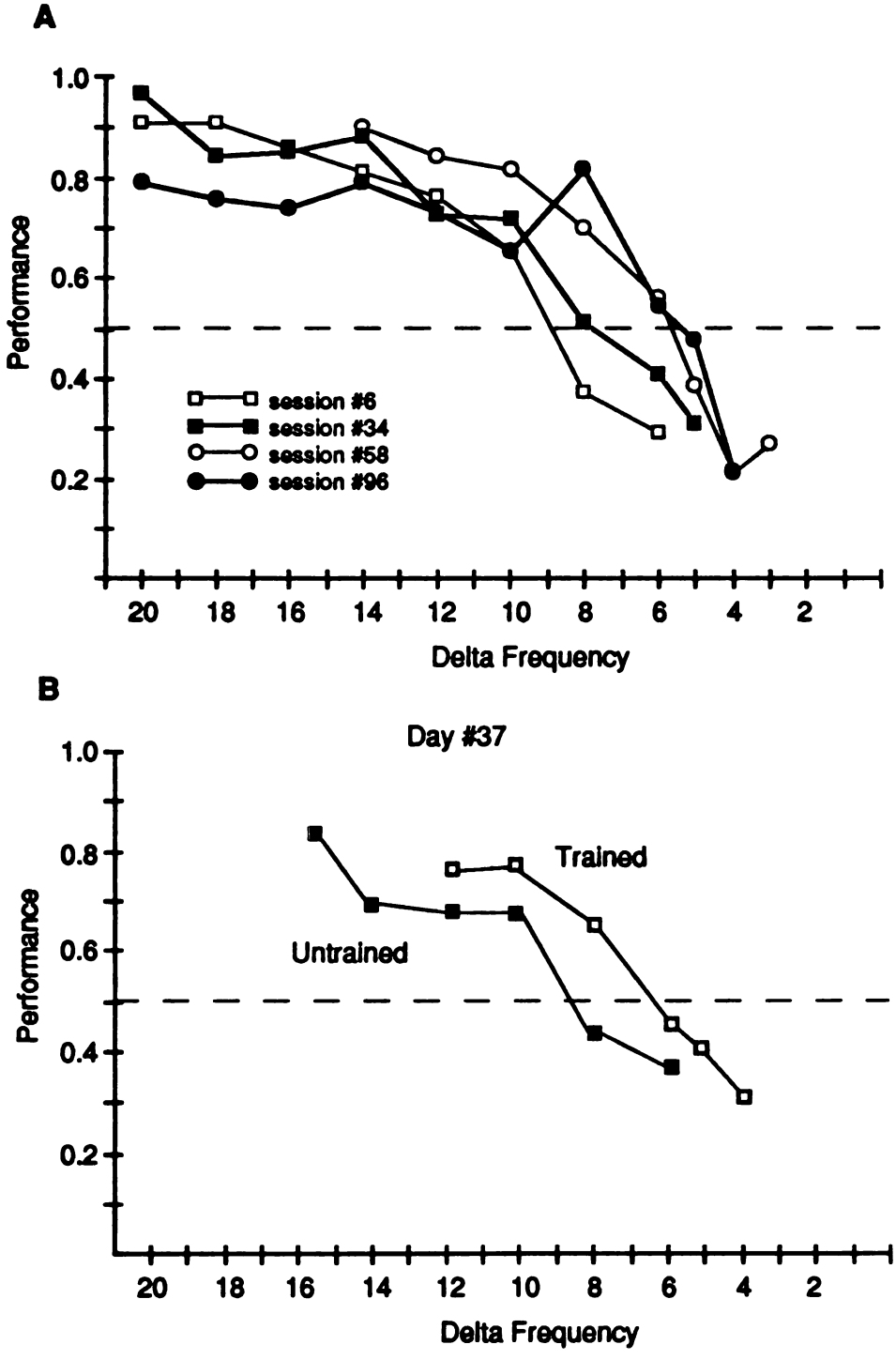

Figure 6. Performance functions on the trained digit on four different sessions for animal E-4 are shown in Part A, the performance functions on Day #37 for the trained digit (open squares) and the adjacent digit (filled squares) are shown in Part B

but also more 'False-Positives'. In this case no improvement of discriminability has actually occurred, and the "signal" and "signal-plus-noise" distributions remain the same. In this case the d' would not change. 2) The discrimination performance of the monkey could improve by increasing the separation of the two distributions. In this case the d' would increase.

Three observations in the behavioral data demonstrate that the discrimination performance improved on the trained skin in four of the five monkeys. First, the individual performance functions changed in slope with training (see Figures 3 and 5). If the animal were only changing criteria, these performance functions would simply move along the y-axis. Second, the False-Positive rate for each of these animals was relatively constant throughout training (Figure 7). If the improvement in performance were due to a change in criteria, the False-positive rate would increase. Third, the values of d' increased for several frequencies as a function of training. These results are shown in Figure 8. In this typical example, the d' values for 30, 26, 24, and 22 Hz are shown in the left vertical column for animal E-3 (Part A). Although there is considerable variability in these calculated values when compared on a session by session basis, a clear trend of increasing d' values is evident for all frequencies which showed an increase in performance (30, 26 and 24 Hz). The d' values were not increased for 22Hz, at which little improvement with practice was recorded in this monkey.

These results of animal E-3 (Figure 8A) were similar to those of each of the animals that improved in performance with training. This analysis supports the conclusion that the improvements in performance resulted from a true

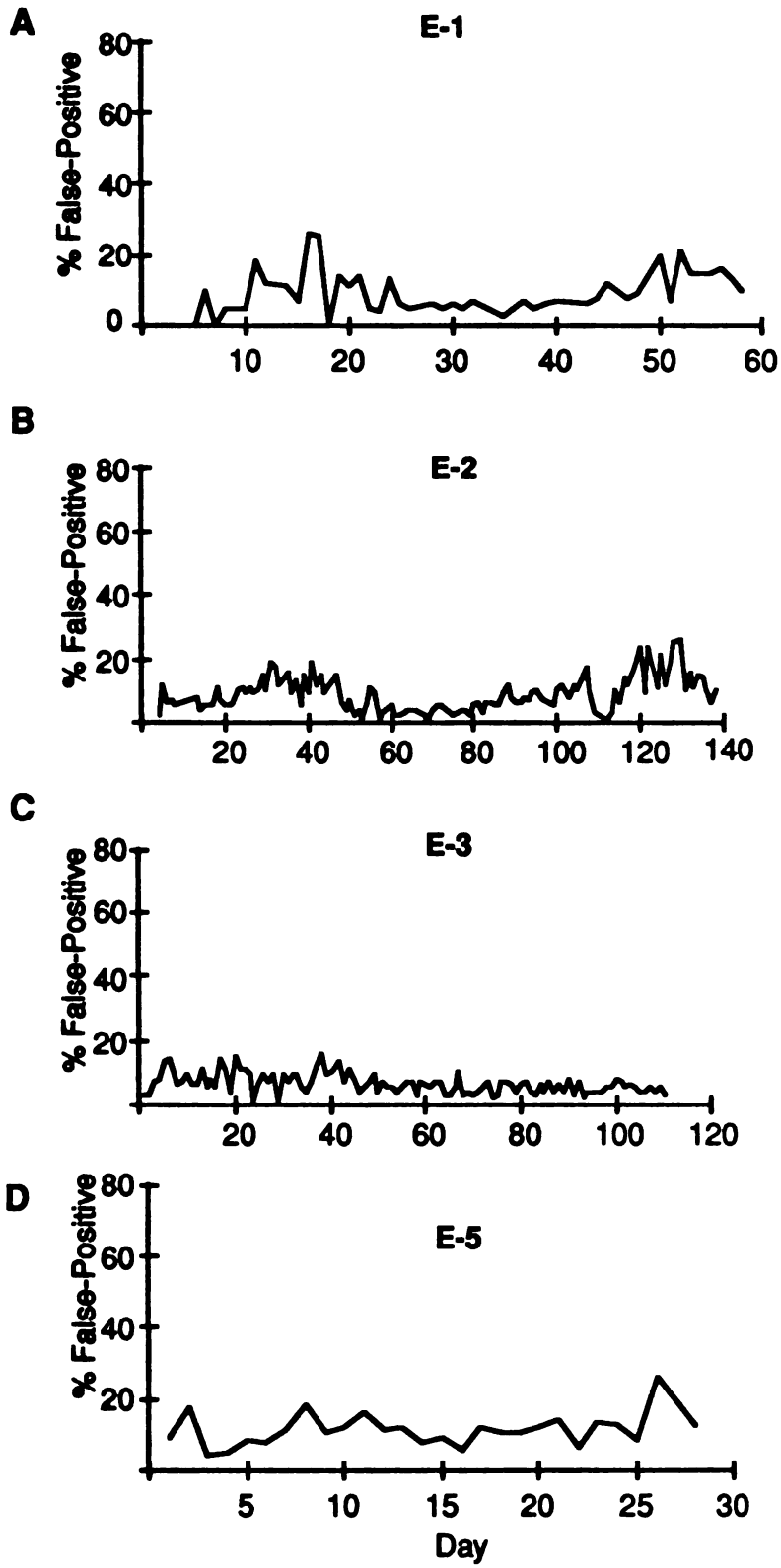

Figure 7. False-Positive rate as a function of consecutive days of training. Each plot is from a different animal which showed improvement in performance with training. Monkey number is denoted in bold type.

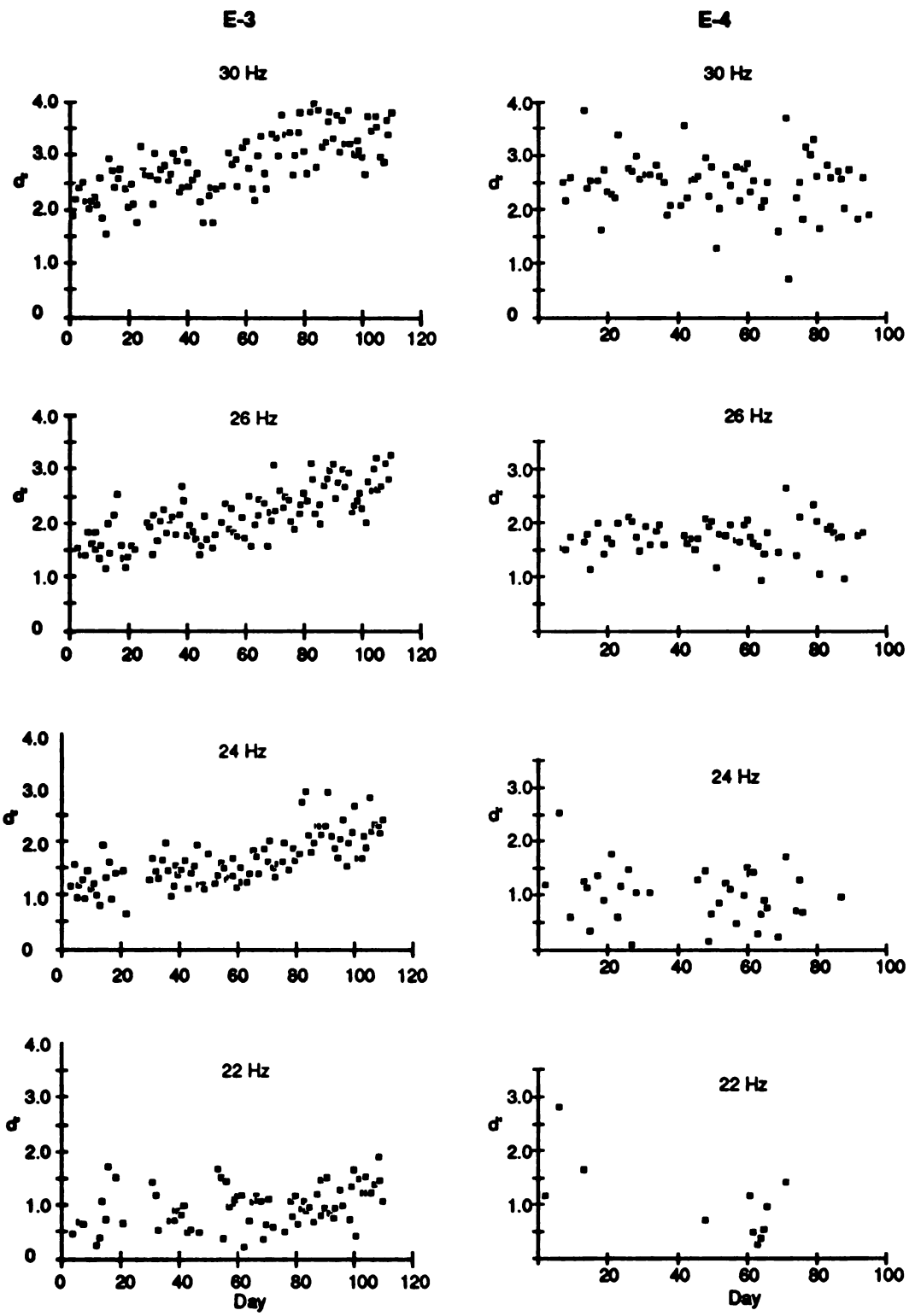

Figure 8. Values of d' calculated from the behavioral data of monkey E-3 (left) and E-4(right) for four different S2 frequencies. d' values of 1.0 represent 1 standard deviation unit.

increase in the frequency discrimination acuity of these trained monkeys. In contrast, the d' values calculated for animal E-4 remained relatively constant across sessions (Figure 8B). The performance functions of this one animal did not steepen with training (Figure 6A). Although some minor improvement could be demonstrated for discrimination of 26 Hz, that improvement was not reflected in changes in the d' values, as was seen for the other four trained animals. This evidence supports the conclusion that frequency discrimination acuity did not improve despite extensive training in this one monkey, animal E-4.

Control Experiments

Several control experiments were performed for each animal to insure that a) the monkey was discriminating the frequency of the tactile stimulus, and b) only the same small region of skin was stimulated each trial. To insure that the performance was not effected by small variations in intensity, the amplitudes of the sinusoidal stimuli presented during a session was periodically increased. One such control of this class is presented in Figure 9. The performance functions at the normal peak-to-peak displacement of 300 μm are shown superimposed with one having 600 μm displacement in this representative example. This difference in stimulus amplitude was perceived as a robust difference in intensity to a human observer. As seen in Figure 9, the performance functions and the calculated threshold are virtually identical under these two conditions of intensity. The independence of behavioral performance with stimulus amplitude, tested over a substantial amplitude range around that used in the training, was observed in all monkeys studied. On the basis of these control experiments it was concluded that intensity effects in this behavioral apparatus and paradigm were negligible.

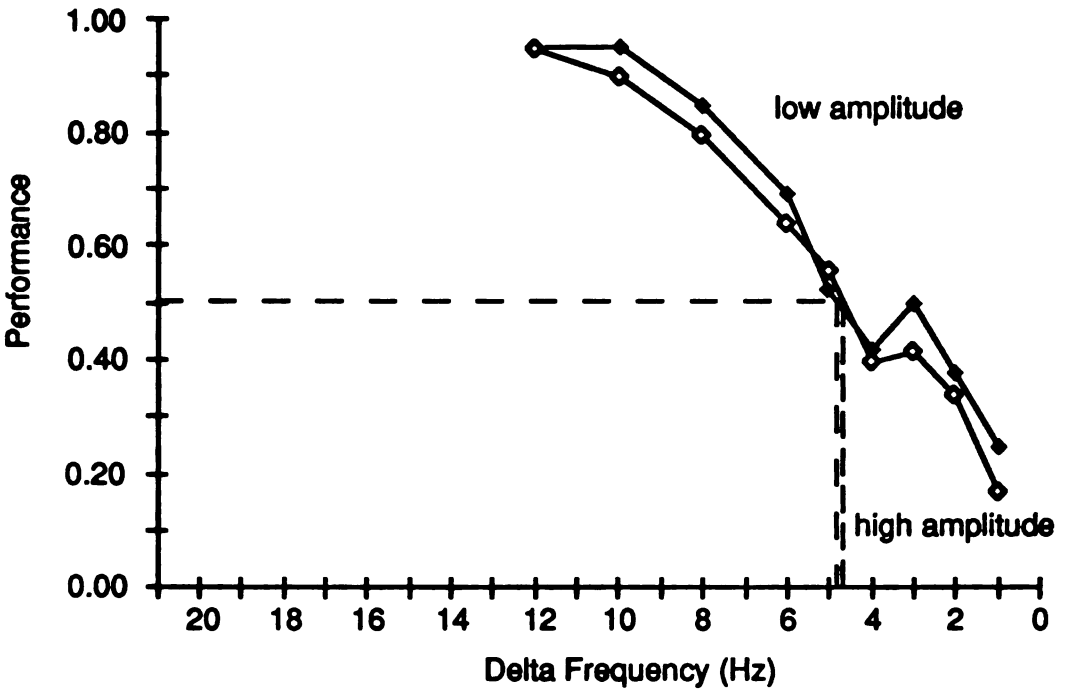

Figure 9. Performance functions of one animal under two conditions of stimulus amplitude. The performance function at a stimulus amplitude of 600 μm peak-to-peak displacement is shown as open diamonds (high amplitude) and the performance function at a stimulus amplitude of 300 μm peak-to-peak displacement is shown as filled diamonds (low amplitude). Dashed lines represent the 50% performance level.

A second concern was the animal's potential ability to move the stimulus probe to a slight degree during the trial. Human observers noticed that pressing the stimulus probe against the hand mold could result in vibration of the entire mold. Although care was taken to ensure that the probe was not in contact with the mold at the start and completion of each session, and visual monitoring of the hand placement behavior did not indicate the animal was moving the probe, we could not be absolutely certain there was never such contact within a given session. Thus, for each animal we purposefully abutted the stimulus probe against the mold in a limited number of trials, creating a clear vibratory cue for the animal. Two examples are shown in Figure 10. The performance during one of these sessions in which the vibration cue was present (digit and mold) is compared to the performance in which the probe did not contact the mold on the previous (Part A) or next (Part B) session (digit only). The psychometric functions were very similar in both conditions. This result indicates that possible signal enhancement attributed to the animal occasionally moving the probe onto the mold was behaviorally inconsequential.

Animals trained in the auditory discrimination task used the same apparatus, including the same hand mold, as did monkeys performing the tactile discrimination task. These animals were not required to discriminate differences in any aspect of the tactile stimulus to obtain a reward. One simple control to ensure they were not attending to the tactile stimulus was to turn the tactile stimulus off for a short period during a session. A typical performance function for an animal discriminating a 8 kHz tone in the presence (open symbols) and absence (filled symbols) of the tactile stimulus is shown in Figure 11. It is clear that the simultaneous presentation of the tactile stimulus had no

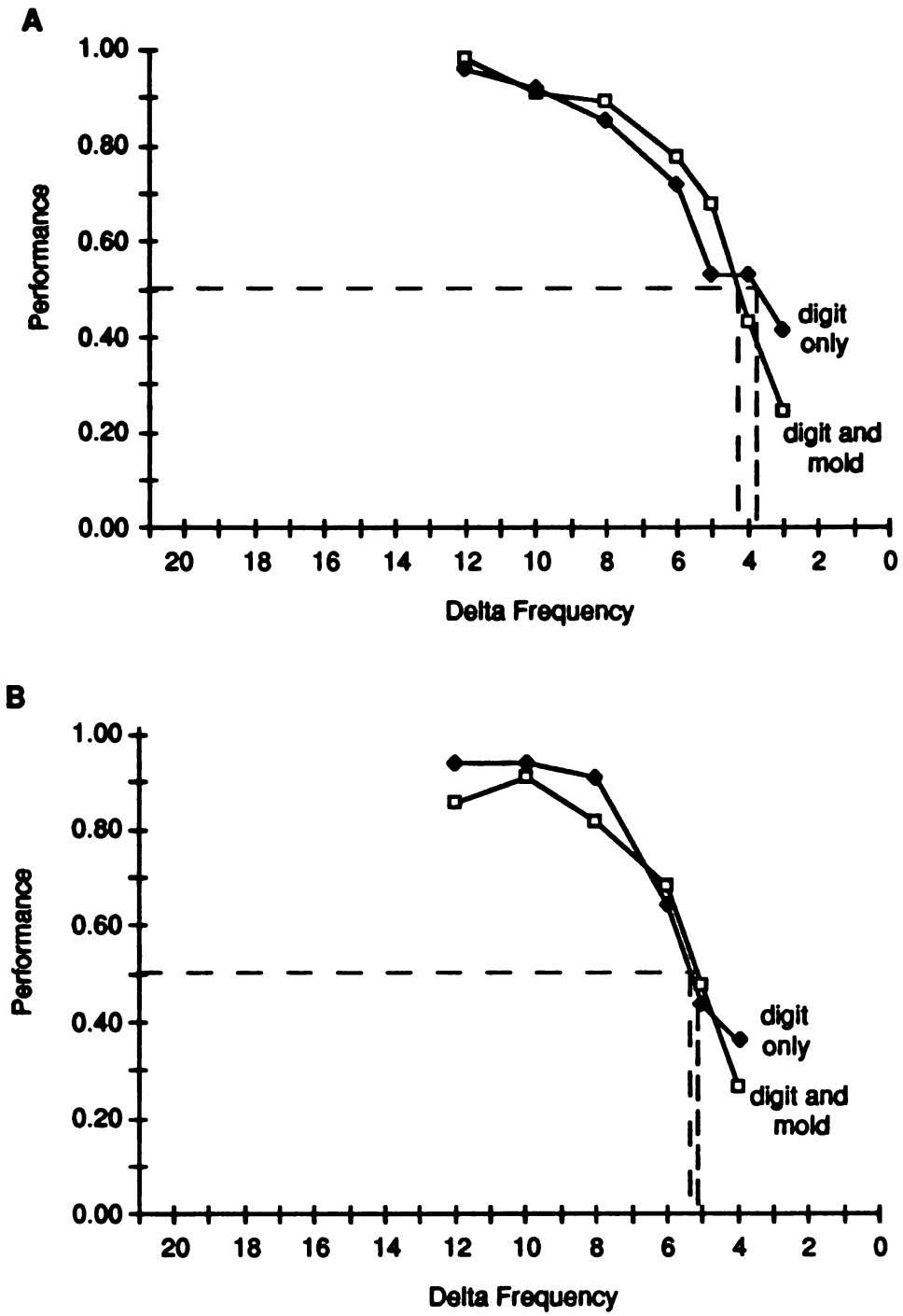

Figure 10. Performance functions from one monkey at two different periods under two different stimulus conditions. Filled diamonds show the performance when the stimulus probe only contacted the skin (digit only). Open squares show the performance when the stimulus probe was deliberately abutted against the hand mold which resulted in the vibration of the entire mold (digit and mold). Performance functions in parts A and B were taken with seven training sessions between them. Conventions as in previous figures.

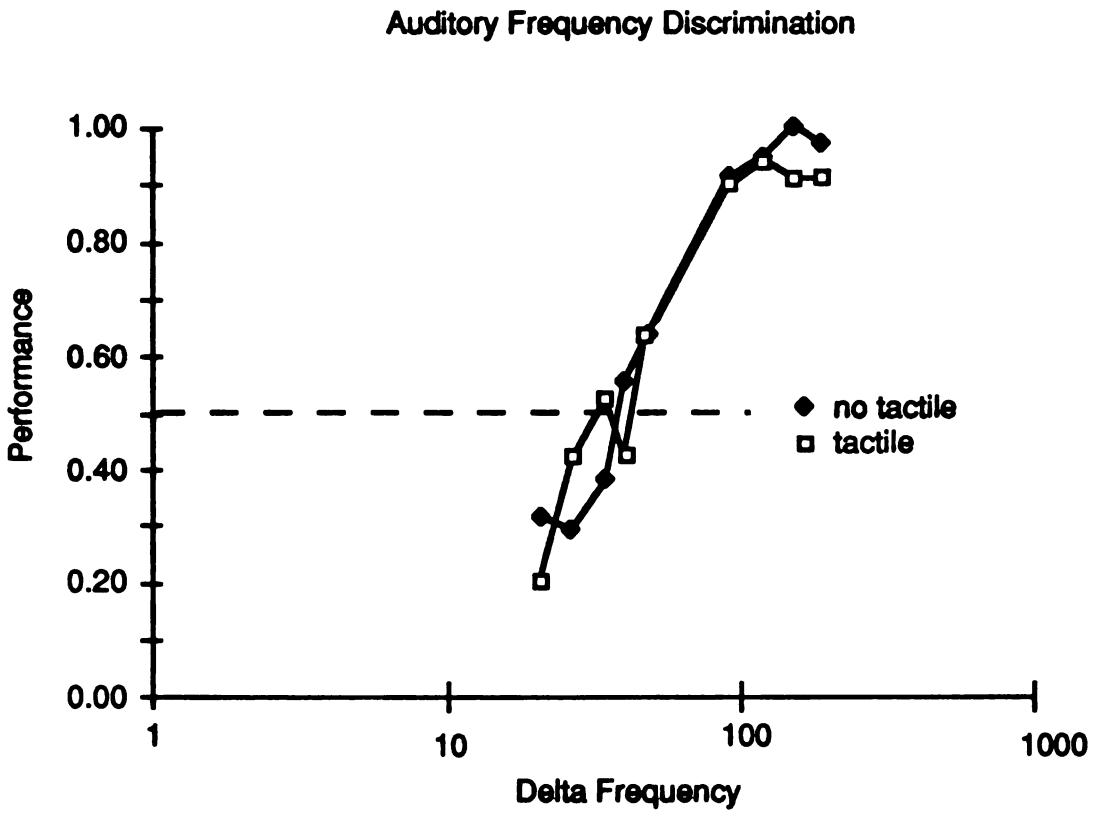

Figure 11. Performance functions of an auditory discrimination animal in the presence of (open squares, tactile) and the absence of (filled diamonds, no tactile) the tactile stimulus. This animal was trained to discriminate the frequency of an auditory stimulus compared to an 8 kHz standard. Delta frequency is plotted on a logrithmic scale.

substantial influence on this animal's behavior. The same finding was made in the other two auditory control animals.

In summary, there was an improvement in performance to stimulation of the digit which was trained for several weeks at the tactile frequency discrimination task in four out of five animals. The improvement varied between individual animals in time course and initial discriminability. The frequency discrimination thresholds measured on the session immediately prior to the electrophysiology experiments were similar among animals, as were the general shapes of the psychometric functions. The performance on the unstimulated digit also improved, but never to the same extent as for the stimulated and trained digit. The Signal Detection Theory analysis of d' and False-Positive rates were consistent with a true increase in acuity and not with changes in criteria in four of the five animals. However, criteria changes could account for the differences in performance for one animal, E-4, whose frequency discrimination performance did not improve despite extensive training and tactile stimulation.

ELECTROPHYSIOLOGY

Electrophysiological experiments were designed to determine the consequences of the discrimination training in somatosensory cortical fields 3a and 3b. They were specifically directed toward determining the neural correlates of the improvement in performance with training. Results are presented by comparing the cortical representation of the trained digit skin with the representation of five classes of controls: 1) The cortical representation of an adjacent finger on the same hand. This digit was also tested psychophysically (open symbols, Figure 2). 2) The cortical representation of the homologous

(same) digit on the contralateral hand. 3) The representation of the adjacent digit on the contralateral hand. 4) The representation of the digit stimulated in the passive-stimulation (auditory discrimination) controls. And 5) The representation of the adjacent digit in the passive-stimulation control group. The cortical representation of the trained digit was thus compared with the representations of 1) digits that had never been stimulated in the behavioral paradigm, 2) digits that were untrained but in which the behavioral threshold was defined, and 3) digits that were stimulated at the same regime but in which the tactile stimulus was behaviorally irrelevant.

The following nomenclature is adopted: The cortical representations of the hands stimulated in the experimental animals will be designated as "EE" with the corresponding animal number. The opposite "control" hemispheres that represent the untrained hand of these same animals are designated "EC". Thus, the hemisphere representing the trained hand in monkey E-1 is designated "EE-1" whereas the representation of the opposite, untrained hand is designated "EC-1". The cortical representations of the stimulated hand in the passive-stimulation control animals are designated "PS". The opposite hemispheres representing the non-passively-stimulated hand are designated as "PC". The cortical representation of the trained hand in the one animal that did not show an improvement in performance with training is designated "ED-4".

Cortical representational "maps"

Cortical mapping data reported in this study was derived in both cortical areas 3a and 3b. The definition of non-cutaneous receptive fields, recorded predominantly in area 3a of control hemispheres, was only rudimentarily

documented and will not be described. This report will focus on the changes in the cutaneous representation of the hand in these two cytoarchitectonically distinct areas.

The cortical representation of the hand in the hemispheres contralateral to the trained hands are shown in Figures 12-15. In these figures, Part A represents the electrode penetration locations as large dots and Part B illustrates the hand surface representations reconstructed from the receptive field locations. Rostral is upward in all illustrations. Thin lines denote boundaries of representation of different digits or digit segments. The representation of the palmar pads were only partially reconstructed and are labeled 'Pads'. Stippled areas denote areas representing the hairy skin of the hand and digits. The heavy line represents the physiologically defined border between areas 3a and 3b. Areas labeled 'NCR' (no cutaneous response) did not respond to cutaneous stimulation but were responsive to taps to the digits, stimulation of deep structures, or joint movement. Microelectrode locations where neurons responded to cutaneous stimulation of the glabrous hand are denoted by heavy cross-hatching; those responding to the hairy skin are denoted by stippling, as in area 3b. Area 3a is discussed in detail below.

Figure 16 shows the representation of the stimulated hand for animal ED-4, which did not show an improvement in performance with practice.

Figures 17-20 show the penetration sites and reconstructions for the control hemispheres from these same animals. The control hemisphere in animal E-5 was not investigated. The representations of the hand in these animals were essentially normal, and did not show any obvious differences in topography

Figures 12-16. Cortical representational "maps" of the stimulated hand in trained owl monkeys. In all figures the filled circles denote electrode penetration sites (Part A). These locations were marked on the 40X image of the cortical surface to correspond to the electrode location relative to the surface cortical vasculature (not shown). The thick line denotes the physiologically defined border between areas 3b and 3a. The medium lines denote boundaries of representation between individual digits, the thinnest lines denote boundaries of representation between the different segments within a single digit (Part B). d:distal phalange, m: middle phalange, p: proximal phalange, s: skin between middle and proximal phalange, stimulated in case EE-2. Bold type denotes the digit (D1=thumb, D5= little finger). "Pads" denote cortical locations with receptive fields on the palmar pads. "NCR" denote cortical locations without a cutaneous receptive field. Stippled areas bound cortical locations with receptive fields on the hairy skin of the digits or hand. Cross-hatched areas bound cortical locations with cutaneous receptive fields rostral of the area 3b-3a border. In all figures illustrating cortical maps, rostral is upward. Scale is 500 μm (horizontal) and 250μm (vertical). Figure 12 represents monkey E-5, digit 2 trained; Figure 13: monkey E-1, digit 3; Figure 14: monkey E-2, digit 3; Figure 15: monkey E-3, digit 4; Figure 16: monkey E-4, digit 3 stimulated.

Figure 12

EE-5

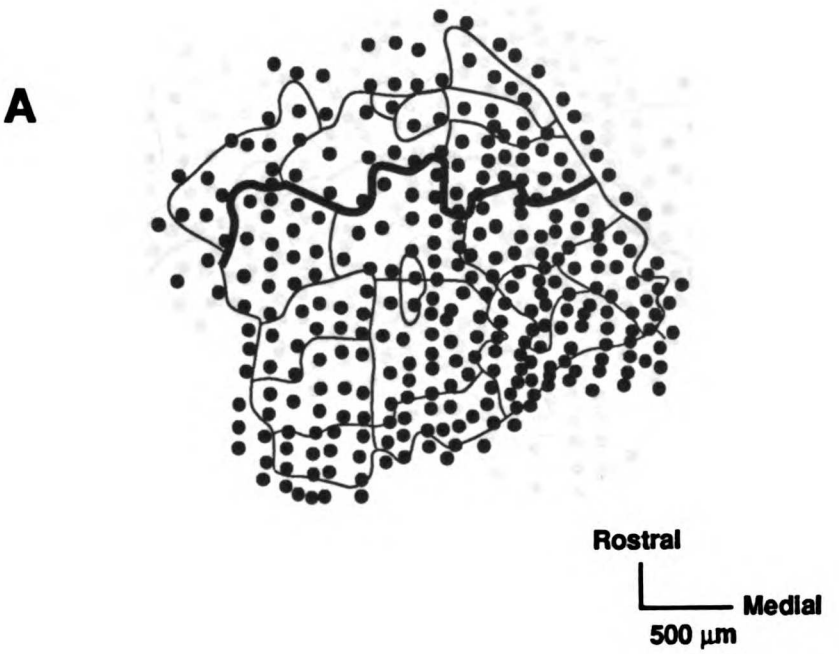

Figure 13

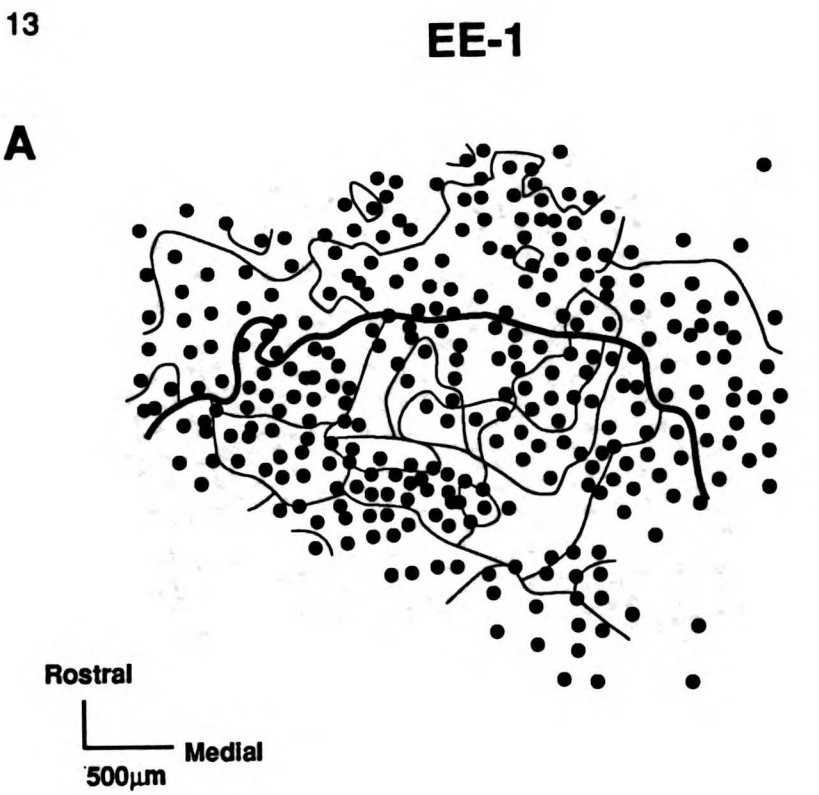
EE-1
A
Rostral
Medial
500μm
B
Penetration Sites
Hairy Skin
Area 3a Glaborous and Cutaneous
NCR Non-cutaneous / Deep Responses Only

Figure 14

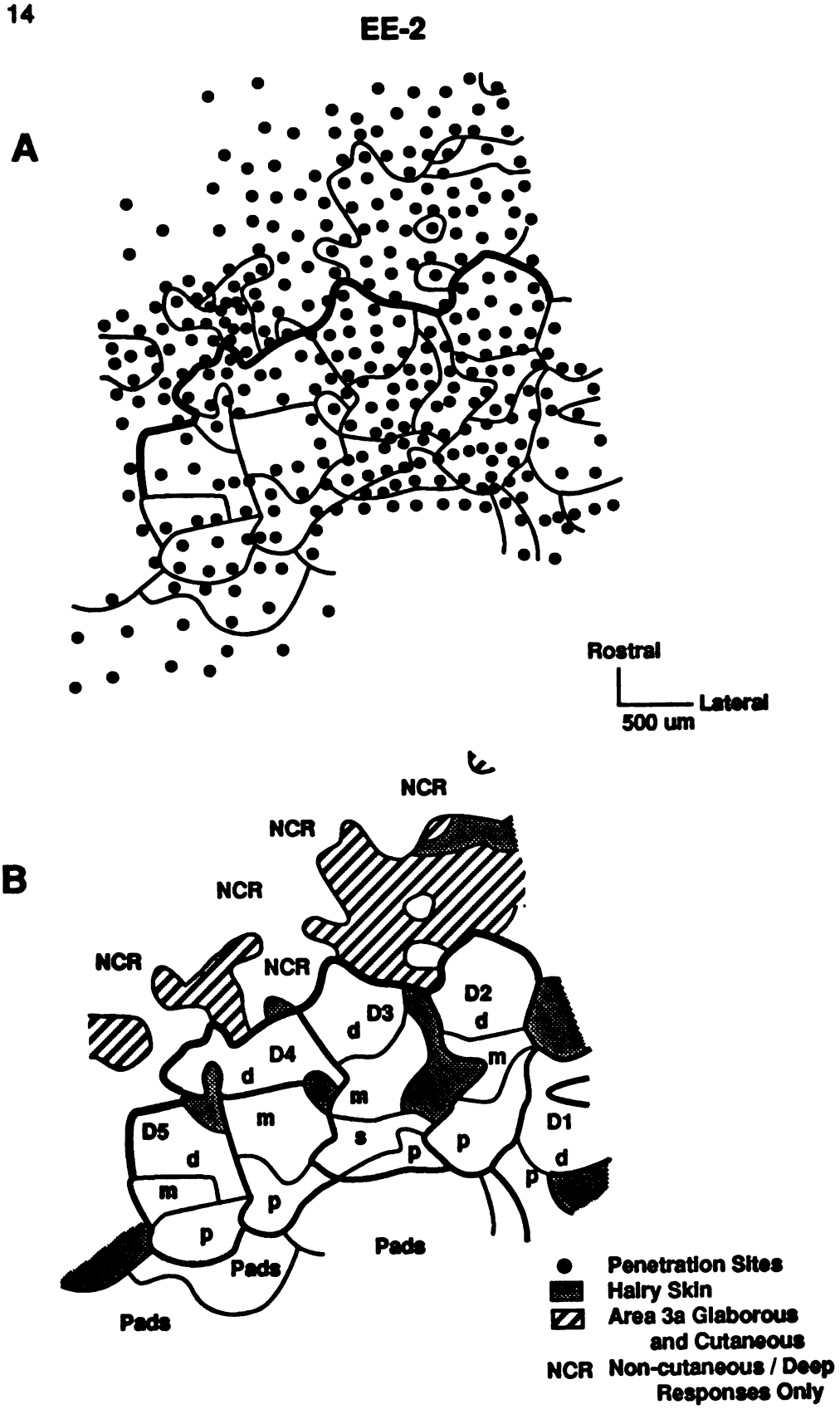
EE-2
A
Rostral
Lateral
500 um
B
NCR
NCR
NCR
NCR
NCR
D2
d
D3
d
D4
d
m
m
m
D5
d
m
s
p
p
D1
d
p
p
p
p
Pads
Pads
Pads
Penetration Sites
Hairy Skin
Area 3a Glaborous and Cutaneous
NCR Non-cutaneous / Deep Responses Only

Figure 15

EE-3

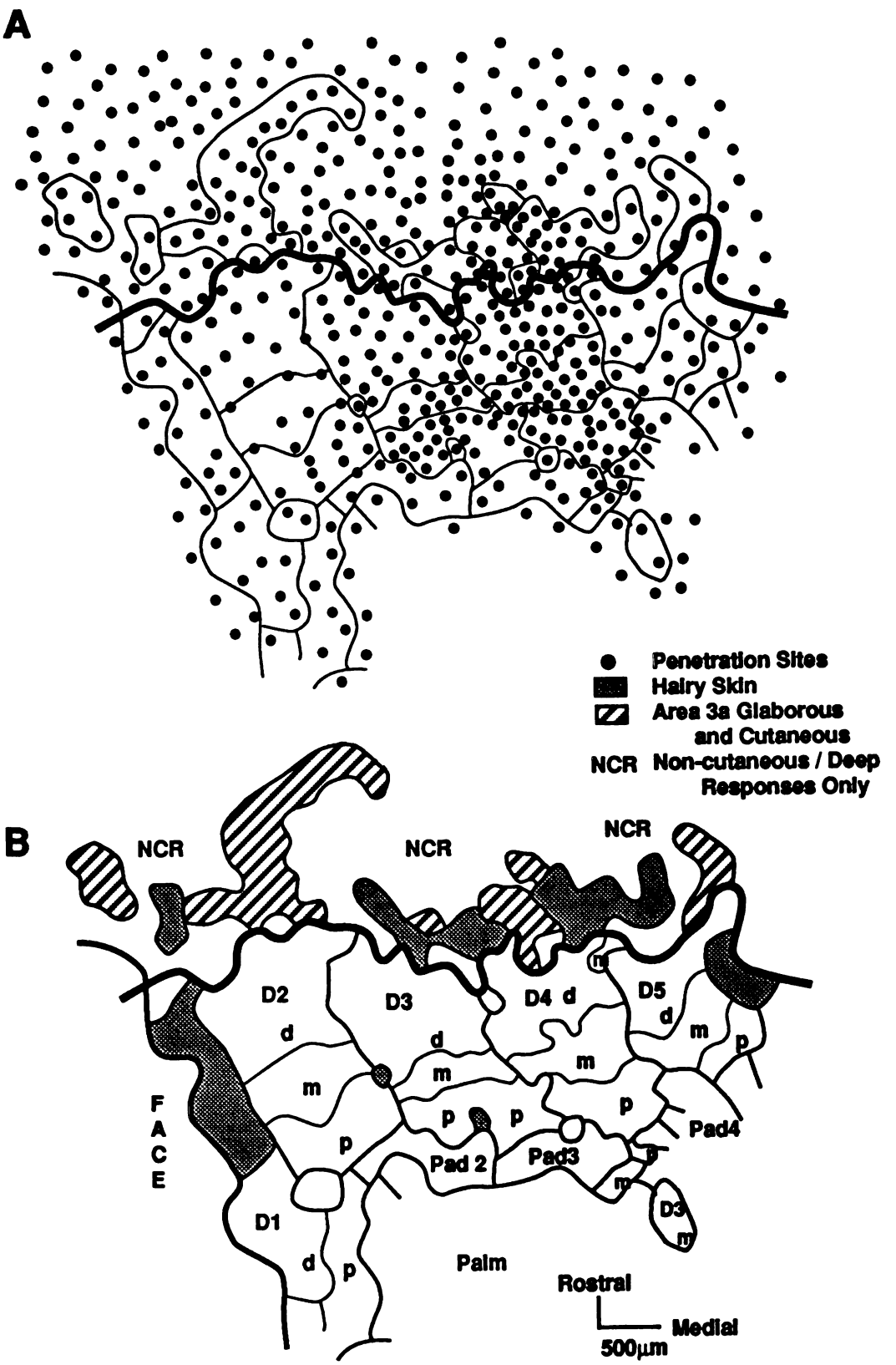

Figure 16

ED-4

A

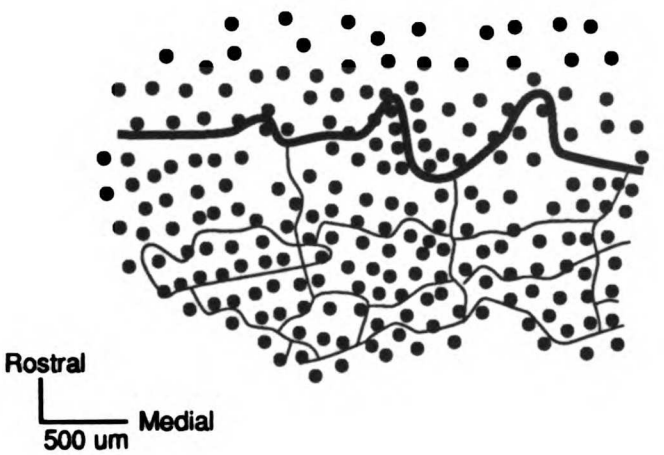

B

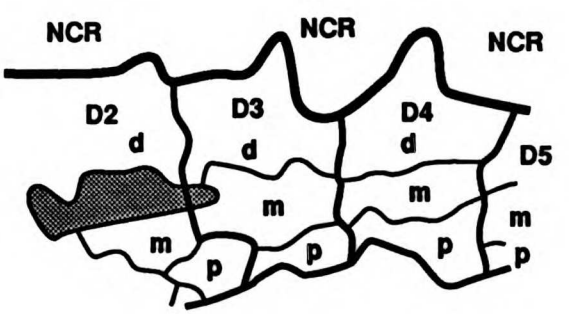

● Penetration Sites
▩ Hairy Skin
▨ Area 3a Glaborous and Cutaneous
NCR Non-cutaneous / Deep Responses Only

Figures 17-20. Cortical representational maps from the control hemispheres representing the untrained hand. Conventions and abbreviations are as in Figures 12-16. Representations from animals E-1, E-2, E-3 and E-4 are illustrated in Figures 17-20, respectively. See text for discussion.

Figure 17

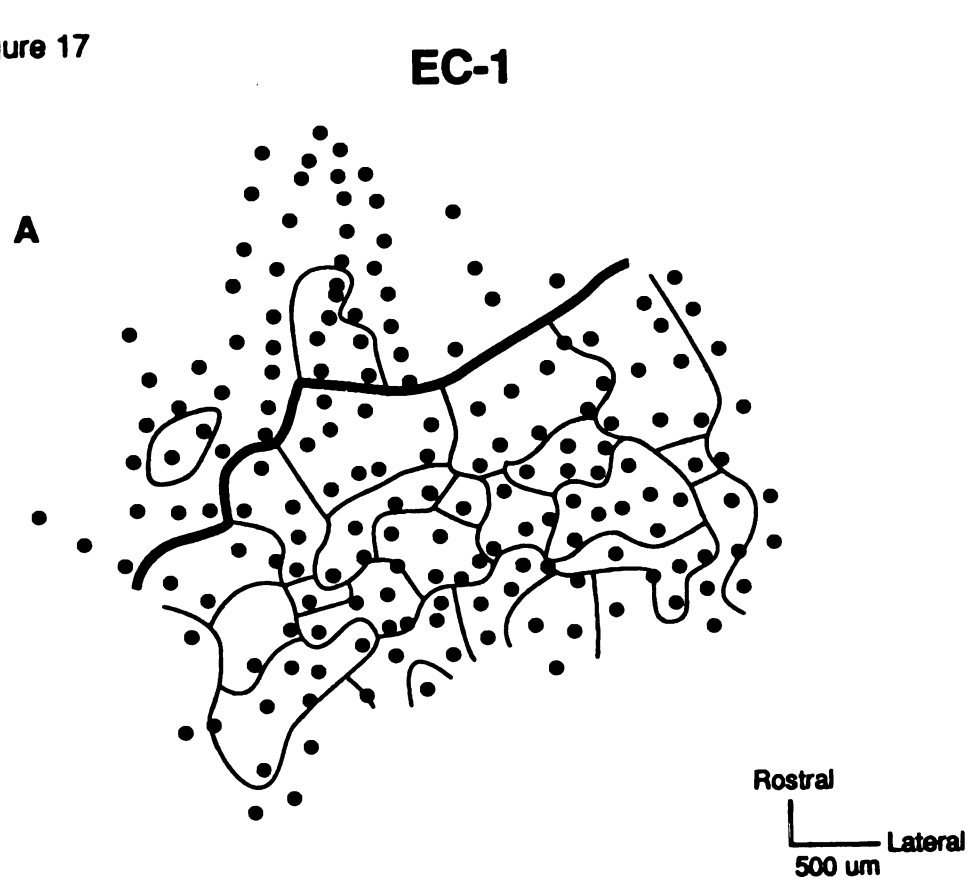
EC-1
A
Rostral
Lateral
500 um
B
NCR
NCR
D3 d
D2 d
m
F
A
C
E
D4
d
m
p
D1
d
D5 d
p
m
p
p
m
PADS
PADS
p
PADS
Penetration Sites
Hairy Skin
Area 3a Glaborous and Cutaneous
NCR Non-cutaneous / Deep Responses Only

Figure 18

EC-2

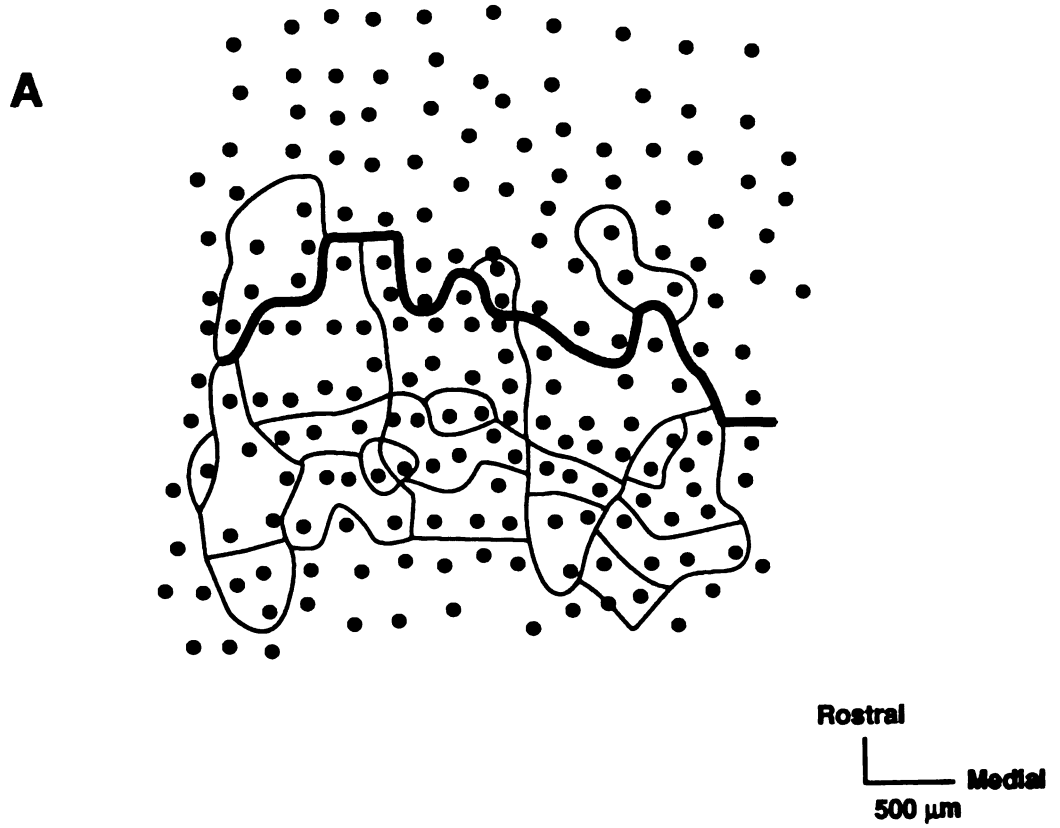

Figure 19

EC-3

A

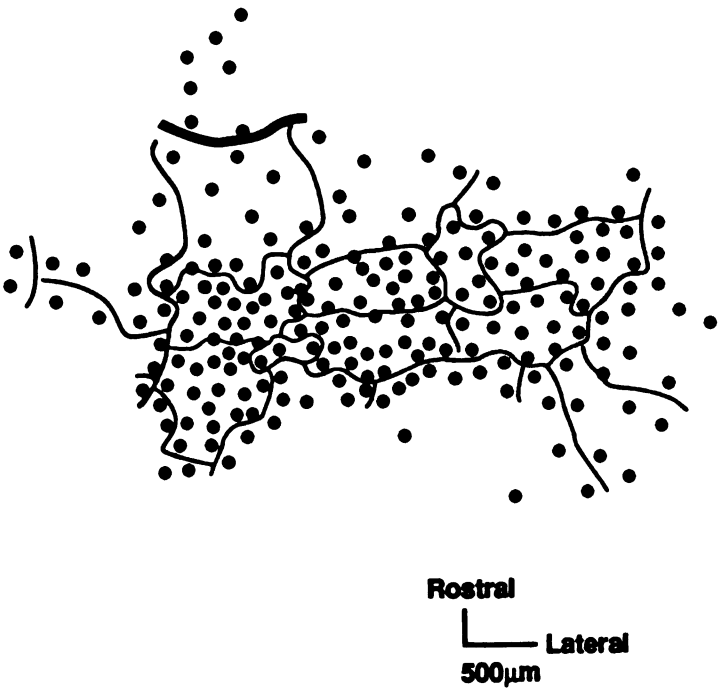

B

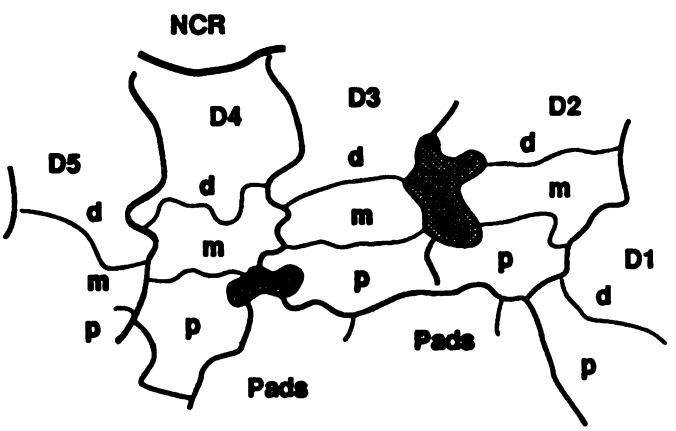

● Penetration Sites
▓ Hairy Skin
▨ Area 3a Glabrous and Cutaneous
NCR Non-cutaneous / Deep Responses Only

Figure 20

EC-4

A

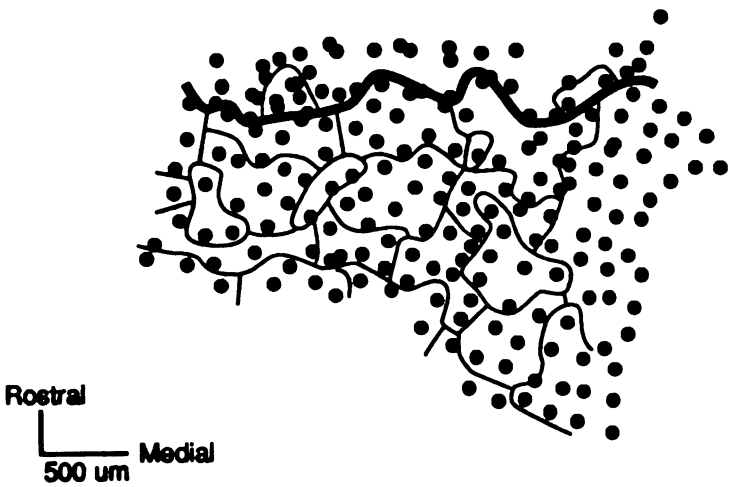

B

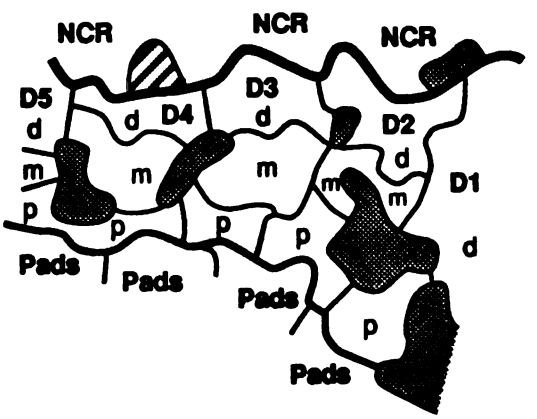

● Penetration Sites
Hairy Skin
Area 3a Glaborous and Cutaneous
NCR Non-cutaneous / Deep Responses Only

1978, 1987). The large cutaneous representation recorded in all experimental hemispheres were not recorded in any of these control hemispheres. Figures 21-23 show the representation of hands that were stimulated tactually during the performance of an auditory discrimination task. These animals had tactile stimulation histories that were equivalent to those of the experimental animals, but the tactile stimulus had no behavioral significance. These cortical representations also appeared to be normal in their topographies and did not have a large cutaneous representation in area 3a. The representation of the unstimulated hand in one passive-stimulation control animal (P-1) is shown in Figure 24.

One distinction of the experimental hemispheres was that the representation of the hand was more complex in the details of topography than in control hemispheres. In each experimental hemisphere there were subtle discontinuities within the representation of the individual digits that were not observed in the hemispheres representing the opposite, control hand. For example, in case EE-5 (Figure 12) the representation of the proximal phalange of digit 2 was nearly bisected by the representation of the middle phalanx of the same digit. Case EE-1 (Figure 13), had a split representation of the middle phalange of digit 3, no representation of the middle phalange of digit 2, and the representation of the middle phalange of digit 4 was not located between the proximal and distal phalanges. Case EE-2 (Figure 14), had a large representation of the skin centered on or near the proximal-middle phalangeal joint of digit 3. This region of skin was stimulated in the behavioral task and is labeled 'S'. Finally, case EE-3 (Figure 15) had two discontinuous 'islands' of representation of the middle phalanx of digit 4, one was located caudally

FIGURES 21-24. Cortical representational maps of passively-stimulated control monkeys. Animals P-2 and P-3 were only investigated thoroughly for digits 3 (stimulated) and 4 (adjacent) and are shown in Figures 22 and 23, respectively. Figure 21 is the stimulated hand from animal P-1. Figure 24 is the opposite, unstimulated hand from the same animal.

Figure 21

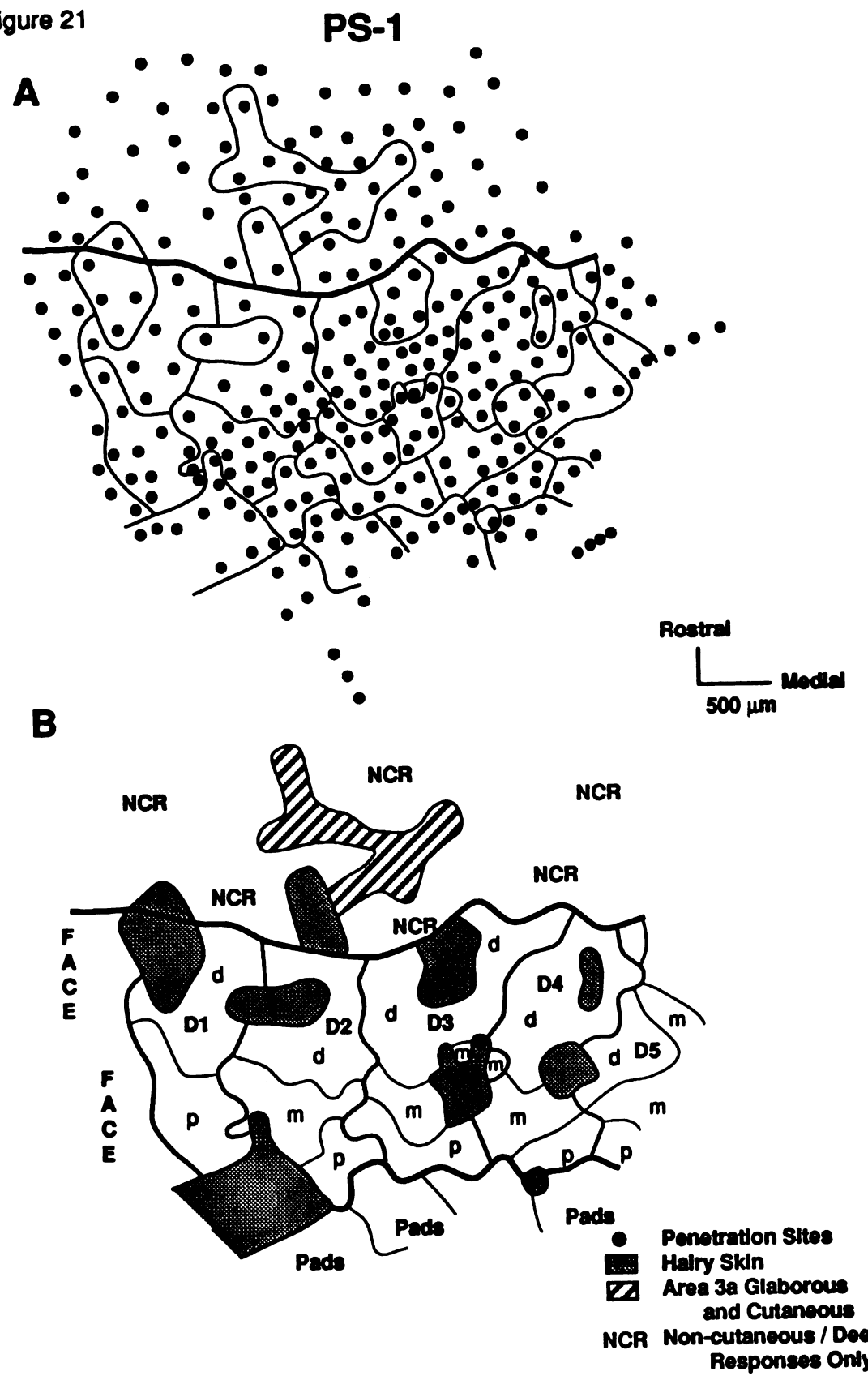
PS-1
A
Rostral
Medial
500 µm
B
NCR
NCR
NCR
NCR
NCR
NCR
FACE
FACE
D1
D2
D3
D4
D5
d
m
p
Pads
Pads
Pads
Penetration Sites
Hairy Skin
Area 3a Glaborous and Cutaneous
NCR Non-cutaneous / Deep Responses Only

Figure 22

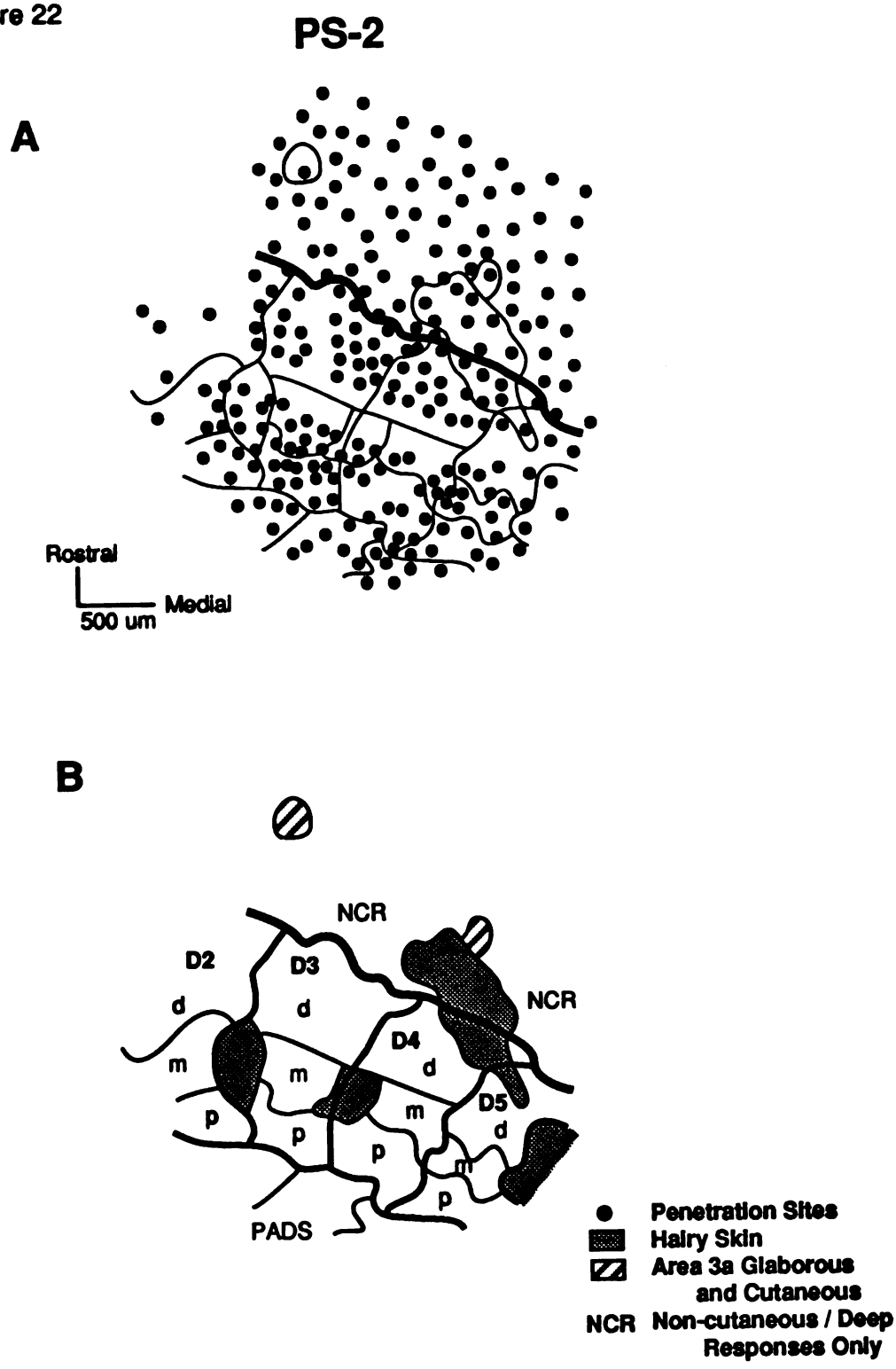
PS-2
A
Rostral
Medial
500 um
B
NCR
D2
D3
d
d
NCR
D4
d
m
m
D5
m
d
p
p
p
m
p
PADS
Penetration Sites
Hairy Skin
Area 3a Glaborous and Cutaneous
NCR Non-cutaneous / Deep Responses Only

Figure 23

PS-3

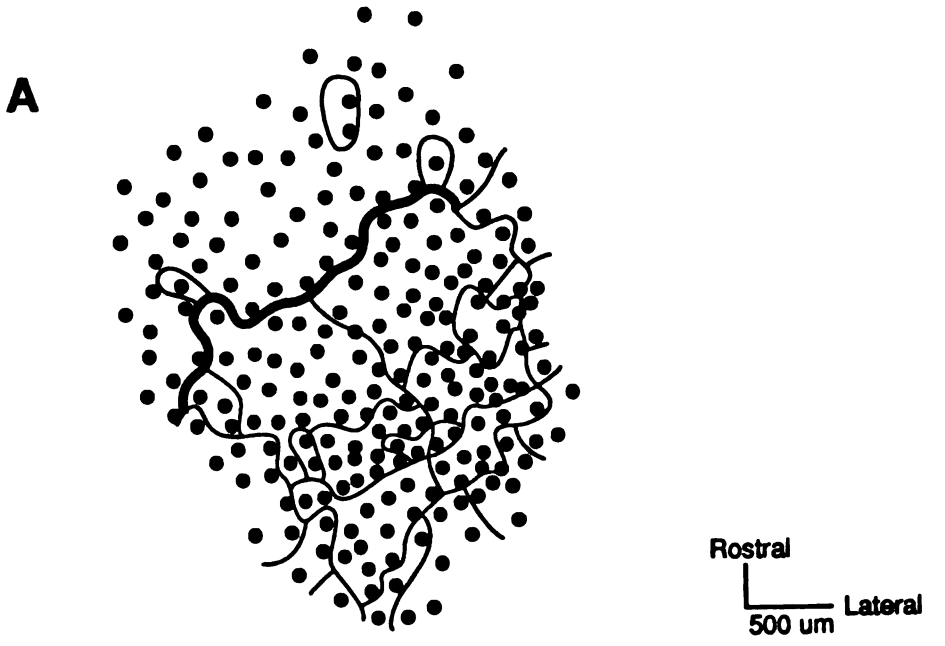

Figure 24

PC-1

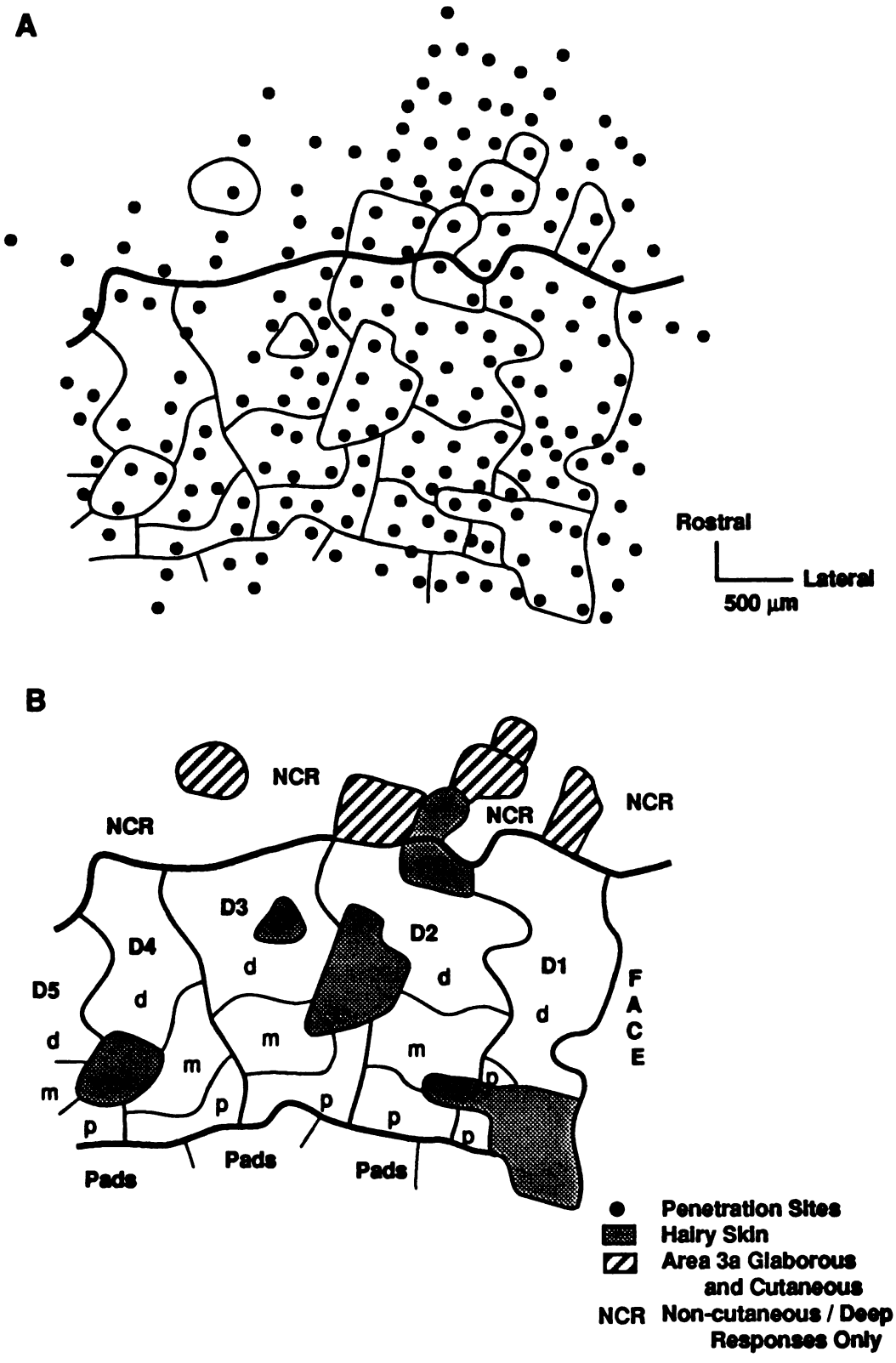

surrounded by the representation of the palmar pads, and the other was located distally, surrounded by distal digit representations and area 3a.

These anomalies of representation were recorded in a simpler form in the passively-stimulated control animals. Case PS-1 (Figure 21) had the representation of the middle phalanx of digit 3 split by the representation of the hairy skin. Case PS-3 (Figure 23) had a similar split in the middle phalangeal representation of digit 3 by hairy skin. The representations of the contralateral, unstimulated hands and the stimulated hand for the animal which did not improve performance (E-4) did not show any equivalent examples of such topographical anomalies. These representations were continuous and the receptive fields progressed in an orderly, topographic manner.

Areal representation of digits in area 3b

The total area of representation for each of the digits in which the entire extent of the digit representation was defined is shown in Figure 24. In each set of histograms, either the trained digit of experimental hands (Part A) or the stimulated digit of passively-stimulated hands (Part C) are highlighted by cross-hatching. The area of representation of any given digit is not appreciably different from the area of representation of any other digit of the same hand. In all cases the representation of any single digit was on the order of one square millimeter, a value consistent with other reports of normal digit representation of the adult owl monkey (Merzenich et al., 1984).

In summary, the topographic boundaries drawn between different digits and digit segments were more complex for the trained hemispheres when compared to the contralateral control hemispheres. Passive-stimulation hemispheres

FIGURE 25. Areas of representation of entire digits are presented as histograms for each case. Only the representations which were completely bounded by electrode penetrations with corresponding receptive fields beyond the digit were considered. Stippled bars denote digits which were not stimulated or trained. Cross-hatched bars denote digits which were trained (Part A), or stimulated in Passive-Stimulation control animals (Part C). Numbers at the bottom of each histogram denote the digit. Bold type denotes the hemisphere.

Figure 25

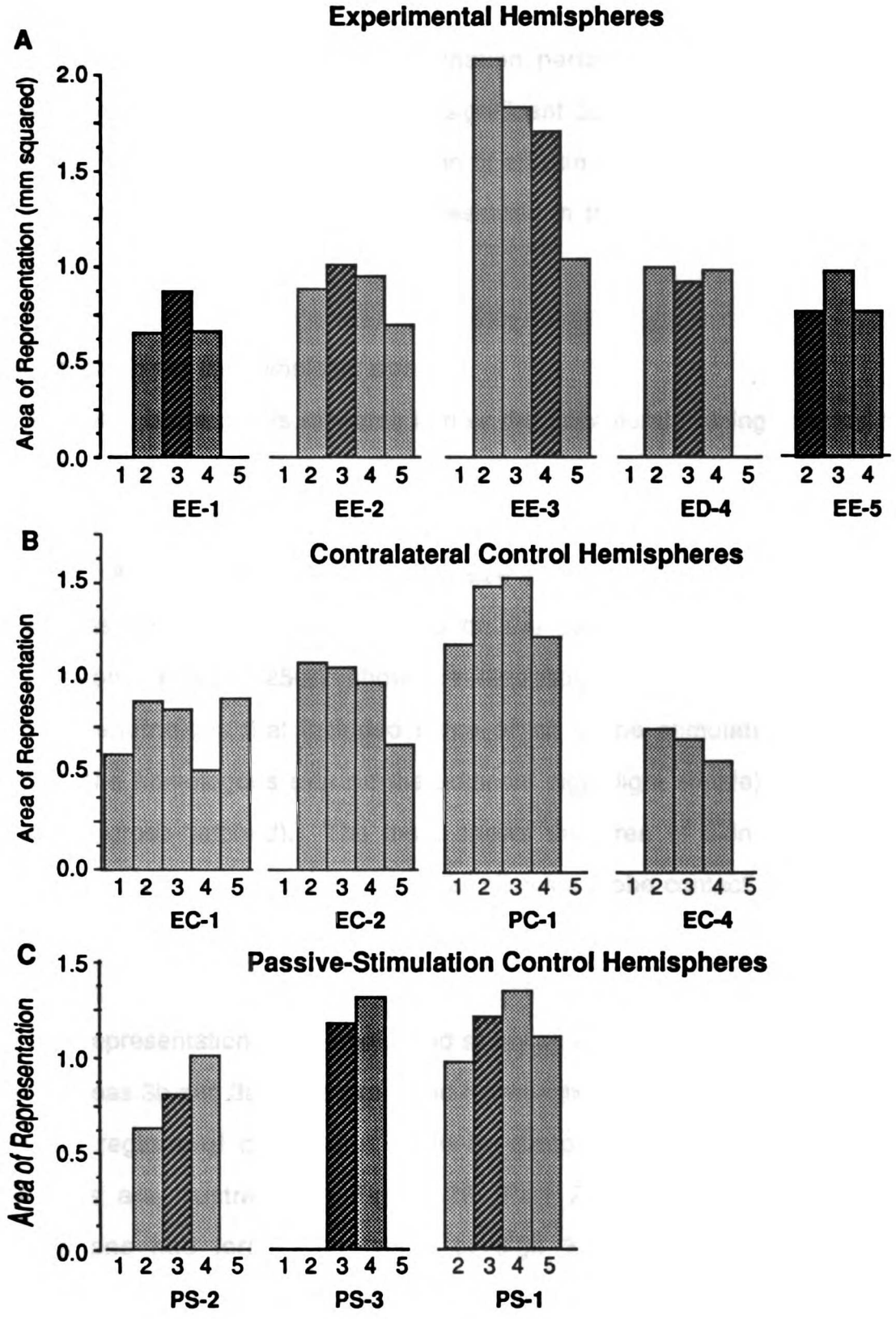
Experimental Hemispheres
A
Area of Representation (mm squared)
2.0
1.5
1.0
0.5
0.0
1 2 3 4 5
EE-1
1 2 3 4 5
EE-2
1 2 3 4 5
EE-3
1 2 3 4 5
ED-4
2 3 4
EE-5
B
Contralateral Control Hemispheres
Area of Representation
1.5
1.0
0.5
0.0
1 2 3 4 5
EC-1
1 2 3 4 5
EC-2
1 2 3 4 5
PC-1
1 2 3 4 5
EC-4
C
Passive-Stimulation Control Hemispheres
Area of Representation
1.5
1.0
0.5
0.0
1 2 3 4 5
PS-2
1 2 3 4 5
PS-3
2 3 4 5
PS-1

were intermediate in topographic complexity when compared to the contralateral control hemispheres and the experimental hemispheres. In all monkeys that improved their discrimination performance, the hemispheres representing the trained hand had a significant cutaneous representation in area 3a. The area of the representation of all skin surfaces of a single digit in area 3b was similar among digits represented in the same hemisphere in all cases.

Representation of the stimulated skin

A central issue of this research is how the behavioral training effected the cortical representation of the trained skin. This question was addressed by defining the cortical representation of the skin area stimulated during the behavior. A skin area of corresponding size and location on the adjacent digit as well as on the homologous digits on the control hands were used for comparison. Figures 25-27 show the reconstructed maps highlighting all cortical penetrations that included some or all of the stimulated skin (dark stipple), the homologous skin on the adjacent digit (light stipple) or both skin surfaces (cross-hatched). The inset shows the area of skin used in this analysis. This skin area encompasses all stimulus probe contact sites over the period measured (see *Methods*).

The representation of the stimulated skin was increased in trained monkeys in both areas 3b and 3a. This expanded representation was not restricted to the adjacent regions of cortex, but could be discontinuous, even in area 3b. Examples are illustrated in Figure 26 (Part A, case EE-1), where two penetrations had formed an island of digit 3 representation within the

representation of digit 2. Similar discontinuities occurred forming islands of representation rostrally (Figure 26A, B and D) as well as caudally (Figure 26C).

In control digits only a single electrode penetration was observed to separate two areas of representation (i. e. Figure 26B, 27C). In these hemispheres, the representation of the homologous skin occupied a very discrete region. This region was topographically aligned within the map, reflecting the orderly progression of receptive field locations encountered.

The reconstructions from the passive-stimulation control animals are shown in Figure 28. Discontinuities were recorded to a lesser extent in these hemispheres. For example, Figure 28B illustrates a discontinuity in the representation of the small skin area of both digit 3 (stimulated) and digit 4 (unstimulated). Similarly, Figure 28C illustrates a single penetration discontinuity for digit 2 (unstimulated). In all of the passive-stimulation control hemispheres the representations were small and were confined to a small area within the 'appropriate' region of 3b.

Finally, Figure 29 illustrates the representation of the stimulated and unstimulated hands for animal E-4, whose discrimination thresholds did not substantially improve with training. The stimulated hand (Part A) showed small discontinuities for both digits 2 and 4. The representation of the stimulated digit (digit 3) occupied a continuous area within the 3b representation. The unstimulated hemisphere (Part B), shows a smaller area of representation of these restricted skin regions for all three digits when compared to the representation of the stimulated hand.

FIGURES 26-29. Cortical representation of restricted skin regions. All cortical locations where the receptive field included any part of the skin region shown in the inset are denoted with heavy stippling (trained / stimulated/ homologous skin) or light stippling (skin of adjacent digit). Hatched regions denote cortical locations where the receptive field included some part of each of the two skin regions. Experimental cases EE-1, EE-2, EE-3 and EE-5 are shown in Figure 26 parts A-D, respectively. Opposite hemisphere control cases EC-1, EC-2, EC-3 and PC-1 are shown in Figure 27 A-D, respectively. Passive-Stimulation control hemispheres PS-2, PS-3 and PS-1 are shown in Figure 28 A-C, respectively. Monkey E-4 is shown in Figure 29.

Figure 26

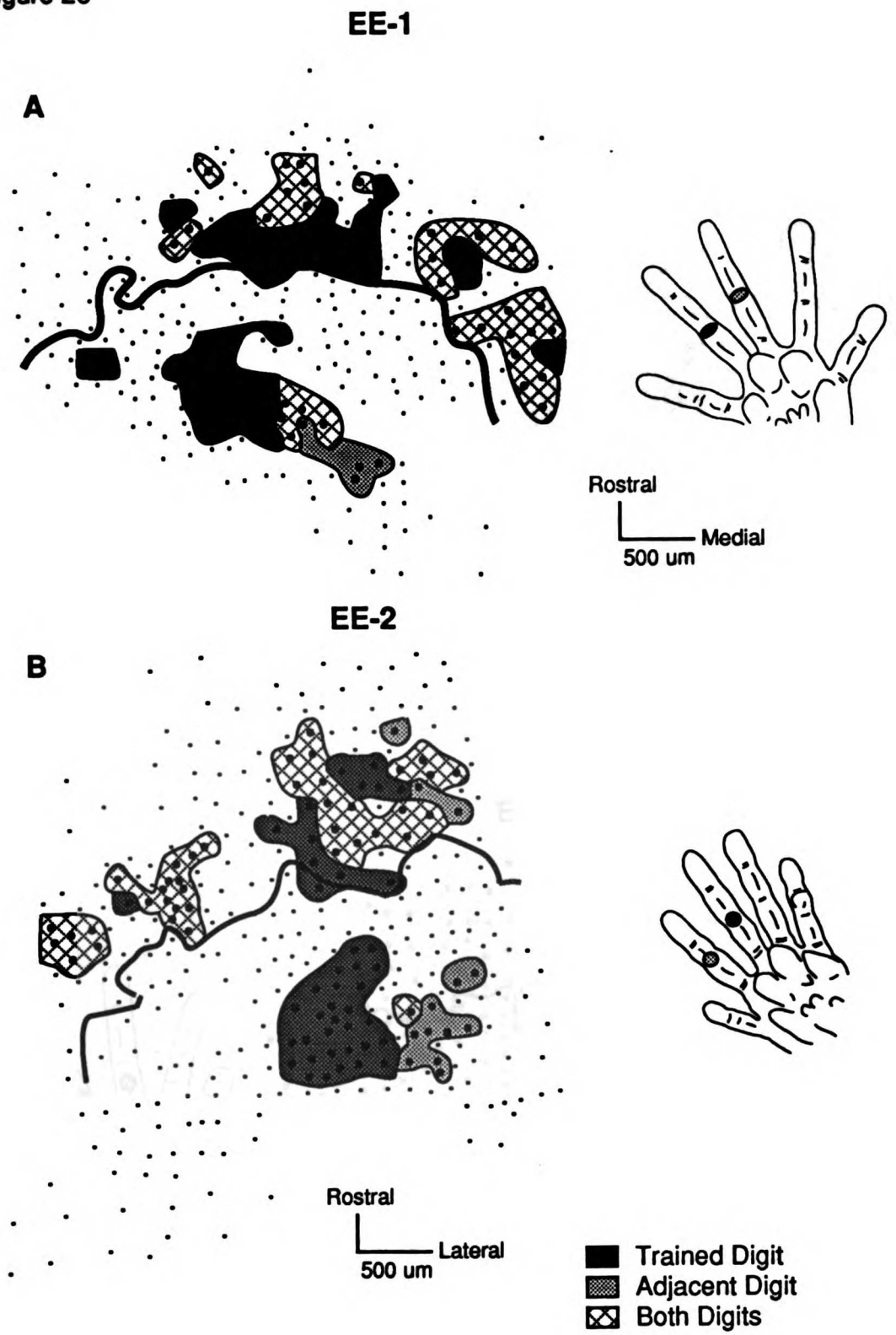
EE-1
A
Rostral
Medial
500 um
EE-2
B
Rostral
Lateral
500 um
Trained Digit
Adjacent Digit
Both Digits

Figure 26

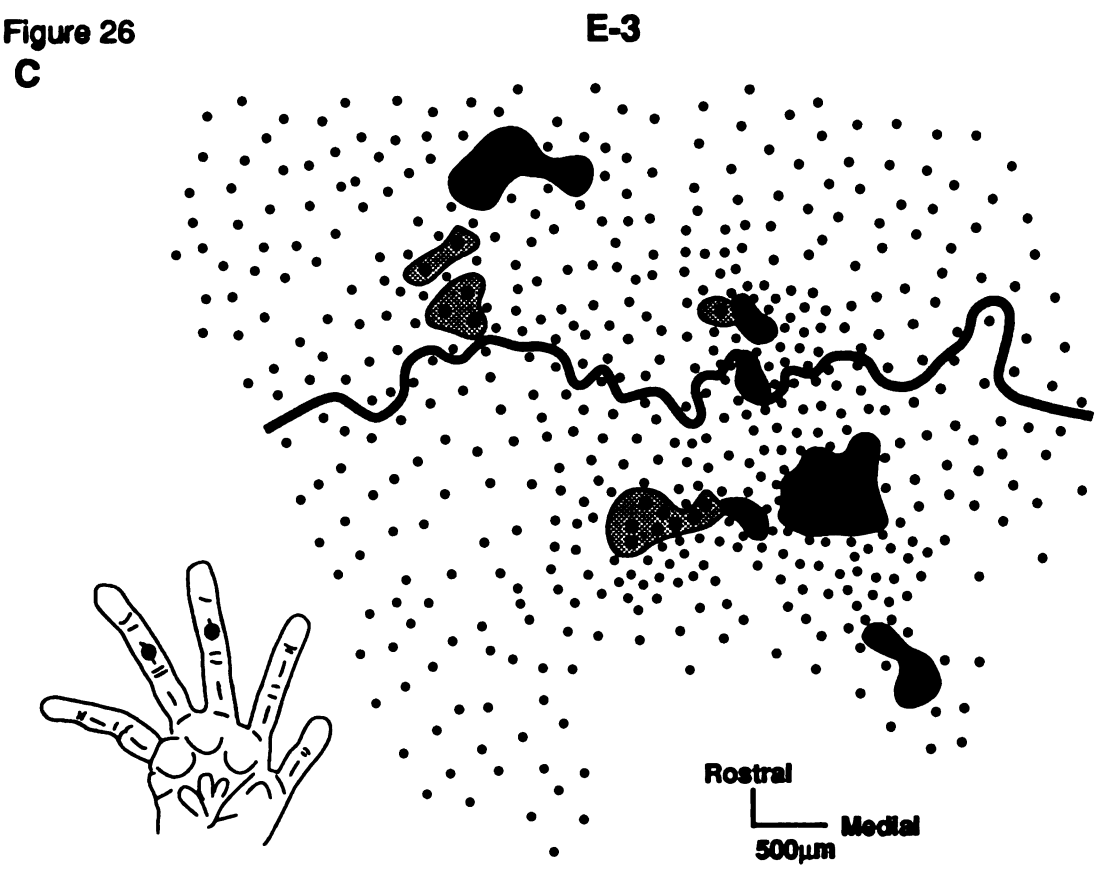
C
E-3
Rostral
Medial
500μm
D
E-5
Rostral
Lateral
500μm
Trained Digit
Adjacent Digit

Figure 27

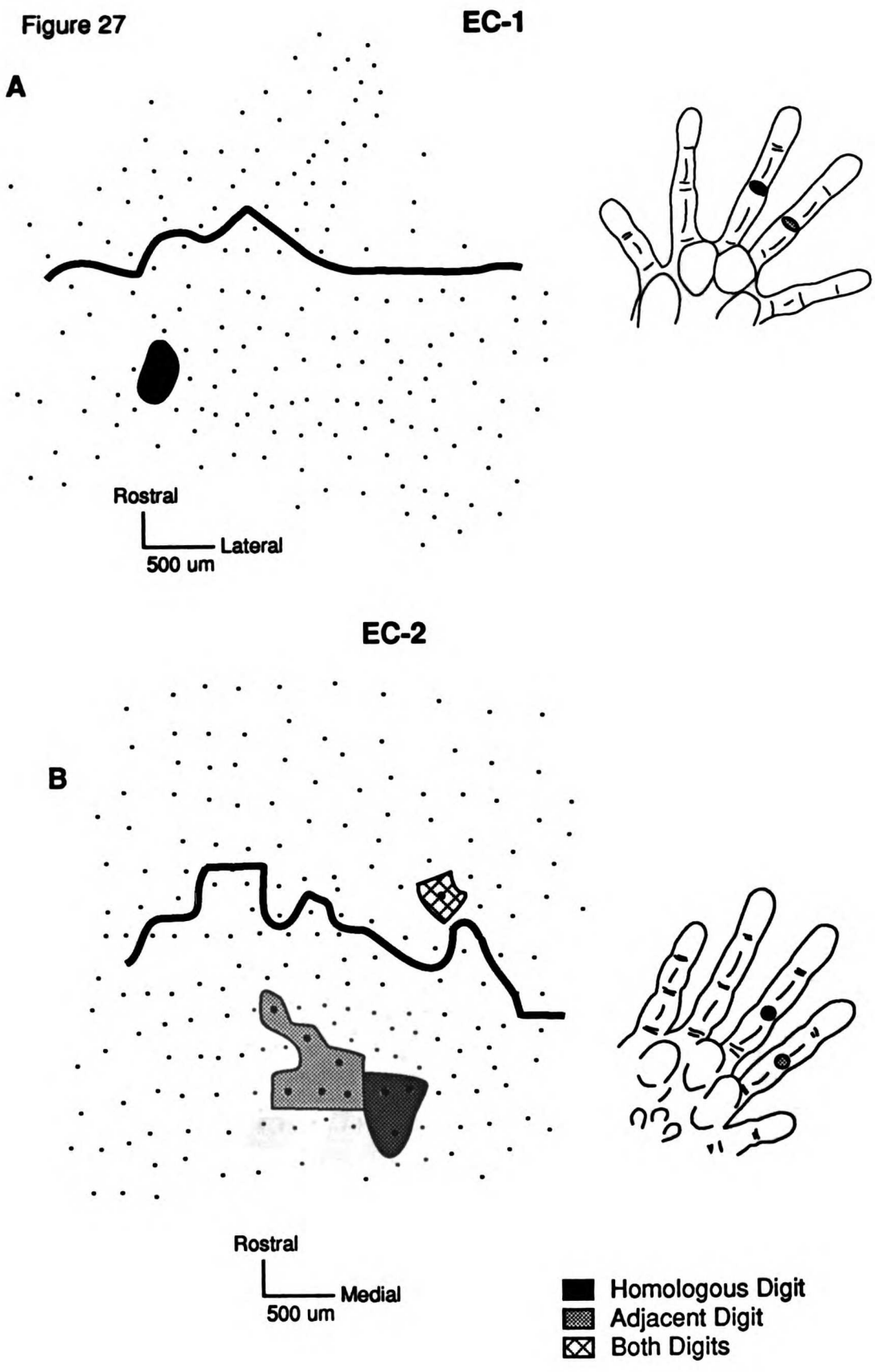
EC-1
A
Rostral
Lateral
500 um
EC-2
B
Rostral
Medial
500 um
Homologous Digit
Adjacent Digit
Both Digits

Figure 27

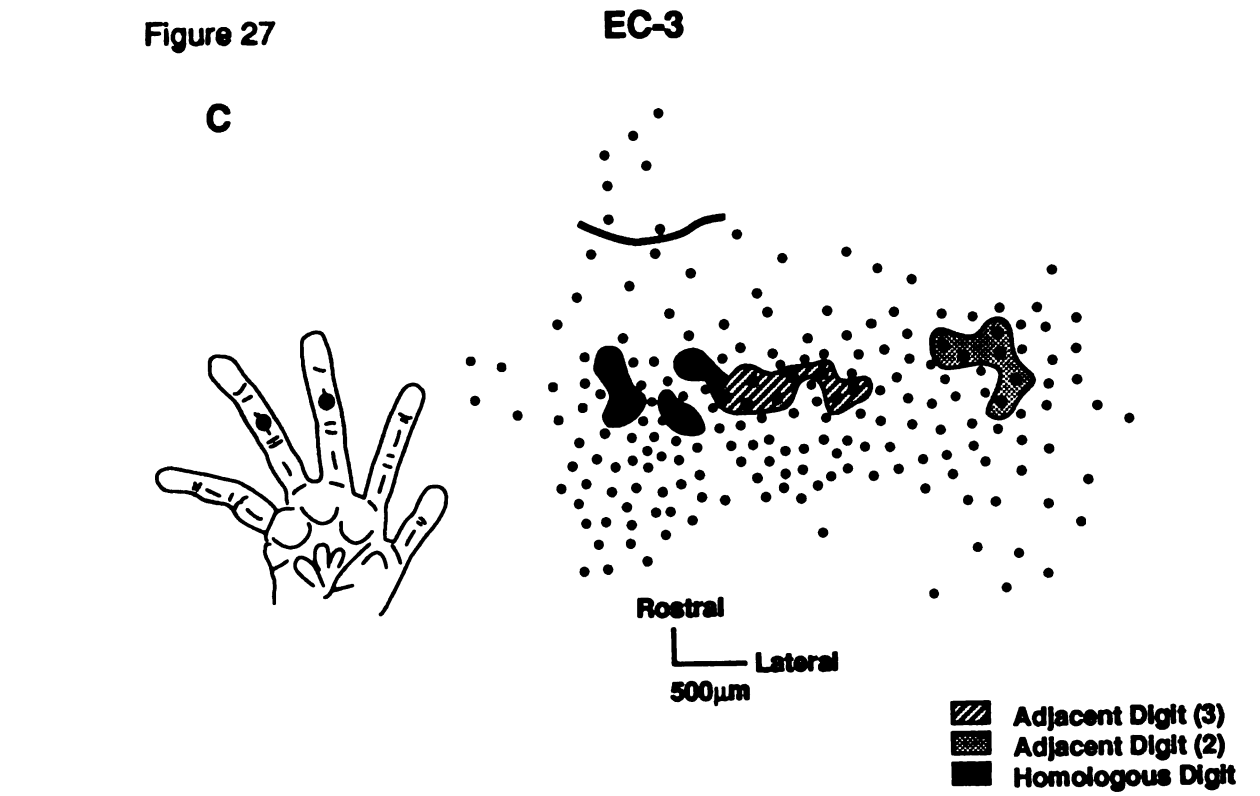
EC-3
C
Rostral
Lateral
500μm
Adjacent Digit (3)
Adjacent Digit (2)
Homologous Digit
PC-1
D
Rostral
Lateral
500 μm
Adjacent Digit (4)
Adjacent Digit (2)
Homologous Digit

Figure 28

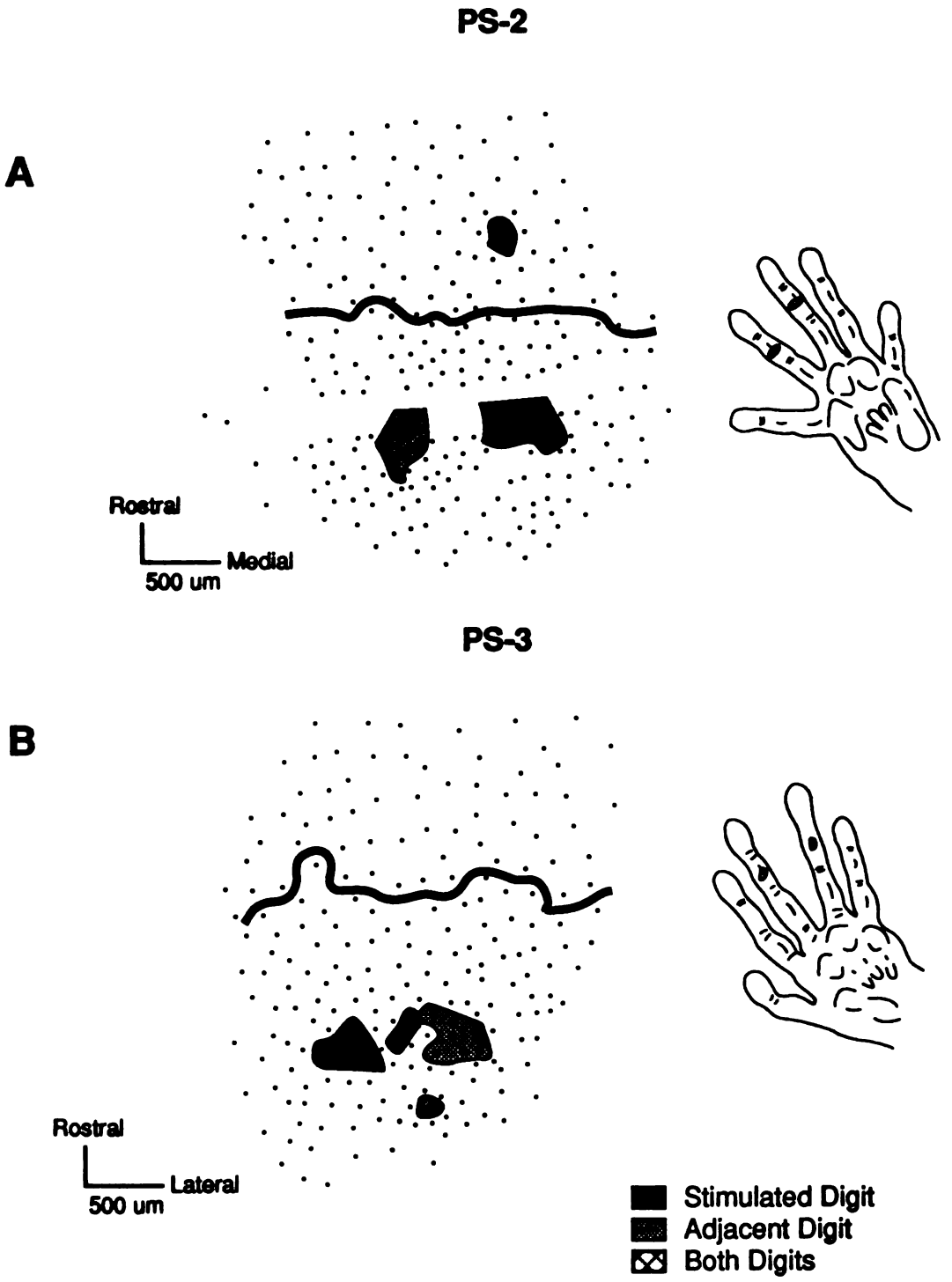
PS-2
A
Rostral
Medial
500 um
PS-3
B
Rostral
Lateral
500 um
Stimulated Digit
Adjacent Digit
Both Digits

Figure 28

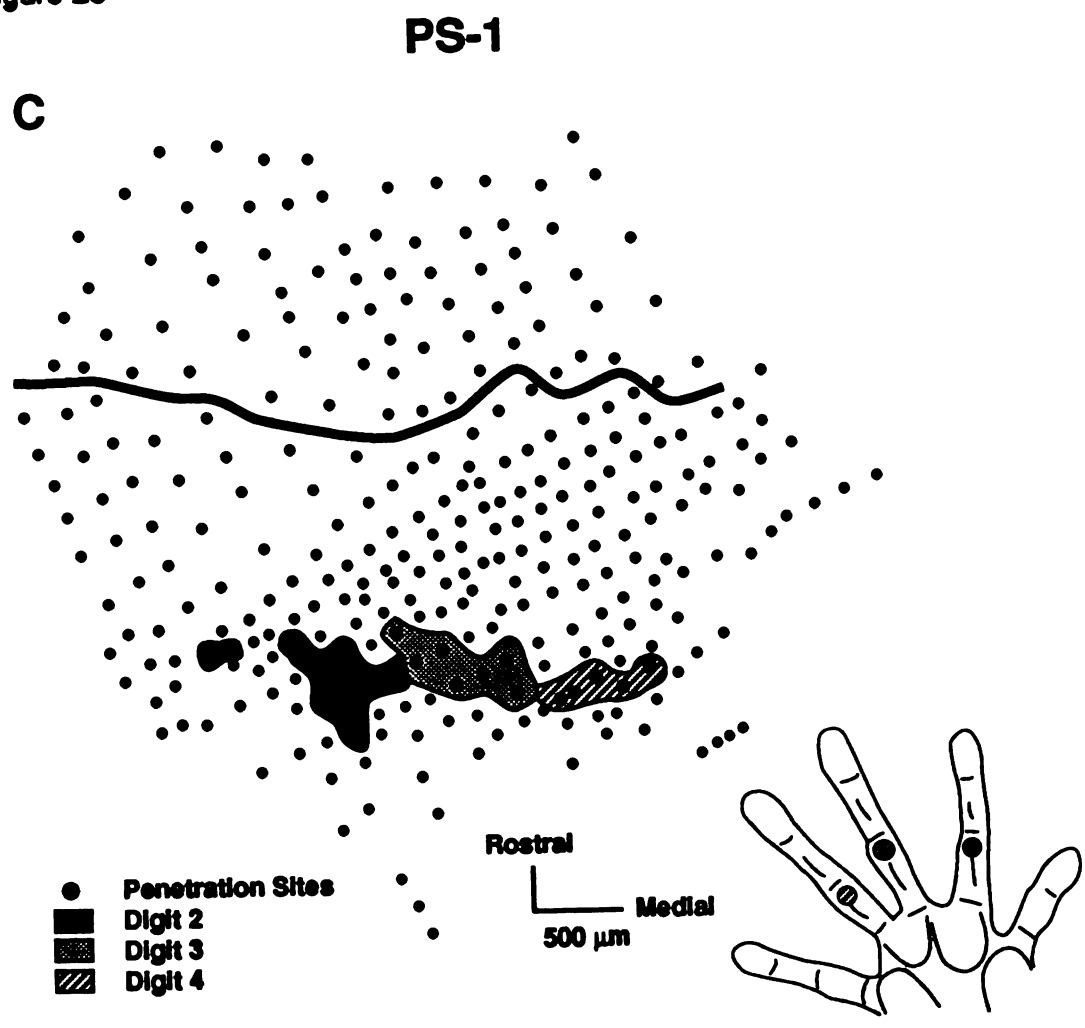
PS-1
C
Penetration Sites
Digit 2
Digit 3
Digit 4
Rostral
Medial
500 µm

Figure 29

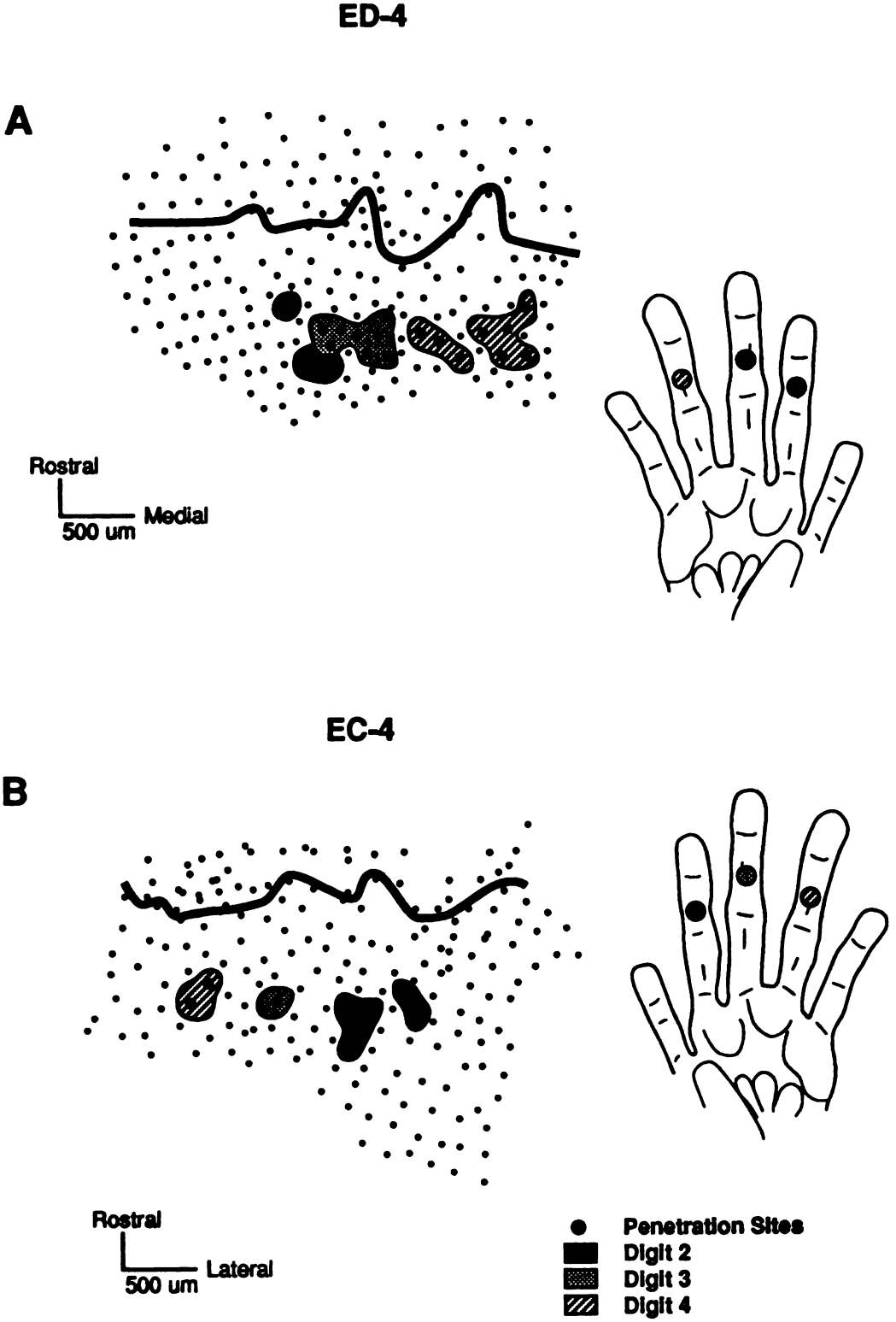
ED-4
A
Rostral
Medial
500 um
EC-4
B
Rostral
Lateral
500 um
Penetration Sites
Digit 2
Digit 3
Digit 4

The discontinuous representation of the stimulated skin was pronounced in area 3a in the experimental hemispheres of the four trained monkeys. Most of the representation of the trained skin was in several clusters. The area of representation of the corresponding skin on the adjacent, untrained digit was also significant. This was in part attributed to the large receptive fields that included this skin region (see below), even though the receptive field was roughly centered on the trained skin. Area 3a in the control and passive-stimulation hemispheres did not have a significant representation of the homologous skin areas. Cutaneous receptive fields that extended over the homologous skin surface were seen in only four penetrations in *all* control and passive-stimulation hemispheres combined.

The results of this analysis qualitatively suggest that the cortical representation of the stimulated skin expanded differentially when compared to similar skin areas on other, non-stimulated digits. This difference is most strikingly illustrated by comparing the absolute area of representation of these restricted skin areas (Figure 30). The representation of the stimulated skin in experimental hemispheres (heavy cross-hatching) is 1.4 to 3.2 time larger than the corresponding area of the adjacent digit (heavy stippling). The area of representation of the homologous skin area in the contralateral hemisphere was always less than that of the experimental hemisphere, and equivalent in area to the representation of its' own adjacent digit. This is most clearly illustrated by case E-3, in which the representation of all non-trained skin areas were about half that of the trained skin area (Part A, right). The area of representation of the trained skin was smallest for the one animal with the poorest behavioral performance (Part B, left). The passive-stimulation control hemispheres showed a similar result. In each case the representation of the

FIGURE 30. Normalized area of area 3b representation of the restricted skin surfaces shown in Figures 26-29. The trained skin is shown by heavy cross-hatching for experimental hemispheres (top). The stimulated skin is also shown by heavy cross-hatching for passively-stimulated control monkeys (bottom). Opposite control hemispheres are shown in the middle panel.

Figure 30

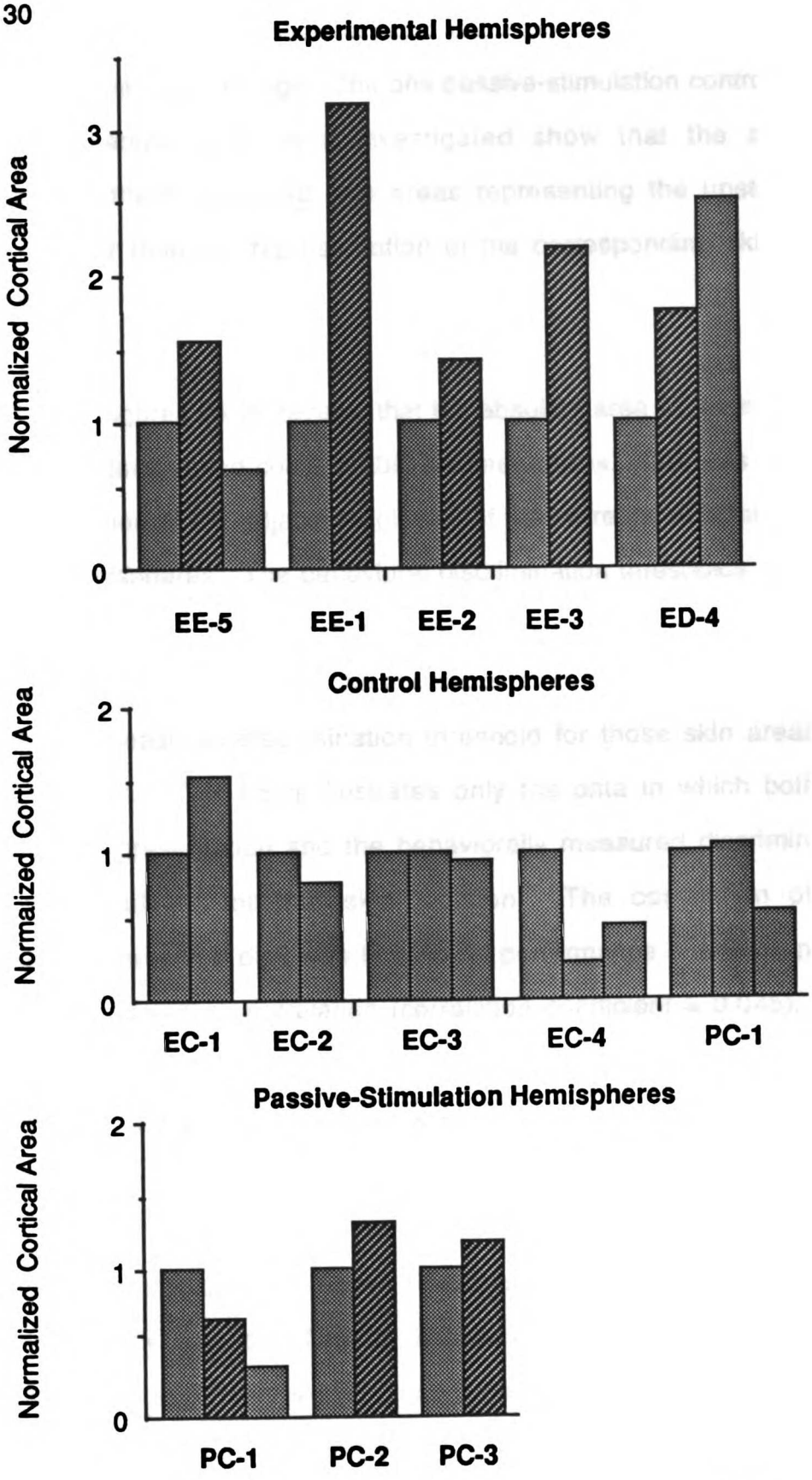
Experimental Hemispheres
Normalized Cortical Area
0
1
2
3
EE-5
EE-1
EE-2
EE-3
ED-4
Control Hemispheres
Normalized Cortical Area
0
1
2
EC-1
EC-2
EC-3
EC-4
PC-1
Passive-Stimulation Hemispheres
Normalized Cortical Area
0
1
2
PC-1
PC-2
PC-3

skin area stimulated in the behavioral task was only slightly larger than the representation of the adjacent digit. The one passive-stimulation control animal in which both hemispheres were investigated show that the areas of representation of these restricted skin areas representing the unstimulated hand were smaller than the representation of the corresponding skin of the stimulated digit.

Inspection of Figures 26-28 reveals that the absolute area of representation of these skin locations varied considerably between cases. This was also true for the representation of the adjacent digit and of the corresponding skin areas in the control hemispheres. The behavioral discrimination thresholds for these skin surfaces also varied, although over a fairly small range. The correlation of the cortical area of representation of the entire digit or of the stimulated skin with the behaviorally measured discrimination threshold for those skin areas are shown in Figure 31. This figure illustrates only the data in which both the cortical area of representation and the behaviorally measured discrimination threshold were defined for that skin location. The correlation of the representation of the entire digit with behavioral performance is shown in Part A. These data showed no correlation (correlation coefficient = 0.045). The correlation with the representation of only the stimulated skin is somewhat better (Part B). The best fit line has a negative slope and a correlation coefficient of 0.75.

In summary, the cortical area 3a and 3b representation of the skin trained in the behavioral task was significantly increased when compared to the representation of an equivalent skin area on adjacent digits of the same hand, or to the representation of the equivalent skin area on the contralateral hand.

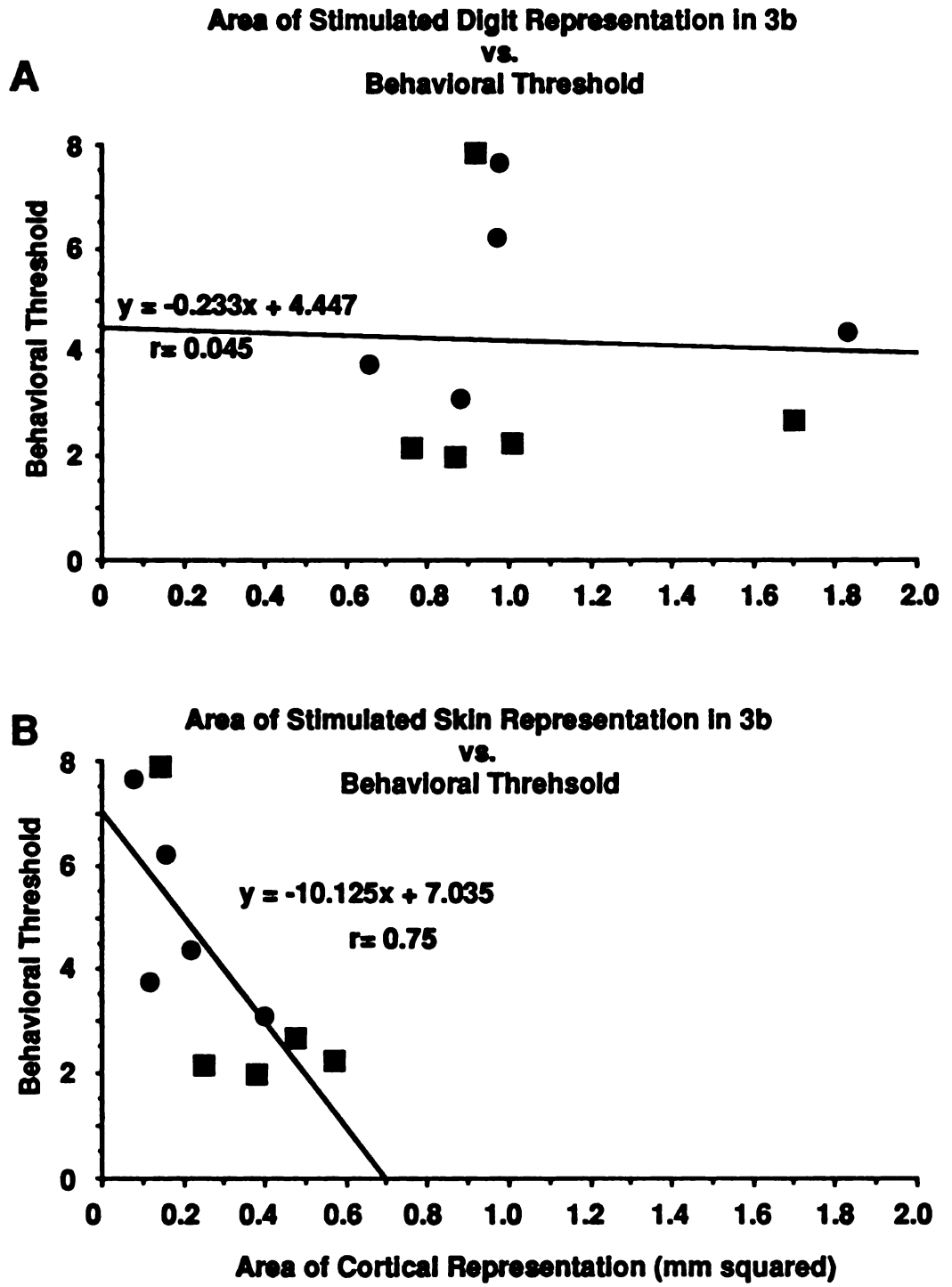

Figure 31. Regression functions plotting the behavioral threshold vs. the area of representation of the entire digit (Part A) or of the restricted skin surface that was stimulated in the task (Part B). The equation at the top of each plot is the r.m.s. best fit line to the data. Correlation coefficients are also shown. Circles denote thresholds on untrained digits, squares are thresholds of trained digits.

This increase occurred to a much lesser extent for the representation of the stimulated skin in passively-stimulated control animals. The area of representation of these restricted skin locations was negatively correlated with the behavioral discrimination performance on that skin, i.e. the skin areas with the lowest thresholds had the largest cortical representation.

Receptive Field Size

Given that the cortical representation of a restricted skin field expanded following training at the frequency discrimination task, one might expect that the corresponding receptive fields over this skin region would be smaller than those in corresponding representations of the other digits. That prediction is based on the "*Inverse Rule*" of normal animals, by which receptive field size is inversely related to the area of the cortical representation of that specific skin area (Sur et al 1981). This "rule" is roughly maintained following a variety of experimental manipulations resulting in topographic reorganizations (Merzenich et al 1983a, 1984; Jenkins et al 1990). During the derivation of these cortical maps it was apparent that the sizes of the receptive fields representing the trained skin did *not* decrease; to the contrary, receptive field sizes *increased* over that region.

The individual receptive fields defined at all cortical locations within area 3b are shown for hands studied in Figures 32-35. The receptive fields defined on the trained hands were distinctly larger and clustered over the stimulated skin region (black dots, Figure 32) when compared to the receptive fields recorded on the opposite, control hand (Figure 33). The only exception was seen in animal E-5 (Figure 32, lower right). The animal's performance did improve, however, and also showed a change in the area of representation in area 3b (see Figure 30). In all of the successfully trained animals, receptive fields were

Receptive Fields of Trained Hands

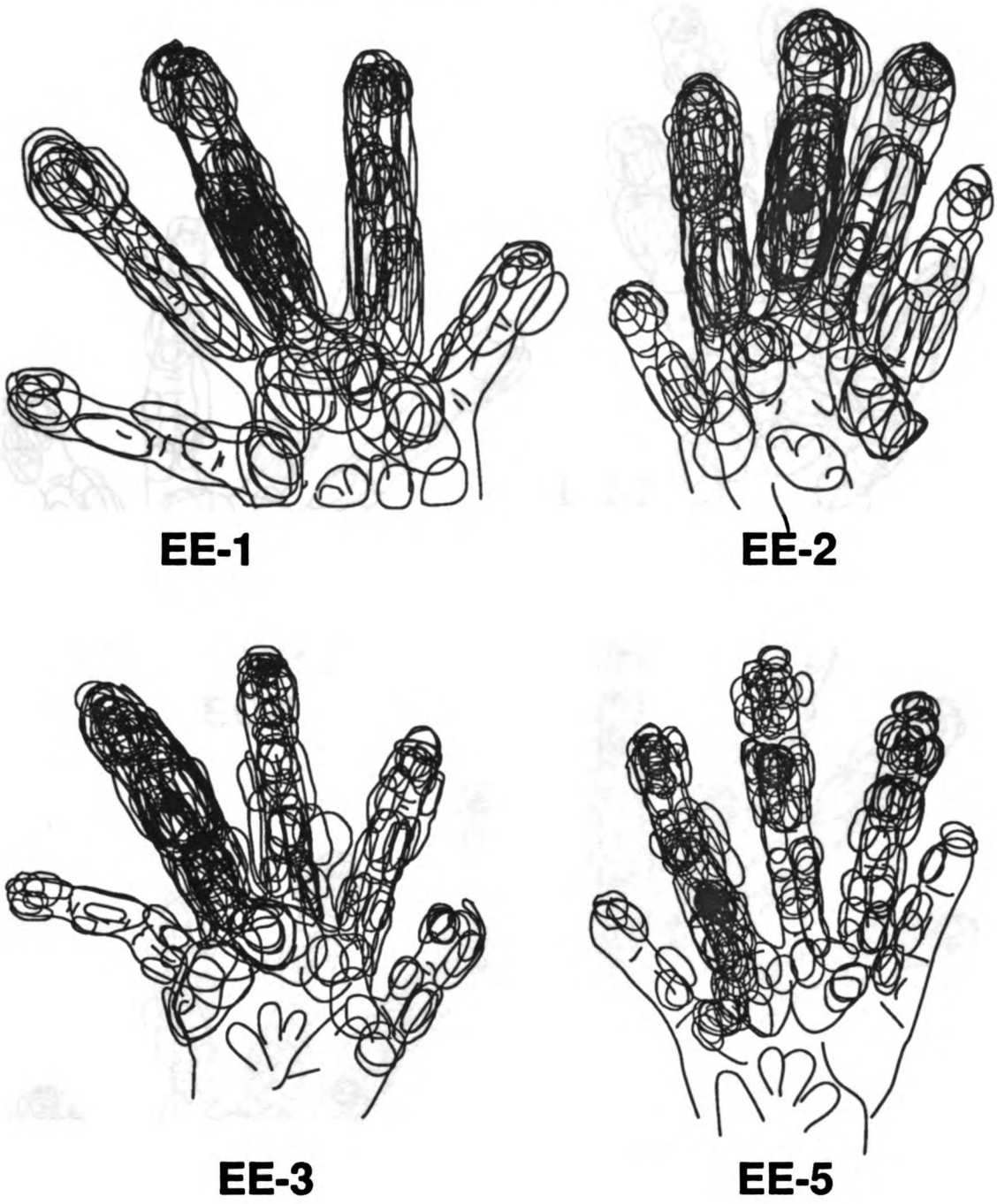

Figure 32. All receptive fields defined in area 3b for hands trained in the frequency discrimination task. The area of skin stimulated in the task is indicated by the black region. The trained digit is Digit 3 for cases EE-1 and EE-2, Digit 4 for case EE-3, and Digit 2 for case EE-5.

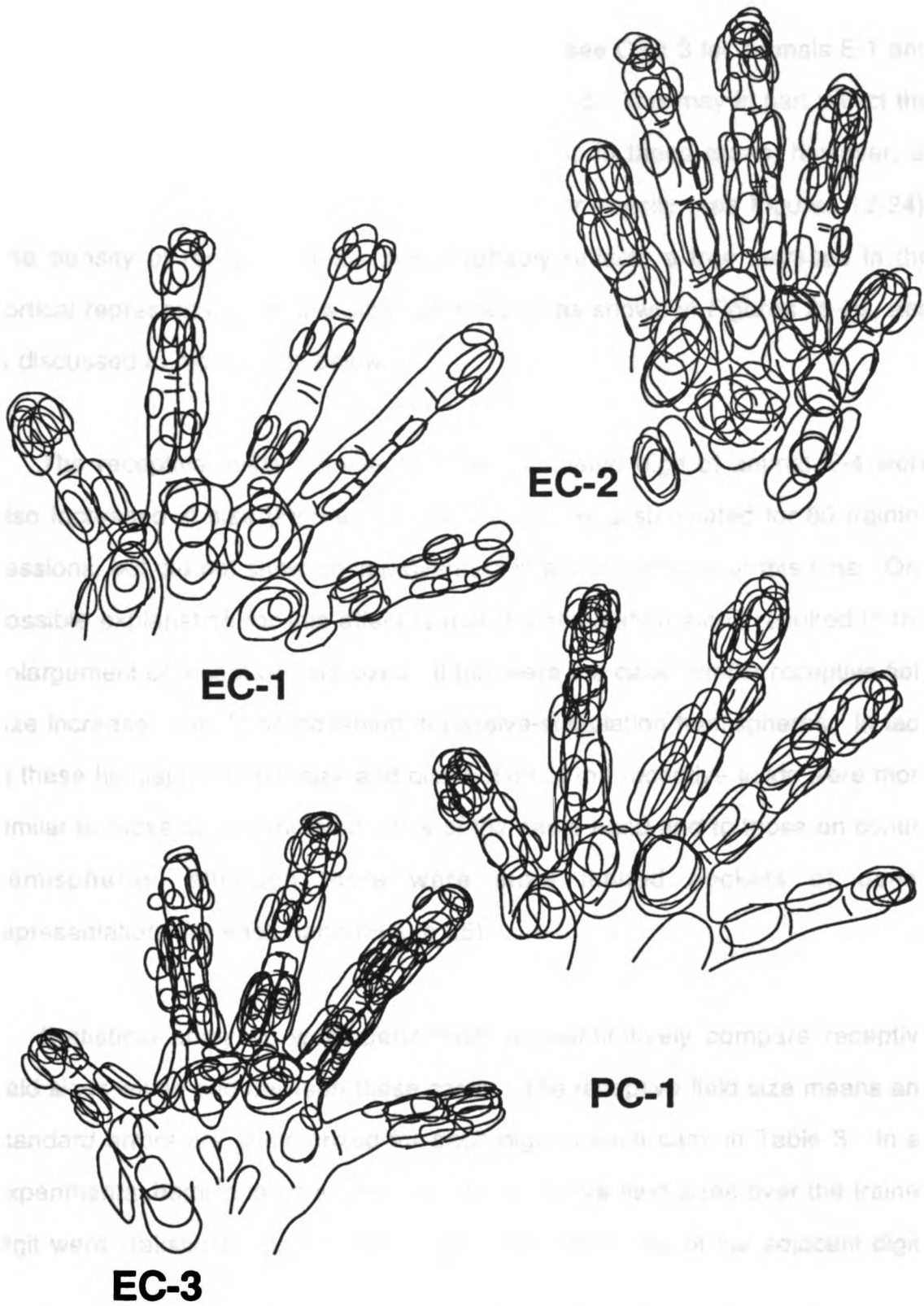

Figure 33. All receptive fields defined in area 3b for the opposite, untrained hands. Hands are from monkeys trained in the tactile discrimination task (EC-1, EC-2 and EC-3), and from the unstimulated hand of a passively-stimulated monkey (PC-1).

more densely distributed on the stimulated digit; see Digit 3 for animals E-1 and E-2, digit 4 for animal E-3 and digit 2 for animal E-5. This may in part reflect the increased density of microelectrode penetrations in these areas, however, at least one adjacent digit was sampled at a similar density (see Figures 12-24). The density of receptive fields most probably reflects a true increase in the cortical representation of this small skin region as shown in Figures 26-29, and is discussed in more detail below.

The receptive fields representing the stimulated digit of animal E-4 were also increased in size (Figure 34). This animal was stimulated for 80 training sessions, but did not show an improvement in performance over this time. One possible explanation for this effect is that the stimulation alone resulted in this enlargement of receptive field sizes. If this were the case, similar receptive field size increases should be observed in passive-stimulation hemispheres. In fact, in these hemispheres the size and distribution of the receptive fields were more similar to those of unstimulated digits of the same hand and to those on control hemispheres, although there were more limited pockets of dense representations for each hand (Figure 35).

Statistical analyses were performed to quantitatively compare receptive field sizes within and between these cases. The receptive field size means and standard errors are summarized for each digit in each case in Table 3. In all experimental hemispheres except E-5, the receptive field sizes over the trained digit were statistically significantly larger than were those of the adjacent digits (two-tailed t-test; $P<0.01$). The single exception was in animal E-1 in which the receptive field sizes on digit 4 were also statistically significantly different from digits 1, 2 and 5, but not different from digit 3. No statistically significant

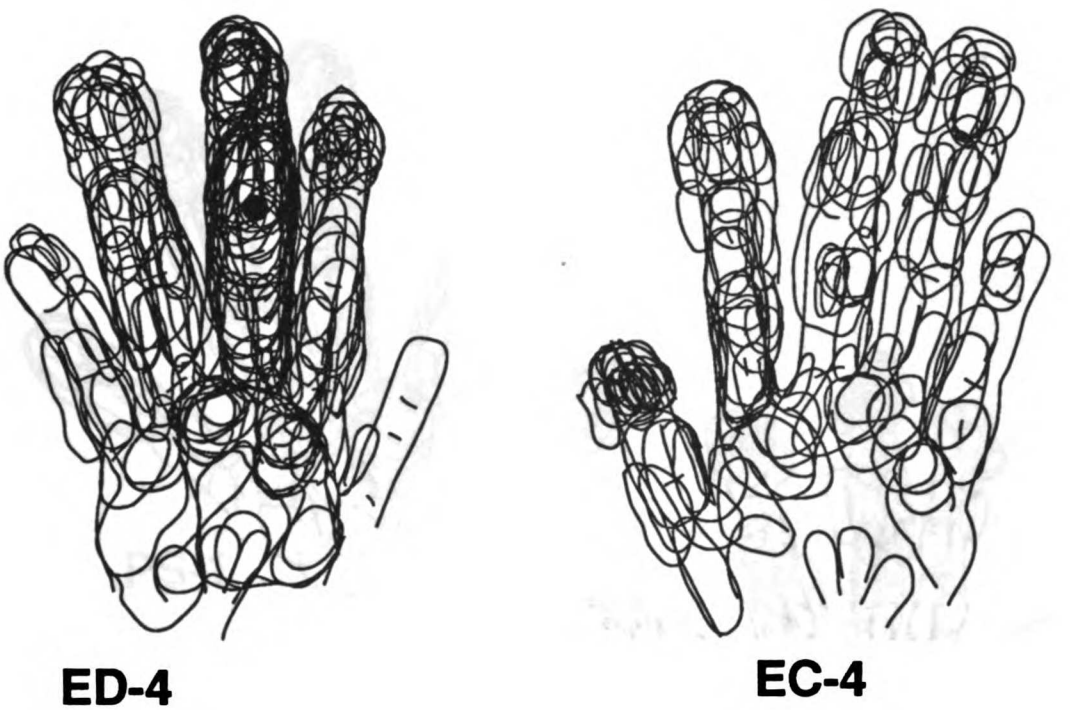

Figure 34. All receptive fields defined in area 3b for both hands of monkey E4. ED-4 represents the hand stimulated in the behavioral apparatus. EC-4 represents the opposite, unstimulated hand. Black circle denotes the area of skin stimulated.

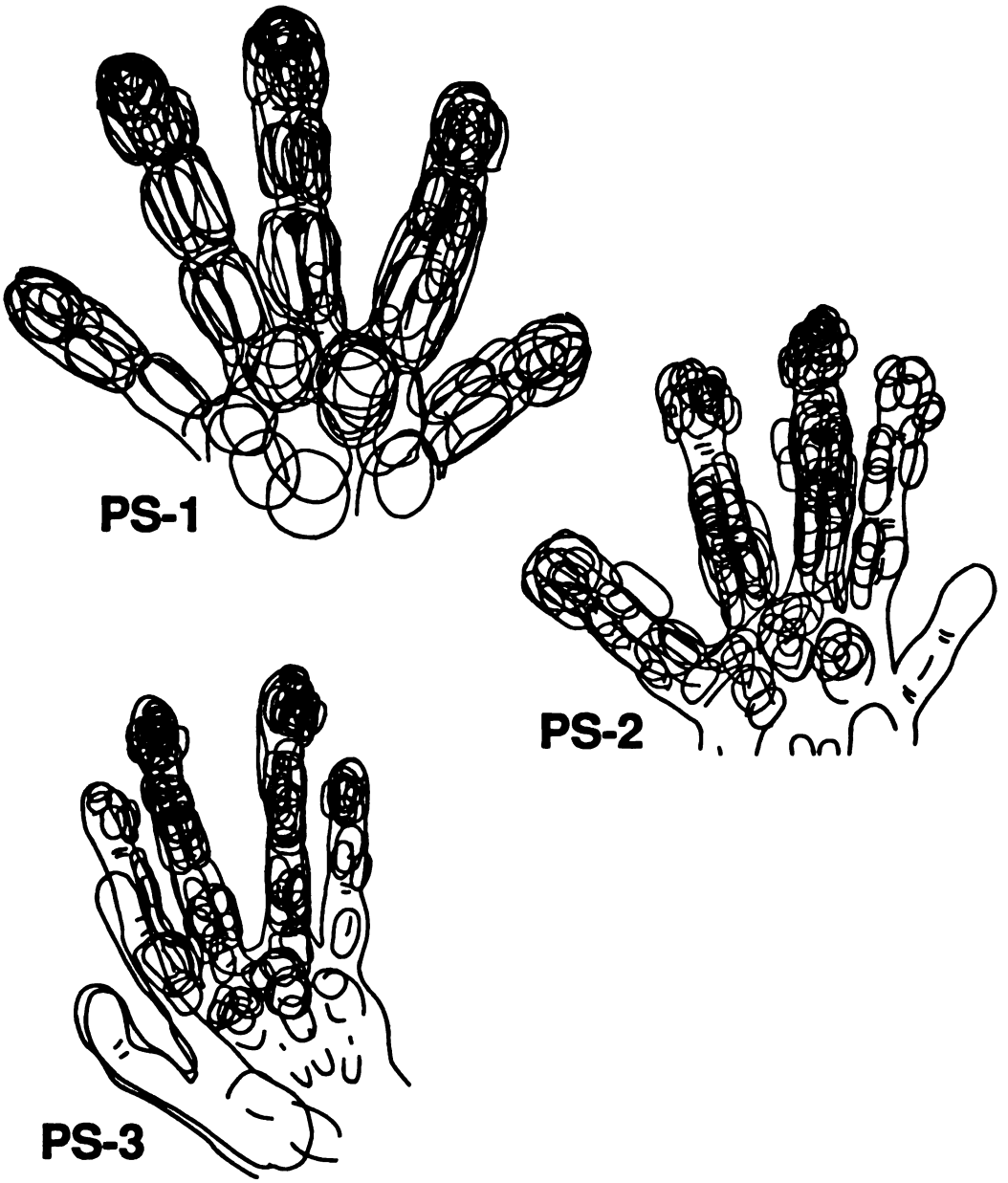

Figure 35. All receptive fields defined in area 3b of passively-stimulated hands. Black circles denote area of skin stimulated in the behavioral apparatus.

differences were found between digits within the control or passively-stimulated hemispheres.

Receptive field sizes were also compared between hemispheres in cases where both hemispheres were studied (Table 4) In every case the receptive field sizes measured on the digit trained in the task (bold type) were significantly larger than those measured on the homologous, unstimulated digit on the contralateral hand. This cross-hemisphere comparison also revealed a statistically significant increase of receptive field sizes on at least one of the adjacent, unstimulated digits on the trained hand in every experimental case.

Distribution of receptive field sizes

The receptive field size increase raises the question of whether all receptive fields increased in size uniformly, or only a subset of receptive fields increased in size. The distribution of receptive field sizes for several representative cases are shown in Figures 36 and 37. In each figure the receptive fields defined in the representation of the stimulated digit or the homologous digit representation in the contralateral hemisphere are shown in the left column and the same analysis for the adjacent digit is shown in the right column. The trained and adjacent digits from animals E-1 and E-2 both have a broad distribution of receptive field sizes when compared to the control hemispheres of these same animals (Figure 36). The increase of large receptive fields is greater for the stimulated digit in the experimental hemispheres, yet the distribution for the adjacent digit is clearly broader in both animals when compared to the control hemisphere. Animal E-3 showed a similar result.

Table 3 Summary of Receptive Field Size Statistics

Experimental Hemispheres

Case	D1	D2	D3	D4	D5
EE-1	44.2 ± 10.6	29.2 ± 4.5	**41.0 ± 4.4***	35.6 ± 5.0*	32.9 ± 8.0
EE-2	12.3 ± 1.7	28.4 ± 3.7	**52.8 ± 5.0***	28.3 ± 24.7	16.9 ± 2.8
EE-3	13.5 ± 1.5	14.1 ± 1.2	**15.2 ± 1.4**	**43.3 ± 5.5***	8.9 ± 2.3
ED-4	i.d.	23.5 ± 3.3	**45.4 ± 4.21***	25.7 ± 3.0	23.5 ± 8.9
EE-5	18.8 ± 8.9	11.5 ± 0.8	**10.5 ± 0.6**	11.1 ± 0.6	9.2 ± 0.4

Control Hemispheres

Case	D1	D2	D3	D4	D5
EC-1	18.9 ± 5.4	i.d.	7.6 ± 0.6	9.1 ± 0.9	7.9 ± 0.5
EC-2	14.3 ± 2.3	11.8 ± 1.2	12.5 ± 1.8	9.5 ± 1.5	7.9 ± 0.5
EC-3	7.8 ± 1.0	6.0 ± 0.6	8.5 ± 1.1	9.07 ± 1.3	10.0 ± 1.23
EC-4	i.d.	19.6 ± 2.3	16.2 ± 3.0	18.2 ± 2.3	19.3 ± 3.5
PC-1	9.7 ± 1.4	13.7 ± 1.7	16.6 ± 1.3	20.0 ± 2.5	14.4 ± 2.1

Passive-Stimulation Hemispheres

Case	D1	D2	D3	D4	D5
PS-1	21.4 ± 2.1	24.1 ± 2.4	**19.0 ± 1.4**	23.9 ± 1.8	20.8 ± 1.7
PS-2	i.d.	9.9 ± 0.8	**15.6 ± 1.8**	15.4 ± 1.9	18.9 ± 2.4
PS-3	i.d.	11.5 ± 2.8	**9.5 ± 0.7**	10.5 ± 1.3	8.0 ± 0.9

i.d. -- insufficient data
Mean and standard errors of receptive fields in mm squared defined on each digit. Bold faced type denotes
the digit trained (Experimental Hemispheres) or stimulated (Passive-Stimulation Hemispheres) digit.
* indicates $p<0.01$ for that digit compared to all others of that hemisphere. For case EE-1, the receptive fields on digits 3 and 4 were significantly different than those on digits 1, 2 and 5

Table 4 Summary of Receptive Field Size Comparisons Between Hemispheres

Animal	Digit 1	Digit 2	Digit 3	Digit 4	Digit 5
E-1	n.s.	n.s.	*	**	*
E-2	n.s.	n.s.	**	*	n.s.
E-3	n.s.	**	**	**	n.s.
E-4	i.d.	n.s.	**	*	n.s.
P-1	**	**	n.s.	n.s.	*

* $P < 0.05$
** $P < 0.01$
i.d. -- insufficient data
Statistical tests of receptive field size comparing homologous digits between hemispheres. Bold faced type denotes the digits that were trained or stimulated in the behavioral apparatus.

FIGURES 36-37. Distribution of receptive field sizes from several different animals. The number of receptive fields are plotted by size in 10 mm squared bins. Figure 36 shows receptive fields from the trained (left) and adjacent (right) digits or their homologues on the opposite hand for monkeys E-1 (to two) and E-2 (bottom two).

Figure 37 shows the same receptive field size distrbutions for monkey E-4 (top two panels), monkey E-5 (third panel) and passive-stimuation control monkey P-3 (bottom panel).

Figure 36

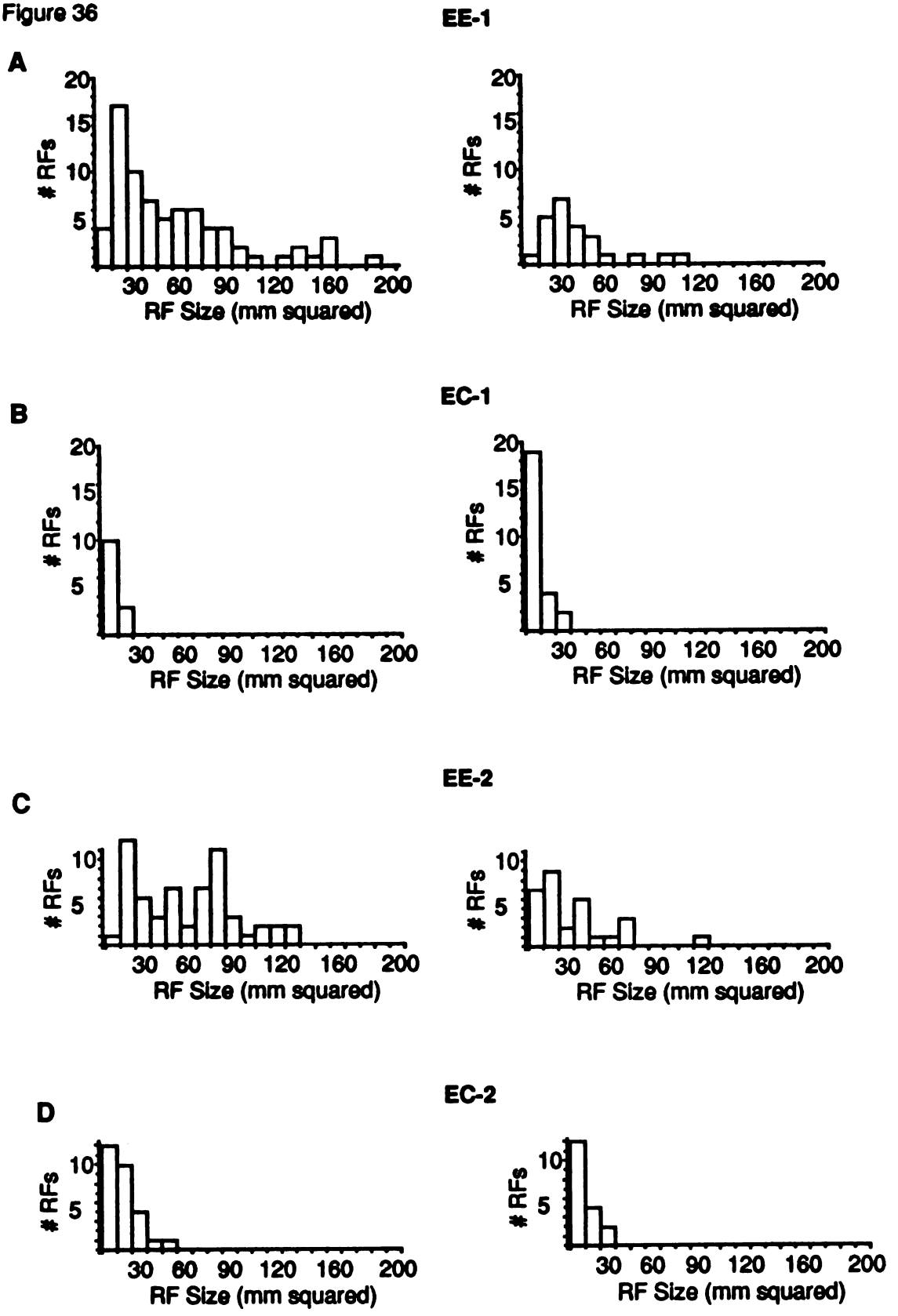
A
EE-1
B
EC-1
C
EE-2
D
EC-2
RFs
RF Size (mm squared)
30 60 90 120 160 200
5 10 15 20

Figure 37

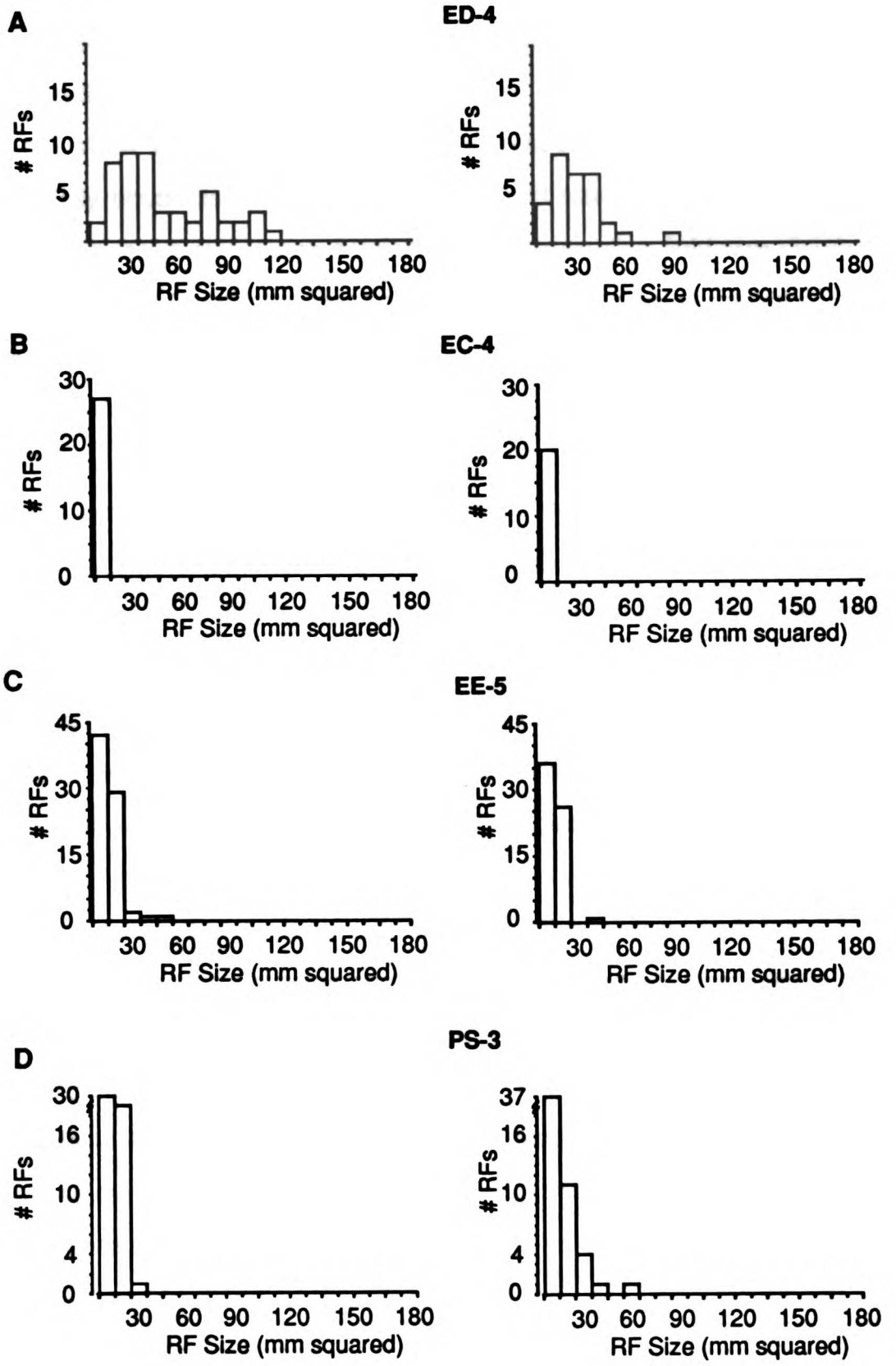

For animal E-4 the distribution of receptive field sizes on both the stimulated and an adjacent digit was also greater for the stimulated hemisphere when compared to the opposite hemisphere (Figure 39A and B). Animal E-5, which did not show a statistically significant increase in receptive field size, had essentially equal distributions of receptive field size for the two digits (Figure 37C). In passive-stimulation hemispheres the receptive field size distributions were essentially identical to those of the control hemispheres (Figure 37D). It is concluded that only a subset of receptive fields increased in size as a result of the behavioral discrimination training.

The cortical location of the largest receptive fields are illustrated for two experimental hemispheres in Figures 38 and 39. In these figures, the location of cortical penetrations are illustrated in the top panels. The lines running through the large circles are labeled to correspond to the offset graphs illustrated in the bottom panels. Small circles indicate data points not included in this analysis. Receptive fields located on different digits are indicated by the symbol (filled circles: digits 1,3 and 5; open circles: digits 2 and 4; squares: receptive fields on the stimulated skin). In the bottom panels, the graphs are offset for clarity. The data derived from case EE-2 is shown in Figure 38. Most of the largest receptive fields correspond to an area of representation of the stimulated skin (squares). There was also some increase in size for the immediately adjacent cortical penetrations. Case EE-3 is shown as a second example in Figure 39. Again, the largest receptive fields were centered on locations representing the stimulated skin. The receptive fields neighboring this region were also increased in size.

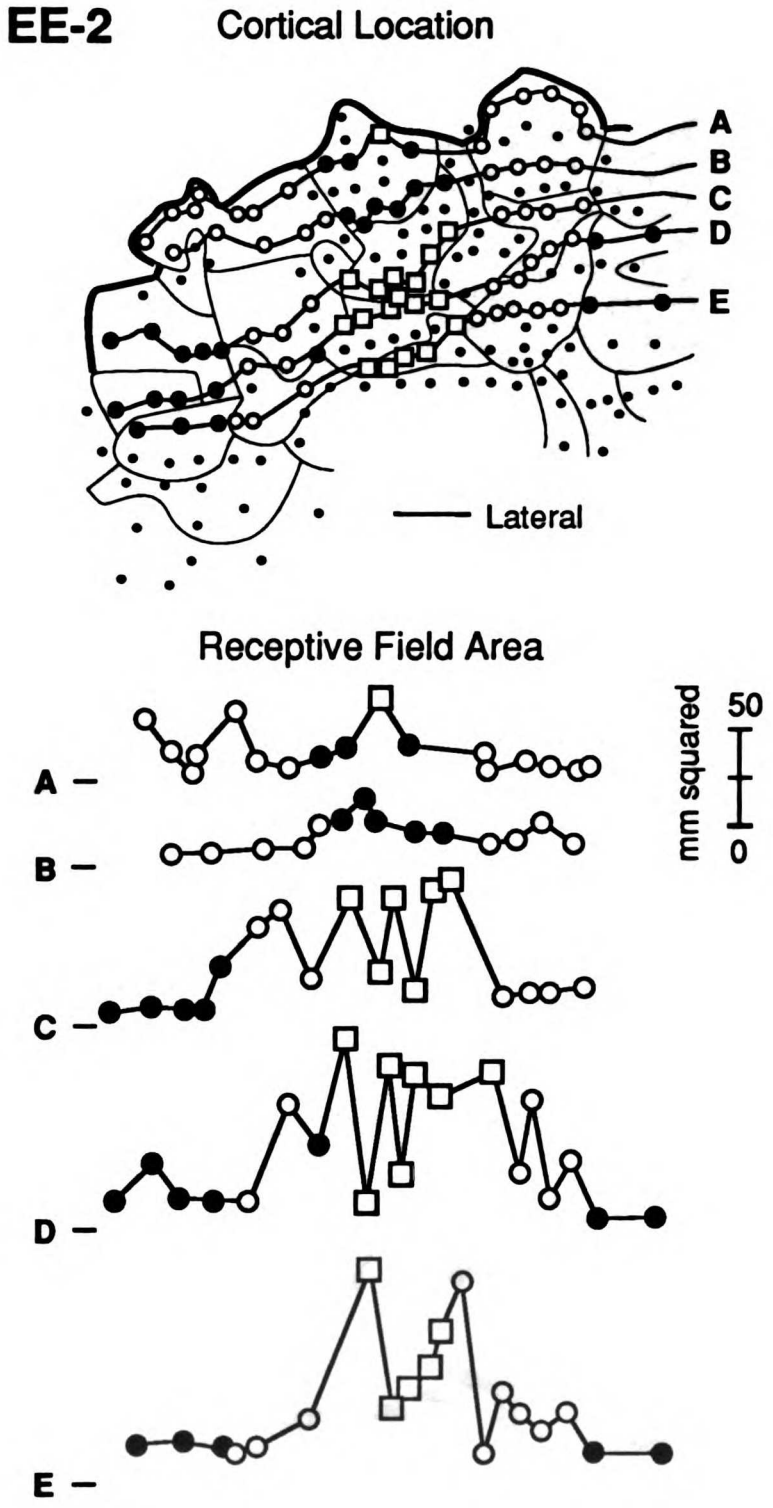

Figure38. Receptive field size as a function of cortical location for case EE-2. Top panel shows the cortical locations of the data points used in constructing the plots shown below. Small dots denote cortical locations with receptive fields located on the extreme radial or ulnar aspect of the digit, and are not included in this analysis. Tic marks denote zero on the offset graphs in the bottom panel. See text for details.

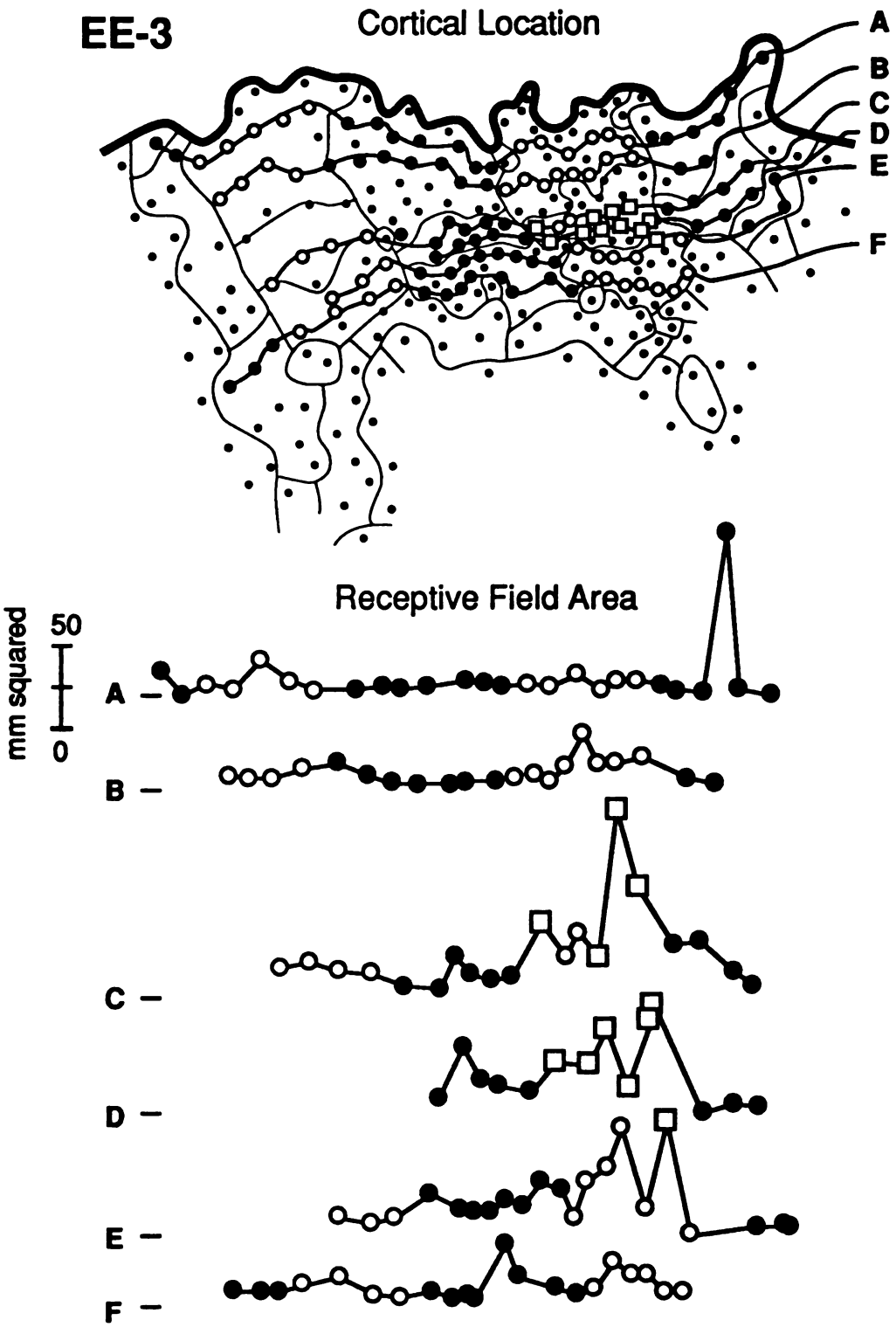

Figure 39. Cortical receptive field size as a function of cortical distance for case EE-3. Abbreviations as in Figure 38.

In summary, the sizes of receptive fields defined in the representation of the trained digit were statistically significantly larger than those defined in the representations of the adjacent digits on the trained hand, as well as to those defined in the representation of the homologous digits on the opposite hemisphere. This inter-hemispheric difference in receptive field size was also true for many of the untrained, adjacent digits. The largest receptive fields were defined within the representation of the stimulated skin and the immediately surrounding cortical region. The receptive field sizes in the representation of passively-stimulated control digits were not statistically significantly larger than those defined on the unstimulated digits of the same or opposite hemispheres.

Internal topography of single digits

The receptive field size increase could be accounted for in one of three ways: 1) All the receptive fields near the stimulated skin could have expanded symmetrically; 2) the receptive fields located near the stimulated skin could have expanded asymmetrically to now represent the stimulated skin; or 3) the receptive fields could have enlarged and moved to become centered on the stimulation site. The obvious clustering of receptive fields over the stimulated skin (Figure 32) supports possibilities (2) and (3) above. To further address this question the distance from the base of the digit to the geometric center of each receptive field was plotted as a function of the distance of the corresponding electrode penetration measured from a line drawn orthoganal to the representation along this axis of the digit. This compresses the two dimensional data into a single dimension of linear distance. If the receptive fields expanded symmetrically the geometric centers of the receptive fields would not change and this function would form a straight line. If the expansion was asymmetric, the geometric centers would cluster near the stimulated skin, causing the slope

of this function to decrease. If the receptive fields moved to incorporate the stimulated skin, receptive fields with the same geometric center would be observed over a large cortical distance.

The results of this analysis for the representation from three experimental hemispheres are shown in Figure 40. The cortical distance was plotted on the x-axis, and the distance from the base of the digit to the geometric center of the corresponding receptive field is plotted on the y-axis. The top panel shows this relationship for the trained digit of monkey E-1 (left) and monkey E-3 (right). The bottom panel shows the results from the trained digit (left) and the adjacent, untrained digit (right) on monkey E-2. In every case the receptive field centers on the trained digit clustered around a skin distance corresponding to the stimulus probe location (arrows). Receptive fields with geometric centers in this region were represented over a cortical distance of over 500 μm. In contrast, the adjacent digit showed a more linear relationship between receptive field center and cortical location (Figure 40, bottom right). This result was also seen in all control digits (Figure 41). This figure shows two digits from control hemispheres (top) and two passively stimulated digits (bottom). In these cases there is no expression of a particular receptive field center over a significantly large cortical area. This result indicates that the receptive fields either expanded asymmetrically or moved to become centered on the stimulated skin of the trained digit.

Percent overlap of receptive fields with cortical distance

As an additional test of how the receptive fields expanded over the trained skin the percent overlap of receptive fields representing these digits was defined and compared to the distance between these cortical locations. The

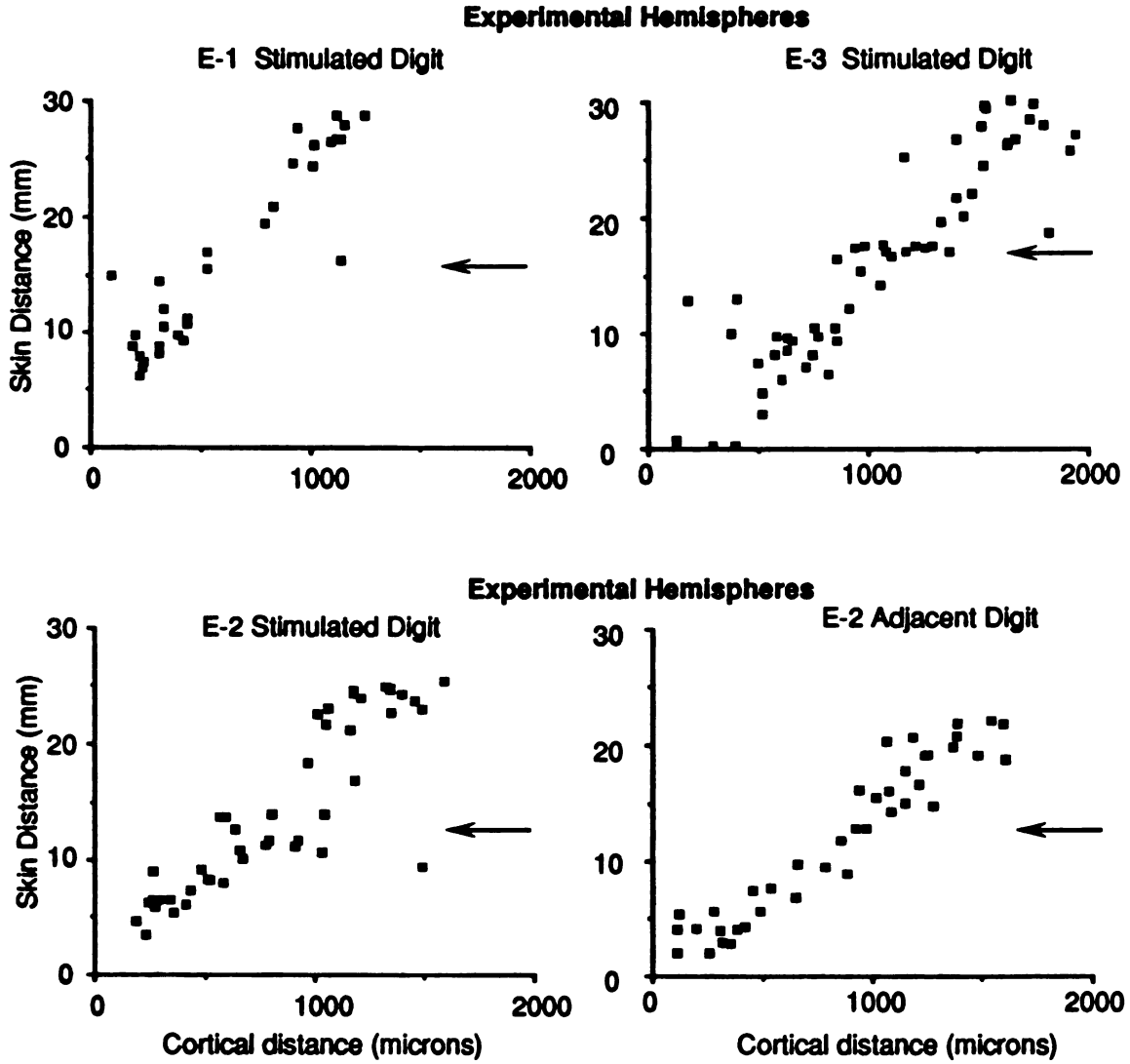

Figure 40. Receptive field geometric center as a function of cortical distance. The geometric center of receptive fields located on the central one-third of the digit measured from the proximal base is plotted on the y-axis. The distance of the corresponding cortical location along a line drawn orthoganal to the axis of representation of that digit in area 3b is plotted on the x-axis. Data are from the trained digit of cases EE-1 and EE-3 (top), and from the trained digit of case EE-2 (bottom left) and the adjacent digit of the trained hand in case EE-2 (bottom right). The arrow indicates the approximate location of the center of the stimulation site.

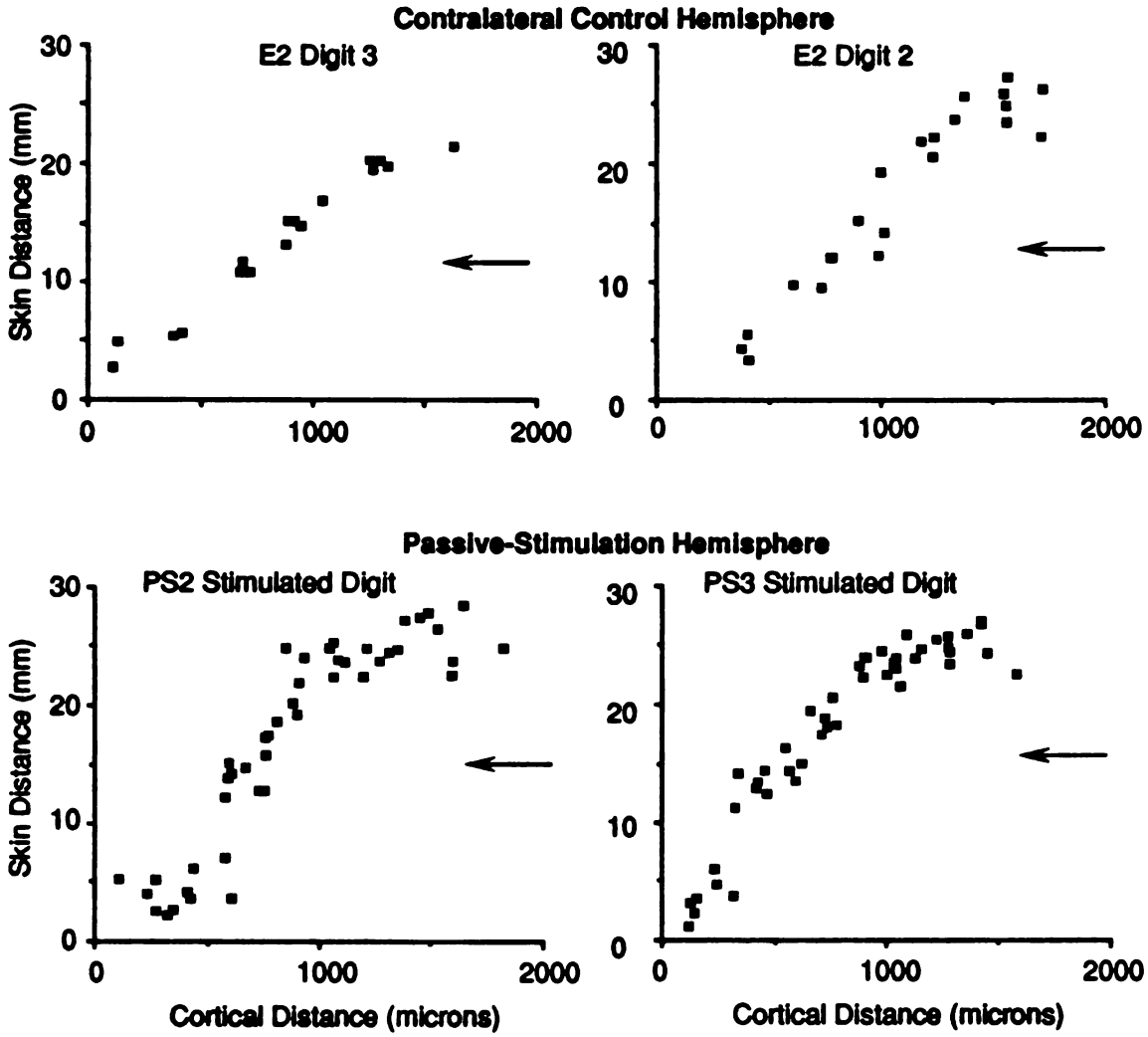

Figure 41. Geometric center of receptive fields plotted as a function of cortical distance for four control digits. Top panel shows these functions from two digits on the opposite hemisphere of monkey E-2. The bottom panel shows the functions from the passively-stimulated digits of two passive-stimulation control monkeys (PS-2 and PS-3). Arrow indicates the approximate location of the stimulation site (bottom panel), or the corresponding skin of the untrained hands. See text for details.

percent overlap between two receptive fields is roughly inversely related to the cortical distance between the two cortical locations (Sur et al 1981; Merzenich et al 1983). This relationship holds true regardless of the body surface represented, and thus regardless of receptive field size. If receptive fields expanded asymmetrically to include the trained skin, there should be a modest increase in overlap between receptive fields located near the stimulation site, but this overlap would not be complete as the expanded receptive fields would still retain some of their original, non-overlapping portion. Alternatively, if receptive fields moved to be centered on the stimulation site, the percent overlap would approach 100% for receptive fields representing the stimulated skin.

This analysis was done by restricting the sample of cortical locations studied to those with receptive fields on the central third of the glabrous skin of the digit, thus eliminating receptive fields located on the most ulnar and radial aspects of the digit. The percent overlap of 6-8 of these locations ('standard' receptive fields, see *Methods*), which had receptive fields scattered throughout the proximal-distal aspect of the digit, were then measured for every other cortical location in that sample. The percent overlap was taken as the area of overlap divided by the area of the standard receptive field. This percent overlap was then plotted against the cortical distance between the two locations. The combined results from all of the standard receptive fields are plotted for three different digits of animal E-2 in Figure 42. Included in these plots are the theoretical function of receptive field overlap ranging from 100% at zero cortical distance to 0% overlap at a cortical distance of 600μm (thin line). The percent overlap with cortical distance does not decrease uniformly for the trained digit (Figure 42A). In several instances, receptive fields overlapped by 100% at

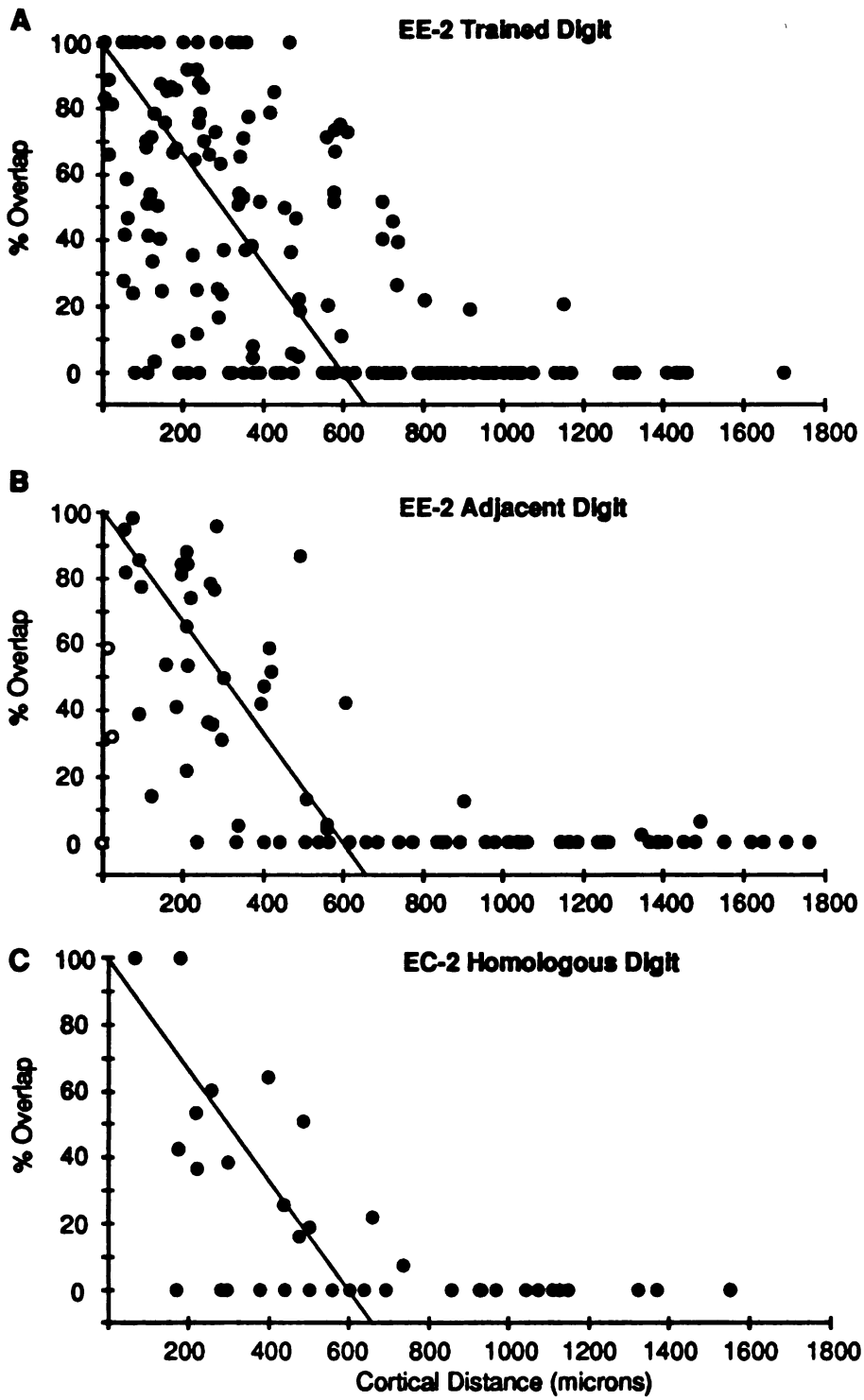

Figure 42. Percent overlap of receptive fields as a function of the distance separating the cortical locations. Only locations with receptive fields located on the central one-third of the digit are considered. Top panel shows a representative example from a trained digit (EE-2), middle panel is from an adjacent digit and the bottom panel is from an opposite hemisphere control digit.

cortical distances of up to 500 microns. Significant overlap was also observed beyond 600 microns in cortical distance. The same analysis on the adjacent digit of this monkey were roughly inversely related, but several exceptions were also noted (Figure 42B). Only in three instances was there any overlap of receptive fields recorded between cortical locations separated by more than six hundred microns. The percent overlap functions for the contralateral hemisphere were reasonably inversely related to cortical distance (Figure 42C). The function shown in this graph is in good agreement to that of the normal owl monkey (Sur et al., 1981).

The analysis presented above suggests that in the trained digit the percent overlap of receptive fields was maintained at a high value over a significant cortical distance. To determine if this effect was limited to a restricted portion of the digit representation, the results were plotted with respect to the cortical location in the rostra-caudal axis, shown in Figure 43. Three cortical locations were selected which had receptive fields on the proximal (filled circle), middle (filled diamond) or distal (filled star) segment of the digit. All cortical locations were assigned a distance value that increased in one dimension along the representation of the long axis of the digit. The horizontal axis of the graphs corresponds to this axis, as does the cortical representation shown at the top. The percent overlap measured as the distance along this axis with respect to the selected cortical location are shown in the graphs below. The representation of the trained digit is to the left. The middle panel represents the results from the overlap of a receptive field that was centered on the trained skin. In this case there was a very high degree of overlap for a significant horizontal distance in both directions.

FIGURE 43 Percent overlap of receptive fields with cortical distance as a function of cortical location. Cortical maps for the trained (left) and adjacent (right) digits are shown at the top. Rostral is to the right. Small dots denote cortical locations not used in this analysis as they had receptive fields on the extreme ulnar or radial aspects of the digit. Open circles denote locations where the receptive field overlap was measured relative to each of the three reference receptive fields (filled symbols). The filled diamond at the left represents a receptive field that was centered on the trained skin.

Figure 43

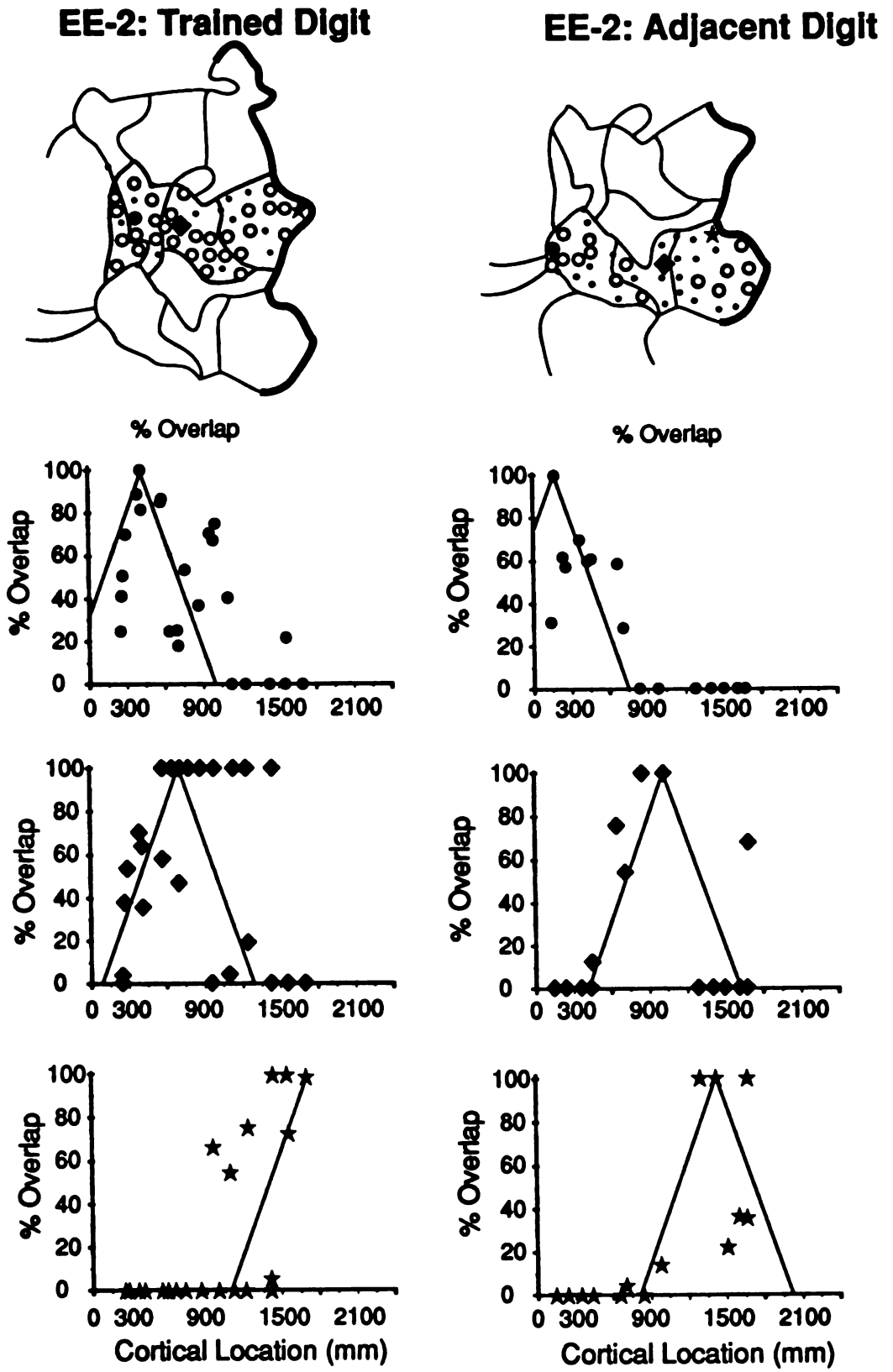
EE-2: Trained Digit
EE-2: Adjacent Digit
% Overlap
% Overlap
% Overlap
% Overlap
% Overlap
% Overlap
% Overlap
% Overlap
100
80
60
40
20
0
0 300 900 1500 2100
Cortical Location (mm)
Cortical Location (mm)

The results from the adjacent digit were better described by a roughly inverse function. There was a high degree of overlap at two nearby locations for the most rostral comparison point.

In summary, the location of the receptive field centers, and the percent overlap of receptive fields in the cortical area representing the stimulated skin area, indicate that the majority of these receptive fields were roughly centered on the stimulated skin. The increase in receptive field size is best explained by an increase in size and a shift in location to be roughly centered on the stimulated skin.

Cutaneous representation in cortical area 3a

The cytoarchitectonic area located immediately rostral to area 3b, area 3a, was also investigated in these monkeys. A significant area of cutaneous responses were recorded in area 3a of monkeys trained at the tactile task. Cutaneous responses are only rarely observed in area 3a of normal monkeys (Merzenich et al 1978, 1987; Kaas et al 1979; Cusick et al 1989). Some details of the cutaneous representation of the hand in area 3a of experimental and control hemispheres are shown in Figures 44-46. In control hemispheres the most common response was non-cutaneous (small dots). At these locations neurons responded to elongation of muscles, joint movement, heavy mechanical vibration or taps. Neurons at the most rostral locations were unresponsive except for vigorous stimulation to the hand. In monkey E4, there were no cutaneous responses recorded in area 3a of either hemisphere. This animal is not considered further in this section.

The area 3a cutaneous representation was classified into five categories. 1) Pacinian-like receptive fields responded briskly to very light stimulation over a large area of the hand, as well as to taps to the table or the clay holding the hand. These units were not always tested for frequency-following responses at vibratory frequencies, yet fulfilled all other criteria for being responsive to input from Pacinian corpuscles. 2) Multiple digit receptive fields included more than a single digit. These units had response characteristics which were more consistent with the rapidly-adapting or slowly-adapting cutaneous inputs, and were essentially identical to responses seen in area 3b except for the large receptive field size. Neurons at these locations did not respond to taps to the table or clay and were not considered to have inputs from Pacinian corpuscles. 3) Single-digit receptive fields covered less than an entire single digit, with non-Pacinian response characteristics. 4) Palm receptive fields were located on the palm and were not classified as Pacinian-like. Finally, 5) Hairy skin receptive fields responded to movement of single hairs on the dorsal surface of the hand. In no instance did we find receptive fields that responded to both stimulation of the hairy and glabrous skin in area 3a, nor did we observe any receptive fields with both Pacinian-like and non-Pacinian components.

The cutaneous representation of the hand in area 3a of trained animals was highly variable between individuals when receptive fields were categorized as described above (Figure 44). In case EE-5 the majority of the cutaneous responses were classified as single digit and had small receptive fields (E-5, Figure 44D, see also Figure 49). In other monkeys the responses at many cortical locations were classified as Pacinian-like (EE-1, Figure 44A), or the majority of responses were classified as multiple-digit (EE-2,EE-3 Figures 44B and C, respectively). In each animal that showed a significant improvement in

FIGURE 44-46. Cutaneous representation of the hand in area 3a. Receptive fields were classified into five different categories. Filled circles denote cortical locations at which no cutaneous receptive field was defined. The heavy line denotes the physiologically defined 3a-3b border. Each panel illustrates a different animal. Figure 44 shows hemispheres representing hands trained in the task. Figure 45 shows the opposite hand control hemispheres, and Figure 46 shows the passive-stimulation control hemispheres. Monkey E-4 had no cutaneous receptive fields in area 3a and is not shown.

Figure 44

Area 3a Cutaneous Representation

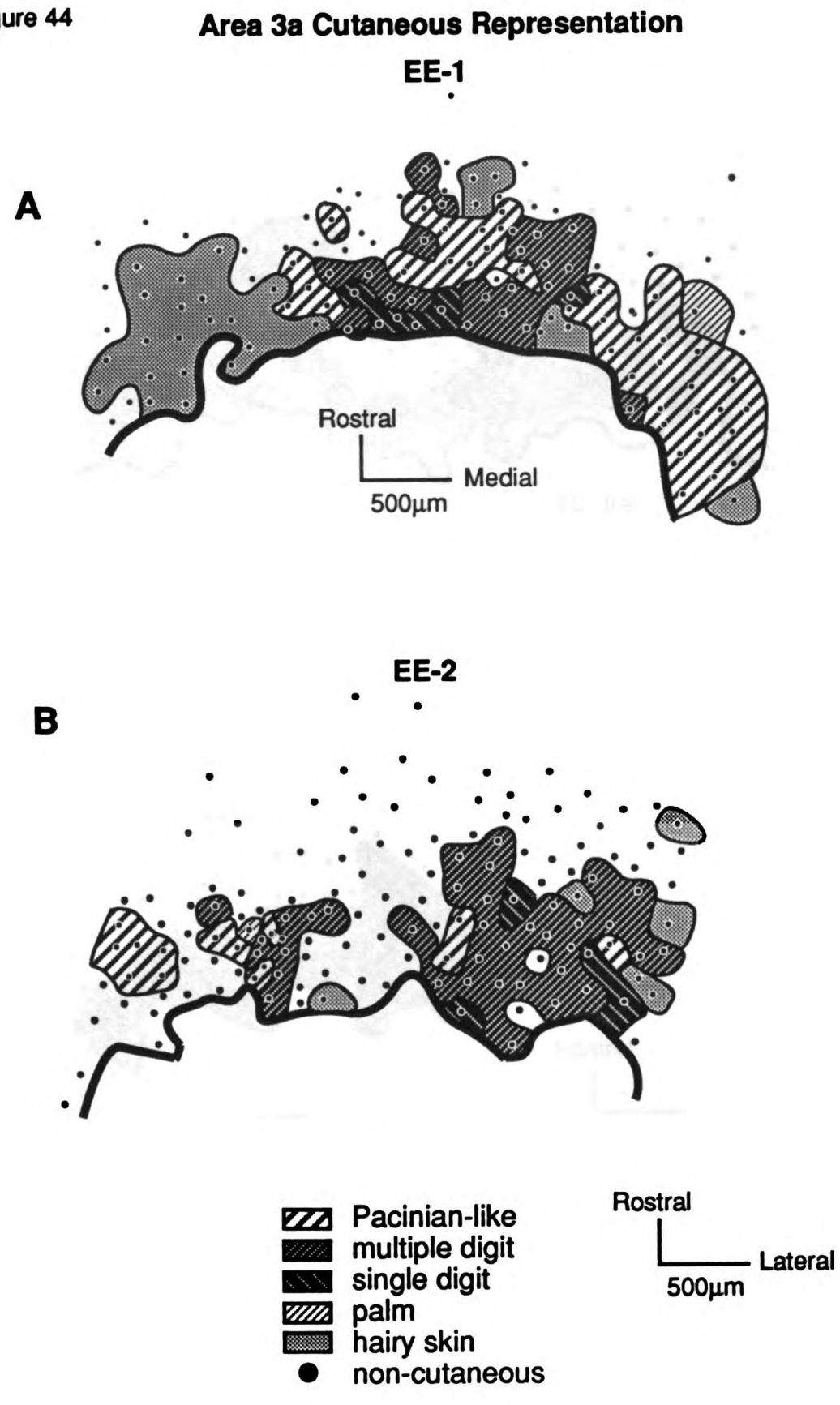

Figure 44 **Area 3a Cutaneous Representation**

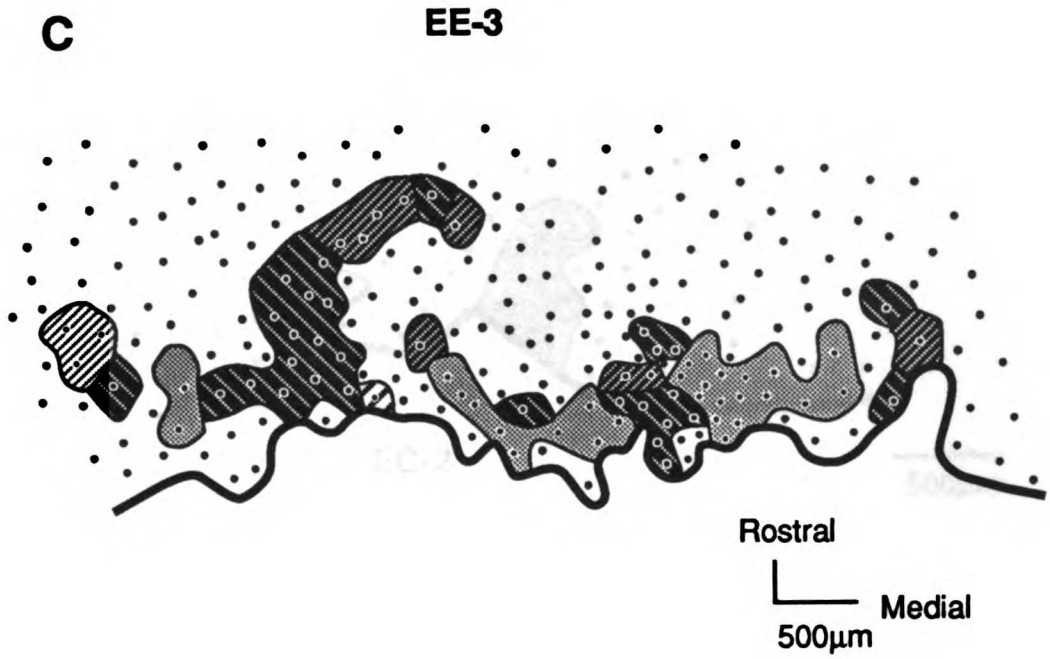

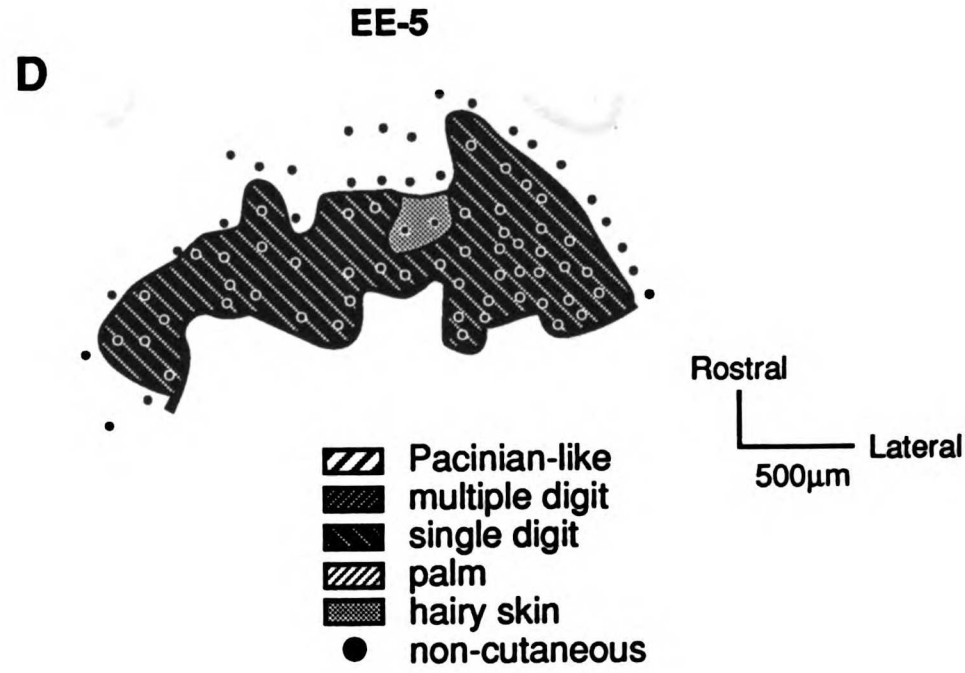

Figure 45 **Opposite Control Hemispheres**

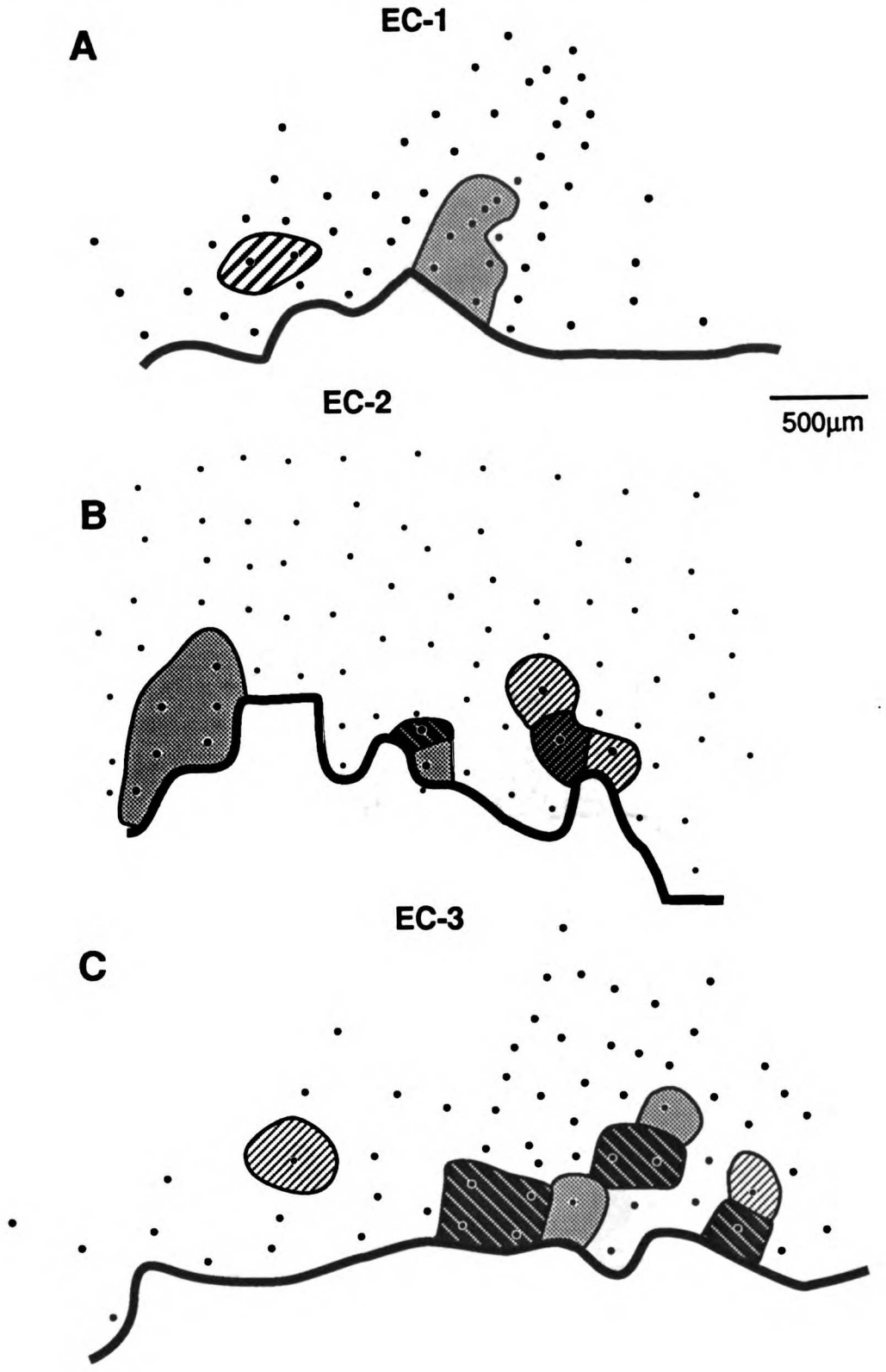

Figure 46 **Passive-Stimulation Control**

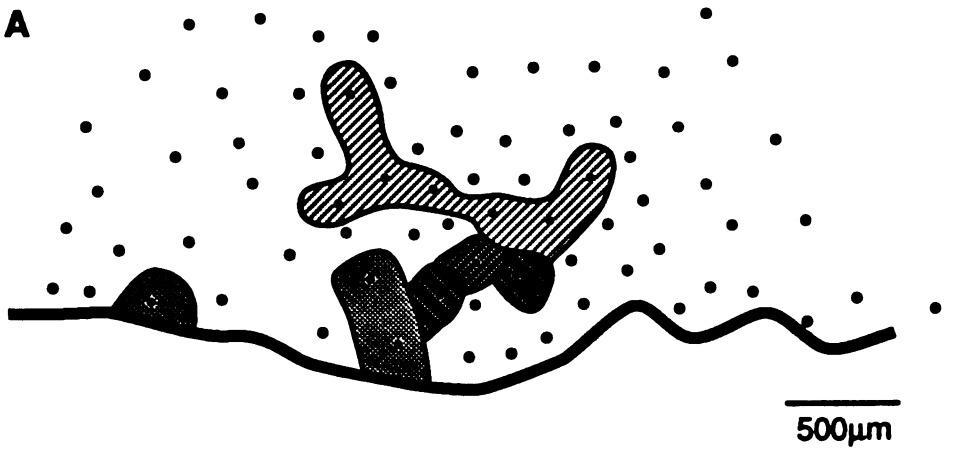

the discrimination threshold, the zone of cortical area 3a responding to cutaneous stimulation of the hand was significant.

By contrast, in the contralateral control hemispheres of the trained monkeys only a small zone of cortical area 3a was responsive to cutaneous stimulation (Figure 45). Most area 3a cutaneous receptive fields in these hemispheres responded to stimulation of the hairy skin. The representation of the glabrous skin was limited to the area near the 3a-3b border. Results from the passive-stimulation control animals were similar (Figure 46). In the case with the most prominent 3a cutaneous region, (Figure 46A) most of the cutaneous receptive fields recorded were located on the palm, with only three penetration sites representing the glabrous skin of the digits. In the other two cases only 1 and 3 cutaneous receptive fields were located on the digits.

Despite the cutaneous responses in area 3a, the physiological 3a-3b border was still distinctive. The receptive field classification, location, and size abruptly changed across this border. Examples of receptive fields recorded across this border are shown in Figure 47 for cases EE-5 and EE-2. In case EE-5 there was a clear reversal in the topographic location of receptive fields across the 3a-3b border. In each of the three examples shown, the receptive field reversed direction from progressing distally in area 3b (bold numbers) to progressing proximally in area 3a (italic numbers). In each case, the receptive field encountered before the reversal was located at the very distal tip of the digit, near or under the fingernail. This receptive field location is commonly encountered within area 3b at the 3a-3b border in normal owl monkeys (see Merzenich et a, 1978).

FIGURE 47. Examples of receptive field sizes and locations on either side of the physiologically defined area 3a-3b border. Numbers represent the caudal-to-rostral progression of receptive fields. Bold type denotes receptive fields defined in area 3b. Italic type denotes receptive fields defined in area 3a. Part A is from animal E-5. Digits 2 through 4 are shown left to right, respectively. Figurines represent the glabrous surface of the digits. "Under nail" denotes receptive fields not shown in the figure which were located on the glabrous skin immediately adjacent to the nail.

Figure 47

EE-5

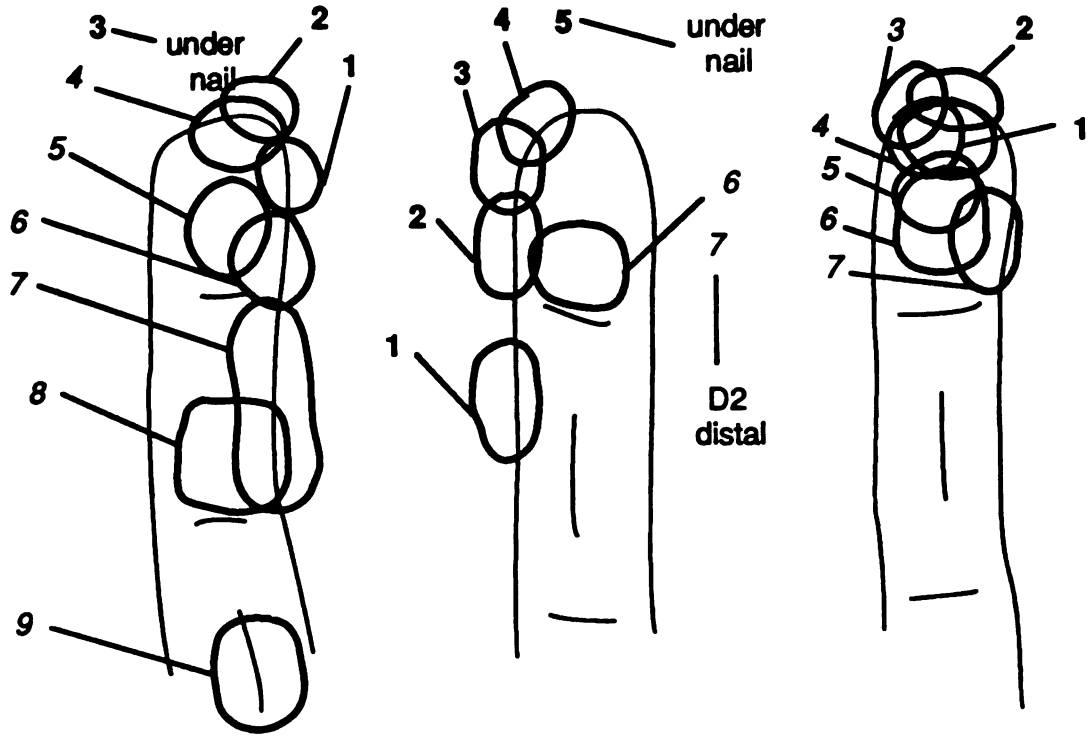

EE-2

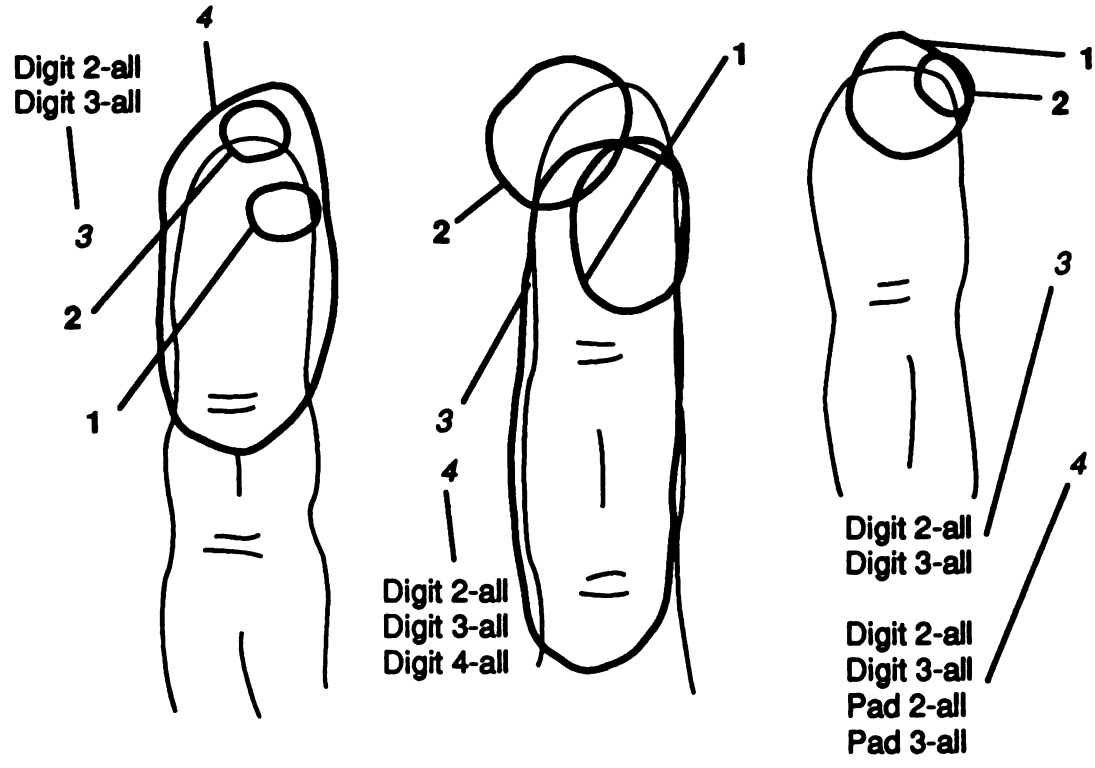

The definition of the 3a-3b border was also clear for the three other successfully trained monkeys. Case EE-2 is illustrated as a representative example of these hemispheres (Figure 47). Receptive field locations progressed in a distal direction in area 3b, as was seen in the control hemispheres. At the area 3a-3b border the receptive field either abruptly increased in size to include several digits (two of three cases illustrated), or increased in size and moved in location out of topographic sequence (middle example). These transitions were encountered in every caudal-to-rostral penetration sequence. These physiological distinctions made an estimation of this border unambiguous.

This physiological boundary closely corresponded to the cytoarchitectonic boundary between areas 3a and 3b. The transition between area 3b and 3a is most easily marked by an overall thickening of the cellular layers in area 3a, an increase in layer V thickness and a decrease in layer IV thickness. Location of the electrode tracts and electrolytic lesions in the histological material allowed for the alignment of the cytoarchitectonic boundary with the physiologically defined boundary. Figure 48 illustrates a section cut through the rostro-caudal axis aligned by an electrolytic lesion with the physiologically defined map for EE-1 The anatomical and physiological map are shown at the same scale. The cytoarchitectonic border between areas 3a (top) and 3b (bottom) was was in good agreement with the physiologically defined border. All other hemispheres that were studied were subjected to the same analysis and showed the same result.

In summary, a cutaneous representation of the hand in area 3a emerged in experimental hemispheres. This emergence was not seen in control

FIGURE 48. Alignment of the cytoarchitectonic area 3a-3b border with the physiologically defined border. The left shows a cresyl violet stained section cut in the parasagital plane as indicated by the thick vertical line to the right. The section is to the same scale as the physiologically defined map of case EE-1. The white matter is to the left, the pia is to the right, rostral is upward. An ink mark and a small part of an electrolytic lesion indicates the physiologically defined border, made at the time of the experiment. Cytoarchitectonically, area 3a is marked by the thicker cellular layer and more prominent layer V. Area 3b is marked by the overall thinner cellular layers, and a more prominent layers IV and VI. A short transition zone of approximately 300 μm separates these two distinct cytoarchitectonic areas. The alignment of the electrolytic lesion made at the physiological border (heavy black horizontal line), and the cytoarchitectonic border was seen in every studied hemisphere. Scale bar is 500 μm for both

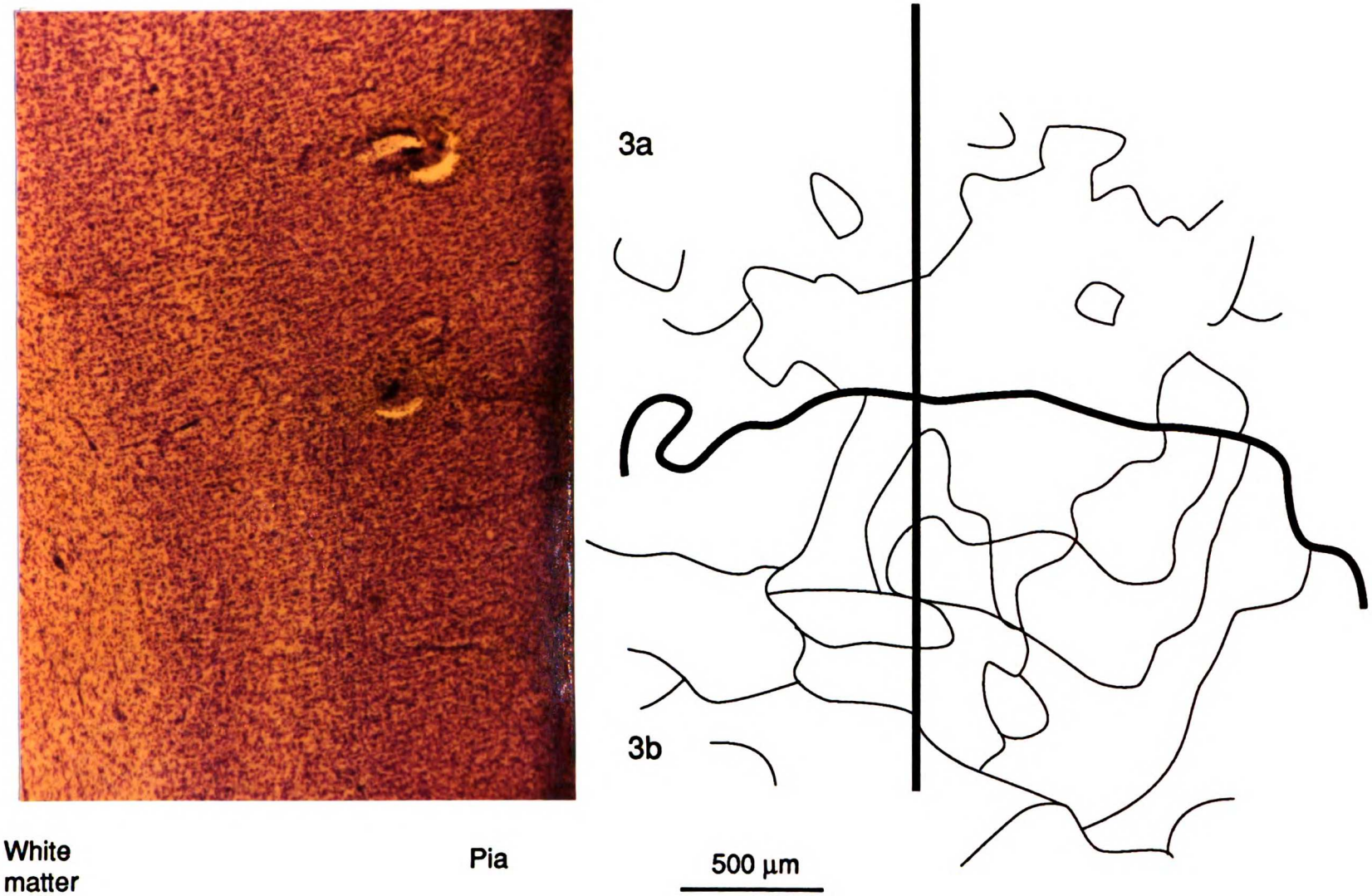
3a
3b
White matter
Pia
500 µm

hemispheres or passively-stimulated hemispheres. The area 3a cutaneous representation in experimental hemispheres showed considerable variation between individuals both in the area of representation and in receptive field characteristics. The border between cytoarchitectonic areas 3a and 3b was reliably estimated on the basis of physiological responses in all studied cases.

Receptive fields in area 3a

All non-Pacinian cutaneous receptive fields in area 3a recorded in two trained animals are shown in Figure 49. The small 3a receptive fields of EE-5 (Figure 49, top) were similar in their sizes to those defined in area 3b of the same case. There was a higher density of receptive fields that represented the stimulated skin (black circle on digit 2). Part B illustrates the receptive fields of EE-1, which were similar to those of the other two successfully trained animals (EE-2 and EE-3). These receptive fields were much larger than were those seen in area 3b. Virtually the entire skin surface of the hand was represented in area 3a even though the total cortical area of cutaneous representation was much smaller than was that of area 3b. Many receptive fields included multiple digits, and usually extended across a large aspect of each digit. The majority of these large receptive fields also included the trained skin as part of the receptive field. In all experimental hemispheres the density of receptive fields over the stimulated skin was significantly greater than the density of receptive fields over other digits. The few receptive fields defined on the control and passive stimulation hemispheres were varied in size. The absolute number of these receptive fields was too small to make any general comparisons.

In summary, the receptive field sizes in area 3a of hemispheres representing the trained hand in three animals were larger than were those

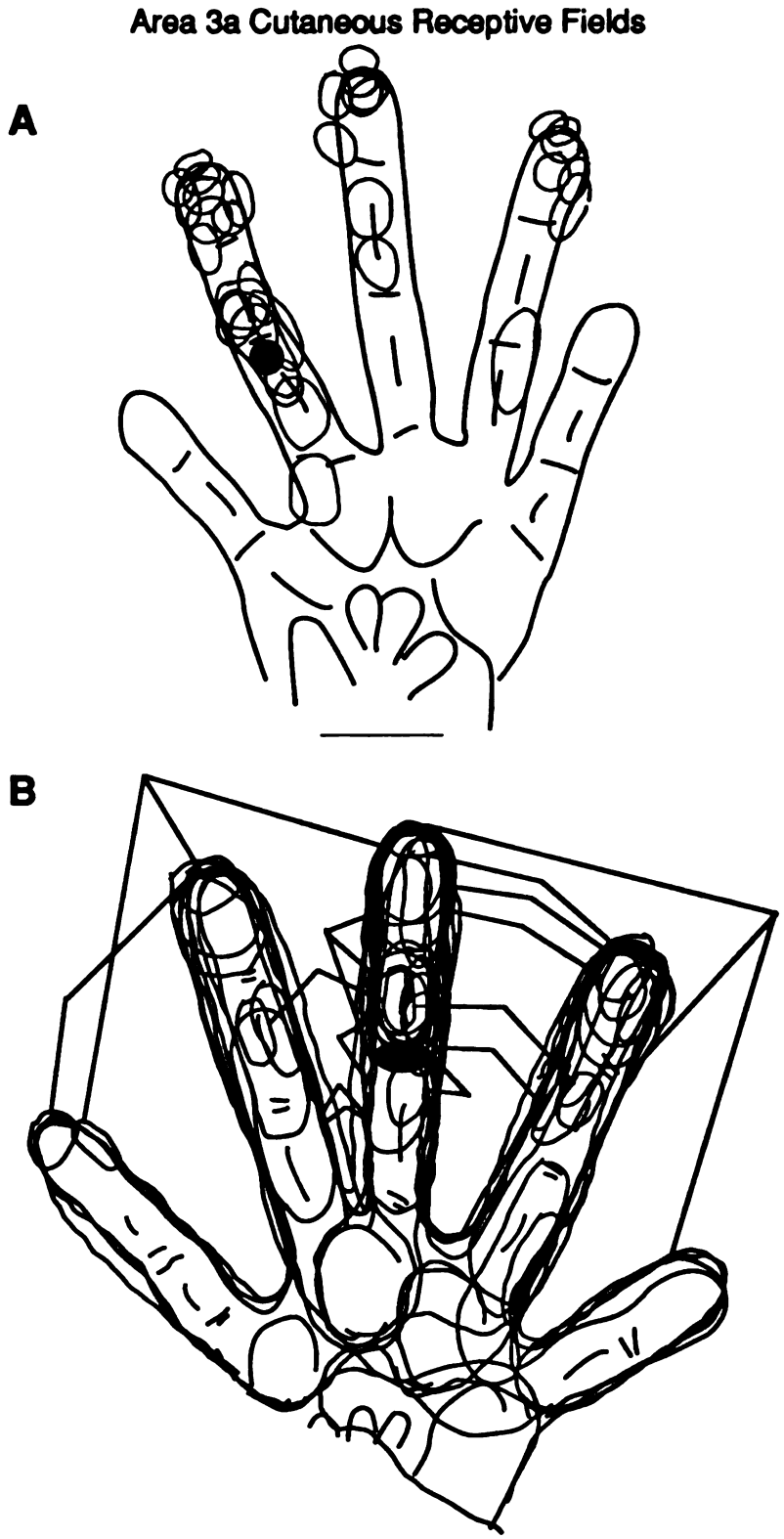

Figure 49. Cutaneous receptive fields defined in area 3a for case EE-5 (Part A, top) and case EE-1 (Part B, bottom). Pacinian-like receptive fields are not included. Straight lines join components of receptive fields on different digits. Black area denotes area of skin stimulated in the behavioral apparatus.

recorded in area 3b, and commonly included several digits. The receptive field sizes in area 3a of one well trained animal (E-5) were not significantly larger. In this animal, the receptive field sizes in area 3b were similarly small, and the discrimination thresholds were very low. Cutaneous receptive field sizes were varied in one trained animal with poor behavioral performance (E-4), in the contralateral control hemispheres and in the passive-stimulation control hemispheres. In these cases the cutaneous representations, and thus the sample size, were too small to make any general conclusions.

QUANTITATIVE RESPONSES

The behavioral task required the animal to discriminate temporal features of the stimulus. Improvements in discrimination performance might be expected to be reflected by differences in the temporal responses of cortical neurons to application of behaviorally relevant stimuli. To investigate this possibility the response to stimulation of the trained skin and to the corresponding skin of the adjacent digit was defined at all cortical locations that responded to sinusoidal stimulation of these skin locations. Data are presented below from six hemispheres: three experimental hemispheres (EE-1, EE-2, EE-3), two passive-stimulation control hemispheres (PS-2, PS-3), and the hemisphere representing the stimulated hand from the monkey which showed poor behavioral performance (ED-4).

Distribution of phase-locked responses

The first level of analysis defines the representation of cortical neurons providing temporal information about these behaviorally relevant stimuli. Cortical locations that showed temporal synchronization or "phase-locking" to

the tactile stimuli with a vector strength greater than 0.50 were considered to be 'frequency-following' and are the only locations included in this analysis (see *Methods*). The distribution of these locations for two experimental hemispheres are shown in Figure 50. The small dots represent cortical locations tested that did not have a frequency-following response. The area in which cortical neurons responded in a frequency-following manner is much greater for the trained skin (open circles) as compared to the adjacent digit (filled circles) or for both digits (stippled circles). The trained skin was represented over a large continuous area within the hand representation in area 3b, as well as in discontinuous regions scattered throughout both area 3b and area 3a. Many locations with receptive field centers away from the stimulated skin, sometimes on different digits, nonetheless provided temporal information about this behaviorally significant stimulation.

The cortical locations with frequency-following responses to stimulation of the adjacent digit were much fewer in absolute number. These cortical locations were also scattered throughout area 3b. The cortical locations with frequency-following responses to this low-frequency stimulation was also significant, particularly in area 3a. The total number of penetrations with frequency-following responses in area 3a was about half that found in area 3b. Results from case EE-3 (not shown) were similar.

The distribution of frequency-following responses in the two passively-stimulated hemispheres studied were much more limited in location number and area of distribution (Figure 51). The distribution of frequency-following responses was consistent with the estimated area of representation of this skin in cortical area 3b based on receptive field definitions (Compare Figure 51 with

FIGURE 50-51. Cortical locations with frequency-following responses in two experimental hemispheres (Figure 50) and two passive-stimulation control hemispheres (Figure 51). Open circles denote cortical locations with frequency following responses to stimulation of the trained or stimulated skin. Filled circles denote cortical locations with frequency following responses to stimulation of a corresponding site on the adjacent digit. Stippled circles denote cortical locations with frequency following responses to stimulation on both the trained and adjacent digit skin. Small filled circles denote cortical locations in which no frequency-following response was observed.

Figure 50

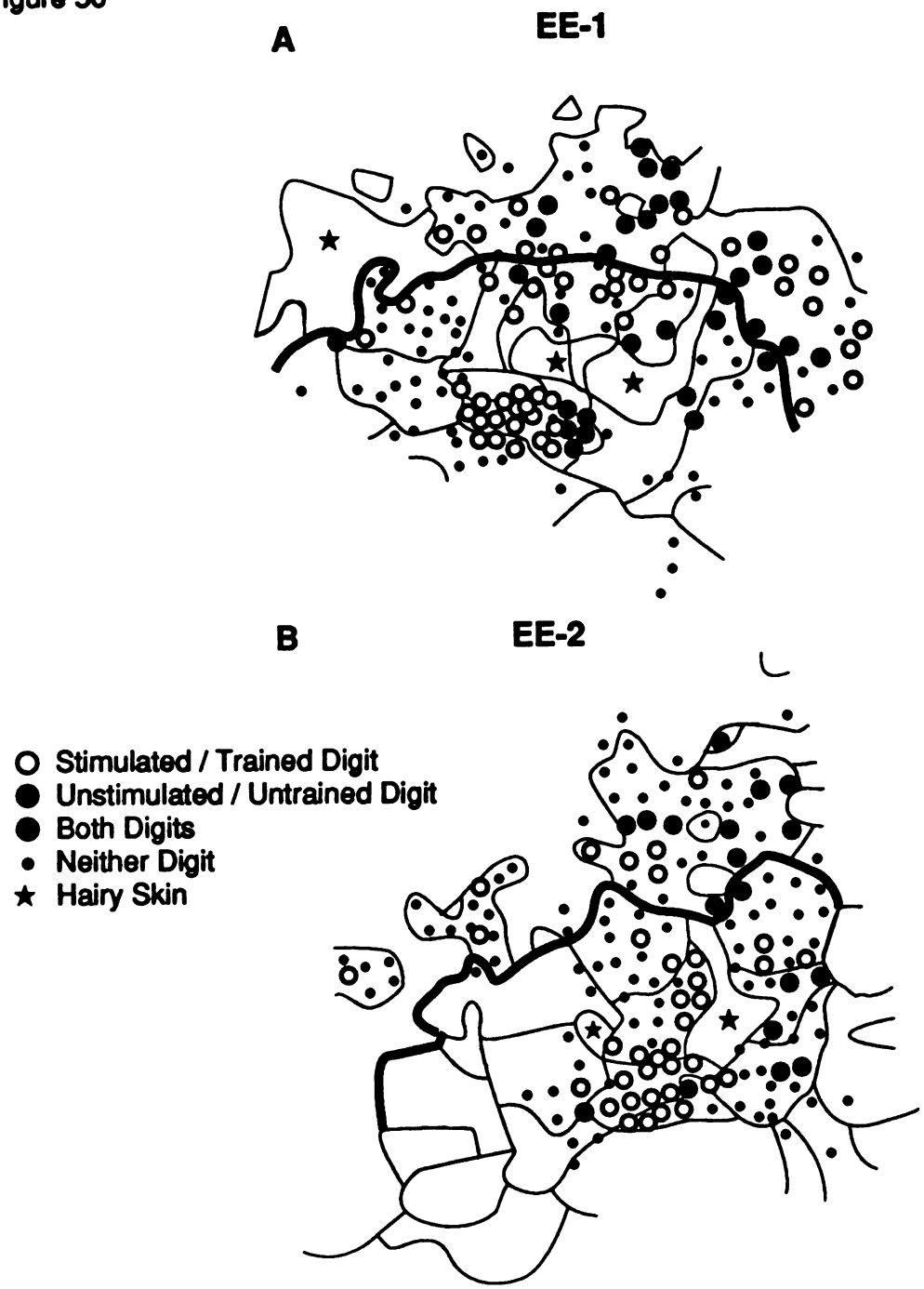
A
EE-1
B
EE-2
Stimulated / Trained Digit
Unstimulated / Untrained Digit
Both Digits
Neither Digit
Hairy Skin

Figure 51

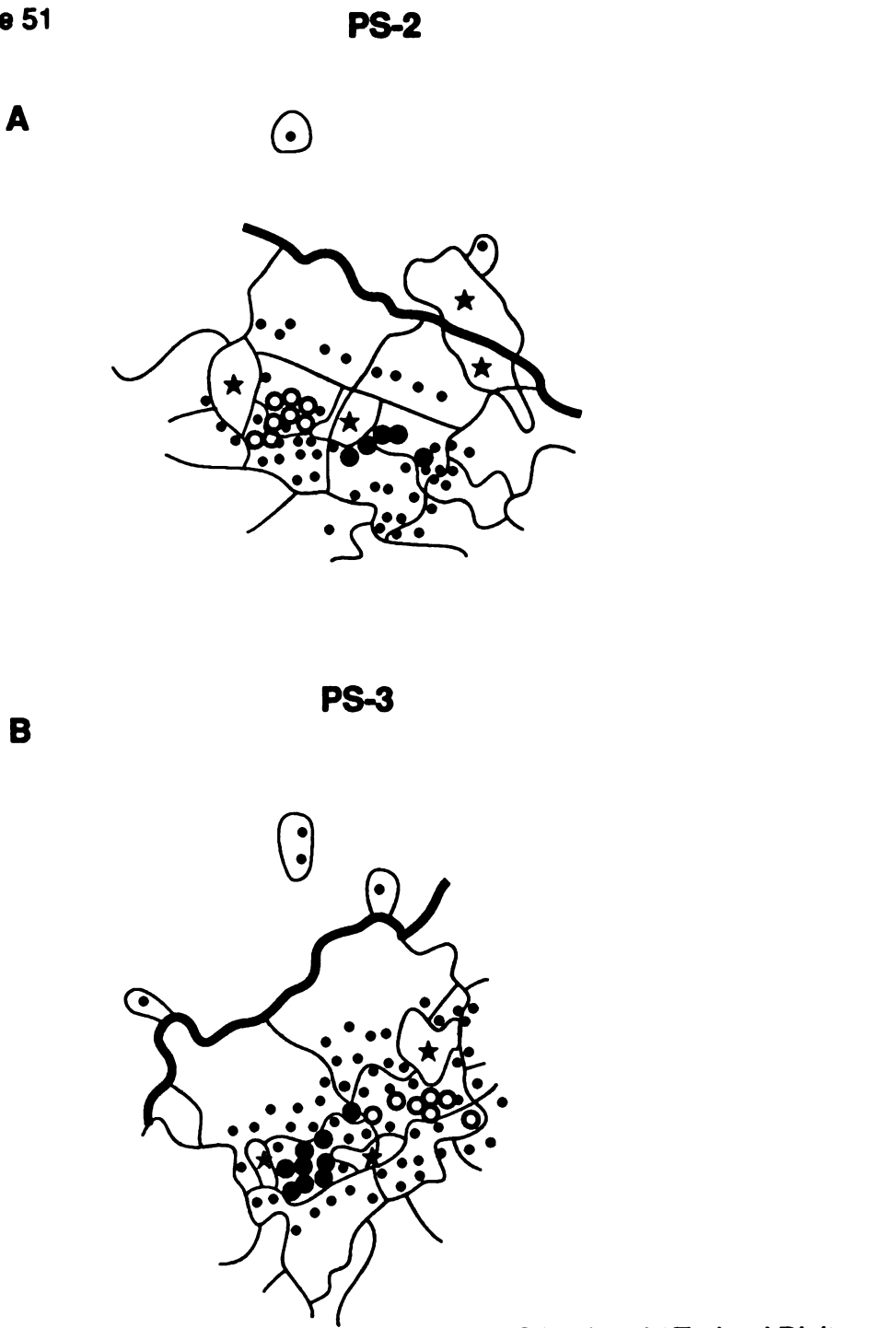
PS-2
A
PS-3
B
Stimulated / Trained Digit
Unstimulated / Untrained Digit
Both Digits
Neither Digit
Hairy Skin

Figure 28). The distributions of entrained responses were similar for both the stimulated and adjacent digits in these hemispheres.

The total area of cortex with entrained responses to stimulation of these two skin surfaces is summarized for all six cases in Figure 52. The experimental hemispheres (top panel) show a much larger representation of the trained skin (cross-hatched bars) when compared to the representation of the adjacent digit. These areas were significantly smaller in the two passively-stimulated monkeys. Monkey E-4, which did not show an improvement in performance, nonetheless did have a greater area of representation of frequency-following responses to stimulation of the trained digit when compared to an adjacent, untrained digit.

An important issue when determining the temporally-locked responses of multiple-unit records is how many neurons are being recorded from at each cortical location. As described in Methods, the window discriminator was set such that only large amplitude waveforms characteristic of single neurons were studied. Smaller amplitude "hash" responses were not collected. The accepted waveforms appeared by eye to be composed of 3-5 single neurons. A second method to estimate the number of neurons recorded from at each location is to take advantage of the response properties of SI neurons to this type of flutter-frequency tactile stimulation. The responses of single neurons in SI in the awake macaque to stimuli that are essentially identical to those used in this study have been extensively studied (Mountcastle et al 1969, 1990; LaMotte and Mountcastle 1975; Hyvarinen et al 1980; see also Gardner 1988). In these studies, single neurons responded with 1-4 action potentials for every stimulus cycle presented to the skin. In order to estimate the number of responses per stimulus cycle in this study, the average number of accepted waveforms per

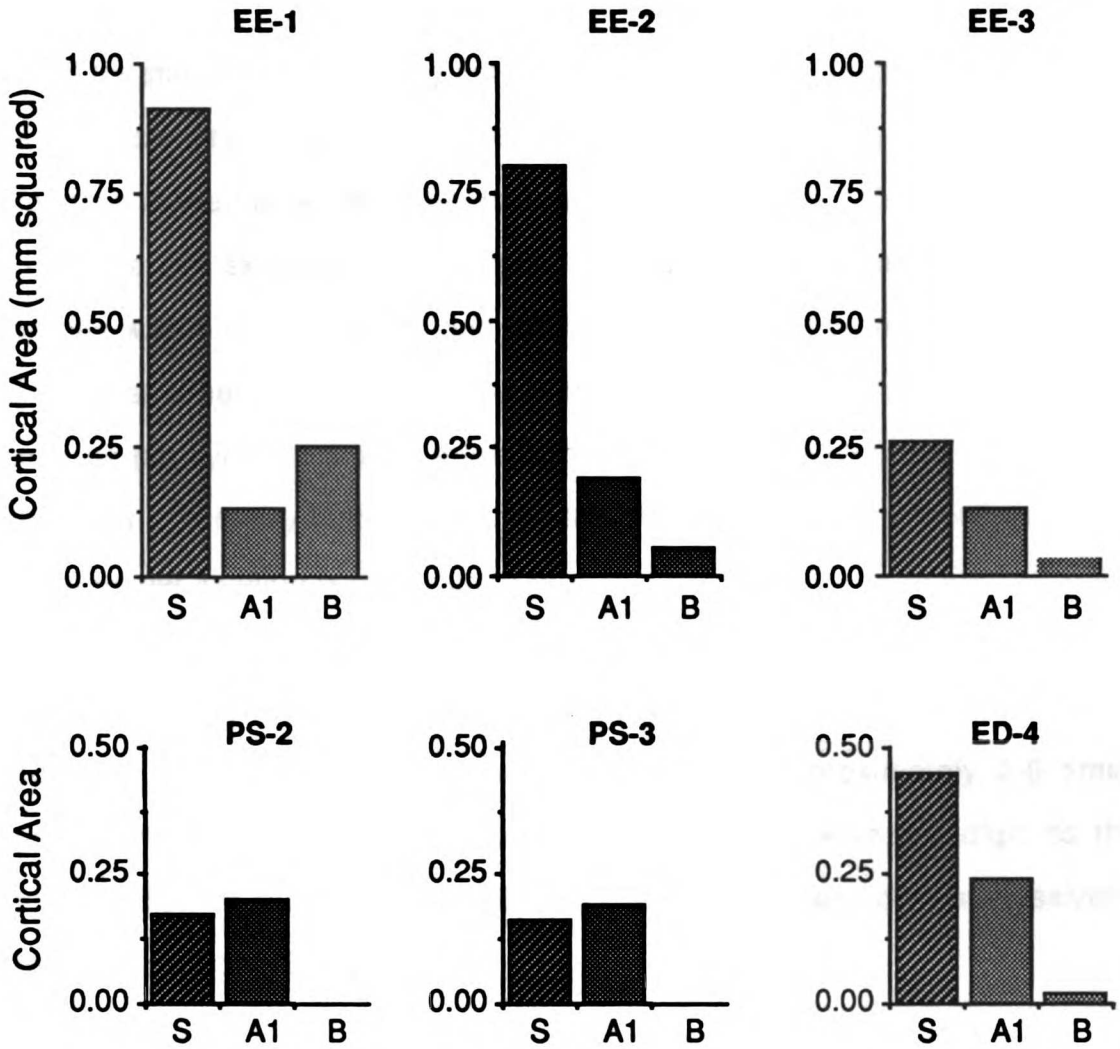

Figure 52. Cortical area of representation of frequency-following responses to stimulation of the trained or stimulated digit (S), to stimulation of the adjacent, untrained digit (A) or to both digits (B). Trained hemispheres are shown in the top panel, the two passively-stimulated control hemispheres and the stimulated hemisphere of monkey E-4 are shown across the bottom panel.

cycle was calculated for every cortical location that responded in a frequency following manner. These locations were pooled as responding to either a trained (or stimulated) digit or to the adjacent, unstimulated digit. The results of this analysis are shown in Figure 53, where the filled symbols represent responses to the trained skin site, and the unfilled symbols represent responses to the adjacent skin site. The largest average response seen in all cortical locations was 8 spikes / cycle, and the majority was less than five. This result implies that either neurons recorded in this preparation respond with less than one spike per cycle, or that no more than 8 neurons were recorded in any given penetration. In reality both possibilities are probably true and the estimate of 3-5 neurons per location is an accurate one.

In summary, the total area of the representation of frequency-following responses to stimulation of the trained skin were approximately 2-6 times greater when compared to the representation of the adjacent digit, to the representation of the stimulated digit, or to the adjacent digit in passively-stimulated control animals.

Receptive fields of Frequency-following locations

All cutaneous receptive fields were defined with punctate stimuli using the criteria of just-visible skin indentation with small diameter probes. At some cortical locations that responded in a frequency following manner, the receptive field defined as above did not include the stimulation site. It was of interest to compare the receptive field properties of locations providing precise temporal information about the behaviorally relevant stimuli. Results from all animals are shown in Figures 54 and 55. The receptive fields are shown for cortical locations that had frequency following responses to stimulation on the trained

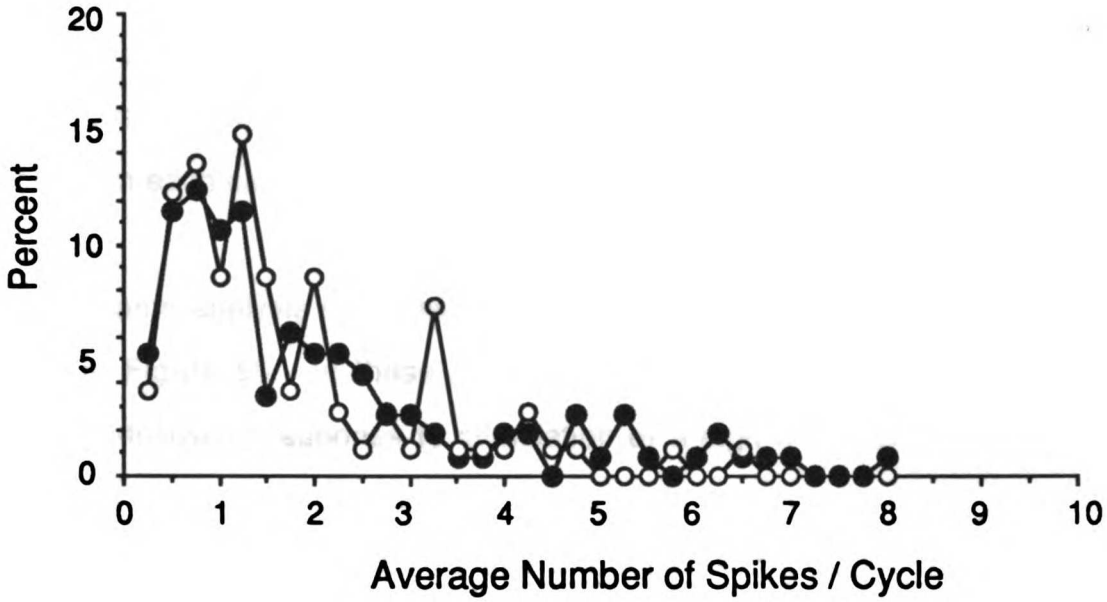

Figure 53. Distribution of the mean number of spikes recorded from for each stimulus cycle. Data are pooled for all locations responding to stimulation of the trained digit (filled circles) and all locations responding to the adjacent digit (open circles). Data are expressed as a percentage of the total number of locations responding.

digit (left) and the adjacent digit (right). In each case the majority of receptive fields included the stimulated skin, however several clear exceptions were observed. Animal EE-1, for example, had several receptive fields located on the distal phalanges of the adjacent digits, as well as on the stimulated digit. These receptive fields did not overlap the trained skin. Similar examples were recorded in each case.

The same analysis of the two passive-stimulation control hemispheres are shown in Figure 55. In these two cases all cortical locations which had a frequency-following response to stimulation of a digit had their receptive field located on the same digit. These receptive fields were much smaller than were those on the experimental hands and did not extend onto the adjacent digit. Most receptive fields overlapped with the stimulation site.

In summary, the majority of cortical locations that responded in a frequency-following manner also represented the stimulated skin as part of their receptive field. Some exceptions were observed in each of the trained hemispheres, where receptive fields could be located on the adjacent digit. Smaller disparities were noted in passive-stimulation control hemispheres.

Temporal coding of behavioral frequencies

The above analysis showed that the absolute number of cortical locations faithfully representing the temporal features of stimulation on the trained skin was increased in successfully trained animals. The next level of analysis was directed toward determining if the precision of temporal entrainment itself was modified with training, and if this modification could account for the improvement in discrimination thresholds in these animals. To qualitatively

Figure 54

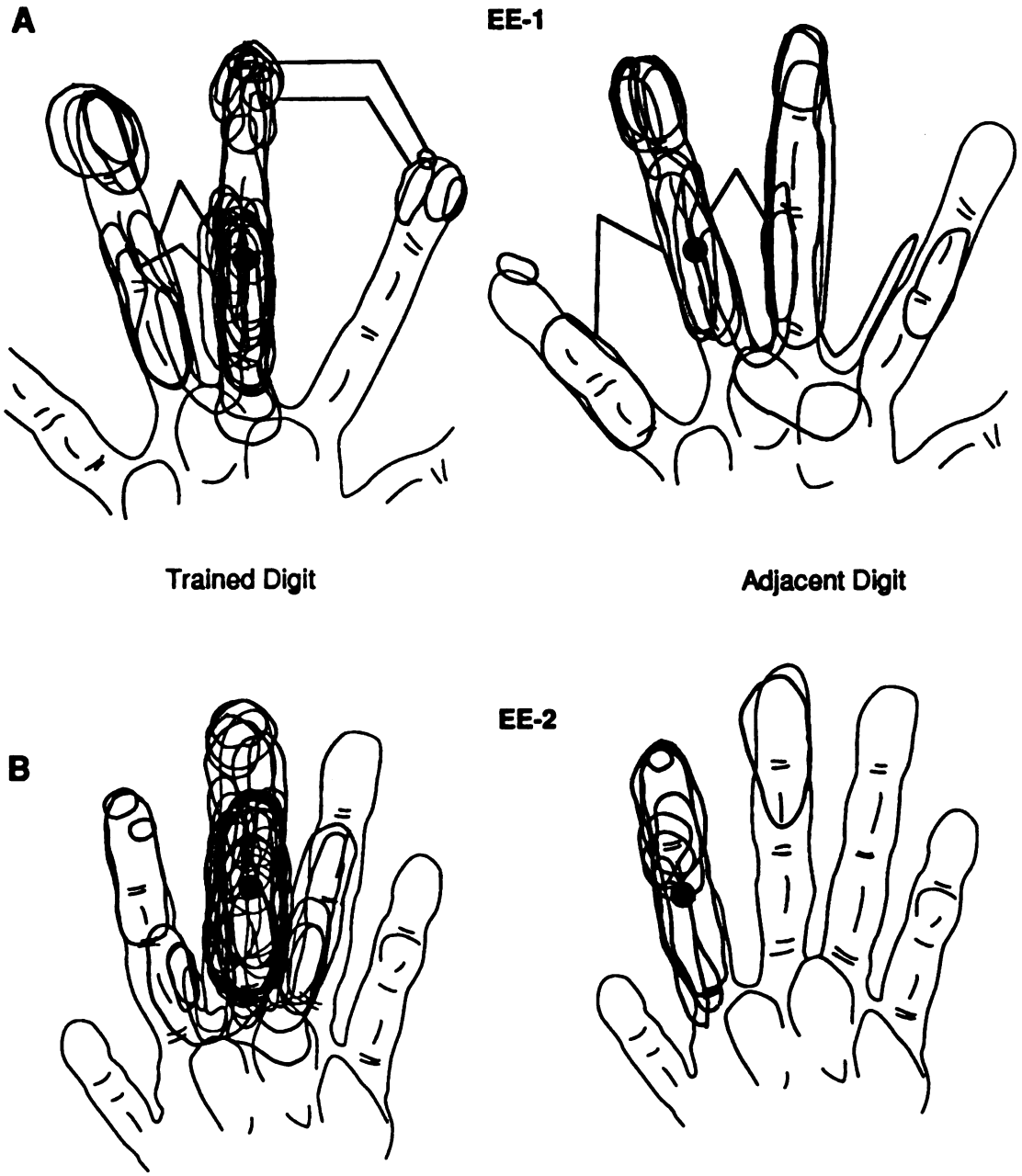

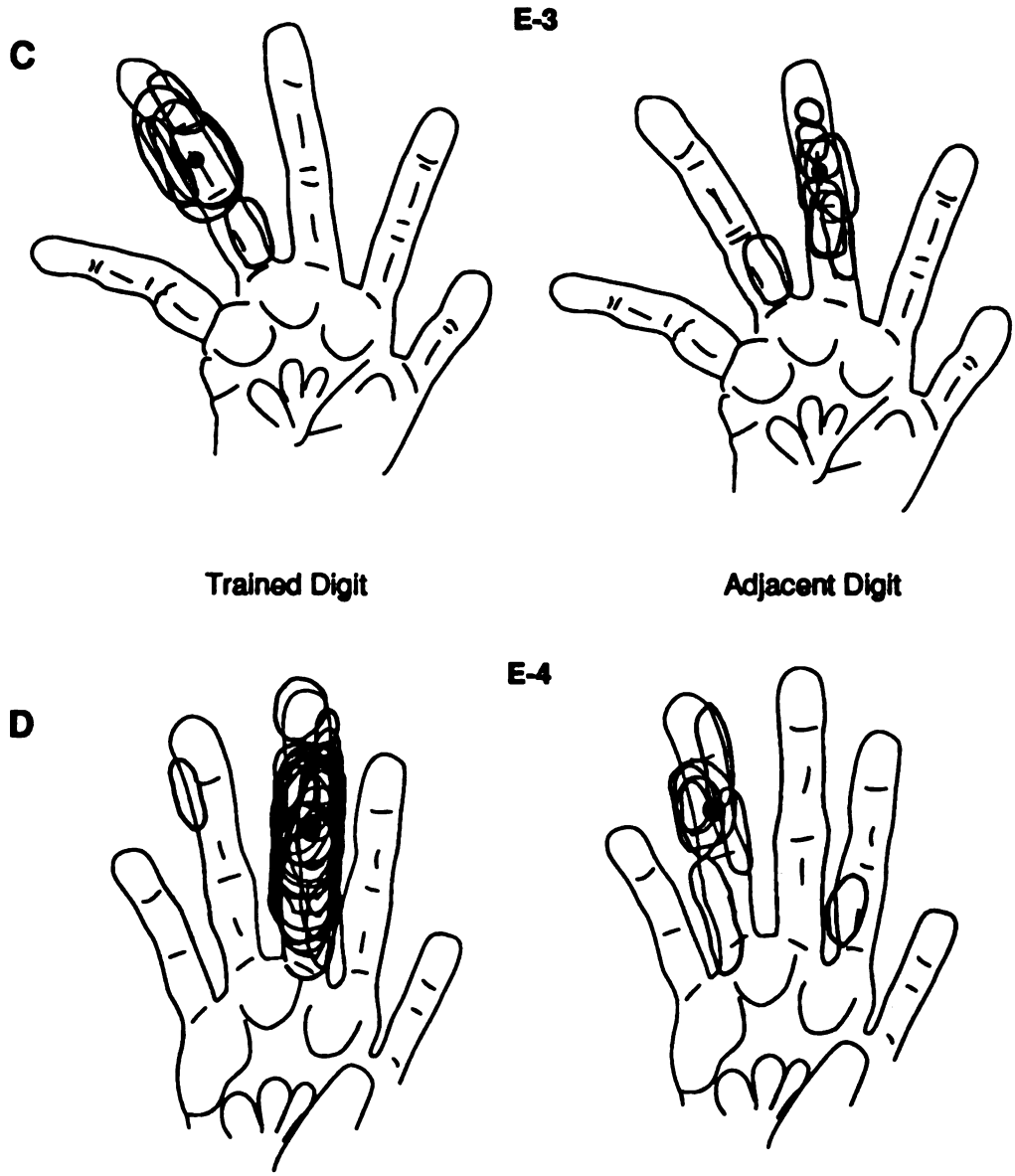

Figure 54. All receptive fields defined with frequency-following responses in aea 3b to stimulation of the trained digit (left panel) or the corresponding location on an adjacent, untrained digit (right panel) Data are derived from cases EE-1 (Part A, previous page), EE-2 (Part B), EE-3 (Part C) and EE4 (Part D).

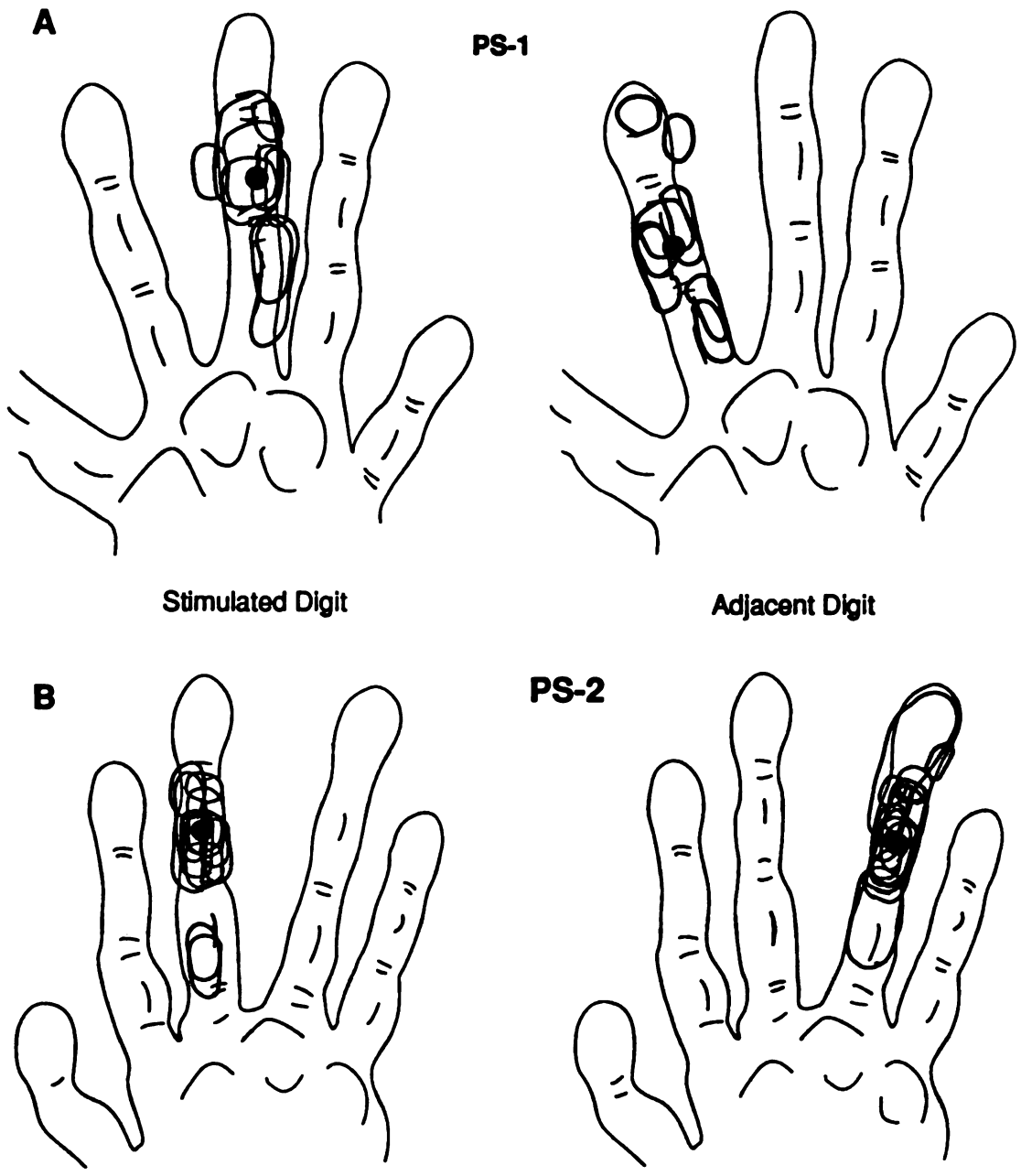

Figure 55. All receptive fields with frequency-following responses in area 3b to stimulation of the skin region stimulated in the behavioral apparatus (left panel) or the the corresponding region of skin on the adjacent digit (right panel). Data are taken from the two passively-stimulated control monkeys, PS-2 (Part A) and PS-3 (Part B).

measure the entrainment of the neural response to the tactile stimulus, the vector strengths at each of five different frequencies at all cortical locations with a frequency-following response were measured. Vector strength (see *Methods*) varies from 0 (no entrainment, the response in not dependent on the stimulus cycle) to 1.0 (perfect entrainment, the response always occurs at the same phase of the stimulus cycle).

An alternative possibility is that individual neurons are 'tuned' to a specific frequency. This could be reflected by either: 1) the vector strength reaching a maximum at a single 'best' frequency, or 2) by neuronal firing rates reaching a maximum at a single 'best' frequency.

Vector strength analysis

The results of this analysis are presented in Figures 56 and 57, where the vector strength at each cortical location is plotted as a function of frequency. Each column shows the data from a single digit of one monkey. The vector strength functions were arbitrarily categorized into three classes for clarity of view: 1) Flat functions, in which the vector strength did not change as a function of frequency; 2) sloping functions, in which the vector strengths either increased or decreased with increasing frequency; 3) tuned functions, in which the vector strengths showed local maxima or minima as a function of frequency.

The main result of this analysis was that there was no consistent difference in the vector strength functions that could account for the difference in behavior. The sloping functions were very steep and downward for case EE-1, but they were similar to those of case PS-2, which was not trained at the task, and steeper than case EE-2, whose behavioral performance was slightly better than

FIGURE 56-57. Vector strength plots for each cortical location with a frequency following response to stimulation of the trained skin in experimental animals E-1 (Part A) and E-2 (Part B) in Figure 56, and from two control monkeys E-4 (Part A) and P-3 (Part B) in Figure 57. Each line represents the vector strength at a single cortical location for each of five frequencies plotted on the x-axis. Responses were arbitrarily classified into three categories for clarity: flat functions (top), sloping functions (middle) and tuned functions (bottom).

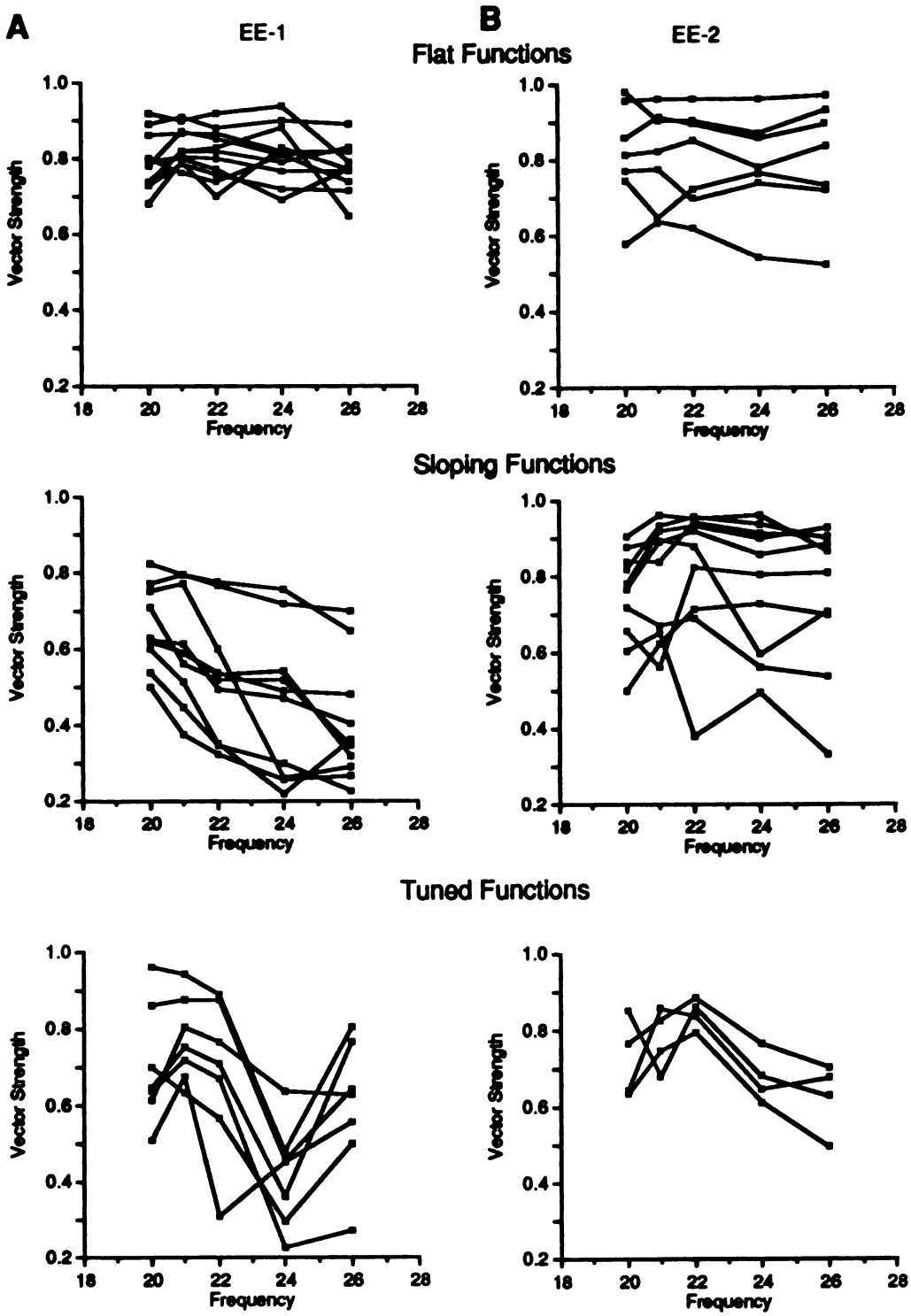
A
EE-1
B
EE-2
Flat Functions
Sloping Functions
Tuned Functions
Vector Strength
Frequency
1.0
0.8
0.6
0.4
0.2
18
20
22
24
26
28

Figure 57

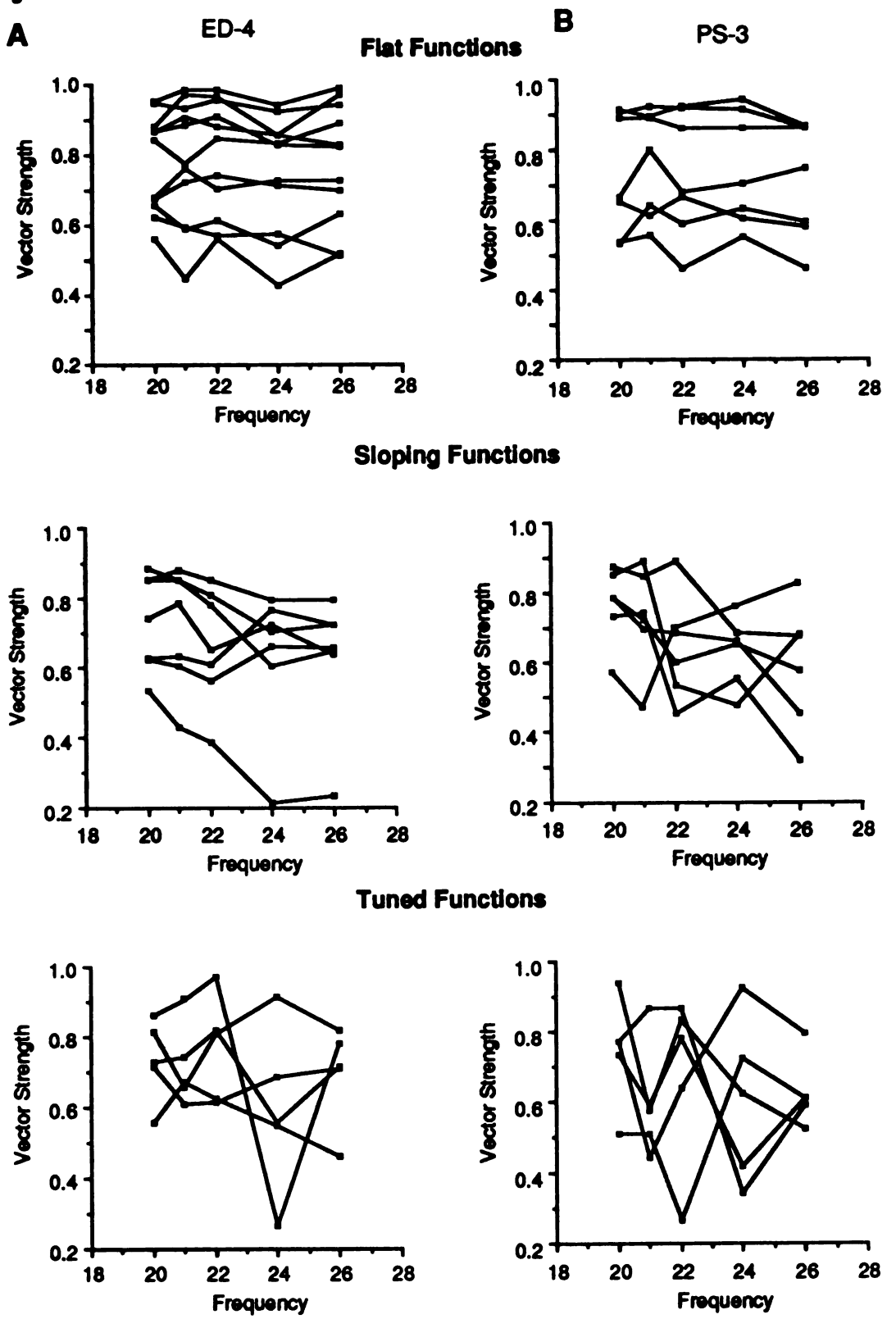
A
ED-4
B
PS-3
Flat Functions
Sloping Functions
Tuned Functions
Vector Strength
Frequency
1.0
0.8
0.6
0.4
0.2
18
20
22
24
26
28

EE-1. The sloping functions for EE-2 and ED-4 were very similar, although the behavioral performance of these two animals was much different. The sloping functions of EE-2 were mostly upward. The responses at single sites in the other three well-trained animals did not have remarkable upward functions.

The tuned functions show inconsistent differences between cases. EE-1 had functions with minima at 24 Hz, which was above threshold, while EE-2 had functions with maxima at 22 Hz, which was below threshold. The other two hemispheres did not have a consistent tuned function. The analysis of vector strengths does not reveal a consensus of how the animal could have used this temporal information to make frequency discriminations. These data indicate that each individual animal may have used a different class of responses: downward functions in EE-1, upward sloping functions and tuned functions for 22 Hz in EE-2.

The vector strength plots for the adjacent digits were similar to those seen in the control hemispheres. However, there were very few locations with vector strengths greater than 0.5 (see Figure 50). Inspection of these functions did not show a clear distinction from those of Figures 56 and 57.

Firing rate analysis

A second parameter that may be used to code the frequency of a stimulus is the overall firing rate. The number of stimulus cycles occurring over a given time will increase with stimulus frequency. To test this possibility, the absolute number of spikes during a 350 msec window starting at stimulus onset was counted. The firing rates for each penetration at five different frequencies are shown as single functions for two experimental hemispheres in Figure 54. The

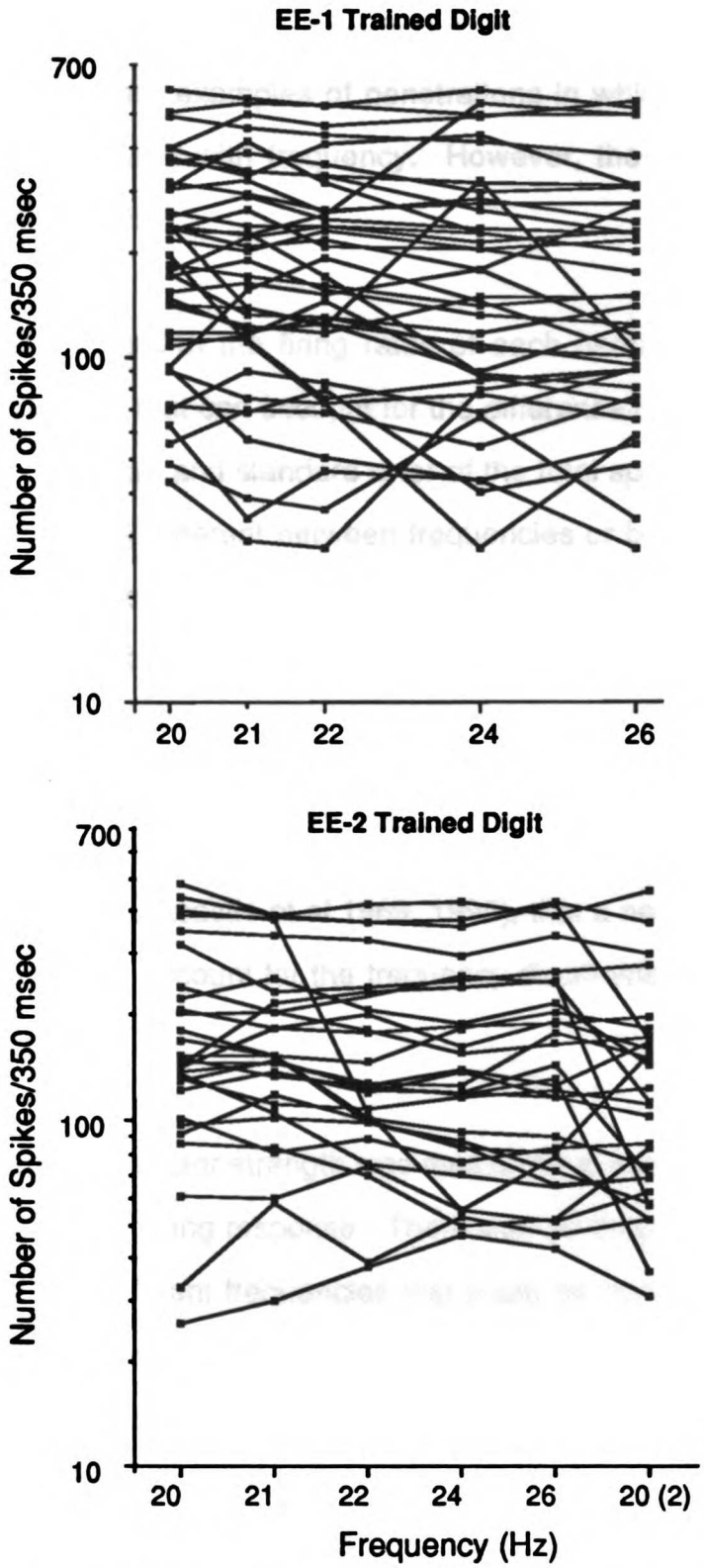

Figure 58. Total number of spikes taken during a 350 msec period of stimulation at each frequency shown on the x-axis. Each line represents the data from one cortical location. Response to stimulation of the trained digit of EE-1 is shown in (A), case EE-2 in (B).

overall firing rate could vary considerably between penetrations (note log scale), and there were examples of penetrations in which the firing rate either increased or decreased with frequency. However, the overall slope of these lines is very near 0 (flat).

Statistical analysis of the firing rates of each hemisphere do not show a significant difference that can account for the difference in performance (Figures 59 and 60). The mean and standard error of the total spikes for each frequency were not consistently different between frequencies or between the trained and adjacent digits in the experimental hemispheres (Figures 59) or in the control hemispheres (Figure 60). Small increases in frequency resulted in a slight decrease in the magnitude of the response. Statistical comparisons, however, did not reveal a consistent difference between the 20 Hz comparison frequency and larger, discriminable frequencies. It is concluded, consistent with the reports of others (Mountcastle et al 1969, 1990), that a neural rate code in these cortical areas cannot account for the frequency discrimination abilities of trained monkeys.

In summary, the vector strength was measured at each cortical location that gave a frequency-following response. There was no consistent difference in the vector strength at different frequencies that could be correlated with or account for the behavioral performance of the trained monkeys. Similar analysis of the firing rate at each cortical location was conducted. This measure was also inadequate to reveal possible mechanisms to explain the monkey's ability to discriminate differences in frequency.

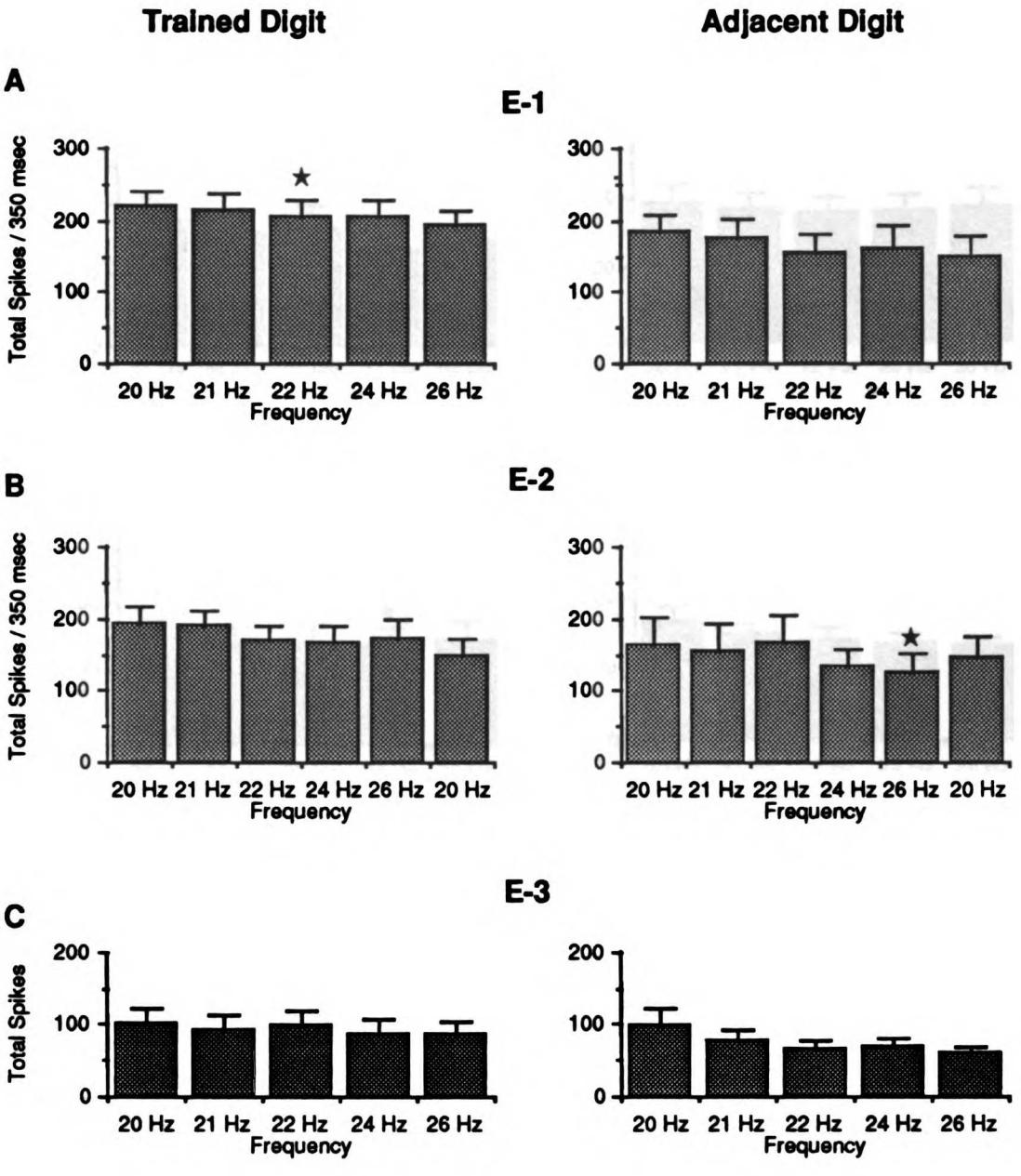

Figure 59. Mean and standard error of total number of spikes recorded at each cortical location for each of five presented frequencies. All statistical comparisons were made relative to the 20 Hz standard. Stars denote P values <0.05 (two-tailed t-test). Results from stimulation of digits trained in the task are shown on the left, results from adjacent, untrained digits are shown on the right. All data are from well-trained monkeys.

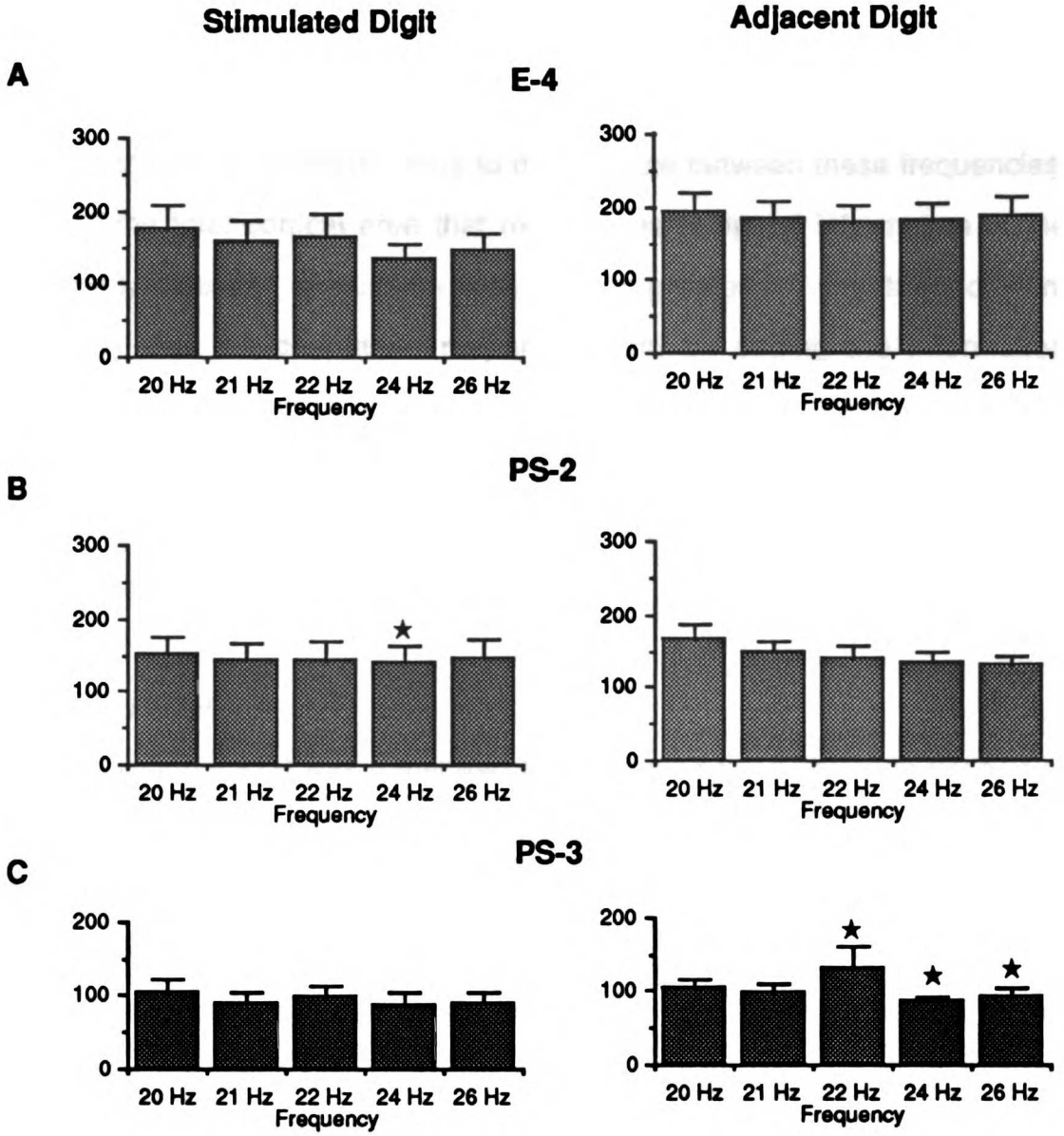

Figure 60. Mean and standard error of total number of spikes recorded to stimulation of the digit stimulated in the behavioral apparatus (left) or to the adjacent, untrained digit (right) in three control monkeys. Stars indicate P values <0.05. All statistical comparisons were made relative to the response recorded at 20 Hz.

Population Analysis

The analysis of neural responses to stimulation at the behaviorally relevant frequencies, when considered on a location-by-location basis, did not show a clear correlate to the animals' ability to discriminate between these frequencies. However, the total cortical area that represented temporal information of the behaviorally relevant stimulation was clearly greater for the trained skin, suggesting that the population response could be coding the information necessary for the animal to make the discrimination. To address this possibility, the temporal responses of all cortical locations with frequency following responses were summed to derive population PSTHs and cycle histograms (see *Methods*).

Population PSTH

A population PSTH was generated by combining the spike data defined at all locations at which a frequency-following response was recorded for stimulation at each designated skin site. All spikes were summed into 2 ms time bins. The results of this analysis demonstrate an increase in both the absolute response magnitude as well as an increase in the temporal fidelity of the response for the trained digit. The population PSTHs for the trained and the adjacent untrained digit for case EE-1 (Part A) and EE-2 (Part B) are shown for two frequencies in Figure 61. Note that these responses are not normalized, but are plotted on the same scale. The two most obvious differences between these representations of the trained and untrained digits were: 1) An increase in the overall response to stimulation of the trained digit (upper), and 2) an overall increase in the temporal fidelity of the response to each cycle of the stimulus presented to the trained digit. The better representation of the individual cycles of the stimulus presented to the trained digit is clearest for

FIGURE 61. Population peri-stimulus time histograms from two experimental animals. The PSTH to a 20 Hz stimulus is shown at the left, and to a 26 Hz stimulus at the right. Parts A and B are from animals E-1 and E-2, respectively. For each animal, the PSTH to stimulation on the trained digit (above) and an adjacent control digit (below) are shown.

Figure 61

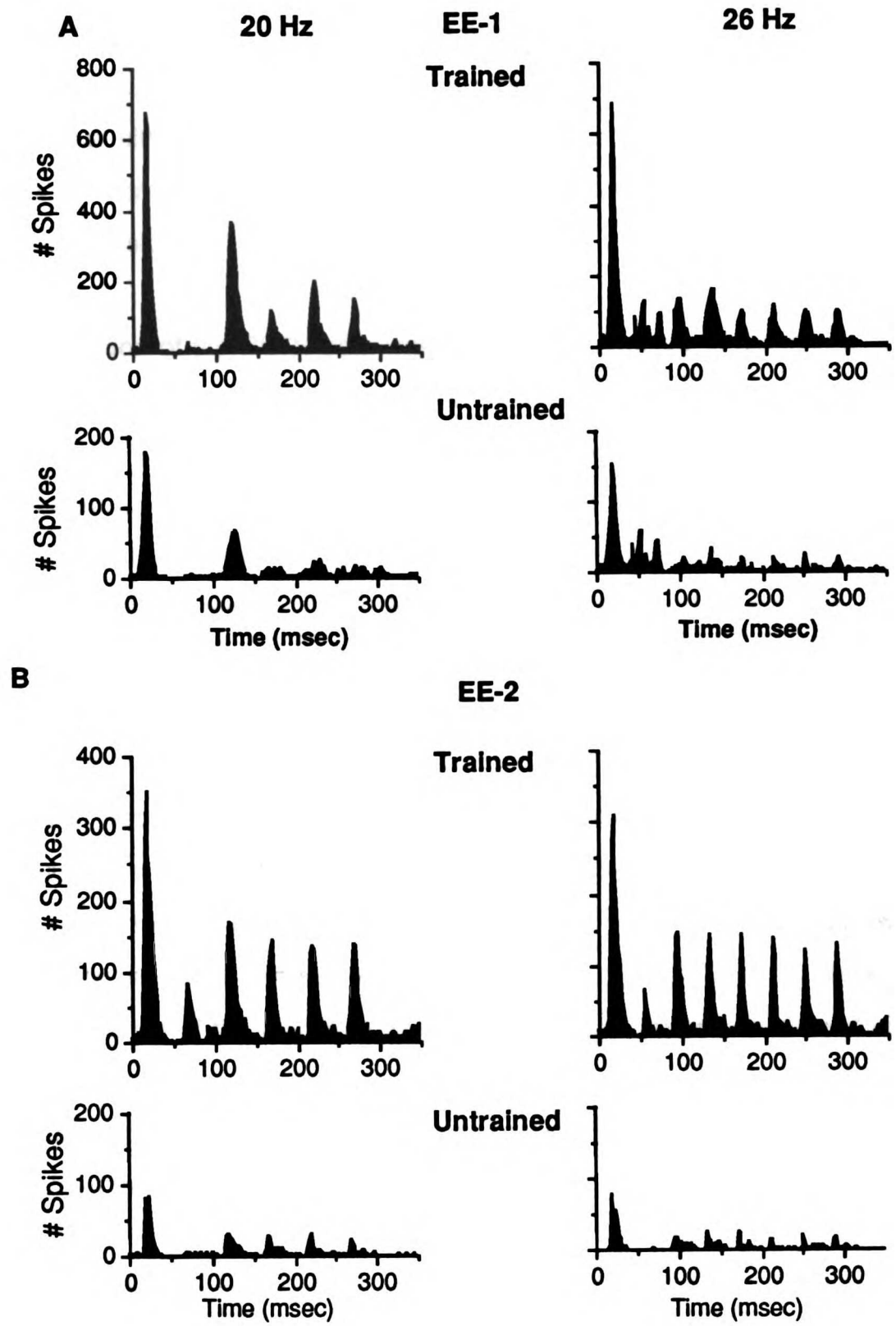
A
20 Hz
EE-1
26 Hz
Trained
Untrained
Spikes
Time (msec)
B
EE-2
Trained
Untrained
Spikes
Time (msec)

case EE-2 (Part B), where every cycle of the stimulus was represented by a sharply defined response. This effect is most clear for the 26Hz stimulus for the trained digit. The untrained digit did not respond to the second cycle of the stimulus at either frequency in this case. The details of the temporal features of the population response are better illustrated by the cycle histograms, which are presented below.

Collection of the PSTH data was done by sequentially presenting each of the frequencies for ten repetitions, with each repetition delivered once per second. To ensure that the recording was stable during this period, 20 Hz was presented as both the first and last stimulus of the series. The population response to these two presentations of the same frequency are shown in Figure 62. Responses were virtually identical at these two time periods. This procedure was also followed for cases EE-3, ED-4, PS-2 and PS-3, with the same result.

The population PSTH derived in the passive-stimulation control hemispheres was not significantly different between the stimulated and unstimulated digits (Figure 63). The population PSTH for both digits were essentially the same with respect to the magnitude and timing of the response. The magnitude of the response was much less than that of the trained digits shown in Figure 61. The "sharpness", or temporal precision of the response to each stimulus cycle, was also reduced for the passive-stimulation animal as compared to experimental animals.

The finding that the population response on the trained digit was greater in absolute magnitude was expected, given the increased area of this

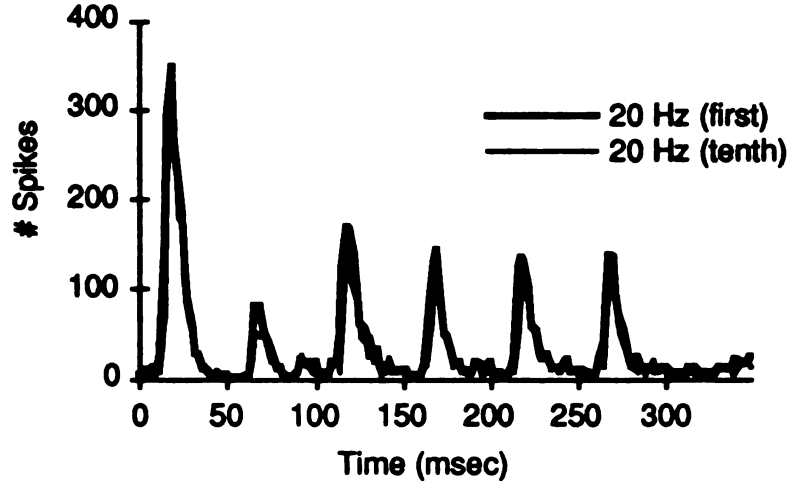

Figure 62. Population PSTH to stimulation of the trained digit with a 20 Hz stimulus presented as the first stimulus (heavy line) or the tenth stimulus (thin line) of a stimulation series. Each histogram is made from ten consecutive stimulus presentations. Eight different frequencies were presented for ten repetitions each between collection of the first and tenth response. See text for details.

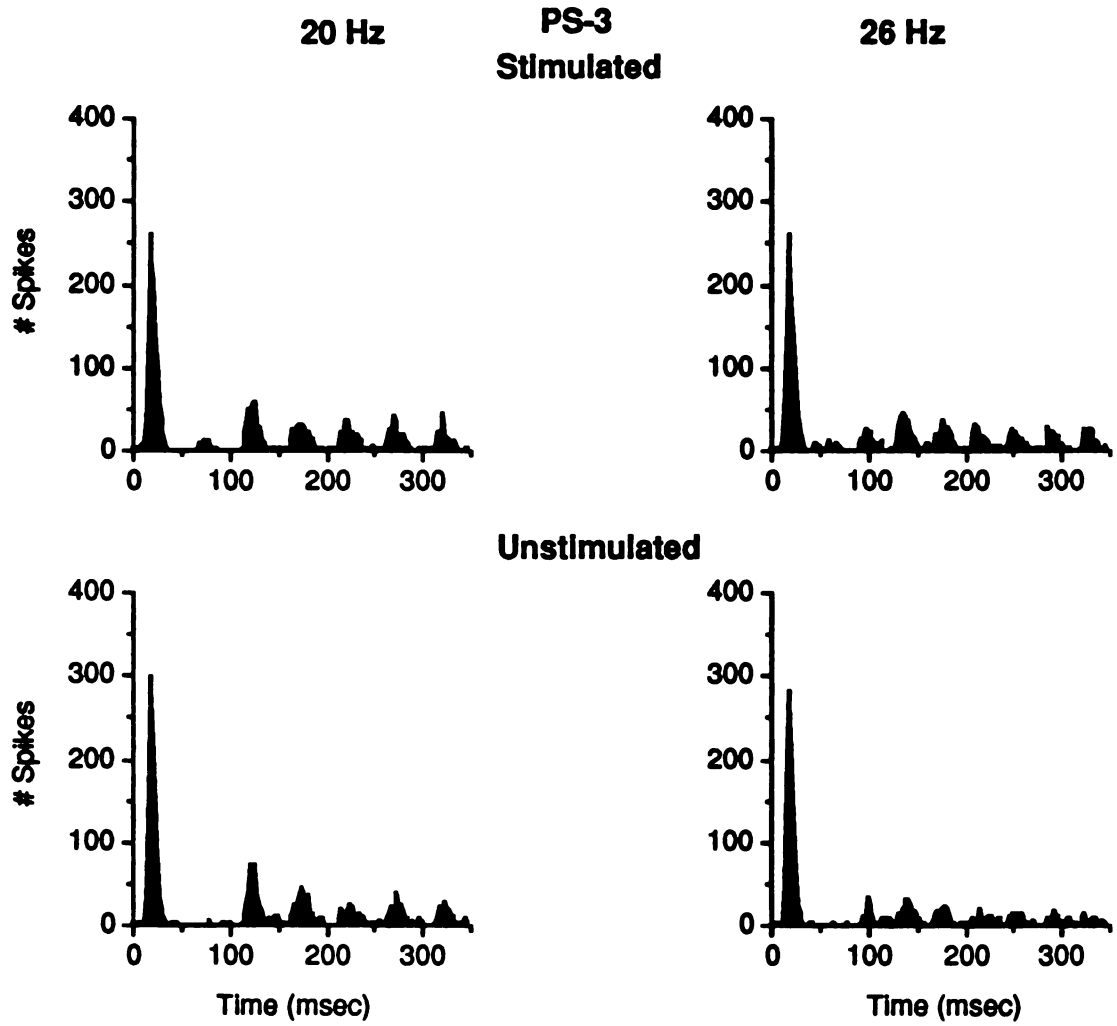

Figure 63. Population PSTH for stimulation to the digit stimulated in the behavioral apparatus (top) or to the adjacent, unstimulated digit (bottom) for 20 Hz (left) and 26 Hz (right) stimulation of passive-stimulation control monkey PS-3.

representation. More cortical locations were contributing to this response. This raises the question of whether the increased area of representation provides a complete explanation of the effect. This was tested by normalizing the population PSTH by the number of locations tested. The results are shown in Figure 64 for the 20 Hz stimulus for the same cases illustrated earlier. The magnitude of the mean response was similar between the trained and untrained digits, although it was somewhat greater at later stimulus cycles for case EE-1 (Figure 64A). Similarly, there was no clear difference for the passively-stimulated control case (Figure 64C).

The differences in the magnitudes of the response are summarized in Figure 65. The total number of spikes occurring for each cycle of the stimulus on the trained digit was divided by the total number of spikes occurring for each cycle of the stimulus on the adjacent digit and plotted as a single line for each frequency. The dashed line is drawn through a value of 1 (no difference). The data are plotted on a semi-log scale. These results show that for the trained digits (Parts A-C) the total response was much greater for the stimulated digit as compared to the adjacent digit. The differences were 200-400% greater for case EE-1, approximately 600% greater for case EE-2, and approximately 50-500% greater for case EE-3. The animal that did not learn the task actually had a smaller response on the stimulated digit when compared to an adjacent, untrained digit (Figure 65D). The passive-stimulation control animals showed only small deviations form the ratio of one (no difference), primarily restricted to the second cycle. (Figure 65 E and F). This figure also shows that there is very little difference in the overall firing to different frequencies presented to the same digit.

FIGURE 64. Mean population peri-stimulus time histograms from each animal illustrated in Figures 61 and 63. The response at each time bin in the population PSTH was divided by the total number of cortical locations comprising the population PSTH. All data are derived from the presentation of a 20 Hz stimulus. Parts A -C are from animals E-1 , E-2, and P-3, respectively. The stimulated digit is shown to the left, the adjacent digit to the right.

Figure 64

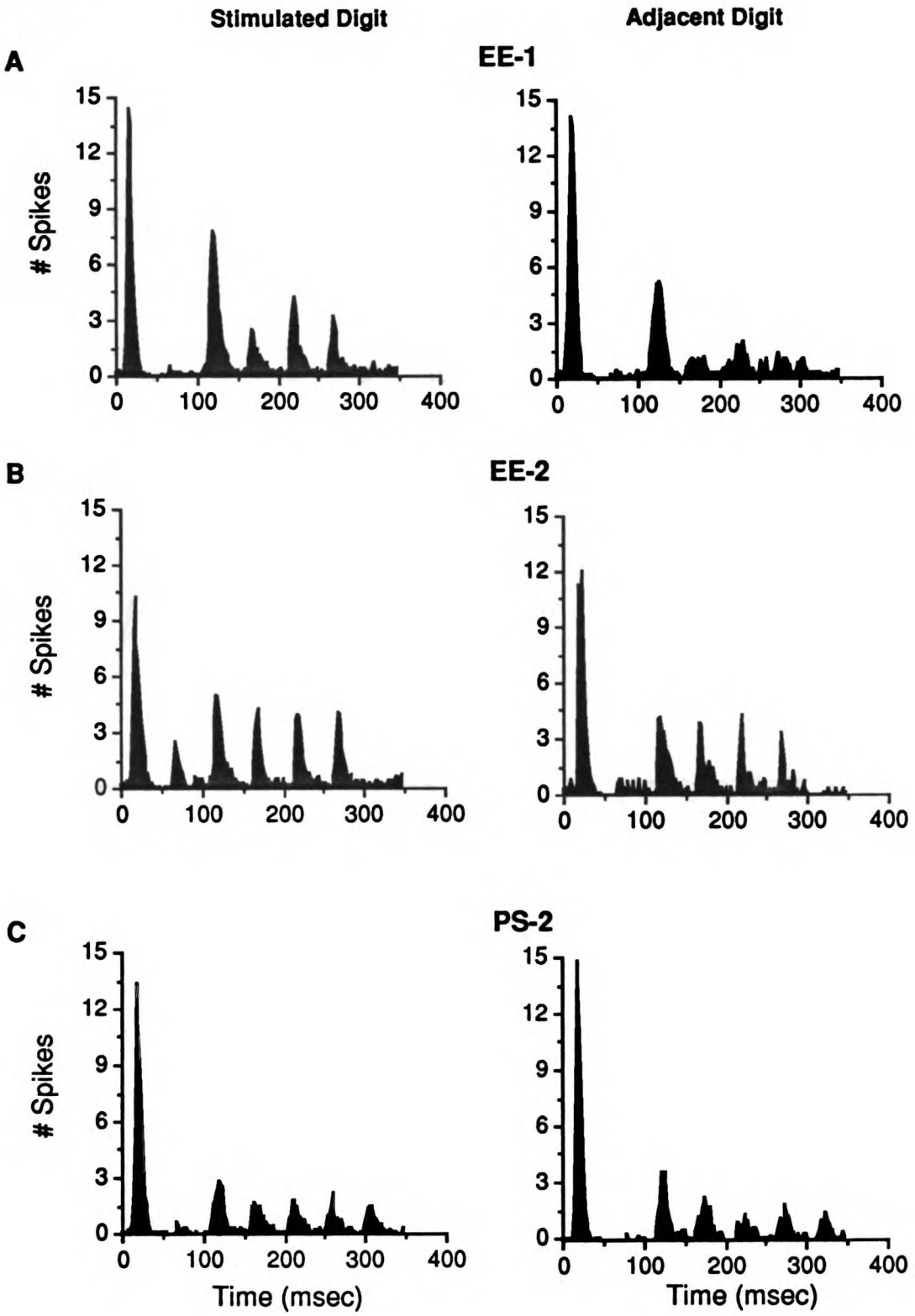
Stimulated Digit
Adjacent Digit
A
EE-1
B
EE-2
C
PS-2
Spikes
Time (msec)
0
3
6
9
12
15
0
100
200
300
400

Figure 65

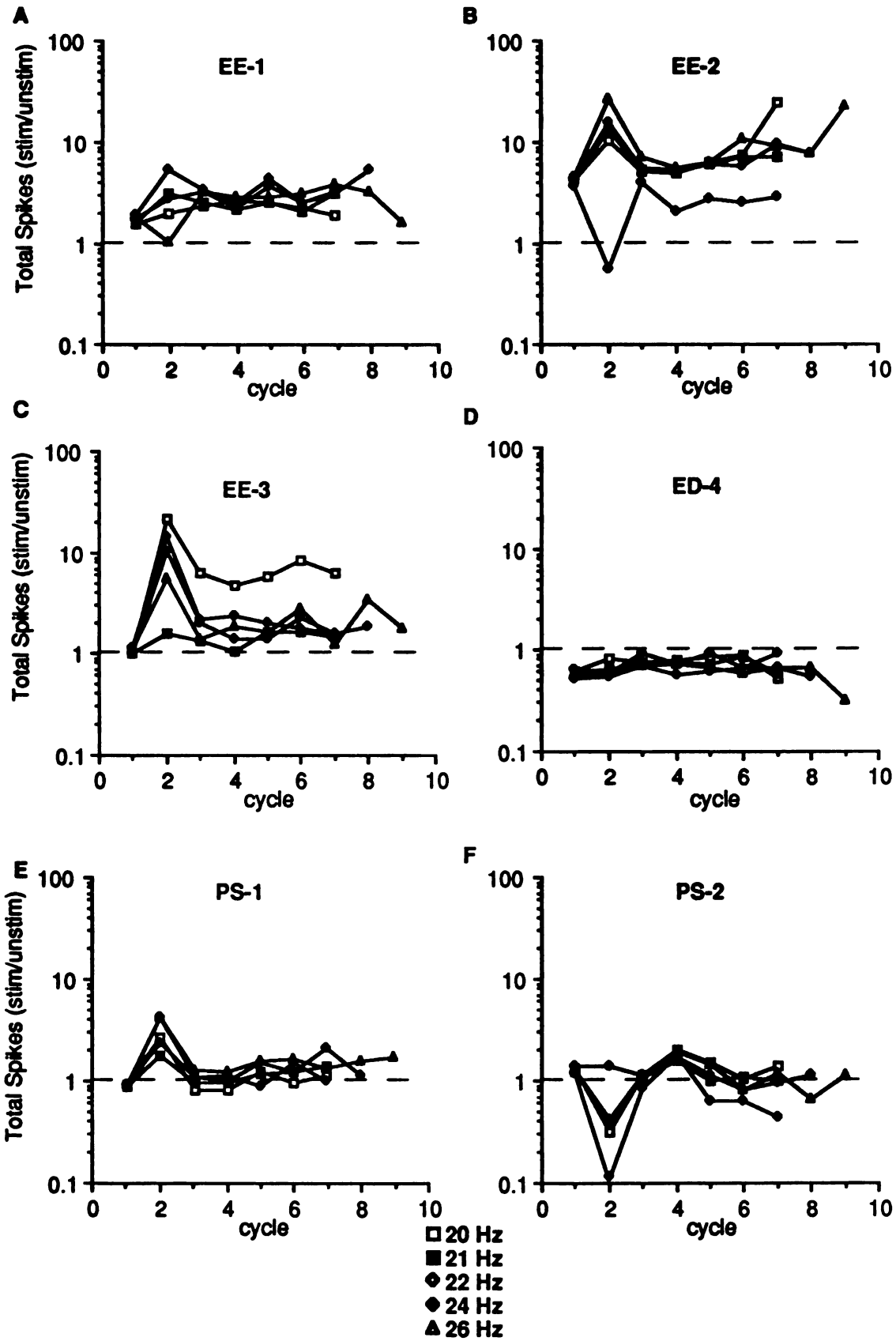
A
EE-1
B
EE-2
C
EE-3
D
ED-4
E
PS-1
F
PS-2
Total Spikes (stim/unstim)
cycle
100
10
1
0.1
0
2
4
6
8
10
20 Hz
21 Hz
22 Hz
24 Hz
26 Hz

In summary, the population PSTH analysis shows that the absolute magnitude of the response to stimulation of the trained digit was increased when compared to unstimulated digits and passively-stimulated digits. This difference in absolute magnitude could be explained as an overall increase in the total number of cortical locations contributing to the response. This increased rate was reflected in each cycle of the stimulus.

Population cycle histograms

The population PSTH shown for case EE-1 (Figure 61) indicates that the timing of the response was more narrowly distributed for the trained digit when compared to the untrained digit. This was investigated further by creating cycle histograms from the population PSTH. All spikes that occurred during the time period of a single stimulus cycle were summed for each cycle of presentation. The first, or onset, cycle was omitted from this analysis to avoid biasing the results with the large onset response (see *Methods*). The cycle histograms of the trained (heavy line) and adjacent (thin line) digits from cases EE-1 (top) and EE-2 (bottom) to a 20Hz stimulus are shown in Figure 66. The cycle histograms are plotted on a real time axis, where zero corresponds to the onset, or zero cross, of the stimulus cycle. The differences in timing of spike occurrence within the cycle are clear for animal E-1. The time of occurrence of the peak response differed by 8-10 msec compared to the response to stimulation of the adjacent, untrained skin location. The overall shape of the histogram was considerably wider for the adjacent digit when compared to the trained digit.

Cycle histograms from the animal that showed poor behavioral performance, and from one animal which was passively-stimulated are shown in Figure 67. The population response in cases ED-4 (top) and PS-3 (bottom)

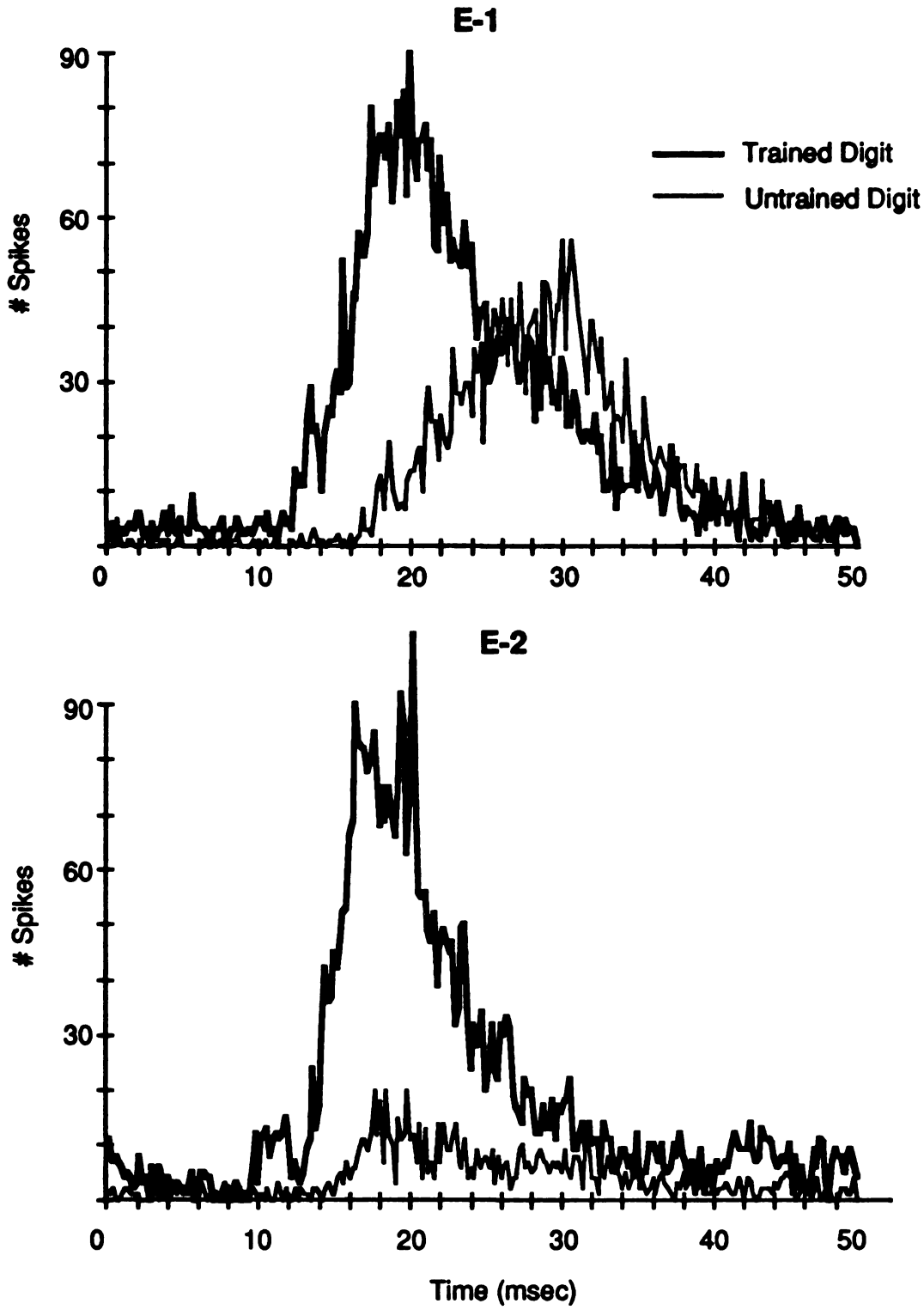

Figure 66. Population cycle histograms to stimulation of the trained digit (heavy line) or to an adjacent, untrained digit (thin line) from two well trained monkeys E-1 (top) and E-2 (bottom). Stimuli were 20 Hz. The time axis begins at the zero-cross of each stimulus cycle.

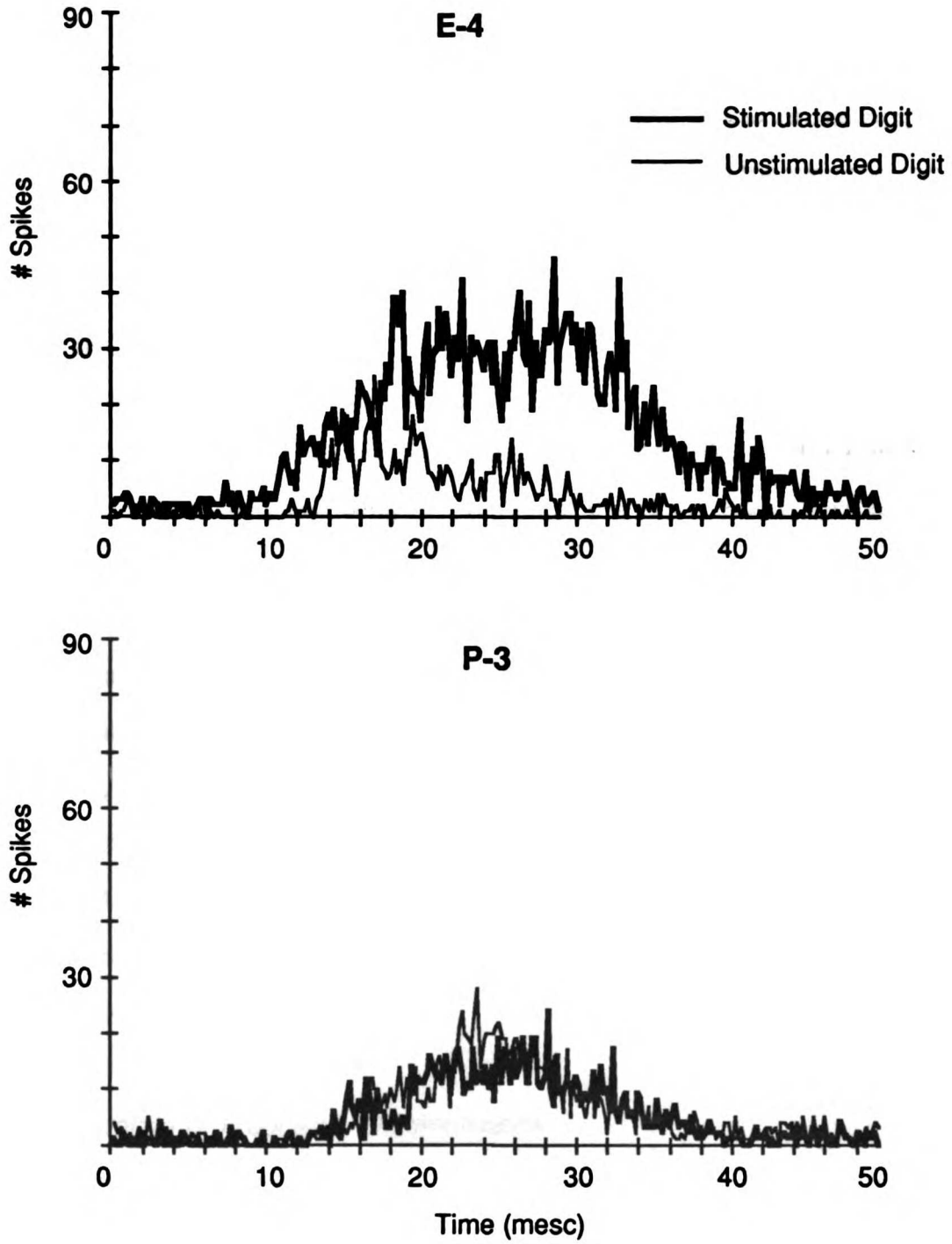

Figure 67. Population cycle histograms from two control monkeys for stimulation of the digit stimulated in the behavioral apparatus (heavy line) or an unstimulated, adjacent digit (thin line). Conventions as in Figure 66.

were clearly reduced in amplitude when compared to the cycle histograms from the trained digits illustrated earlier. A difference in amplitude between the stimulated and adjacent digits is evident for case ED-4, but not in either of the passively-stimulated animals. In both animals, the sharpness of the response for the trained (or stimulated) skin regions is similar to that of the skin regions on the adjacent digit of the experimental hemispheres.

Cycle histograms in area 3a

The quantitative responses of cortical locations in area 3a were also subjected to the same analysis for cases EE-1 and EE-2. The number of locations with frequency-following responses in the other cases was too small to create population histograms. The population cycle histograms for these two cases from area 3a are shown in Figure 68. The total magnitude of the response is considerably attenuated for this cortical field when compared to area 3b (compare Figures 68 with 66). The width of the spike distribution, or the sharpness, is only slightly improved with respect to the untrained digit. However, the rising phase for the response to the trained digit in case EE-1 (Figure 68A) is very steep when compared to the untrained digit. This indicates a sharp temporal precision to the onset of each cycle. This was not as apparent for case EE-2.

Neural Correlate of Frequency Discrimination

Previous studies of tactile frequency discrimination proposed that the 'entrainment' or cycle-for-cycle responses of neurons in SI could account for the behavioral performance at a frequency discrimination task of the animal (Mountcastle et al 1969,1990). They proposed that a decision theory-based analysis of the cycle histograms could predict the behavioral performance

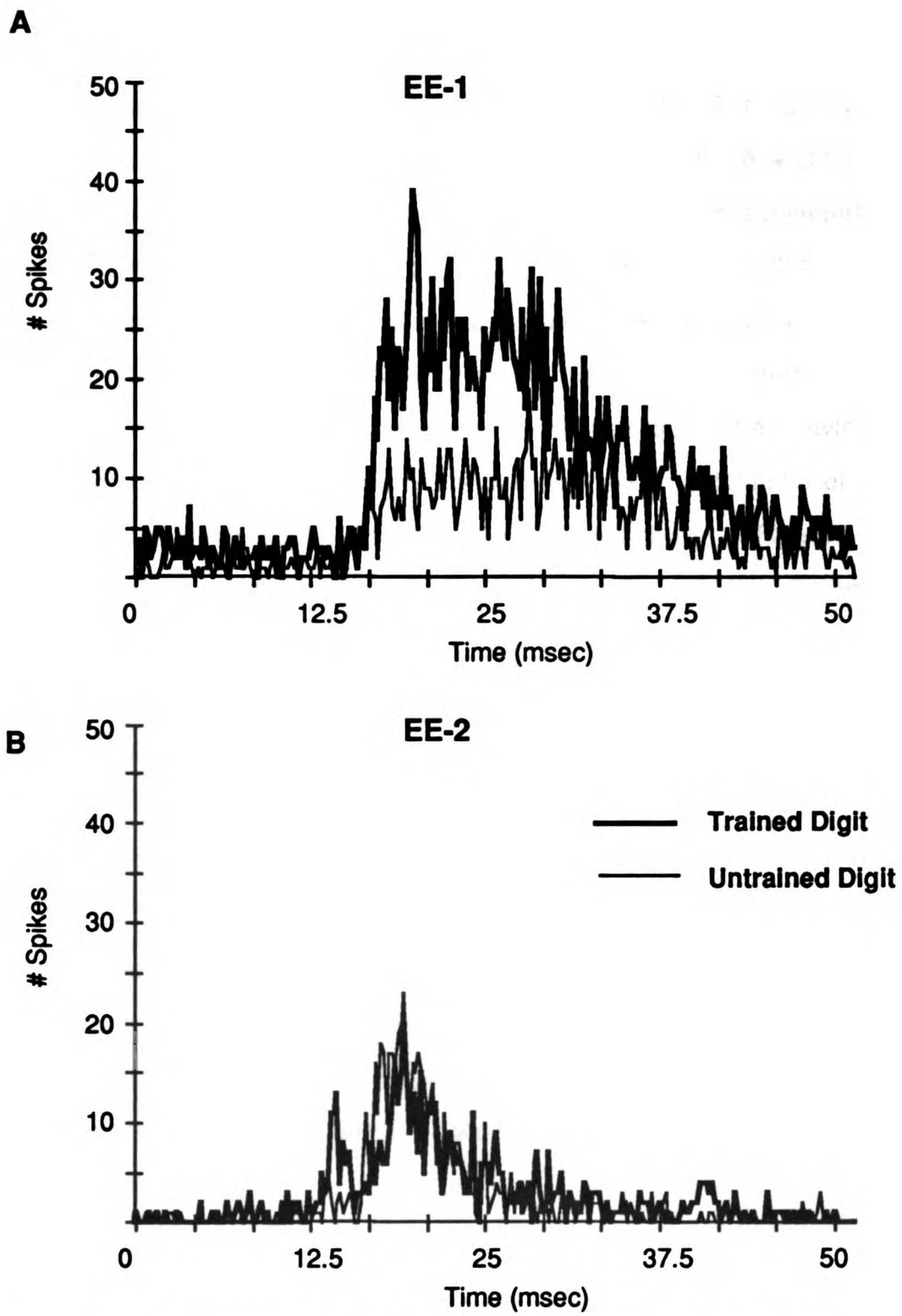

Figure 68. Population cycle histograms taken from area 3a from two well-trained monkeys. Heavy line is the response to stimulation of the trained digit, thin line is the response to stimulation of the adjacent digit. Stimulus frequency was 20 Hz.

(Mountcastle et al 1969). As explained earlier, decision theory predicts that the ideal observer can discriminate between two signals if the peaks of their distributions are separated by one standard deviation or more. The population cycle histograms to the 20Hz stimulus collected for each of the eight skin surfaces in which behavioral thresholds were also defined were subjected to this analysis (trained and adjacent digits of EE-1, EE-2, EE-3 and ED-4). The standard deviation of the cycle histogram was defined in real time (1 s.d. = the time period in which the middle 66.67% of the response occurred). The minimally detectable frequency difference from 20 Hz was defined as having a period length of (50msec-1s.d.). This value was plotted as a function of the behavioral threshold measured for that skin surface and is shown in Figure 69A. The solid line is the best fit to the data, the dashed line corresponds to a perfect correlation. The best fit line has a slope of 0.014 and a correlation coefficient of 0.03. Decision-theory analysis of the entire cycle histogram is clearly insufficient to explain the behavioral data.

Closer inspection of the cycle histograms gives an indication of why this analysis failed. Decision theory analysis makes two assumptions about the distributions of the two signals: 1) They have equal variance and 2) they can be fit by a Gaussian distribution. The cycle histograms for the trained digits in Figure 66 are not Gaussian, but are skewed to the left (shorter latency). This results in an overestimate of the variance, and thus, in an overestimation of the predicted threshold.

An alternative and more appropriate approach is to analyze the data with respect to the onset of the response to each cycle. The discrimination task demanded that the subject determine the period of the sinusoids presented to

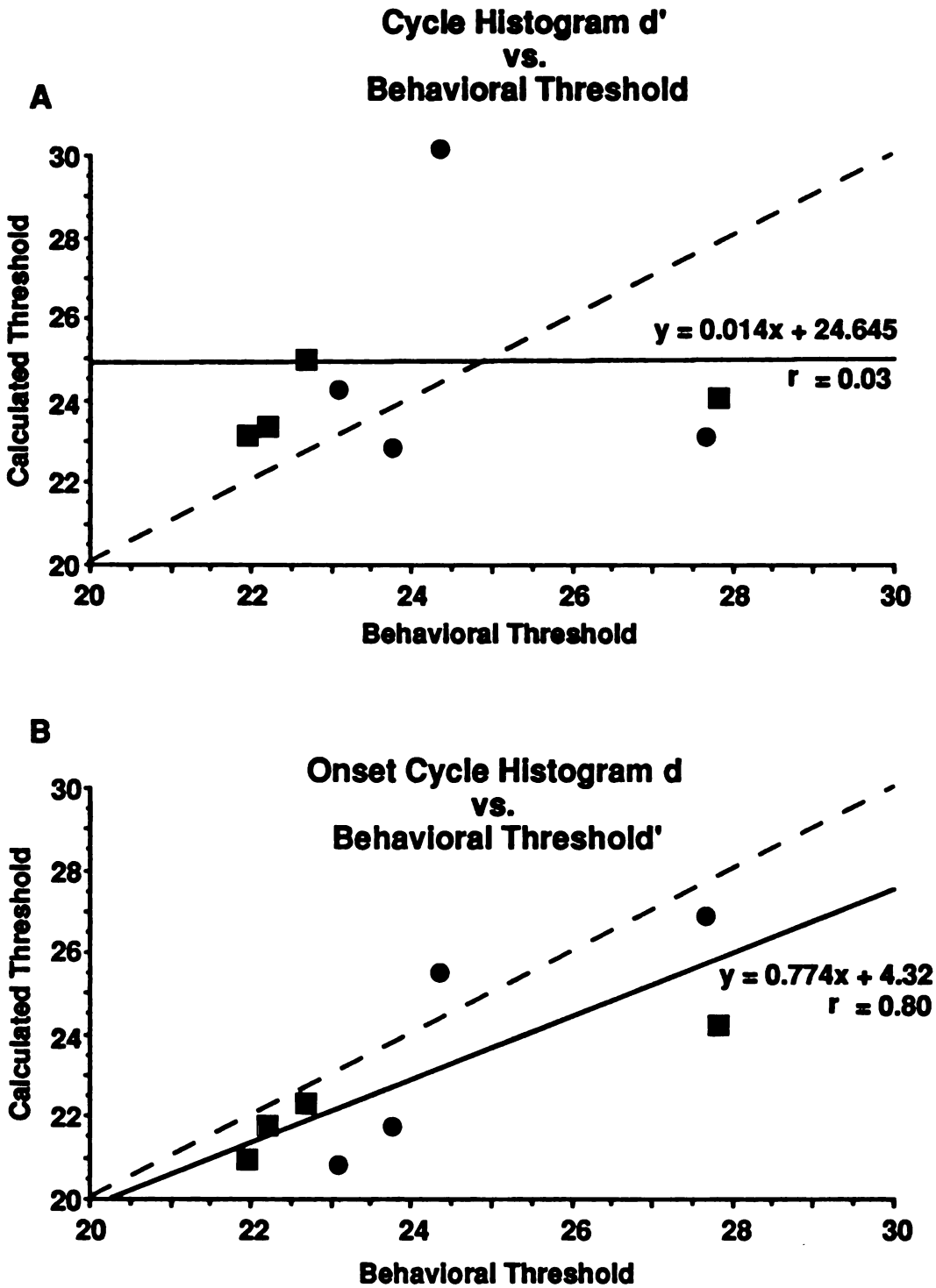

Figure 69. Regression analysis of detection theory analysis of the neural data based on the cycle histograms vs. the behavioral thresholds. In A the detection theory analysis was performed on the entire cycle histogram. In B only the onset portion of the cycle histogram was used for the analysis. Squares denote trained skin regions, circles denote untrained skin regions.

the skin. This could be accomplished by comparing the relative lengths of time between these onset responses, while the remaining response during each cycle could be used to encode other features of the stimulus, for example the cycle length or intensity. The ability to discriminate frequency would then depend on the variance of the response to the onset of each cycle, as opposed to the variance of the response about the peak. The variance of the onset response is reflected in the rising phase of the cycle histogram.

The decision-theory analysis was performed with respect to the rising phase of the cycle histogram, and the predicted threshold plotted as a function of the behaviorally measured thresholds (Figure 69B). The rising phase of the cycle histogram was defined as starting at the first increase in the firing rate over four consecutive time intervals and ending at the first decrease in the firing rate over four consecutive intervals. This part of the histogram was considered as the first half of an 'onset' cycle histogram and subjected to the analysis described above. This restricted analysis provided a better fit between the predicted and behavioral thresholds, with the correlation coefficient increasing to 0.80, accounting for 64% of the variance in the data. This analysis suggests that the onset is a more appropriate measure, but it is still an unsatisfactory explanation of the behavioral performance.

The steep rising phase of the cycle histograms representing stimulation of the trained digit could be accounted for by either: 1) An increase in the onset response of all neurons responding to the stimulation; or 2) by an increase in the onset response by only a subset of neurons. To investigate this further, the latency to the peak firing rate of each cycle histogram from an individual location was measured. This latency measure formed a unimodal distribution in

all but the trained digit in experimental animals. In these hemispheres the latencies fell into two distinct distributions. Examples of these latency distributions are shown for two experimental hemispheres (top two panels), a passively-stimulated hemisphere (middle, bottom) and monkey E-4 (bottom) in Figure 70. The two experimental hemispheres show a clear bimodal distribution of latency, as indicated by the vertical arrow corresponding to a latency of 74 msec. This arrow is projected down onto the two control hemispheres. The distributions in these, as well as all other control hemispheres, is not clearly bimodal, but more unimodal.

For the experimental cases, the two distributions were separated and a population cycle histogram was constructed from each set of the data (Figure 71). The short latency population (heavy line) is very similar in appearance to the total population histogram illustrated previously. The long-latency population (thin line), is very similar in shape and magnitude to the adjacent digit of the same hand and of the control digits of other animals (compare Figure 71 with Figures 66 and 67).

The distribution of these two populations of responses within area 3b are shown in Figure 72. The large filled circles show the cortical locations used in constructing the short-latency cycle histograms; the large open circles show the cortical locations used in constructing the long-latency cycle histograms. In both cases the short-latency locations were clustered in a central region, but could also be found in a wider extent throughout area 3b, while the long-latency locations were all located more peripherally.

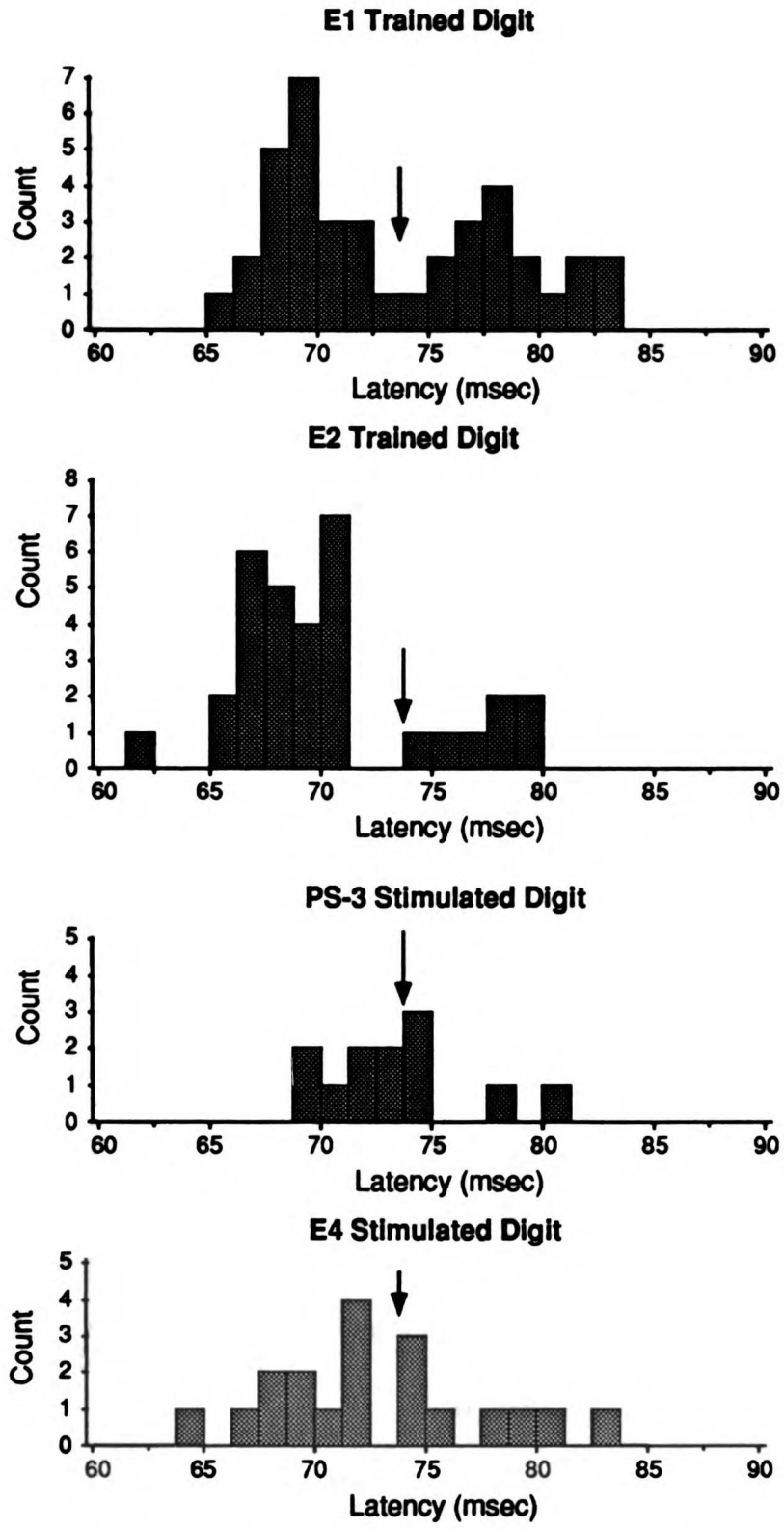

Figure 70. Distributions of latencies for cortical locations with frequency following responses to stimulation of the trained or stimulated digit in four different monkeys. Locations with latencies outside the range of 60-90 msec are not included. The arrow at 74 msec was used to divide the distribution into two different populations for the trained hemispheres only.

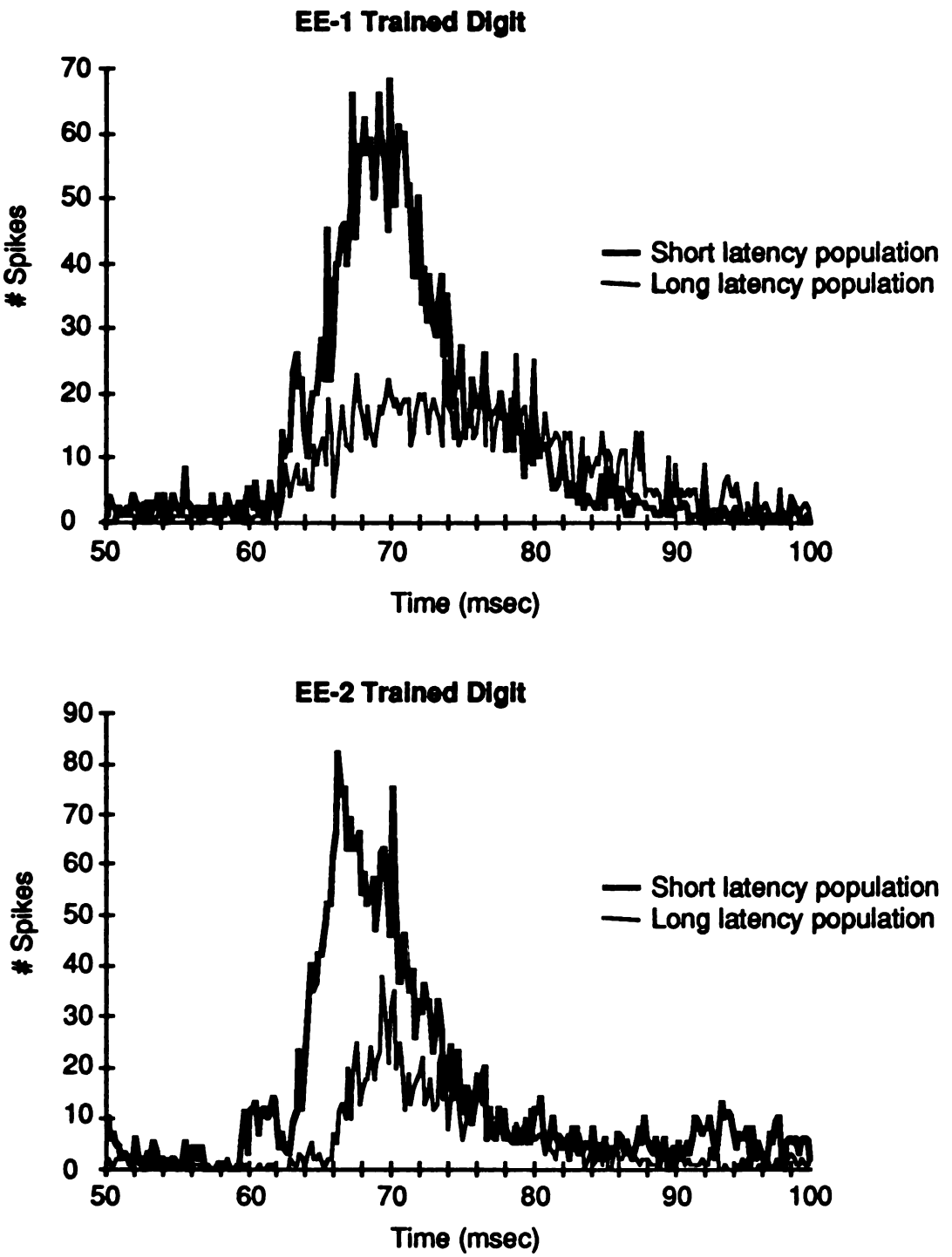

Figure 71. Population cycle histograms to 20 Hz stimulation of the trained digit for monkey E-1 (top) and monkey E-2 (bottom). The total population was divided into a short latency population (heavy line, latency < 74 msec) and a long latency population (thin line, latency >74 msec).

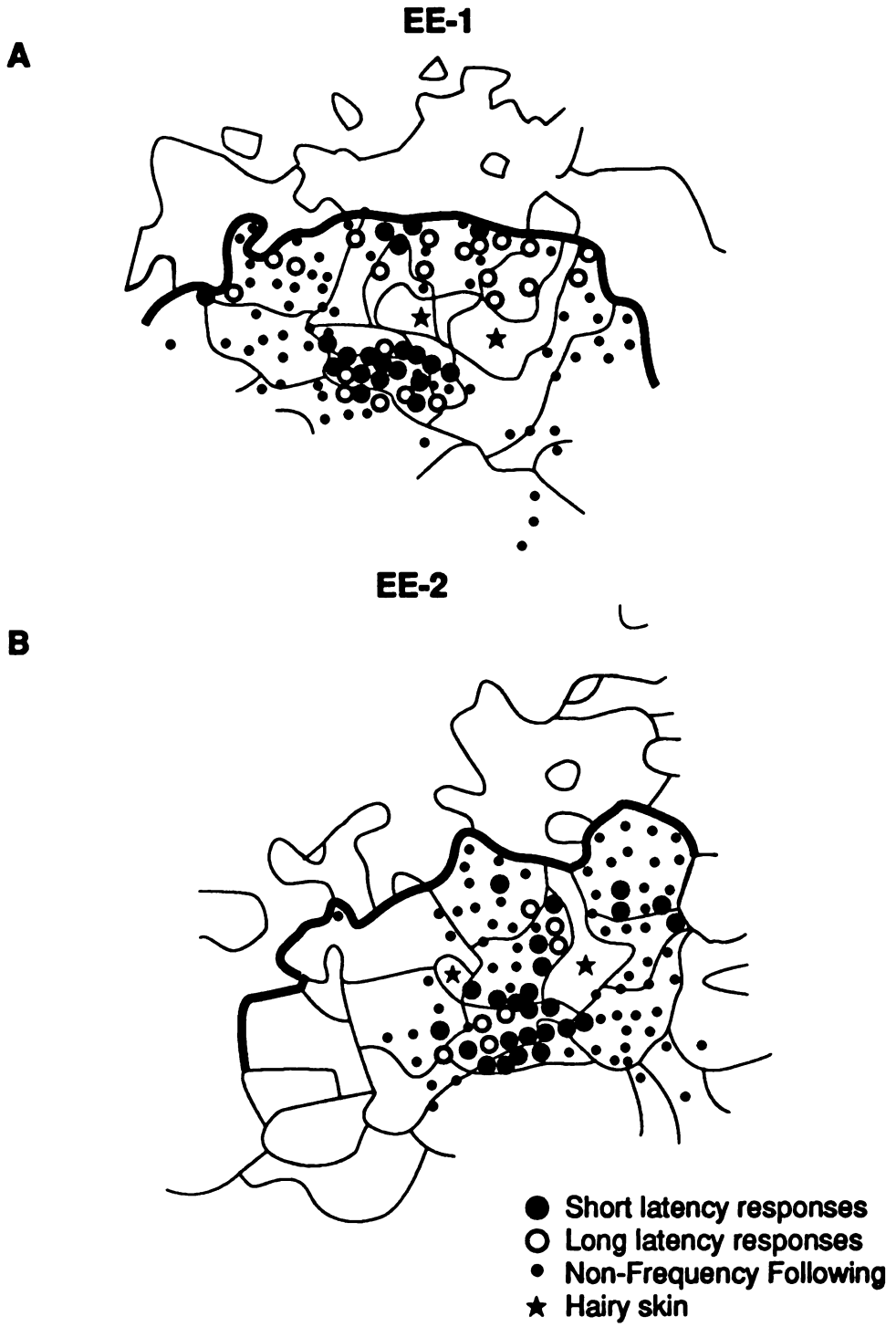

Figure 72. Distribution of cortical locations that gave a short latency (<74 ms) response (filled symbols) or a long latency response (>74 ms) to stimulation of the trained digit of monkeys E-1 (top) and E-2 (bottom).

The subpopulation of neuronal responses with a short latency and steep rising phase could be the basis of the improved performance. Detection theory analysis of these responses is still inappropriate, as the overall shape of each of the cycle histograms, while very similar at close frequencies, differ substantially at higher frequencies. Figure 73 demonstrates this difference for case EE-1. Given the unequal distribution of the response to different frequencies, an alternative analysis was to use the neural data themselves as the distributions representing the different frequencies. The neural response for all locations in the control hemispheres, and only the short latency responses for the trained hemispheres, were used in this analysis. Cycle histograms were constructed as before, except that the period of time used for analysis was two stimulus cycles. The second of the two cycle histograms thus represents the distribution of responses, in time, since the preceding burst of impulses (see Methods). By superimposing the first cycle of the response at the zero-cross of the stimulus, the second cycle represents the differences in the time of the response between cycles. This difference in the response in time is illustrated by plotting the second cycle of the S2 histogram with that of the second cycle of the 20Hz standard (Figure 73).

For S2 frequencies of 21, 22, 24 and 26 Hz, the neural response to the rising phase was calculated for the cycle histogram to the 20 Hz stimulus, as described above. A measure of the temporal difference between two stimulus frequencies was taken as the integrated neural response to the S2 frequency which was non-overlapping with the neural response of the comparison (20Hz) frequency (see Methods, Figure 1). This value was divided by the total integrated response to the S2 frequency. Thus, the number ranged from 0 (complete overlap with the comparison) to 1.0 (complete non-overlap). If this

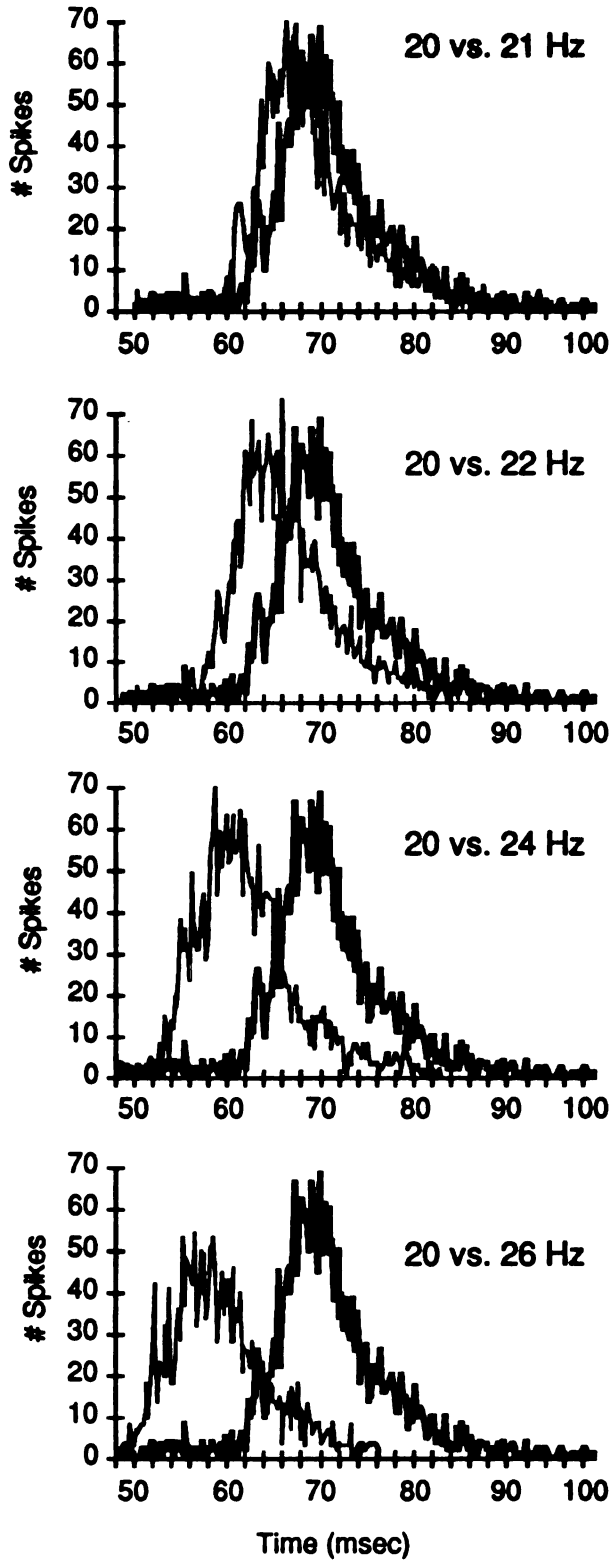

Figure 73. Second cycle of two-cycle histograms for case EE-1. Only short latency responses are considered. Heavy line is the 20 Hz response, thin line is the response to the frequency indicated.

value is presented as a percentage of non-overlap (1-100%), it can be compared directly to the behavioral results of frequency discrimination which are presented as a percentage of correct responses.

The results of this analysis for the trained digit are shown in Figure 74 for animals E-1 (Part A) and E-2 (Part B). Open symbols represent the behaviorally measured values; closed symbols represent the values predicted from the above analysis. A similarly close correspondence between the performance predicted from the neural response and the behaviorally measured performance was seen for both the trained and the adjacent, untrained digit in each animal tested.

This analysis was performed on each of the eight skin surfaces in which both behavioral and electrophysiological data were obtained. Predicted thresholds were computed from the predicted performance functions by the same method used for the behavioral data. These 'neural thresholds' were then plotted against the thresholds measured behaviorally and presented in Figure 75A. This method provides a close fit between the predicted and measured thresholds (correlation coefficient =0.96, accounting for 93% of the variance). The predicted thresholds were usually slightly better than those measured behaviorally, as indicated by most points falling below the dashed line representing an exact match.

The same analysis used in predicting the behavioral performance based on the rising phase of the cycle histogram was conducted for area 3a (Figure 75B). The predicted and measured thresholds were not as closely matched as was the case for the area 3b cycle histograms. Based on this poorer match, it is

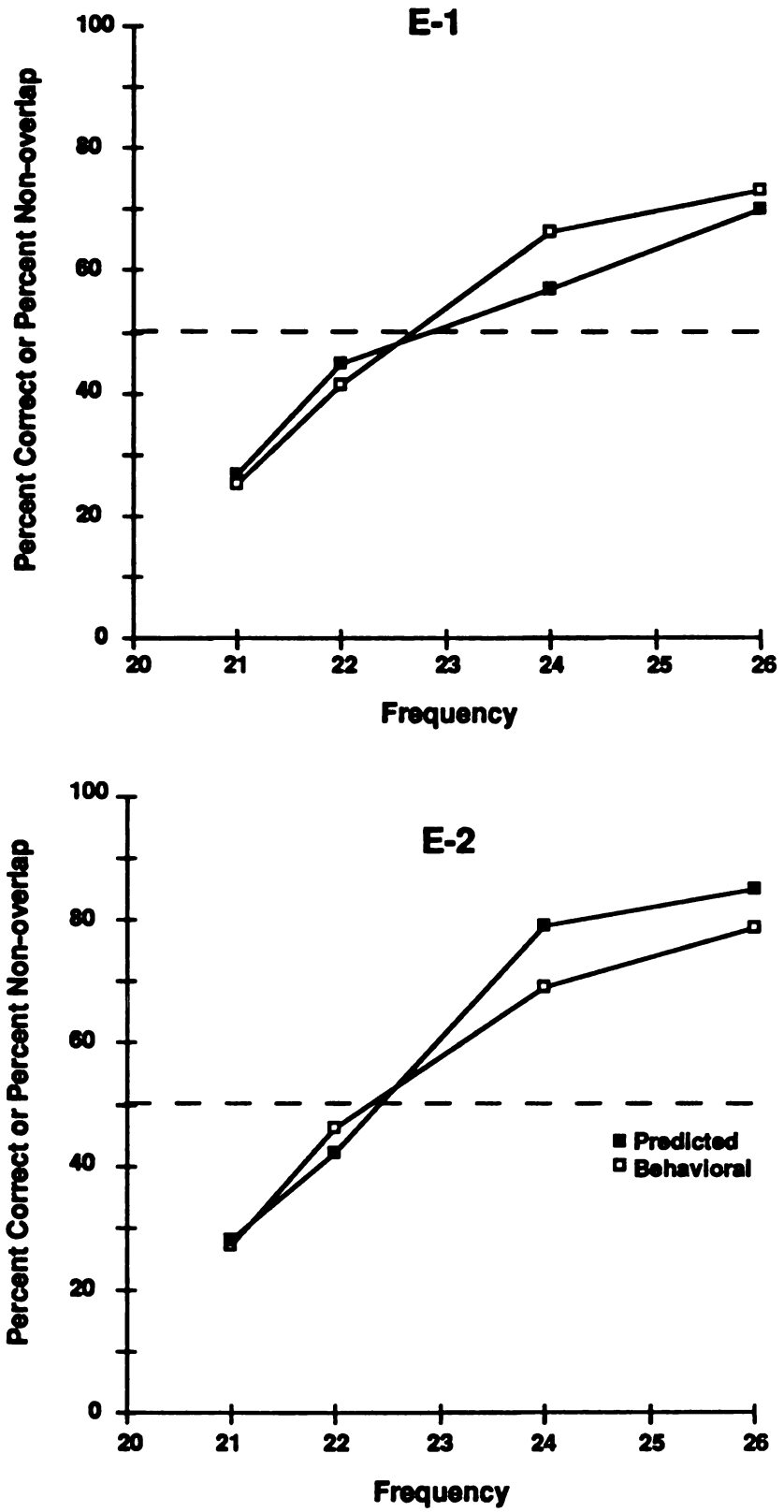

Figure 74. Functions of percent overlap of the second cycle of two-cycle histograms (filled symbols) or behavioral performance (open symbols) as a function of S2 frequency.

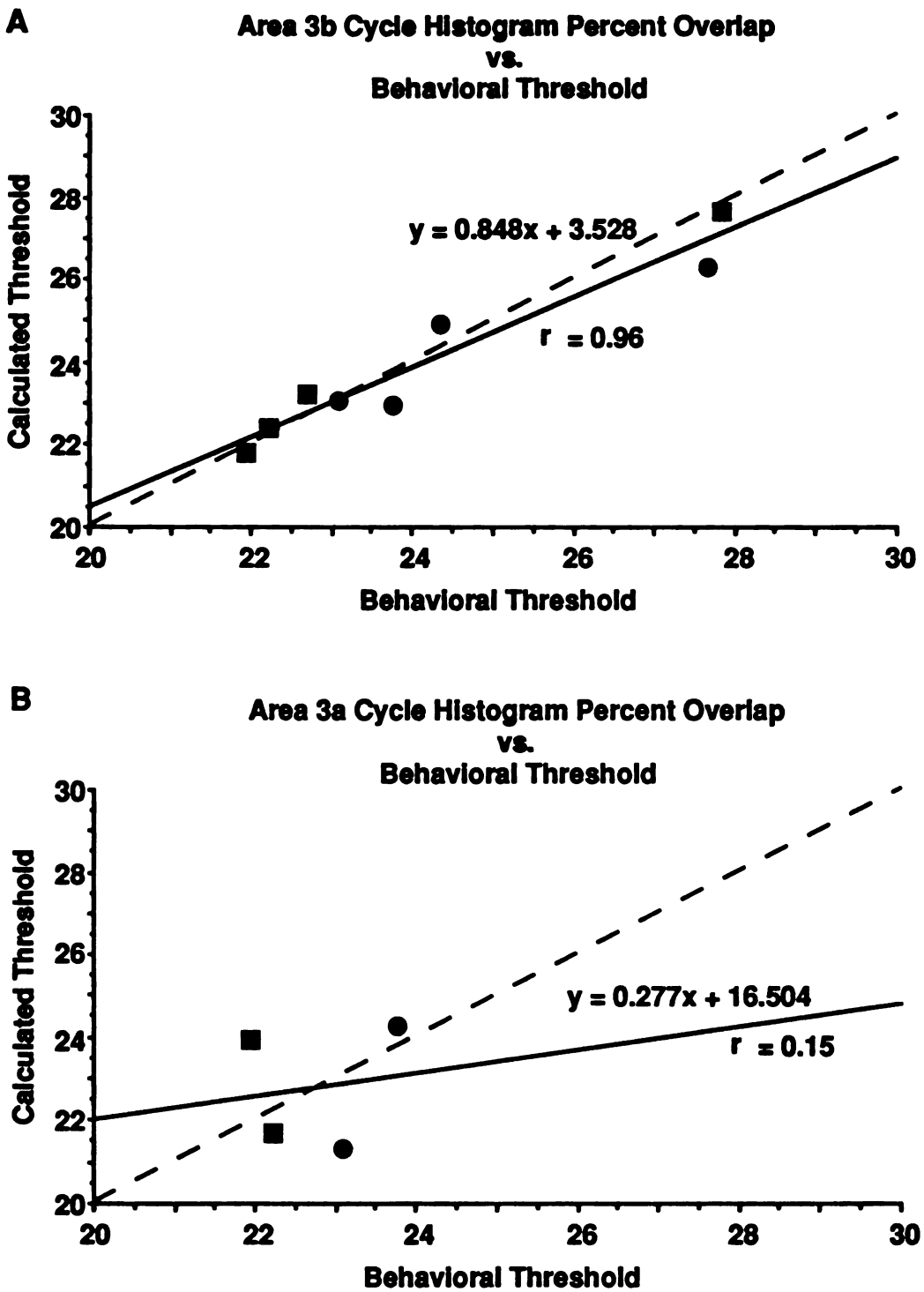

Figure 75. Regression analysis of the threshold predicted from the neural data (Calculated Threshold) with the behaviorally measured thresholds. The predicted thresholds based on area 3b responses are shown in (A), from 3a responses are shown in (B). Squares denote trained skin surfaces, circles denote adjacent skin surfaces. Area 3a responses are from E-1 and E-2 only.

concluded that the compound response of neurons in area 3a is not sufficient in itself to account for the behavioral performance.

Finally, given the finding that the rising phase of the cycle histogram, and thus only the onset response to each stimulus cycle, is theoretically necessary to perform the task, the above analysis of percent overlap of the neural response was performed when the response was restricted to the rising phase of the cycle histogram. The neural response considered for this analysis was confined to the time between the cycle onset (zero cross) and the time period defining the end of the rising phase of the 20 Hz stimulus (i.e. 50-69 msec for the trained digit of case EE-1). The difference in the response between the cycle histogram for the S2 frequency and for the 20 Hz standard within this time period was normalized by the total response at the S2 frequency. The results of this analysis, using the same behavioral measure as done previously, shows an even better correlation (0.98, accounting for 96% of the variance; Figure 76)

In summary, population cycle histograms were constructed by summing the total neural response to stimulation of a single digit. These cycle histograms were largest in overall magnitude and had the sharpest rising phase in the representation of the trained digits. The increased slope of the rising phase of the population histogram could be accounted for by a decrease in the onset time and an overall sharpening, or increase in the temporal precision, of the response to each stimulus cycle of a subpopulation of neurons within area 3b. The increase in temporal precision enhanced the differences in timing in the response to different stimulus frequencies and this enhanced difference could account for the improvements in performance of frequency discrimination tasks with training.

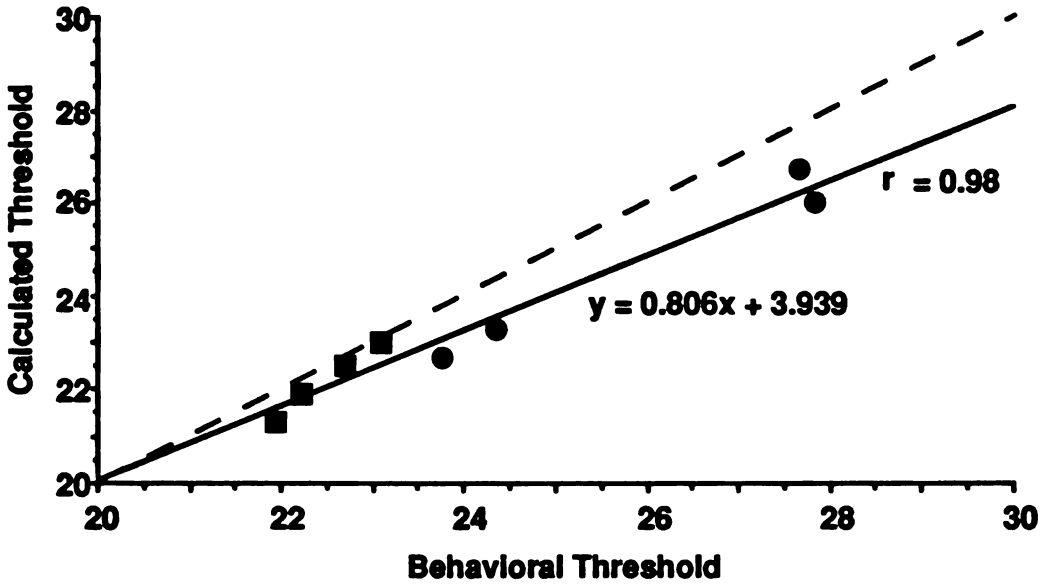

Figure 76. Regression analysis of the predicted threshold based on the rising phase, or onset portion, of the neural response with the behaviorally measured threshold. Conventions as in Figure 75.

DISCUSSION

The goal of this study was to determine the consequences of tactile discrimination training on the topographic representation of the skin surface in areas 3a and 3b in adult primates. The cortical representations of the hand surface defined in animals trained to discriminate the frequency of a tactile stimulus were compared to the representations of the opposite, untrained hand from these same animals, and to the representation of the hands from other monkeys that received the same tactile stimulation but attended to an auditory discrimination task. Several results are described: 1) Improvements in performance with training were recorded in four of five trained monkeys. This improvement progressed by an initial improvement at all S2 frequencies, followed by a more gradual improvement at S2 frequencies near threshold. 2) Performance at S2 frequencies near threshold improved the slowest. 3) Some transference of this improvement was evident on the adjacent, untrained digit. 4) The cortical area of representation of the trained skin increased in both areas 3a and 3b in the four animals whose performance at the tactile discrimination task improved with training. This effect was not observed in one animal whose performance did not significantly improve. 5) The receptive fields defined over the trained skin increased in size when compared to the adjacent digit of the same hand or to the same digit of the contralateral hand, in four of five trained animals. 6) The receptive fields defined on the digits adjacent to the trained digit were also significantly larger than were receptive fields defined on the same digit of the contralateral hand in the same four of five trained animals. 7) For one monkey the receptive field sizes representing the stimulated digit did not increase even though the discrimination performance improved with training. 8) These four well-trained monkeys also showed an emerged

cutaneous representation in area 3a. In all but one monkey the cutaneous receptive fields defined in area 3a were larger than were those in area 3b, and collectively represented most if not all of the glabrous surface of the hand. Many of these receptive fields included the trained skin. 9) The summed population response across area 3b was greater in absolute magnitude and better resolved the temporal features of flutter-frequency stimulation of the trained skin. 10) A sub-population of area 3b neurons in the well trained animals had shorter response latency and were more sharply tuned to each stimulus cycle. 11) The difference in timing between the neural response to S2 frequencies presented to the skin and the rising phase response to the comparison frequency could account for the animals' behavioral performance. 12) Passive-stimulation had a limited effect on the area of representation in area 3b when compared to the unstimulated, contralateral control hemispheres. No significant changes in the spatiotemporal representation of flutter frequencies were recorded in these passively stimulated control hemispheres. 13) Training in one hemisphere did not result in any clear changes in homotypic area 3a or 3b sites in the opposite hemisphere.

Based on the results summarized above it is concluded that: 1) The topographic and functional reorganization of the cortical representation of the skin surface by tactile stimulation is facilitated by attention to the stimulus. 2) The observed increases in receptive field sizes cannot account for the improvement in performance with training as one animal did improve performance without enlarged receptive fields, and one animal did not improve performance but did have enlarged receptive field sizes. 3) The absolute area of representation, although positively correlated with the improvement in performance at the tactile discrimination task, is not sufficient in itself to account

for the improvement in performance. 4) The distributed and temporally more precise responses evoked by stimulation of the trained skin can best account for the behaviorally defined frequency discrimination thresholds measured for that skin area. 5) The functional organization of the somatosensory cortex defined at any given time in the life of an animal reflects the recent behaviorally relevant stimulation-history of that animal. 6) This reorganization is likely to be accomplished by an alteration in the synaptic efficacies distributed throughout a significant horizontal extent within the cerebral cortex. These synaptic efficacy changes result in an enlarged group or area of cortical neurons that act in concert to process tactile information from a single skin location.

TECHNICAL CONSIDERATIONS

Area of representation measurements

The area of representation of the stimulated skin was shown to be significantly increased for the trained skin only. These areas were estimated by drawing the boundaries of representation as the midpoint between electrode penetrations representing adjacent skin locations. The density of electrode penetrations assured that these area estimates were very accurate. The amount of error has been defined mathematically and empirically by other investigators to be 10-20% (Stryker et al 1987) for microelectrode penetrations at the density described in this study. This error cannot account for the changes in representation seen for the following reasons: 1) Area comparisons were measured in the same way for each of the compared skin surfaces. Thus any error inherent in the technique would be consistent across cases and thus not differentially effect the measurement of some digits but not others. 2) By defining boundaries as the midpoint between electrode penetrations, the

number of small errors by overestimations should be roughly equal to the number of small errors by underestimations and would thus sum to zero.

Limitations of multiple unit recording

All neural responses were recorded extracellularly, recording from several neurons (approximately 3-5) at each location. All multiple unit discharges were passed through a window discriminator that only accepted waveforms that were greater than 2X the spike-free neural 'noise' level in that preparation. Inspection of the accepted waveforms had shapes characteristic of single neurons in both time and amplitude. In recording the response properties to sinusoidal stimulation of the skin, we encountered firing rates never greater than an average of 8 spikes/cycle within the stimulus train. Single neuron data derived from macaque under the same stimulus conditions (Mountcastle et al 1969, 1990; Hyvarinen et al 1980; see also Gardner 1988) showed firing rates of only 1-4 spikes / cycle. The distribution of spikes accepted / stimulus cycle in our experiments suggests that either 1) the neural responses in this preparation could give less than one spike per cycle. This was undoubtedly the case in some instances, where there were clearly some cycles not represented (usually the second, see Figures 61, 64) or 2) very few single neurons (1-2) made up the bulk of the responses recorded in these penetrations. In either case it is clear that at the majority of locations recorded responses were made up of less than 10 neurons.

An important advantage of multiple-unit recording is the surveillance of several hundred locations in a single hemisphere, as receptive field definitions can be derived easily and rapidly when compared to single unit recording. However, multiple unit recording does have limitations. One consideration is

how distant from the electrode tip neurons can be recorded from. This distance can be empirically estimated by recording across the clear discontinuities between representations of different hand surfaces. For example, the cortical location that responds to stimulation of only hairy skin can be separated by less than 100μm from a location that responds to only glabrous skin. Thus the effective "seeing distance" of the electrode cannot be more than 50μm.

Multiple unit recording could also be expected to increase the receptive field size, as many neurons with slightly different receptive fields are recorded simultaneously. This possibility cannot effect the results described in this study, as all cortical receptive fields were defined using equivalent multiple unit recording. The possibility that sprouting of peripheral afferents or changes in the skin mechanics of the the trained skin could effect receptive field definition is discussed below.

A third potential limitation is that recording from several neurons simultaneously, some of which are undoubtedly reciprocally connected, might be expected to broaden the temporal response. In spite of this, the temporal responses recorded at individual locations and across a large cortical area in this preparation were very reproducible and represent the temporal features of the stimulus with high fidelity. This implies that the majority of neurons recorded at each cortical location had highly correlated activity, at least over the time scales used in this study. In experimental hemispheres this correlated activity could extend over several hundred microns in area.

Population Histograms

By summing responses at many cortical locations we were able to estimate the neural response in time over a large cortical area. The response to a stimulus at two different locations at two different times is not necessarily the same as the response at both locations at the same time. Ideally, one would record simultaneously from a large number of neurons during presentation of the tactile stimulus. Limitations of the technique used in this study are that the stimulus probe may not be aligned in exactly the same manner for each stimulus run, small differences in anesthetic state (see below) or hydration level may effect the response, or the cortical electrode may be in a different cortical layer or sampling from different classes of cortical neurons. Every attempt was made to control for these possibilities. The tactile stimulator was placed in the identical location on the skin, which was marked in indelible ink. The initial contact force and the stimulus amplitude was constant throughout the experiment for each animal. The anesthetic state and hydration state were monitored closely during the experiment and were not allowed to fluctuate. The cortical electrode was always placed 750-900 μm below the cortical surface.

These efforts cannot rule out any of the above caveats, but the quantitative neural data strongly suggest that these possible sources of error are small. All data were collected using the same method, thus any persistent error would not be expected to differ between trained and untrained skin surfaces. Individual and population histograms from these data are equivalent to those derived in the awake macaque (Mountcastle et al., 1969, 1990; Hyvarinen et al 1980). The slope of the rising phase in the cycle histograms was very steep for the trained digit in experimental hemispheres. If artifactual variations were imposed onto the data by the technique, they would result in an overall increase in the

variance and in a decrease in response fidelity. Moreover, recorded neural responses provided a good prediction of the behavioral data (see below).

Anesthetic state

These experiments were performed on animals anesthetized with barbiturate. Barbiturates have been described as having only minimal effects on excitatory cutaneous receptive fields defined using the techniques employed in this study (Mountcastle and Powell 1959; Stryker et al 1987), but do seem to effect inhibitory receptive fields (Mountcastle and Powell 1959). This analysis of topographic representation in cortical layers III and IV, which is based on excitatory cutaneous receptive fields, is probably a reasonable estimate. In other cortical layers and in other somatosensory cortical fields, anesthetics have been seen to result in a decrease of receptive field sizes (McKenna et al 1982), or can effect neural responses to sustained stimuli (unpublished observations).

Comparisons of receptive fields in anesthetized and awake monkeys show that they are equivalent in size and sensitivity. The attentional state of an animal can, however, influence the response properties of cortical neurons (see Robinson et al 1978; Mountcastle et al 1981, 1987; Bushnell and Goldberg 1981; Sato 1988; Spitzer et al 1988). It is possible that the representation of the stimulated skin would be seen to differ in these animals as they performed this behavioral task. However, Mountcastle et al (1990), and Hyvarinen et al (1980) compared the temporal response of single neurons in areas 3b and 1 during active and passive presentation of the same flutter-frequency stimulus and saw no differences in the response properties.

Receptive field definition

The receptive field was defined using the criteria of just-visible skin indentation. This corresponds to skin indentation levels of several hundred microns, equivalent to displacement levels used in the behavioral task. Nonetheless, some receptive fields that gave frequency-following responses did not include the stimulation site, while some receptive fields that did represent the stimulation site did not have frequency-following responses. The latter finding was particularly true for area 3a receptive fields. The apparent mismatch between the receptive field locations and the temporal response to the behaviorally relevant stimulus could have resulted from one of at least three reasons. 1) The sinusoidal stimulus was superimposed onto a trapezoidal skin indentation to simulate the behavioral condition, thus the stimulus-skin coupling might be superior to that achieved with a hand held probe. 2) The step indentation may result in limited skin stretching, which could effectively increase the area of stimulated skin. 3) The contact surface area of the stimulus probe used in the training and in quantitative testing was several times greater than the tips of the hand held probes used in receptive field mapping. 4) Finally, the temporal nature of the stimulus could have increased the probability of a neuronal response.

Many authors have argued about the merits of different stimuli used in defining somatosensory receptive fields. Some believe that higher intensity stimuli should be used to define the maximum responsive area of a given cortical location (Calford and Tweedale 1988), whereas others have pointed out that some neurons are most responsive to complex or moving stimuli (Killackey 1990).

Defining minimal receptive fields in this study revealed: 1) The essentially normal somatotopic representation of all but the trained digit, 2) the emergence of low threshold cutaneous receptive fields in area 3a and 3) training induced increases in receptive fields sizes. These data are critical for understanding which inputs are most effective in driving cortical neurons, and how these inputs may have been altered as a result of the experimental manipulation (see below).

The temporal response properties of neurons necessitated the use of suprathreshold stimulation. The definition of frequency following responses revealed the spatial and temporal representation of the behaviorally relevant stimulus in the cortex, and allowed analysis of the possible mechanisms by which the nervous system can discriminate flutter frequency. Similarly, questions relating to the animals ability to process motion information on the skin would require investigation of the neural response to moving stimuli. Thus, the appropriate stimulus used to define the response properties of cortical neurons is in fact not constant, but is dependent on the question under study.

Opposite hemisphere control

One set of control data was derived from the hemisphere representing the untrained hand in the same animals in which experimental data were derived. This opposite hemisphere control has the advantage that it is from the same animal and thus reflects the same physiological and behavioral history as the experimental hemisphere. These 'normal' maps also provided data from hands which were neither stimulated nor directly used in the task. The disadvantage is that they may have been affected either directly by projections of cortical neurons across the midline through the corpus callosum, or indirectly as a result

of the untrained hand being used in other aspects of the task such as grasping the cage to maintain balance.

The callosal projections between the hand area in SI are small in most primates, if not entirely nonexistent (see Killackey et al 1983 for owl monkey and Shanks et al 1985a for macaque). There is some projection of SII to its homologue on the contralateral hemisphere, as is true of most for the parietal cortex. The indirect influence of the stimulated SI on the contralateral control SI surely exists to some extent, as area 3b does project to the ipsilateral SII (Shanks et al 1985b; Cusick et al 1989). While the extent of this indirect projection is not clear, it should be stressed that the representations of the hand surface in areas 3a and 3b in these control hemispheres were, by all subjective criteria, equivalent to those in normal, untrained hemispheres (see Merzenich et al 1987; Kaas et al 1979). It is concluded that for cortical areas 3a and 3b, any effects from the contralateral hemisphere with respect to the topographic representations and receptive field properties were minimal in these experimental animals.

Passive-Stimulation hemispheres

The second set of control data were derived from passively stimulated animals. These animals had the same requirements as the experimental monkeys to perform the hand placement behavior, and they also received equivalent tactile stimulation in both duration and frequency. It is unlikely that the owl monkeys were more than rudimentarily aware of the tactile stimulus as they were performing the auditory discrimination. This contention is supported by the close correspondence between the auditory psychometric functions in

the presence and absence of the tactile stimulus (See Figure 11), and the similarities of their somatosensory cortical representations to those of normal monkeys.

Small differences in the representations of the hand surfaces were noted in these passive-stimulation control animals. These effects were consistent across the three hemispheres studied. In the one case where both hemispheres of a passive-stimulation animal was investigated, the passively-stimulated skin did have the greatest area of representation when compared to the three other control skin surfaces. However, this increase was much smaller than was seen in for the trained skin in experimental monkeys. Unfortunately the data sample is too small to make any firm conclusions, yet the limited data available does suggest a modest effect on cortical representations as a result of passive stimulation.

In summary, the results presented in this study are most consistent with an alteration of the functional organization of SI in animals trained to discriminate the frequency of a tactile stimulus presented to a restricted skin area. This reorganization occurred in parallel with the improvement in performance at the behavioral task. Two fundamental questions are raised by these results: 1) In what manner are the response properties of neurons in the cerebral cortex altered to account for the observed reorganization? and 2) What mechanisms can account for the frequency discrimination behavior and the improvement in discrimination performance with training?

POSSIBLE MECHANISMS OF REORGANIZATION

The mutability of the primary somatosensory cortex, particularly area 3b in the primate, has been demonstrated repeatedly. Two classes of interpretation have been put forth to account for this cortical plasticity: 1) The anatomical connections to and within the cortex have changed by sprouting and/or pruning of axonal and dendritic arbors, or 2) the efficacies of existing synapses have changed, but not the physical connections of pre- and post-synaptic cells. The most straightforward evidence for an anatomical explanation would be if the anatomical divergence in the somatosensory system was not sufficient to account for the observed plasticity.

Anatomical divergence of input

Intracellular injections of HRP into physiologically characterized thalamic afferents that project to SI provide the most direct evidence of the anatomical divergence in the cortex. In the owl monkey, 20 thalamo-cortical afferents were injected with HRP in the white matter 500-2500 μm below layer VI and the axonal processes were reconstructed (Garraghty et al 1989). These arbors covered a horizontal distance in cortex of 100-900μm, with a mean of approximately 350μm. The majority of synaptic bouton morphologies were most densely located in an area 350μm in diameter for all but the smallest afferents. The diameter of afferent arbors was larger in the macaque, ranging from 350-800μm in diameter (Garraghty and Sur 1990). Afferents that had multiple branches were observed in both studies. These axons had several separate clusters of terminations, all approximately 350μm in diameter and extending 1-3 mm in the tangential plane. These types of axons were seen in 5 of 20 owl monkey afferents and 1 of 8 macaque afferents. A study using the Golgi method to stain thalamic afferents was conducted in the squirrel monkey

(Jones 1975a). In this study thalamic afferents were reported to arborize over a distance of not less than 300μm.

Studies that address the dendritic spread of individual neurons in cortex have shown a similar range in values. These studies have mainly involved reconstruction of single neurons either injected intracellularly with HRP (Schwark and Jones 1989), or stained using a Golgi method (see Jones 1975b; Peters and Jones 1984). Pyramidal and spiny stellate cells in layer III-IV, where the thalamic afferents terminate, have dendritic spreads of 300-500 μm. Combining these data indicate that the 350μm diameter distributions of terminals can contact the dendrites of cell bodies at least 200μm on either extreme, making a total distribution of 750μm. Any single thalamic cell can potentially influence the firing rate of neurons within a distribution of at least 750μm.

Small injections of tracers into the ventrobasal thalamus or SI, which label many (hundreds) neurons at the injection site, suggest an even greater divergence of thalamic inputs in the cortex. In the central nucleus of the ventrobasal thalamus, neurons with very similar, almost completely overlapping receptive fields are organized into rostro-caudally oriented clusters or 'rods' (Jones and Friedman 1982a, b). These rods can extend for 500-800μm in the rostrocaudal direction. Afferent fibers from the dorsal column nuclei seem to project along these structures, making contact with most cells within a single rod (Rainey and Jones 1983). Single injections of tracer into one location of a single rods show a similar distribution of anterograde label in SI as do multiple injections elongated in the rosto-caudal axis which are presumably restricted to a single rod. The elongated injections are more densely labeled, suggesting

that the afferents from a single rod project to a densely overlapping zone two or more millimeters in diameter in SI cortex (Jones and Friedman 1982b; E.G. Jones, personal communication).

Studies in which the receptive fields of neurons at the injection site are defined suggest that label restricted to the representation of one or two digits in the thalamus projects to an area several millimeters in width in the cortex, which represent three to five digits (Lin et al 1979; Jones and Friedman 1982a, b; Cusick and Gould 1990). Anterograde labelling experiments are consistent with this result (Lin et al 1979; Mayner and Kaas 1986; Cusick and Gould 1990).

These anatomical data may not represent the total spreads of potential inputs for several reasons. First, intracellular injections of single afferents may not fill the entire axon, for example by restricted transport of the label. Second, injections made distal to major branch points may only fill a single branch, and the proportion of multiple branching axons seen (12-25%) may be underestimated. Third, the injection technique may selectively fill the largest diameter axons leading to overestimates of the actual values. The bulk injection data can lead to overestimates because the label can spread at the injection site, or the label can be taken up by axons of passage which are damaged by the injection pipette. Underestimates are possible by injection failure, the lack of uptake, or insufficient transport of the label. Although these caveats cannot be ignored, the emerging picture is that small regions of the thalamus directly influence a cortical area of at least 750μm and probably 1-3 millimeters in horizontal extent.

Physiological spread of inputs

Pharmacological manipulations of GABAergic inhibition have shown that cortical neurons receive input from a large skin area. Iontophoretic application of GABA antagonists in cat SI result in 4-10 fold increases of the receptive field size (Alloway et al 1989; Bautev et al 1982; Hicks and Dykes 1984). These changes occur on the order of seconds and are reversible. The same techniques applied in the thalamus do not result in a consistent increase in receptive field size (6/48 cells increased; Hicks et al 1986). These data indicate that the receptive field of a cortical neuron defined at any moment presumably represents only a fraction of the excitatory input available to that neuron.

The extent of afferent arborization has been measured at 250-830μm in cat SI using intracortical microstimulation (Snow et al 1988). These measurements were derived by defining the horizontal dimensions over which cortical microstimulation can cause antidromic action potentials recorded in a single thalamic neuron. Cortical receptive fields could be on completely different digits than the receptive fields of thalamic neurons antidromically activated from the cortical site. Zarzecki and Wiggin (1982) recorded sub-threshold responses of cortical neurons to electrical stimulation of peripheral cutaneous nerves. Their results suggest that inputs from at least two cutaneous nerves are present in 50% of SI cortical neurons.

Metabolic labeling of the cortex during the course of either electrical or mechanical stimulation have shown much larger areas of representation than would be predicted on the basis of the electrophysiological mapping studies. In adult cats, a cortical area 713μm across increased uptake of a metabolic label (2-deoxy-glucose) following mechanical stimulation of a single skin site (Juliano et al 1989). The area of increased uptake expanded to a width of 1266μm with

the treatment of the GABA antagonist bicuculine. Application of these same techniques in the primate showed that large patches one to five millimeters in extent were labeled in SI cortex following mechanical stimulation of a single digit with a 1cm diameter probe (Juliano and Whitsel 1987, 1985).

In summary, the limited pharmacological, physiological and metabolic evidence available indicates that a single location in SI cortex receives input from an area of skin many times larger that the receptive fields defined using single or multiple unit recording methods. This large area of skin that can potentially activate a cortical neuron can be accounted for by the estimated anatomical divergence of 750μm as discussed above. The data derived from cortical plasticity experiments, including the results described in this report, are largely confined within this estimated limit of 750 μm. The representation of any given skin surface was mainly contained within this limit. The few exceptions were still well within 1-2 mm, which is within the range of some thalamocortical afferents previously documented (Garraghty et al 1989). Receptive field overlap dropped to zero within approximately 800μm of cortical separation, even in experimental cases, which is consistent with the estimate of anatomical divergence. In short, the anatomical divergence known to exist in normal animals is sufficient to account for these observed physiological results.

Although it is not necessary to hypothesize sprouting of axonal or dendritic processes as a mechanism of reorganization, these results cannot exclude the possibility. It also does not eliminate the possibility that local changes in dendritic or synaptic morphology occurs (e.g. see Connors and Diamond 1982). A definitive experiment would be to compare the arborizations of single thalamic afferents and/or dendritic processes within and beyond a known area

of reorganized cortex. This type of study has been done in the visual cortex, taking advantage of the restricted arborizations of lateral geniculate afferents in ocular dominance columns (Katz et al 1989) and has shown that the dendritic arborization of neurons in the middle cortical layers respect these ocular dominance boundaries, whereas those of neurons in the upper and lower layers do not. Studies have also been reported in which the dendritic morphology of neurons in motor cortex of rats have been altered by training in a simple motor task (Greenough et al 1985; Withers and Greenough 1989). These investigators found a significant increase in dendritic length of 25-50 μm in layer V pyramidal cells. This magnitude of change was clearly less than those reported in this and other functional representational plasticity studies.

Physiological mechanisms of reorganization

Two general classes of physiological mechanisms have been proposed to account for cortical topographic reorganization. Each produces changes in representation by changing the effectiveness of inputs to cortical neurons at existing synapses, without the necessity of altering anatomical distributions. The difference lies in whether the transmission of impulses is altered by inhibitory or excitatory mechanisms.

Models of inhibition

Cortical receptive fields have been described as a product of excitatory and inhibitory processes (Laskin and Spencer 1979; Mountcastle and Powell 1959). In cat, receptive fields appear to have inhibitory components that are larger than and completely overlap with the excitatory receptive field (Laskin and Spencer 1979), whereas in primate the inhibitory receptive field is said to surround the excitatory receptive field (Mountcastle and Powell 1959).

Inhibitory receptive fields are rarely encountered (<10%) in primates. This may result from the difficulty in defining inhibitory receptive fields due to the low rate of spontaneous activity in SI cortex and their sensitivity to barbiturate anesthesia (see Mountcastle and Powell 1959).

Excitatory neurons, spiny stellate and small pyramidal cells, are known to synapse on neighboring, presumptively inhibitory neurons (see Peters and Jones 1984). These neurons project densely into the surrounding area. This anatomical construction has been hypothesized to be the basis of surround inhibition (Mountcastle, 1978). The latencies of inhibitory responses are generally longer than are those of excitatory responses. The main contention of inhibitory models is that cortical reorganization, for example following dennervation, arises by a release of inhibition through the silencing of inputs to the inhibitory neurons. This release from inhibition then allows previously sub-threshold inputs to fire cortical neurons in response to stimulation of the neighboring skin field. In time, these new driving inputs reorganize the inhibitory surrounds, and this process returns the receptive fields into topographic order.

A finding consistent with this model is that receptive field sizes increase following dennervation, and the receptive field location moves onto a dennervated region of skin (Calford and Tweedale 1988; Wall 1977; Merzenich et al 1983b). The Calford study in the flying fox suggested that the expanded receptive field always included the area of skin that was to become the stable receptive field. The Merzenich study in the owl monkey showed that 30% of the receptive fields recorded weeks after dennervation did not overlap with the receptive field recorded immediately after dennervation.

Studies which pharmacologically alter the inhibitory influence on cortical neurons clearly demonstrate the capacity of receptive field sizes to increase following the release of inhibition (studies cited above). Inhibitory inputs have also been proposed to shape the responses of auditory cortical neurons (see Abeles and Goldstein 1970; Suga and Tsuzuki 1985) and orientation selectivity in visual cortex (Sillito 1975). The GABA producing enzyme GAD, has been shown immuno-histochemically to increase in the cerebral cortex following selective stimulation of the periphery (Welker et al 1989b), and dennervation results in a decrease in GAD expression (Welker et al 1989a; Hendry and Jones 1988).

Hebbian-like synapse models

An alternative hypothesis to account for cortical plasticity is that the excitatory synapses change in effectiveness as the result of differences in their temporal activity (see Edelman 1978, 1987; Merzenich et al 1988; von der Malsburg and Singer 1988). These hypotheses evoke a Hebbian synapse (Hebb 1949), which increases its efficacy for firing the post synaptic neuron when both the pre- and post synaptic cells fire simultaneously. By this view, the co-activation of input from adjacent receptors in the skin is sufficient to activate the neuron, resulting in the correlated activity of the pre- and post-synaptic elements. Such temporally coincident inputs strengthen these synapses, whereas inputs which are not temporally correlated are not strengthened. An important feature is that the synapses are not necessarily only of the thalamo-cortical type, but can also be from local cortico-cortical connections. These cortico-cortical connections allow interaction of neighboring cortical neurons to operate in either a synergistic or antagonistic way. The resulting receptive field

is the product of the competition between the excitatory inputs from the thalamic afferents and the local cortical neurons with the inhibitory influence from the surrounding cortical neurons. The topography of the representation can therefore be maintained by this competitive balance.

There are several examples throughout the nervous system in which the efficacy of excitatory synapses are altered by temporal activation. The most widely known system studied is long-term potentiation (LTP) in the hippocampus (Bliss and Lomo 1973), in which tetanic stimulation of the input to the dentate gyrus potentiates subsequent responses to discrete inputs. LTP has also been demonstrated in motor cortex (Iriki et al 1989; Sakamoto et al 1987). Neurons in rat SI can respond to stimulation of a second whisker if stimulation of that whisker was paired with the whisker of its initial receptive field (Delacour et al 1987). The response of cat SI neurons to tactile stimulation is enhanced if the stimulation is paired with the iontophoretic application of acetylcholine (Metherate et al 1987). The response of auditory cortex can be altered by classical conditioning paradigms in which the response to tones is enhanced by pairing the tone presentation with foot shock (Diamond and Weinberger 1986 1989), or intracortical microstimulation (Buchalter et al 1978). Prevention of simultaneous pre- and post-synaptic activity can block the plasticity of synaptic efficacy in the visual cortex (Reiter and Stryker 1988).

Neural network models that modify excitatory synapses in a Hebbian manner show topographic reorganization similar to those described experimentally (Pearson et al 1987; Grajski and Merzenich 1990). No models based on changes of inhibition have been published that show the same result.

This negative result is perhaps due to lack of effort: however one such attempt is known to have failed (Grajski, personal communication).

The excitatory/Hebbian hypothesis is capable of explaining all experimental data thus far available. A simple example is the topography of the representation of a single digit and the sharp discontinuity of representation between two digits. The synchronous activity of peripheral receptors on a single digit will tend to strengthen the synapses of these inputs to the cortical neurons. The cortico-cortical interactions would then shape the receptive fields into topographic order through competitive mechanisms, as neighboring receptors will have the most temporally synchronous inputs, and this synchrony would decrease with distance. In the extreme the receptors are on different digits, and thus have much less temporal coactivation. This results in a sharp discontinuity through the cortico-cortical interactions and surround inhibition, even though anatomically the inputs overlap between these two cortical areas. An elegant experimental test of this scenario was done by surgically fusing the skin of two adjacent digits, thus creating a single, continuous digit. This manipulation resulted in a loss of the discontinuity between the digits as predicted (Clark et al 1988; Allard et al 1991).

The Hebbian-synapse models account for the immediate effects following dennervation as the result of the release from inhibition, as the inhibitory models propose. In contrast, the excitatory model predicts that the inhibitory portion of the receptive field is similarly plastic, as it directly reflects the input from the excitatory neuron (and therefore the receptive field). There is not a requirement that the new excitatory receptive field must be contained within the

enlarged receptive field, as is seen in 30% of the owl monkey receptive fields following dennervation (Merzenich et al 1983b).

The experimental data available to distinguish between the two models is not conclusive. Although somewhat circumstantial, the weight of the available evidence falls in favor of alterations of the excitatory synapse. Inhibitory models suffer in that a simple disinhibition without changes in synaptic efficacy predicts no difference between the immediate and long-term effects of dennervation. I favor the excitatory class of hypothesis and will advance this model in interpretations of the specific findings of this study, as discussed below.

Sub-cortical contribution to topographic changes

Changes in the topographic representation measured at the cortical level could be reflected by changes at any level throughout the somatosensory system. Changes in the periphery, for example sprouting of peripheral afferents or increased sensitivity of the individual receptors, is one possible mechanism which could account for the increased receptive fields size. In addition, the formation of calluses could plausibly contribute to the changes in the representations described here. These possibilities cannot be eliminated by the data collected in these studies, although the work of others suggests that sprouting of peripheral afferents is unlikely. For example, peripheral afferents were not seen to cross the suture line when two digits were surgically joined (Clark et al 1988; Allard et al 1991). Digital nerves allowed to reinnervate the digit will not invade the area of skin that was not dennervated (Allard et al 1988; see also Horch 1981). Although this evidence in indirect, it does indicate that the possibility of sprouting in the absence of dennervation is unlikely. Similarly, close inspection of the hand surface at the time of the electrophysiological study

did not reveal any calluses or other abnormality of the skin engaged in the behavior.

It is possible that topographic changes occur in subcortical relay nuclei. Changes in the somatotopic representation have been documented in the dorsal column nuclei (Millar et al 1976; Dostrovsky and Millar, 1977; McMahon and Wall, 1983) as well as the ventrobasal thalamus (Fadiga et al 1978; Pollin and Albe-Fessard, 1979). The greater divergence of anatomical connections in the cerebral cortex as compared to subcortical nuclei has been argued as an indication of the cerebral cortex being the focus of this reorganization (see Merzenich et al 1988, 1991). In fact, cortical reorganization has been observed in the absence of activation of peripheral nerves, and thus bypassing the normal subcortical nuclei (Recanzone et al 1988; Dinse et al 1990). These studies, of course, cannot eliminate the possibility of subcortical mechanisms of reorganization but do indicate that some portion of the reorganization takes place within the cerebral cortex itself.

SPECULATION ON NEURAL MECHANISMS

Any model of the mechanism of cortical reorganization must invoke intracortical interactions that maintain the normal topographic representation. The hypothesis that the response properties of cortical neurons reflect activity-dependent efficacy of excitatory synapses and intracortical interactions can account for all of the main results described in this study.

Neural mechanism of changes in topography and receptive field size

The receptive field size increased within the representation of the trained skin, and to a lesser extent this effect was present in the representation of the

analogous skin on the adjacent digit. The absolute area of representation of the trained skin site was also increased when compared to control digits, yet there was no significant increase in the representation of the entire digit. This violation of the overlap 'rule' was achieved by an increase in the number of receptive fields that were roughly centered on the stimulated skin. This conclusion is supported by: 1) Inspection of the receptive field sizes and locations recorded over that region. Many receptive fields appeared to be essentially identical and representing the same skin area; 2) The density of receptive fields that had their geometric centers located near the stimulation site; and 3) The distortion in the percent overlap of receptive fields in this region with respect to cortical distance. Receptive fields located near the stimulated skin could overlap completely for a cortical distance of over six hundred microns. Receptive fields representing the proximal and distal portions of the trained and adjacent digits and the receptive fields over the digits in control hemispheres had normal overlap-with-distance functions.

In the behavioral task, the area of skin stimulated in a temporally synchronous manner was of the order of the area of a typical cutaneous receptive field. This synchronous input from an invariant skin location would strengthen the synapses representing the stimulated skin. The neighboring cortical neurons which initially represented some portion of the stimulated skin would be activated simultaneously, thereby strengthening all local-circuit synapses of this group or cluster of neurons. The tighter coupling of these neighboring neurons would result in the group of neurons firing to any stimulus sufficient to fire one or some small subset of neurons. Thus, the synapses that initially excite any significant subset of the group could now fire all neurons of the group, resulting in the large and constant receptive field size.

The above model predicts that if the skin site stimulated was not restricted to a single location, but was instead positioned at different locations across the skin, the changes in topography and receptive field size would not result. A study of frequency discrimination in macaque, in which the tactile stimulus was presented to different locations on the skin, did not report differences in receptive field sizes (Mountcastle et al 1990).

As this large group of cortical neurons representing the stimulated skin expanded, the competitive influences of neurons representing the neighboring, unstimulated skin would become more competitive. Thus, these neurons that initially represented skin removed from the stimulation site would retain most of the original synaptic efficacies and therefore represent the same skin area. These competitive interactions can account for the constant area of representation of the entire digit.

The result of animal E-2 illustrates the best example of this phenomenon. In this case the receptive field overlap in the area representing the stimulated skin was very high over a cortical distance of approximately 800μm. This overlap then dropped dramatically at the margins of this cortical area. The receptive field size was also largest over the area of representation of the stimulated skin. This area could therefore be considered one large or 'super' group of tightly interconnected neurons. Three other experimental cases that showed the increase in receptive field sizes, cases E-1, E-3 and E-4, were consistent with the above model.

Influences of attention

The above model as stated must be expanded to include effects of attending to the tactile stimulus, as passively-stimulated control animals did not show a statistically significant increase in receptive field sizes. The enhancement of neural responses due to attention have been hypothesized to be regulated by chemical neuromodulators (see Farley et al 1985). Neuromodulators have also been implicated in normal developmental cortical plasticity (see Kasamatsu and Pettigrew 1976; Bear and Singer 1986). The best experimental evidence indicates that these neuromodulators include acetylcholine and/or norepinepherine (see Armstrong-James and Fox 1983; Sillito and Kemp 1983; Metherate et al 1987). These substances increase the responsiveness of neurons to natural stimulation, and improve the signal to noise ratio of the response. This effect is accomplished through an alteration of specific membrane channels activated via second messenger systems (see Nicoll et al, 1990 for review) that normally result in accommodation of the response to sustained stimuli. By blocking accommodation (e.g. see Madison et al 1986, 1988), the probability of synchronized pre- and post synaptic activity is increased, thereby increasing the efficacy of the effected synapses.

The increase of receptive field sizes cannot by itself account for the changes in behavioral performance. The receptive field sizes increased in the animal which had only limited improvement in performance (E-4). This animal clearly attended to the stimulus, as it responded at high delta frequencies. In a second animal which did show an improvement in performance (E-5) there was no increase in receptive field size. Interestingly, the receptive field sizes noted in area 3a of this animal were approximately the same size as the 3b receptive fields, and were much smaller than receptive field sizes measured in area 3a of other experimental hemispheres. Passively stimulated animals, which were

presumably not attending the stimulation, did not show an increase in receptive field size even though they were stimulated for a time equivalent to the tactually trained animals.

Emergence of a cutaneous representation in area 3a

The mechanisms described to explain the reorganization in area 3b can also account for the emergence of cutaneous receptive fields in area 3a. Cutaneous inputs to area 3a have been demonstrated to be sub-threshold in the anesthetized cat (Zarzecki and Wiggin 1982; Zarzecki and Herman 1983), and have been reported in the awake (Nelson 1987; Nelson and Douglass 1989) and anesthetized primate (Merzenich et al 1978, 1987; Kaas et al 1979). The increased attentional state coupled with cutaneous stimulation might be expected to selectively strengthen cutaneous inputs. The results of Nelson and Douglass (1989) suggest that input from motor and pre-motor areas modulate the responses of area 3a neurons. Inputs from these cortical areas onto area 3a neurons, coupled with cutaneous inputs from both area 3b and the ventrobasal thalamus, would be activated simultaneously and thus are expected to be strengthened. This strengthening of the cutaneous inputs would be seen using the experimental techniques used in this study.

This explanation is not meant to imply that the emergence of cutaneous receptive fields in area 3a is an epiphenomenon. The function of the cutaneous representation in area 3a may be indicated on the basis of the emergent cutaneous receptive field properties. At least three possible functions can be assigned to this "new" cutaneous representation. First, area 3a in these animals could have provided necessary inputs for correct hand placement and maintenance. One common feature of all animals trained in the apparatus was

that they very seldom used visual cues for hand placement. The information the animal could use to make correct hand placement was virtually entirely from the hand itself, and was presumably both cutaneous and proprioceptive.

Second, area 3a may have been providing temporal information about the stimulus which was used to discriminate frequency differences. The population cycle histograms from this cytoarchitectonic area, although smaller in absolute magnitude than the population cycle histogram measured in area 3b, were nonetheless sharply tuned (see below).

Third, area 3a could have been actively involved in performance of the behavioral response, which was to release the hand mold as soon as the frequency difference was detected. This hand release response was very stereotypic, usually initiated by the simultaneous extension of each of digits 2-5. Area 3a is known to project to area 4, the primary motor area, and it also has extensive projections down the spinal cord (Jones and Porter 1980; Zarzecki et al 1982, 1983). Thus, the functional alteration of area 3a may reflect its contribution to the behavioral response, providing feedback to motor areas facilitating hand release.

These hypotheses presented to account for changes in area 3a are not mutually exclusive. All animals that were successfully trained at the task had a significant cutaneous representation in area 3a, whereas control animals and the one animal that did not significantly improve its performance did not have a significant area 3a cutaneous representation. This implies that the cutaneous representation may be related to the improvement in temporal acuity. However, analysis of the temporal response properties in area 3a did not fit the behavioral

performance as well as neurons in area 3b, and there were significantly fewer of these responses. The distinction between the processing of information relating to hand position vs. the behavioral response cannot be made by the data collected in these experiments. One can speculate that the single animal that did not improve in performance was not relaying the appropriate neural information to area 3a, probably via the parietal lobe (see below), and thus not appropriately gating the cutaneous information. This would suggest that the function of area 3a is related to the behavioral response.

Neural correlate of frequency discrimination

Several features of the temporal response analyzed at individual cortical locations could not reliably account for the tactile frequency discrimination behavior. The firing rate, considered either at individual cortical locations or in the entire representation as a whole, was not consistently different between frequencies. This finding is consistent with those of other investigators (Mountcastle et al 1969, 1990). The phase-locking of neurons at individual locations were variable within and between individual animals, and did not show a clear correlation with the behavioral performance.

Tactile frequency discrimination has been hypothesized to be accounted for in SI cortex by the response to the individual cycles of the stimulus described by the cycle histogram (Mountcastle et al 1969, 1990). These investigators subjected the cycle histograms of 13 macaque cortical neurons and the behavioral performance of a well trained human to the same decision-theory analysis (Mountcastle et al 1969). The threshold predicted by the cycle histograms were only slightly higher than the performance of a single, well-trained human subject. The psychophysical detection and discrimination

thresholds were later shown to be similar between the two species (LaMotte and Mountcastle 1975). More recently, Mountcastle et al (1990) performed essentially the same experiments in awake animals during performance at the task, and compared the responses to those derived with identical stimulation without the behavioral contingency. They found that the temporal coding of the response, as measured by the power spectrum, was tuned to the presented frequency, that is, the power spectrum for a 20 Hz stimulus had the majority of energy at 20Hz, with only smaller amounts of energy at other frequencies. The same was true of the other frequencies presented. Their conclusion was that frequency discrimination could be based on this temporal information, but they did not elaborate how this could be done.

A similar analysis was conducted in this study based on the population response as opposed to the response of single neurons. In contrast to the Mountcastle studies, the cycle histograms in this study did not predict the behavioral thresholds, when considered as a whole. It was not until a subpopulation of area 3b responses were considered that a good fit to the behavioral data was obtained. This fit could be improved by only considering the rising phase of the histogram, corresponding to the onset response to each stimulus cycle. This finding makes intuitive sense when one considers the task. In order to determine the frequency, the animal must have knowledge of the occurrence in time of each of the stimulus cycles. Comparison of the time between cycle occurrence would then give a clear representation of the frequency. One way to increase the ability to discriminate small differences in frequency would then be to sharpen the tuning of the response to only a narrow range with respect to the phase of the stimulus. By sharpening the onset response to each stimulus cycle the coding of the timing between cycles would

be sharpened and hence the frequency discrimination performance would be improved. The remaining, temporally less well-defined responses to the stimulus cycle could then be used to code other aspects of the stimulus, for example the intensity or duration of each stimulus cycle.

Analysis of the neural data showed that the above hypothesis resulted in a close agreement between the predicted and measured performances at each frequency. The shape of the cycle histogram was not constant between frequencies, so simple detection theory analysis was not appropriate. It was necessary to analyze the neural data with respect to the difference between the representation of the S2 frequencies to that of the 20 Hz (S1) frequency. It is unclear from this data if the animal is able to use only the onset response, or if it uses the entire response, or in fact if it uses some entirely different mechanism. The finding that only considering the rising phase of the histogram gives the best fit to the data suggests that the animal may be biasing the weight of the input to the onset response.

Neural mechanisms of improvement in performance

The results of this study suggests that frequency discrimination is based on the difference between the representation in time of the occurrence of each stimulus cycle of the standard frequency and the S2 frequency. The improvement in performance could then be the result of the decreased variance of the response to each cycle of the presented stimulus. This decreased variance was achieved by a decrease in the latency of the response to the stimulus of a subset of neurons in area 3b.

The results from animal E-4 strongly support the above hypothesis. This animal had an overall increase in the population response, but the rising phase of the cycle histograms had a shallow slope. This paralleled the poor behavioral performance. Alternatively, the population response on the adjacent digit for animal E-2 was smaller but the cycle histograms showed a steep onset and the behavioral performance was better than was that of monkey E-4.

The mechanism presented above to account for the changes in topography of areas 3b and 3a can also adequately explain the improvement in behavioral performance with training at this task. The behavioral stimulus would coactivate inputs responding to the behavioral stimulus, thereby increasing synaptic efficacies. The shortest latency inputs are presumably the direct inputs from the thalamocortical afferents. By increasing the efficacy of these short latency inputs, the variance of the first response to each stimulus cycle would decrease, resulting in an increase in the slope of the rising phase of the cycle histogram. Similarly, the increased coupling between cortical neurons representing the stimulated skin could enhance the probability of a response of all neurons in the network to the appropriate thalamic input. This is supported by the observation that the rising phase of the cycle histograms of the trained digits are nearly identical, while the rising phase of the cycle histograms of the untrained digits were more varied. The somewhat degraded response at the higher frequencies used in the behavioral task (i.e. 26 Hz for E-1) could be explained by fatigue of the neurons, or by a relative refractory period of the network which decreases the response at this higher frequency. The fact that the predicted performance for this frequency is consistent with the behavioral results suggests that the two signals are different enough that the temporal code does not need to be so refined.

Finally, the fact that the neural signal was neither Gaussian in distribution, nor of equal variance for the different frequencies, could explain why the analysis of the behavioral data using signal detection theory was so variable. The calculated values of d' in the behavioral data did show an increase, but was variable between sessions. This is expected if the variance between the signals that are discriminated is changing over time.

Effects of Passive-Stimulation

Experiments addressing cortical topographic reorganization following a variety of manipulations have not directly addressed the function of selectively attending to tactile stimulation. Jenkins et al (1990) suggested that this may in fact be an important factor in cortical reorganization. Human observers noted that the tactile discrimination task used in this study demanded their complete attention in order to perform it successfully, implying that the monkeys devoted similar attention to the tactile stimulus. By directly comparing the results from the cortical representational maps of passively-stimulated hands to those used in the behavioral task, and to those of the contralateral, unstimulated and untrained hands, the effects of passive-stimulation can be addressed.

The first feature to note is the relative complexity of the hand representation. The hand representations of the unstimulated and untrained hands were well within the range of 'normal' with respect to cortical topography (see Merzenich et al 1984, 1987). Small irregularities were noted in the passive-stimulation hemispheres, mainly in discontinuities of the proximal portions of the digits. There also appeared to be a few discrete regions of the hand which were represented over a greater cortical area than other, similar

hand surfaces. This was reflected in an accumulation of receptive fields over those skin surfaces. These irregularities were much smaller than those observed in trained hemispheres. In addition, the cutaneous representation of the hand in area 3a was similar to that found in the contralateral control hemisphere.

The second feature to note was the area of representation of the stimulated skin. The limited data derived from these representations suggests that there was a small increase in the representation of the stimulated skin. This was most evident when comparing the area of representation of these skin surfaces between hemispheres in the one monkey studied.

The third feature was that the receptive field sizes representing the stimulated digit were not statistically significantly different than those representing other, unstimulated digits on the same hemisphere. The receptive field sizes on two adjacent digits were statistically significantly larger than those recorded on the homologous digit in the contralateral hemisphere in the one studied monkey.

The fourth feature to note is that the cortical locations of neurons with entrained responses were topographically restricted to a small, continuous area in passively-stimulated hemispheres. This is in contrast to the more diffusely located sites with entrained responses in the trained and adjacent digits of the experimental hemispheres. The temporal resolution of the stimulus, as measured by the population PSTH and cycle histograms, was similar to those on unstimulated digits.

These results collectively imply that the passive-stimulation regime was not sufficient in itself to generate the dramatic changes in cortical topography seen in the experimental hemispheres. The only effects seen were those relating to the topography of the hand representation. The passive-stimulation control animals were required to make the appropriate hand placement in order to initiate a behavioral trial, and these animals commonly did not visualize the hand mold to do so. These irregularities in cortical topography may simply reflect consequences of the hand placement behavior.

The auditory discrimination paradigm also required attentional vigilance to successfully perform the discrimination. This could very well have resulted in the animal actively ignoring the tactile stimulus that was simultaneously presented. Studies of selective attention in a task have been reported to influence the response properties of neurons at a wide variety of cortical areas (Robinson et al 1978; Mountcastle et al 1981, 1987; Bushnell and Goldberg 1981; Sato 1988; Spitzer et al 1988; Corbetta et al 1990). The study reported herein has provided unequivocal evidence that the behavioral relevance of a tactile stimulus strongly influences the effects of that stimulus on cortical topography. In retrospect it may have been prudent to test a third set of animals that passively received the same tactile stimulus, but were not engaged in any behavioral task.

Conclusions and implications

This study provides the first experimental evidence that the distributed response properties of cortical neurons are altered in concert with changes in the perceptual acuity of the animal. These kinds of changes, distributed

throughout the cortical mantle, could provide the neural substrate for learning through repetition.

This study also provides a new paradigm in which to test the hypotheses and models of cortical organization (see Edelman 1978, 1987; Mountcastle 1978; Merzenich et al 1987, 1988, 1990; von der Malsburg and Singer 1988). A key feature of this work which distinguishes it from that of previous investigators is that the behaviorally relevant stimulus was presented to a constant, invariant location on the skin. This resulted in a non-competitive input to a limited cortical region, resulting in an expansion of representation of that input. This result is exactly that predicted by the competitive, coincidence-based models of cortical organization proposed above, namely, cortical neurons over a significant horizontal extent became tightly coupled and responded to nearly-identical stimulation. This was dramatically evident in the very high resolution of the temporal responses to the behaviorally relevant sinusoidal stimuli. In spite of the distance between the cortical locations and the laborious process of defining the temporal response at each individual cortical location, the response to each stimulus cycle was very tightly locked in time. This implies that during presentation of the behavioral stimulus a large cortical area was *simultaneously* active. Through this tight coupling of cortical neurons, essentially a single module or positively coupled group of neurons was formed which occupied a large cortical area.

The creation of a large cortical area in which the receptive fields are highly overlapping also results from the synchronous activation of cortical neurons through intracortical microstimulation (Recanzone and Merzenich 1988; Dinse et al 1990). These effects occurred over a short period of time but were not as

great in magnitude as were those described in the present study. The driven and spontaneous activity of neurons at two cortical locations came to be correlated in time following the ICMS. The increased correlation of spontaneous activity suggests that the synaptic efficacies from the thalamic afferents were increased in these animals. In the present study, the increase in synaptic efficacy at the thalamocortical synapse is also suggested. The expansion of the short latency response area can be accounted for by an increase in the efficacy of this thalamocortical synapse.

A third implication is the relative influence of creation of this large neuronal group on the neighboring cortical area. In every case, the changes noted in the topographic representation and receptive field size for the trained skin was evident to a lesser extent on the adjacent digit. This effect was clearly evident with respect to receptive field size increases. Receptive field sizes were increased on the adjacent digit when compared to the contralateral control. Inspection of the cortical locations of these larger receptive fields showed that the largest among them were located adjacent to the representation of the trained skin. Cortical locations with entrained responses on the adjacent digit were also scattered throughout area 3b, as was seen for the trained digit. This finding was in contrast to the localized distribution of entrained responses seen in passively-stimulated controls. Presumably, this horizontal influence of neurons representing the trained skin would contribute to the temporal domain and in effect account for at least some of the observed transference of the improvement in performance.

Increases in receptive field size was noted in four of the five behaviorally trained animals. This increase did not, however, correlate with the behavioral

performance. One well-trained animal did not have large receptive fields. This was true of both area 3b and area 3a. On the other hand, the monkey with poor behavioral performance did have increased receptive field sizes in area 3b. The animal with no receptive field size increase was also trained for the fewest training session, whereas the other animal did receive a large number of training sessions, equivalent to that of the other well-trained animals. However, the total amount of stimulation in the animal with fewest training sessions nonetheless did receive an extensive period of training at that digit. This observation coupled with the lack of effects on receptive field size in passively-stimulated control cases, and the larger receptive fields on the adjacent digit of trained animals, indicates that receptive field size increases are not a simple function of stimulus presentations.

Alternatively, the differences may reflect a difference in the location of the tactile stimulus. If an animal were able to vary the stimulus location on the skin, the mechanism proposed above would not predict increased receptive field size. In fact, in studies in which the stimulus location was varied, no increases in receptive field size were noted (Mountcastle et al 1969, 1990; Hyvarinen 1980). Careful inspection of the video-taped sessions did not indicate more variability in hand position compared to the other animals, however. Thus it is difficult to reconcile this possibility with the available data.

Finally, the differences may reflect differences in the strategy used by the different animals to achieve improved frequency discrimination performance. It may be that the attention to the stimulus over the relatively long training period results in the increased receptive field size by the mechanism proposed above. This would result in an initial expansion of receptive field sizes to increase the

signal to noise ratio. The temporal responses are then subsequently sharpened to respond to only a limited segment of the stimulus cycle, and this sharpening of the response could then account for the improved performance. Animal E-5 may have had sufficient temporal resolution in the neural representation of flutter-frequency stimuli and thus the increase in receptive field sizes was unnecessary.

In each of the experimental hemispheres studied, there was considerable variability in the details of the topographic representation of the hand. These differences most probably reflect differences in the animal's neural and behavioral strategy in solving the task, and the predisposition of the animal's nervous system to perform the task. Ultimately all animals decreased the variance of the neural response to the tactile stimulus, however, the rate at which they did this varied considerably. It is intriguing to speculate that these differences would be illustrated by changing the task and challenging these animals in a similar but different enterprise. For example, changing the range in tested frequencies from a flutter to a vibration range may be easily met by an animal with many Pacinian-like responses, but take considerably more time to train animals which do not. Similarly, changing the task to an absolute location task, which presumably utilizes small receptive fields, would be easily transferred to by an animal that retained small receptive fields, but poorly for those with enlarged receptive fields. These examples may very well be the reason these animals showed considerable differences in the number of training sessions necessary to have equivalent performance.

The results presented herein provide strong evidence for models of functional cortical organization based on competitive interactions of cortical

neurons and coincidence of inputs. It also confirms the proposition that the functional organization of the cortex is alterable throughout life, and that this organization reflects the behavioral capacities of the animal. The demonstration of the alterability of the distributed responses properties has profound implications for other cortical areas, and thus other behaviors and perceptions, if the phenomenon and principles outlined in this thesis are generalizable to other areas of the neocortex.

Cited References

Abeles, M. and Goldstein, M.H. Jr. (1970). Functional architecture in cat primary auditory cortex: columnar organization and organization according to depth. *J. Neurophysiol* 33:172-187.

Allard, T.T., Clark, S.A., Grajski, K.A. and Merzenich, M.M. (1988). Plasticity in primary somatosensory cortex after digital nerve section and regeneration in adult owl monkey. *Soc. Neurosci. Abstr.* 14(2):844.

Alloway, K.D., Rosenthal, P. and Burton, H. (1989). Quantitative measurements of receptive field changes during antagonism of GABAergic transmission in primary somatosensory cortex of cats. *Exp. Br. Res.* 78:514-532.

Anderson, J.R. (1981). *Cognitive Skills and Their Acquisition.* Hillsdale, New Jersey:Erlbaum.

Armstrong-James, M. and Fox, K. (1983). Effects of iontophorised noradrenaline on the spontaneous activity of neurones in rat primary somatosensory cortex. *J. Physiol.* 335:427-447.

Batuev, A.S., Alexandrov, A.A. and Scheynikov, N.A. (1982). Picrotoxin action on the receptive fields of the cat sensorimotor cortex neurons. *J. Neurosci. Res.* 7:49-55.

Bear, M.F. and Singer, W. (1986). Modulation of visual cortical plasticity by acetylcholine and noradrenaline. *Nature* 320:172-176.

Bliss, T.V.P. and Lomo, T. (1973). Long-lasting potentiation of synaptic transmission in the dentate area of the anesthetized rabbit following stimulation of the preforant path. *J. Physiol.* 232:331-56.

Brodmann, K. (1905). Beitrage zur histologischen lokalisation der grosshirnrinde. Dritte mitt eilusns: Die rindenfelder der niederen affen. *J. Psychol. u. Neurol.* 4:177-224.

Buchhalter, J., Brons, J. and Woody, C. (1978). Changes in cortical neuronal excitability after presentations of a compound auditory stimulus. *Br. Res.* 156: 162-167.

Bushnell, M.C., Goldberg, M.E. and Robinson, D.L. (1981). Behavioral enhancement of visual responses in monkey cerebral cortex. I. Modulation in posterior parietal cortex related to selective visual attention. *J. Neurophysiol.* 46(4):755-772.

Byrne, J.H. (1987). Cellular analysis of associative learning. *Physiol. Reviews.* 57:329-439.

Calford, M.B. and Tweedale, R. (1988). Immediate and chronic changes in responses of somatosensory cortex in adult flying-fox after digit amputation. *Nature* 332:446-448.

Carlson, M., Huerta, M.F., Cusick, C.G. and Kaas, J.H. (1986). Studies on the evolution of multiple somatosensory representations in primates: the organization of anterior parietal cortex in the New World Callitrichid, *Saguinus. J. Comp. Neurol.246*:409-426.

Carlson, M., Fitzpatrick, K.A. (1982). Organization of the hand area in the primary somatic sensory cortex (SmI) of the prosimian primate, *Nycticebus coucang. J. Comp. Neurol.* 204:280-295.

Carlson, M. (1981). Characteristics of sensory deficits following lesions of Brodmann's areas 2 and 3 in the postcentral gyrus of *Macaca mulatta. Br. Res.* 204:424-430.

Clark, W.E. Le Gros and Powell, T.P.S. (1953). On the thalamo-cortical connexions of the general sensory cortex of *Macaca. Proc. Roy. Soc. Lond.B.* 141: 467-487.

Clark, S.A., Allard, T., Jenkins, W.M. and Merzenich, M.M. (1988). Syndactyly results in the emergence of double digit receptive fields in somatosensory cortex in adult owl monkeys. *Nature* 332:444-445.

Cole, J. and Glees, P. (1954). Effects of small lesions in sensory cortex in trained monkeys. *J. Neurophysiol.* 1:1-13.

Connor, J.R. and Diamond, M.C. (1982). A comparison of dendritic spine number and type on pyramidal neurons of the visual cortex of old adult rats from social or isolated environments. *J. Comp. Neurol.* 210:99-106.

Corbetta, M., Miezin, F.M., Dobmeyer, S., Shulman, G.L. and Petersen, S.E. (1990). Attentional modulation of neural processing of shape, color, and velocity in humans. *Science* 248:1556-1559.

Cronholm, B. (1951). Phantom limbs in amputees. A study of changes in the integration of centripetal impulses with special reference to referred sensations. *Acta Psychiat. Neurologica Scand. Suppl.* 72. 1-310.

Cusick, C.G. and Gould, H.J.III. (1990). Connections between area 3b of the somatosensory cortex and subdivisions of the ventroposterior nuclear complex and the anterior pulvinar nucleus in squirrel monkeys. *J. Comp. Neurol.* 292:83-102.

Cusick, C.G., Wall, J.T., Felleman, D.J. and Kaas, J.H. (1989). Somatotopic organization of the lateral sulcus of owl monkeys: Area 3b, S-II, and a ventral somatosensory area. *J. Comp. Neurol.* 282:169-190.

Delacour, J., Houcine, O. and Talbi, B. (1987). "Learned" changes in the responses of the rat barrel field neurons. *Neuroscience* 23(1):63-71.

Diamond, D.M. and Weinberger, N.M. (1986). Classical conditioning rapidly induces specific changes in frequency receptive fields of single neurons in secondary and ventral ectosylvian auditory cortical fields. *Br. Res.* 372:357-360.

Diamond, D.M. and Weinberger, N.M. (1989). Role of context in the expression of learning-induced plasticity of single neurons in auditory cortex. *Behav. Neurosci.* 103(3):471-494.

Dinse, H.R., Recanzone, G.H., and Merzenich, M.M. (1990). Direct observation of neural assemblies during neocortical representational reorganization. In: *Parallel Processing in Neural Systems and Computers* R. Eckmitler, G. Hartmann and G. Hauske (Eds.) North Holland: Elsevier Science Publishers. pp. 65-70.

Dostrovsky, J.O. and Millar, J. (1977). Receptive fields of gracile neurons after transection of the dorsal columns. *Exp. Neurol.* 56:610-621.

Dykes, R.W. (1983). Parallel processing of somatosensory information: a theory. *Br. Res. Rev.* 6:47-115.

Edelman, G.M. (1987). *Neuronal Darwinism: The Theory of Neuronal Group Selection.* New York: Basic Books.

Edelman, G.M. and Mountcastle, V.B (1978).*The Mindful Brain*: *Cortical Organization and the Group-Selective Theory of Higher Brain Function.* Cambridge: MIT Press.

Fadiga, E., Haimann, C., Margnelli, M. and Sotgiu, M.L. (1978). Variability of peripheral representation in ventrobasal thalamic nuclei of the cat: effects of acute reversible blockade of the dorsal column nuclei. *Exp. Neurol.* 60:484-498.

Farley, J. and Alkon, D.L. (1985). Cellular mechanisms of learning, memory, and information storage. *Ann. Rev. Psychol.* 36:419-494.

Franck, J.I. (1980). Functional reorganization of cat somatic sensory-motor cortex (SmI) after selective dorsal root rhizotomies. *Br. Res.* 186:458-462.

Friedman, D.P. and Jones, E.G. (1981). Thalamic input to areas 3a and 2 in monkeys. *J. Neurophysiol.* 45:59-85.

Gardner, E.P. (1988).Somatosensory cortical mechanims of feature detection in tactile and kinesthetic discrimination. *Can. J. Physiol. Pharmacol.* 66:439-454.

Garraghty, P.E. and Sur, M. (1990). Morphology of single intracellularly stained axons terminating in area 3b of macaque monkeys. *J. Comp. Neurol.* 294:583-593.

Garraghty, P.E., Pons, T.P., Sur, M. and Kaas, J.H. (1989). The arbors of axon terminations in middle cortical layers of somatosensory area 3b in owl monkeys. *Somatosen. Mot. Res.* 6(4):401-411.

Gibson, E.J. (1953). Improvement in perceptual judgments as a function of controlled practice or training. *Psychol. Bull.* 50(6):401-432.

Goldberg, M.E. and Bushnell, M.C. (1981). Behavioral enhancement of visual responses in monkey cerebral cortex. II. Modulation in frontal eye fields specifically related to saccades. *J. Neurophysiol.* 46(4): 773-787.

Graham Brown, T. and Sherrington, C.S. (1911). Observations on the localization in the motor cortex of the baboon (*Papio anubis*). *J. Physiol.* 43:209-218.

Graham Brown, T. and Sherrington, C.S. (1912). On the instability of a cortical point. *Proc. Roy. Soc. Lond. B.* 85:250-277.

Graham Brown, T. (1915). Studies in the physiology of the nervous system. XXII: On the phenomenon of facilitation. 1: Its occurrence in reactions induced by stimulation of the "motor" cortex of the cerebrum in monkeys. *Quart. J. Exp. Physiol.* 9(1):6-99.

Green, D.M. and Swets, J.A. (1966) *Signal Detection Theory.* New York: Wiley.

Greenough, W.T., Larson, J.R. and Withers, G.S. (1985). Effects of unilateral and bilateral training in a reaching task on dendritic branching of neurons in the rat motor-sensory forelimb cortex. *Behav. Neural. Biol* 44:301-314.

Grajski, K.A, and Merzenich, M.M. (1990). Hebb-type dynamics is sufficient to account for the inverse magnification rule in cortical somatotopy. *Neural Computation* 2: 74-81.

Haber, W.B. (1958). Reactions to loss of limb: physiological and psychological aspects. *Annals. New York Acad. Sci.* 74:14-24.

Heath, C.J., Hore, J. and Phillips, C.G. (1976). Inputs from low threshold muscle and cutaneous afferents of hand and forearm to areas 3a and 3b of baboon's cerebral cortex. *J. Physiol.* 257:199-227.

Hebb, D.O. (1949). *The Organization of Behavior: A Neuropsychological Theory.* New York: Wiley.

Henderson, W.R. and Smyth, G.E. (1948). Phantom limbs. *J. Neurol. Neurosurg. Psychiat.* 11. 88-112.

Hendry, S.H.C. and Jones, E.G. (1988). Activity-dependent regulation of GABA expression in the visual cortex of adult monkeys. *Neuron 1:*701-712.

Hicks, T.P., Metherate, R., Landry, P. and Dykes, R.W. (1986). Bicuculline induced alterations of response properties in functionally identified ventroposterior thalamic neurons. *Exp. Br. Res.* 63:248-264.

Hicks, T.P. and Dykes, R.W. (1984). Receptive field size for certain neurons in primary somatosensory cortex is determined by GABA-mediated intracortical inhibition. *Brain Res.* 274:160-164.

Horch, K. (1981). Absence of functional collateral sprouting of mechanoreceptor axons into dennervated areas of mammalian skin. *Exp. Neurol.* 74:313-317.

Hyvarinen, J., Poranen, A, and Jokinen, Y. (1980). Influence of attentive behavior on neuronal responses to vibration in primary somatosensory cortex of the monkey. *J. Neurophysiol.* 43(4):870-882.

Iriki, A., Pavlides, C., Keller, A. and Asanuma, H. (1989). Long-term potentiation in the motor cortex. *Science* 245:1385-1387.

James, W. (1890). *The Principles of Psychology.* Vol. I. New York: Dover Publications, Inc.

Jenkins, W.M., Merzenich, M.M., Ochs, M., Allard, T.T. and Guic-Robles, E. (1990). Functional reorganization of primary somatosensory cortex in adult owl monkeys after behaviorally controlled tactile stimulation. *J. Neurophysiol.* 63(1):82-104.

Jenkins, W.M. (1982). Interfacing the Apple II for the behavioral laboratory. *Behav. Res. Meth. Instrum.* 14(3):345-347.

Johansson, R.S. and Vallbo, A.B. (1979). Detection of tactile stimuli. Thresholds of afferent units to psychophysical thresholds in the human hand. *J. Physiol.* 297:405-422.

Johnson, K.O. and Phillips, J.R. (1981). Tactile spatial resolutions. I. Two-point discrimination, gap detection, grating resolution and letter recognition. *J. Neurophysiol.* 46:1177-1191.

Jones, E.G. (1975a). Lamination and differential distribution of thalamic afferents within the sensory-motor cortex of the squirrel monkey. *J. Comp. Neurol.* 160:167-204.

Jones, E.G. (1975b). Varieties and distribution of non-pyramidal cells in the somatosensory cortex of the squirrel monkey. *J. Comp. Neurol.* 160:205-268.

Jones, E.G. and Porter, R. (1980). What is area 3a? *Brain Res. Rev.* 2:1-43.

Jones, E.G. and Friedman, D.P. (1982). Projection pattern of functional components of thalamic ventrobasal complex on monkey somatosensory cortex. *J. Neurophysiol.* 48(2):521-544.

Jones, E.G., Friedman, D.P. and Hendry S.H.C. (1982). Thalamic basis of place- and modality-specific columns in monkey somatosensory cortex: a correlative anatomical and physiological study. *J. Neurophysiol.* 48(2):545-568.

Juliano, S. L., Whitsel, B.L., Tommerkahl, M. and Cheema, S.S. (1989). Determinants of patchy metabolic labeling in the somatosensory cortex of cats: a possible role for intrinsic inhibitory circuitry. *J. Neurosci.* 9(1):1-12.

Juliano, S. L., Whitsel, B.L. (1987). A combined 2-deoxyglucose and neurophysiological study of primate somatosensory cortex. *J. Comp. Neurol.* 263:514-525.

Juliano, S. L., Whitsel, B.L. (1985). Metabolic labeling associated with index finger stimulation in monkey SI: between animal variability. *Br. Res.* 342:242-251.

Kaas, J.H., Krubitzer, L.A., Chino, Y.M., Langston, A.L., Polley, E.H. and Blair, N. (1990). Reorganization of retinotopic cortical maps in adult mammals after lesions of the retina. *Science* 228:229-231.

Kaas, J.H., Merzenich, M.M and Killackey, H.P. (1983). The reorganization of somatosensory cortex following peripheral nerve damage in adult and developing mammals. *Ann Rev. Neurosci.* 6:325-356.

Kaas, J.H., Nelson, R.J., Sur, M., Lin, C.S., and Merzenich, M.M. (1979). Multiple representations of the body within the primary somatosensory cortex of primates. *Science* 204:521-523.

Kalaska, J. and Pomeranz, B. (1979). Chronic paw dennervation causes an age-dependent appearance of novel responses from forearm in "paw cortex" of kittens and adult cats. *J. Neurophysiol.* 42(2):618-633.

Kasamatsu, T. and Pettigrew, J.D. (1976). Depletion of brain catecholamines: failure of ocular dominance shift after monocular occlusion in kittens. *Science* 194: 206-209.

Katz, L.C., Gilbert, C.D. and Wiesel, T.N. (1989). Local circuits and ocular dominance columns in monkey striate cortex. *J. Neurosci.* 9(4):1389-1399.

Kelehan, A.M. and Deutsch, G.S. Time-dependent changes in the functional organization of somatosensory cerebral cortex following digit amputation in adult raccoons. *Somatosen. Res.* 2:49-81.

Kenshalo, D.R.Jr., Chudler, E.H., Anton, F. and Dubner, R. (1988). SI nociceptive neurons participate in the encoding process by which monkeys perceive the intensity of noxious thermal stimulation. *Br. Res.* 454:378-382.

Kenshalo, D.R. Jr. and Isensee, O. (1983). Responses of primate SI cortical neurons to noxious stimuli. *J. Neurophysiol 50*: 1479-1496.

Killackey, H.P. (1990). Static and dynamic aspects of cortical somatotopy: a critical evaluation. *J. Cog. Neurosci.* 1(1):1-11.

Killackey, H..P., Gould, H.J.III, Cusick, C.G., Pons, T.P. and Kaas, J.H. (1983). The relation of corpus callosum connections to architectonic fields and body surface maps in sensorimotor cortex of new and old world monkeys. *J.Comp. Neurol.* 219:384-419.

Kreig, W.J.S. (1954). Connections of the cerebral cortex. II. The macaque. E. The postcentral gyrus. *J. Comp. Neurol.* 101:101-127.

Krishnamurti, A., Sanides, F. and Welker, W.I. (1976). Microelectrode mapping of modality-specific somatic sensory cerebral neocortex in slow loris. *Br. Behav. Evol. 13*:267-283.

Krubitzer, L.A. and Kaas, J.H. (1990). The organization and connections of somatosensory cortex in marmosets. *J. Neurosci.*10(3):952-974.

Lamb, G.D. (1983). Tactile discrimination of textured surfaces: peripheral neural coding in the monkey. *J. Physiol.* 338:567-587.

LaMotte, J.H. and Mountcastle, V.B. (1979). Disorders in somesthesis following lesions of parietal lobe. *J. Neurophysiol.* 42(2):400-419.

LaMotte, J.H. and Mountcastle, V.B. (1975). Capacities of humans and monkeys to discriminate between vibratory stimuli of different frequency and amplitude: a correlation between neural events and psychophysical measurements. *J. Neurophysiol.*38:539-559.

Laskin, S.E. and Spencer, W.A. (1979). Cutaneous masking. II. Geometry of excitatory and inhibitory receptive fields of single units in somatosensory cortex of the cat. *J.Neurophysiol.* 42(4):1061-1082.

Lin, C.S., Merzenich, M.M., Sur, M. and Kaas, J.H. (1979). Connections of areas 3b and 1 of the parietal somatosensory strip with the ventroposterior nucleus in the owl monkey (*Aotus trivirgatus*). *J. Comp. Neurol.* 185(2):355-371.

Lucier, G.E., Ruegg, D.C. and Wiesendanger, M. (1975). Responses of neurones in motor cortex and in area 3a to controlled stretches of forelimb muscles in cebus monkeys. *J.Physiol.* 251:833-853.

Madison, D.V., Lancaster, B. and Nicoll, R.A. (1987) Voltage clamp analysis of cholinergic action in the hippocampus. *J. Neurosci.* 7:733-741.

Madison, D.V. and Nicoll, R.A. (1982). Noradrenaline blocks accommodation of pyramidal cell discharge in the hippocampus. *Nature* 299:636-638.

Marshall, W.H., Woolsey, C.N. and Bard, P. (1937). Cortical representation of tactile sensibility as indicated by cortical potentials. *Science* 85:388-390.

Marshall, W.H., Woolsey, C.N. and Bard, P. (1941). Observations on cortical somatic sensory mechanisms of cat and monkey. *J. Neurophysiol.* 4:1-24.

Mayner, L. and Kaas, J.H. (1986). Thalamic projections from electrophysiologically defined sites of body surface representations in areas 3b and 1 of somatosensory cortex of cebus monkeys. *Somatosens. and Mot. Res.* 4(1):13-29.

McKenna, T.M., Whitsel, B.L., Dreyer, D.A. and Metz, C.N. (1981). Organization of cat anterior parietal cortex: relations among cytoarchitecture, single neuron functional properties, and interhemispheric connectivity. *J. Neurophysiol. 45*:667-697.

McMahon, S.B. and Wall, P.D. (1983). Plasticity in the nucleus gracilis of the rat. *Exp. Neurol.* 80:195-207.

Merzenich, M.M., Recanzone, G.H. and Jenkins, W.M. (1990). How the brain functionally rewires itself. In *Neural and Artificial Parallel Computations* M. Buchsbaum, W.E. Bunney and R. Hair (Eds) New York: MIT Press.

Merzenich, M.M., Recanzone, G.H., Jenkins, W.M., Allard, T.T. and Nudo, R.J. (1988). Cortical representational plasticity. In:*Neurobiology of Neocortex* T. P. Rakic and W. Singer (eds.). New York: John Wiley & Sons Limited. pp. 41-67.

Merzenich, M.M. (1987). Dynamic neocortical processes and the origins of higher brain functions. In: *The Neural and Molecular Bases of Learning.* pp. 337-358. J.P. Changeux and M. Konishi (eds.) New York: John Wiley & Sons Limited..

Merzenich, M.M., Nelson, R.J., Kaas, J.H., Stryker, M.P., Jenkins, W.M., Zook, J.M., Cynader, M.S. and Schoppmann, A. (1987). Variability in hand surface representations in areas 3b and 1 in adult owl and squirrel monkeys. *J. Comp. Neurol.* 258:281-296.

Merzenich, M.M., Nelson, R.J., Stryker, M.P. Cynader, M.S., Schoppmann, A. and Zook, J.M. (1984). Somatosensory cortical map changes following digital amputation in adult monkey. *J. Comp. Neurol.* 224:591-605.

Merzenich, M.M., Kaas, J.H., Wall, J.T., Nelson, R.J., Sur, M., and Felleman, D.J. (1983a). Topographic reorganization of somatosensory cortical areas 3b and 1 in adult monkeys following restricted deafferentation. *Neurosci.* 10: 33-55.

Merzenich, M.M. Kaas, J.H., Wall, J.T., Sur, M. Nelson, R.J. and Felleman, D.J. (1983b). Progression of change following median nerve section in the cortical representation of the hand in areas 3b and 1 in adult owl and squirrel monkeys. *Neurosci.* 10:639-665.

Merzenich, M.M. Kaas, J.H., Sur, M. and Lin, C.S. (1978). Double representation of the body surface within cytoarchitectonic areas 3b and 1 in "SI" in the owl monkey (*Aotus trivirgatus*). *J. Comp. Neurol.*181:41-74.

Metherate, R., Trembley, N. and Dykes, R.W. (1987). Acetylcholine permits long-term enhancement of neuronal responsiveness in cat primary somatosensory cortex. *Neuroscience* 22(1):75-81.

Millar, J., Bausbaum, A.I. and Wall, P.D. (1976). Restructuring of the somatotopic map and appearance of abnormal neuronal activity in the gracile nucleus after partial deafferentation. *Exp. Neurol.* 50:658-672.

Mountcastle, V.B., Steinmetz, M.A. and Romo, R. (1990). Frequency discrimination in the sense of flutter: psychophysical measurements correlated with postcentral events in behaving monkeys. *J. Neurosci.* 10:3032-3044.

Mountcastle, V.B., Motter, B.C., Steinmetz, M.A. and Sestokas, A.K. (1987). Common and differential effects of attentive fixation on the excitability of parietal and prestriate (V4) cortical visual neurons in the macaque monkey. *J. Neurosci.* 7(7):2239-2255.

Mountcastle, V.B., Andersen, R.A. and Motter, B.C. (1981). The influence of attentive fixation upon the excitability of the light-sensitive neurons of the posterior parietal cortex. *J. Neurosci.* 1:1218-1235.

Mountcastle, V.B. (1978). In: *The Mindful Brain: Cortical Organization and the Group-Selective Theory of Higher Brain Function.* E.G. Edelman and V.B. Mountcastle. Cambridge: MIT Press.

Mountcastle, V.B., LaMotte, R.H. and Carli, G. (1972). Detection thresholds for vibratory stimuli in humans and monkeys: comparison with threshold events in mechanoreceptive afferent nerve fibers innervation the monkey hand. *J. Neurophysiol.* 35:122-136.

Mountcastle, V.B., Talbot, W.H., Sakata, H. and Hyvarinen, J. (1969). Cortical neuronal mechanisms in flutter-vibration studied in unanesthetized monkeys. Neuronal periodicity and frequency discrimination. *J. Neurophysiol.* 32:452-484.

Mountcastle, V.B. and Powell, T.P.S. (1959). Neural mechanisms subserving cutaneous sensibility, with special reference to the role of afferent inhibition in sensory perception and discrimination. *Bull. Johns Hopkins Hosp.* 105:201-232.

Nelson, R.J. and Douglas, V.D. (1989). Changes in premovement activity in primary somatosensory cortex differ when monkeys make hand movements in response to visual vs vibratory cues. *Br. Res.* 484:43-56.

Nelson, R.J. (1987). Activity of monkey primary somatosensory cortical neurons changes prior to active movement. *Br. Res.* 406:402-407.

Nelson, R.J., Sur, M., Felleman, D.J. and Kaas, J.H. (1980). Representations of the body surface in postcentral parietal cortex of *Macaca fasicularis. J. Comp. Neurol.* 192:611-643.

Nicoll, R.A., Malenka, R.C. and Kauer, J.A. (1990) Functional comparison of neurotransmitter receptor subtypes in mammailan central nervous system. *Physiol. Rev.* 70:513-565.

Pearson, J.C., Finkel, L.H. and Edelman, G.M. (1987). Plasticity organization of adult cerebral cortical maps: a computer simulation based on neuronal group selection *J. Neurosci.* 7:4209-4333.

Penfield,W and Boldrey, E. (1937). Somatic motor and sensory representation in the cerebral cortex of man as studied by electrical stimulation. *Brain.* 60:255-281.

Penfield, W. and Rasmussen, T.(1950). *The Cerebral Cortex of Man. A Clinical Study of Localization of Function.* New York: Macmillan

Peters, A. and Jones, E.G. (1984) *Cerebral Cortex. Volume I* .New York:Plenum Press.

Phillips, C.G., Powell, T.P.S. and Wiesendanger, M. (1971). Projection from low-threshold muscle afferents of hand and forearm to area 3a of baboon's cortex. *J. Physiol.* 217:419-446.

Phillips, J.R. and Johnson, K.O. (1981). Tactile spatial resolution. II. Neural representation of bars, edges, and gratings in monkey primary afferents. *J. Neurophysiol.* 46(6):1192-1203.

Pollin, B and Albe-Fessard, D. (1979). Organization of somatic thalamus in monkeys with and without section of dorsal spinal tracts. *Br. Res.* 173:431-449.

Pons, T.P., Garraghty, P.E. and Mishkin, M. (1988). Lesion-induced plasticity in the second somatosensory cortex of adult macaques. *Proc. Natl. Acad. Sci.* 85:5279-5281.

Pons, T.P., Wall, J.T., Garraghty, P.E., Cusick, C.G. and Kaas, J.H. (1987). Consistent features in the representation of the hand in area 3b of macaque monkeys. *Somatosens. Res.* 4:309-331.

Pons, T.P., Garraghty, P.E., Cusick, C.G. and Kaas, J.H. (1985). The somatotopic organization of area 2 in macaque monkeys. *J. Comp.Neurol.* 241:445-466.

Powell, T.P.S. and Mountcastle, V.B. (1959a). The cytoarchitecture of the postcentral gyrus of the monkey *Macaca mulatta. Bull. Johns. Hopkins.*150:108-131.

Powell, T.P.S. and Mountcastle, V.B. (1959b). Some aspects of the functional organization of the cortex of the postcentral gyrus of the monkey. A correlation of findings obtained in a single unit analysis with cytoarchitecture. *Bull. Johns Hopkins Hosp.* 105:133-162.

Rainey, W.T. and Jones, E.G. (1983). Spatial distribution of individual medial lemniscal axons in the thalamic ventrobasal complex of the cat. *Exp. Br. Res.* 49:229-246.

Randolph, M. and Semmes, J. (1974). Behavioral consequences of selective subtotal ablations in the postcentral gyrus of *Macaca mulatta. Br. Res.*70:55-70.

Rasmusson, D.D. (1982). Reorganization of raccoon somatosensory cortex following removal of the fifth digit. *J. Comp. Neurol.* 205:313-326.

Recanzone, G.H. and Merzenich, M.M. (1988). Intracortical microstimulation in somatosensory cortex in adult rats and owl monkeys results in a large expansion of the cortical zone of representation of a specific cortical receptive field. *Soc. Neurosci. Abstr.* 18:92.10.

Reiter, H.O. and Stryker, M.P. (1988). Neural plasticity without post-synaptic action potentials: less active inputs become dominate when kitten visual cortical cells are pharmacologically inhibited. *Proc. Nat. Acad. Sci.* 85(10):3623-3627.

Robertson, D. and Irvine, D.R.F. (1989). Plasticity of frequency organization in auditory cortex of guinea pigs with partial unilateral deafness. *J. Comp. Neurol.*282:456-471.

Robinson, D.L., Goldberg, M.E. and Stanton, G.B. (1978). Parietal association cortex in the primate: sensory mechanisms and behavioral modulations. *J. Neurophysiol.* 41(4):910-932.

Sakamoto, T., Porter, L.L. and Asanuma, H. (1987). Long-lasting potentiation of synaptic potentials in the motor cortex produced by stimulation of the sensory cortex in the cat: a basis of motor learning. *Br. Res.* 413:360-364.

Sanes, J.N., Suner, S. and Donoghue, J.P. (1990). Dynamic organization of primary motor cortex output to target muscles in adult rats. I. Long-term patterns of reorganization following motor or mixed peripheral nerve lesions. *Exp. Br. Res.* 79:479-491.

Sato, T. (1988). Effects of attention and stimulus interaction on visual responses of inferior temporal neurons in Macaque. *J. Neurophysiol.* 60(1):344-363.

Schwark, H.D. and Jones, E.G. (1989). The distribution of intrinsic cortical axons in area 3b of cat primary somatosensory cortex. *Exp. Br. Res.* 78:501-513.

Semmes, J., Porter, L. and Randolph, M. (1974). Further studies of anterior postcentral lesions in monkeys. *Cortex* 10:55-68.

Semmes, J. and Porter, L. (1972). A comparison of precentral and postcentral cortical lesions on somatosensory discrimination in the monkey. *Cortex* 8(2):249-264.

Shanks, M.F., Pearson, R.C.A. and Powell, T.P.S. (1985a). The callosal connexions of the primary somatic sensory cortex in the monkey. *Br. Res. Rev.* 9:43-65.

Shanks, M.F., Pearson, R.C.A., Powell, T.P.S. (1985b). The ipsilateral cortico-cortical connexions between the cytoarchitectonic subdivisions of the primary somatic sensory cortex in the monkey. *Br. Res. Rev.* 9:67-88.

Sillito, A.M. and Kemp, J.A. (1983). Cholinergic modulation of the functional organization of the cat visual cortex. *Br. Res.* 289:143-155.

Sillito, A.M. (1975). The contribution of inhibitory mechanisms to the receptive field properties of neurones in the striate cortex of the cat. *J. Physiol.* 250:305-329.

Singley, M.K. and Anderson, J.R. (1989). *The Transfer of Cognitive Skill.* Cambridge: Harvard University Press.

Snow, P. J., Nudo, R.J., Rivers, W., Jenkins, W.M. and Merzenich, M.M. (1988). Somatotopically inappropriate projections from thalamocortical neurons to the SI cortex of the cat demonstrated by the use of intracortical microstimulation. *Somatosen. Res.*5:349-372.

Spitzer, H., Desimone, R. and Moran, J. (1988). Increased attention enhances both behavioral and neuronal performance. *Science* 240: 338-340.

Stryker, M.P., Jenkins, W.M. and Merzenich, M.M. (1987). Anesthetic state does not affect the map of the hand representation within area 3b somatosensory cortex in owl monkey. *J. Comp. Neurol.* 258:297-303.

Suga, N. and Tsuzuki, K. (1985). Inhibition and level-tolerant frequency tuning in the auditory cortex of the mustached bat. *J. Neurophysiol.* 53(4):1109-1145.

Sur, M., Garraghty, P.E. and Bruce, C.J. (1985). Somatosensory cortex in macaque monkeys:laminar differences in receptive field size in areas 3b and 1. *Br. Res.* 342:391-395.

Sur, M., Wall, J.T. and Kaas, J.H. (1984). Modular distribution of neurons with slowly adapting and rapidly adapting responses in area 3b of somatosensory cortex in monkeys. *J. Neurophysiol.* 51(4):724-744.

Sur, M., Nelson, R.J. and Kaas, J.H. (1982). Representations of the body surface in cortical areas 3b and 1 of squirrel monkeys: comparisons with other primates. *J. Comp. Neurol.* 211:177-192.

Sur, M., Merzenich, M.M. and Kaas, J.H. (1981). Magnification, receptive fields area, and "hypercolumn" size in areas 3b and 1 of somatosensory cortex in owl monkeys. *J. Neurophysiol.* 44:295-311.

Sur, M. (1980). Receptive fields of neurons in areas 3b and 1 of somatosensory cortex in monkeys. *Br. Res.* 198:465-471.

Talbot, W.H., Darian-Smith, I., Kornhuber, H.H. and Mountcastle, V.B. (1968). The sense of flutter-vibration: comparisons of the human capacity with response patterns of mechanoreceptive afferents from the monkey hand. *J. Neurophysiol.* 31:301-334.

Teuber, L., Keieger, H.P. Bender, M.B. (1949). Reorganization of sensory function in amputation stump: two-point discrimination. *Fed. Proc.* 8(1):156.

Thompson, R.F., Donegan, N.H. and Lavond, D.G. (1988). The psychobiology of learning and memory. In: *Stevens' Handbook of Experimental Psychology. Vol. 2: Learning and Cognition.* R.C. Atkinson, R.J.

Herrnstein, R.J., G. Lindzey, and R.D. Luce (Eds.). New York: John Wiley & Sons. pp.245-347.

Torebjork, H.E., Vallbo, A.B. and Ochoa, J.L. (1987). Intraneural microstimulation in man. Its relation to specificity of tactile sensations. *Brain* 110:1509-1529.

Torebjork, H.E. and Ochow, J.L. (1980). Specific sensations evoked by activity in single identified sensory units in man. *Acta Physiol. Scand.* 110:445-447.

von der Malsburg, C. and Singer, W. (1988). Principles of cortical network organization. In:*Neurobiology of Neocortex*T. P. Rakic and W. Singer (eds.). New York: John Wiley & Sons Limited. pp.69-99.

Vierck, C.J. Jr., Favorov, O. and Whitsel, B.L. (1989). Neural mechanisms of absolute tactile localization in monkeys. *Somatosens. and Mot. Res.* 6(1):41-61.

Vierck, C.J.Jr. and Jones, M.B. (1970). Influences of low and high frequency oscillation upon spatio-tactile resolution. *Physiol. Behav.* 5:1431-1435.

Vogt, C. and Vogt, O. (1919). Allgemeinere Ergebnisse unserer Hirnforschung. *J. Psychol. u. Neurol.* 25:279-292.

Wade, D.T., Hewer, R.L., Skilbeck, C. and David, R.M. (1985). *Stroke. A critical approach to diagnosis treatment and management.* pp.175-284. Chicago: Year Book Medical Publishers, Inc.

Wagenaar, R.C., Meijer, O.G., van Wieringen, P.C.W., Kuik, D.J., Hazenberg, G.J., Lindeboom, J., Wichers, F. and Fijswijk, H. (1990). The functional recovery of stroke: a comparison between neuro-developmental treatment and the brunnstrom method. *Scand. J. Rehab. Med.* 22:1-8.

Wall, J.T. and Cusick, C.G. (1984). Cutaneous responsiveness in primary somatosensory (S-I) hindpaw cortex before and after partial hindpaw deafferentation in adult rats. *J. Neurosci.* 4:1499-1515.

Wall, P.D. (1977). The presence of ineffective synapses and the circumstances which unmask them. *Phil. Trans. R. Soc. Lond. B.* 278:361-372.

Welker, E., Soriano, E., Dorfi, J. and Van der Loos, H. (1989a). Plasticity in the barrel cortex of the adult mouse: transient increase of GAD-immunoreactivity following sensory stimulation. *Exp. Br. Res.*78:659-664.

Welker, E., Soriano, E., and Van der Loos, H. (1989b). Plasticity in the barrel cortex of the adult mouse: effects of peripheral depravation on GAD-immunoreactivity. *Exp. Br. Res. 74*: 441-452.

Withers, G.S. and Greenough, W.T. (1989). Reach training selectively alters dendritic branching in subpopulations of layer II-III pyramids in rat motor-somatosensory forelimb cortex. *Neuropsychologia* 27(1):61-69.

Woolsey, C.N., Marshall, W.H. and Bard, P. (1942). Representation of cutaneous tactile sensibility in the cerebral cortex of the monkey as indicated by evoked potentials. *Bull. Johns Hopkins Med. Sch.* 70:399-441.

Zaraecki, P. and Herman, D. (1983). Convergence of sensory inputs upon projection neurons of somatosensory cortex: vestibular, neck, head, and forelimb inputs. *Exp. Br. Res.* 50:408-414.

Zarzecki, P. and Wiggin, D.M. (1982). Convergence of sensory inputs upon projection neurons of somatosensory cortex. *Exp. Br. Res.* 48:28-42.

APPENDIX I

Internal apparatus

The internal apparatus was housed inside a single-walled acoustic chamber. The inside walls and door of the chamber were covered with 4" echo-attenuating foam. The internal apparatus consisted of a cage (see Figure A1), indicator lights located on the ceiling of the chamber, a hand mold and tactile stimulator at one end (front), and a food cup for the pellet rewards. The cage was constructed of 3mm diameter stainless steel rods at 27mm intervals measuring 28cm X 21cm X 48cm (*l* X *w* X *h*). The cage was fastened to the floor of the chamber on a 2cm foam pad to reduce vibrations. The animal extended it's hand and arm outside the cage through a 5 cm X 14 cm opening to make contact with the hand mold.

Hand molds were constructed from poly-form sheet. The mold had five grooves, one for each digit, and the palm-digit angle was approximately 75° when the palm rested on the mold (see Fig. A1). Strips of gold-plated copper foil (3mm X 10mm) were imbedded in each groove with cyanoacrylate. Wire leads from these strips were fastened to the underside of the hand mold with cyanoacrylate and connected to the contact circuitry. The mold was stabilized by four bolts through a U-shaped aluminum brace and fastened to a magnetic-base post.

Openings to allow access to the skin surfaces of interest were made after the mold was formed. The stimulator probe contacted the skin at 90° through the opening. The stimulator probe was a 2mm diameter monofilament rod with a hemispherical tip. The tactile stimulator faithfully delivered sinusoidal

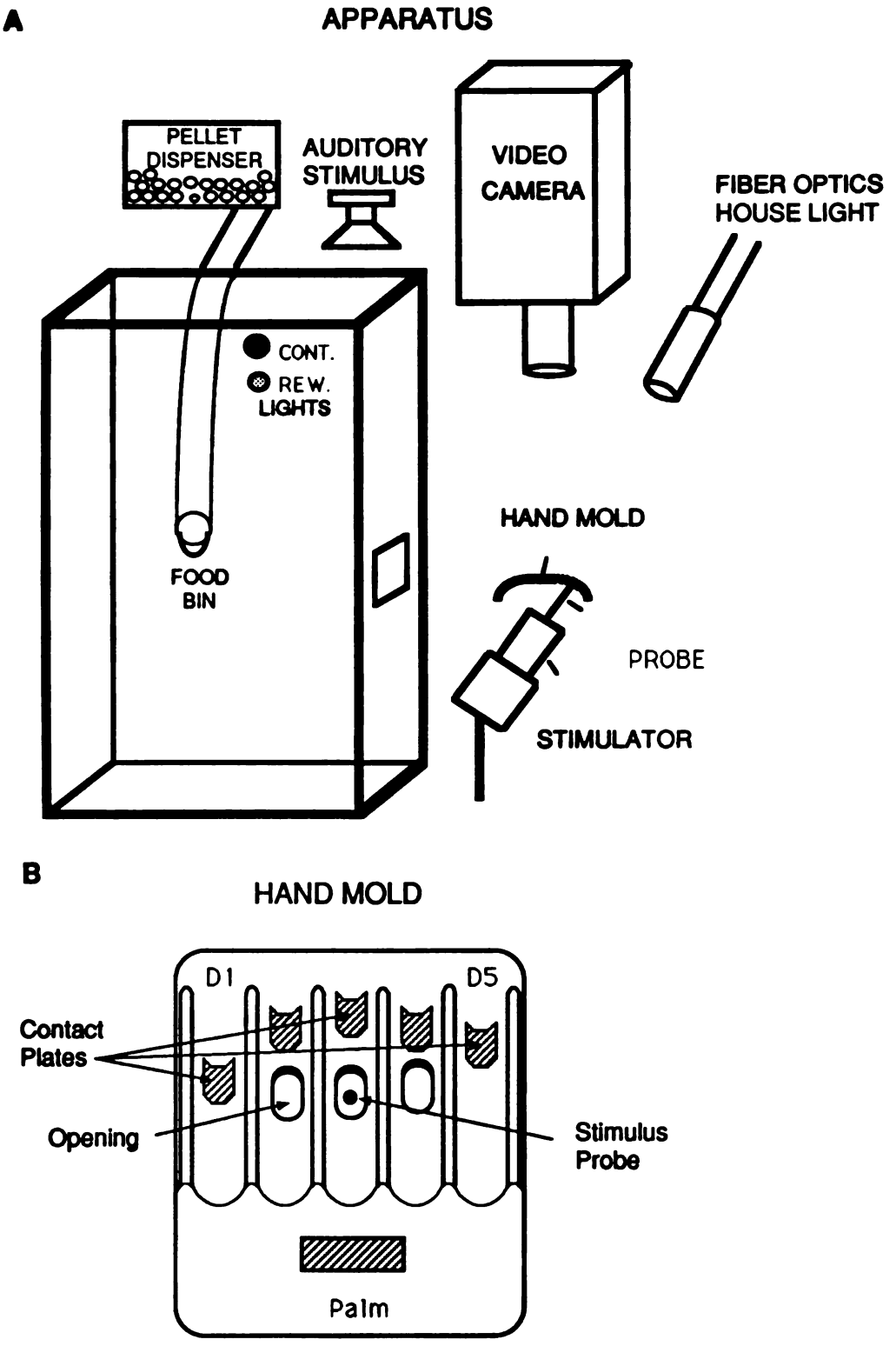

Figure A1. Behavioral apparatus (A) and a top view of a schematic hand mold (B). The apparatus was designed such that only one unique hand position could initiate a trial. The tactile stimulator contacted the skin from underneath the mold. See text.

waveforms at a constant displacement across the frequencies used (Chubbuck 1966).

Rewards were 45mg. banana-flavored food pellets (Bio-Serve, FO382). The number of pellets eaten in a normal session was nutritionally equivalent or superior to the normal diet of chow biscuits (Purina). The automated pellet dispenser (Gerbands D-1) was located outside of the sound booth test chamber. The food cup was located on the side of the cage. A fiber optic light source directed onto the hand mold served as the house light. Two 6.5V incandescent lights of different colors were located at the top of the cage. A video camera was used for continual visual monitoring of hand position. A speaker located directly above the test chamber provided auditory stimuli.

External Apparatus

An Apple II microcomputer with digital interfaces (Jenkins 1982) controlled all aspects of the behavioral procedure, provided on-line feedback of the animals performance, and allowed the experimenter to adjust several stimulus parameters without interruption. The pellet dispenser, indicator lights and the house light were controlled through relay switches within the behavioral interface.

Stimuli consisted of sinusoidal waveforms. The auditory stimulus was amplified (crown D76) and presented through a conventional speaker. The amplifier output and displacement feedback from the Chubbuck stimulator were continuously monitored on an oscilloscope. The contact circuitry delivered a step voltage upon detection of <5 MΩ resistance between the contact plates and the cage floor. The experimenter could set any combination of inputs as

"correct" to initiate a stimulus run.

PSYCHOPHYSICAL PROCEDURE

Subject's task

The tactile frequency discrimination protocol is diagramed in Figure 2A. The subject initiated each run by making "correct" contact with the hand mold, as determined by the contact circuit output, and indicated to the subject by an indicator light. A one second pre-stimulation period began in which the animal could break correct contact without penalty. The pre-period was followed by a ramped displacement of the stimulator tip onto the skin surface. All sinusoidal stimulation for the run was superimposed onto this ramped displacement. A completed run consisted of 2-6 stimulus presentations (bins) of 650 msec duration with a 650 msec pause between bins. In each stimulus bin the probe was set into sinusoidal oscillation at a frequency between 20-40 Hz. The first stimulus presented was always the comparison stimulus (S1; 20 Hz). Presentations 2-5 had an equal probability (0.388) that the stimulus would be a higher frequency (S2), given that S2 had not yet been presented. Thus, the probability that an S2 would occur in the next bin did not increase during a run. Eight lookup tables of bin presentation were created using the values in Table A1 in pseudo-random order. Four of these tables were randomly selected to run in sequential order for each session, the only requirement being that the same table was not used first on two consecutive days. The bin in which the S2 was to be presented in was selected in order from the look-up table. If the animal made a response before the presentation of the S2 (a False-Positive), the same S2 was presented on the next run, in the bin of presentation next in order in the look-up table. Thus each sequence of the bin in which the S2 was presented varied by the particular sequence of False-Positives of the given

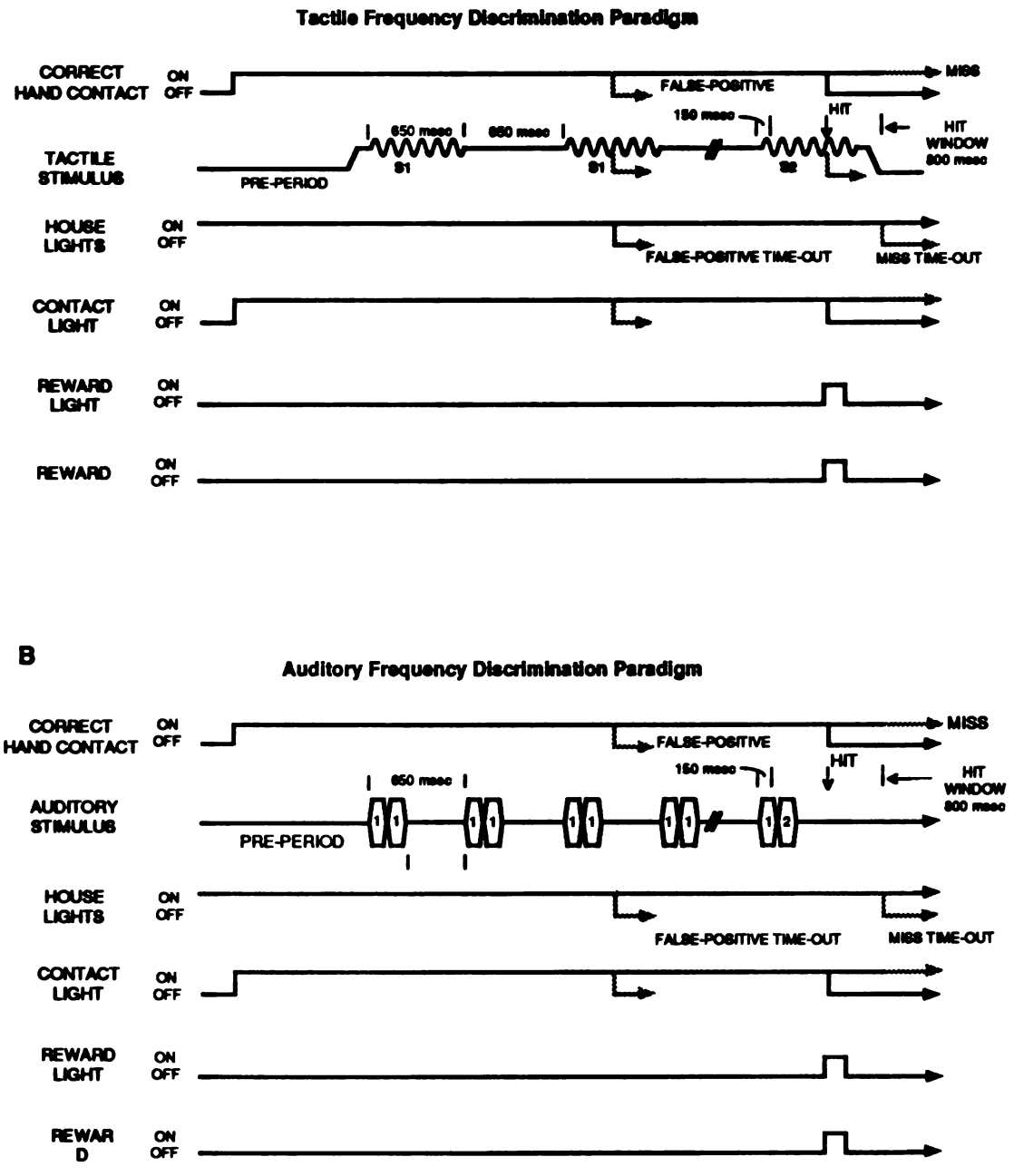

Figure 2. Psychophysical procedure used in the tactile task (A) and the passive-stimulation (auditory) task (B). Correct hand placement initiated a trial in both cases. The tactile stimulus was presented in periods of 650 msec. The auditory stimulus was presented as tone pairs in periods of 325 msec. The two paradims are identical except for the time that the S2 stimulus, either tactile or auditory, could occurr. See text for details.

Table A1. Probability of S2 occurrence by bin.

Tactile Stimulus:

Bin of Presentation	# occurrences/100	Probability
2	37	0.37
3	25	0.40
4	15	0.39
5	9	0.39
6	14	1.00
Mean ± S.D. (Bins 2-5)		0.388 ± 0.012

Auditory Stimulus:

Bin of Presentation	# occurrences/100	Probability
2	0	0.00
3	31	0.31
4	22	0.32
5	15	0.32
6	10	0.31
7	7	0.32
8	5	0.33
9	3	0.30
10	2	0.29
11	3	0.60
12	2	1.00
Mean ± S.D. (Bins 3-10)		0.312 ± 0.014

Number of occurances of the S2 stimulus in each stimulus bin for 100 trials. By changing the number of presentations for each bin, the probability that the next stimulus would be an S2, given that an S2 stimulus had not yet occurred, is maintained relatively constant.

session. This feature in combination with the variable set of possible combinations of tables prevented the animal from "learning" the correct sequence of S2 presentations based on the position in the look-up table.

A rewarded run was one in which correct hand contact was maintained through the S1 stimulus presentation(s) and broken within the reward-window. The reward window began 150 msec after S2 onset and ended 300 msec after S2 offset (800 msec). As the fastest reaction time recorded for this task in these animals was more than 150 msec, this time window did not reward responses initiated before the animal actually "discriminated" the stimulus. The additional time following stimulus offset was still prior to any expected onset of the next stimulus. A white light was briefly illuminated and a food pellet was delivered to the food bin. If the subject did not break contact during the 800 msec reward window all lights were extinguished for a set period (Miss time-out) and no reward was delivered. Responses made prior to the hit window also resulted in a brief time-out (False-Positive time-out).

Catch Trials

In order to maintain the probability of S2 occurrence constant across bin, it was necessary for the S2 to occasionally occur in bin six. Thus, whenever bin six occurred the S2 was presented. These runs were not counted in the data analysis. We also imposed a 1/50-1/100 probability that the S2 stimulus would be equal to the S1 stimulus. In these runs, an animal under stimulus control did not respond. The stimulus probe was moved off the skin on several runs in rare sessions to insure the animal was not using other cues to discriminate the stimulus. Animals under stimulus control did respond in this condition.

Daily Session

Each session was initiated with a "warm-up" period consisting of 2-4 S2 frequencies that were above 90% correct the previous session. The animal was allowed to obtain 50-100 rewards at this criteria. The delta frequency was then gradually reduced over the next 50-100 rewards, ultimately to a frequency range of 6-10 frequencies, with approximately 2 below the 50% correct rate. The order of S2 frequency presentation was randomized for each session. We target the tested frequencies to ensure an overall reward rate (#rewards / #runs) at approximately 60% or greater, with an overall False-Positive rate of 15% or less. A daily session consisted of the number of runs required to deliver the appropriate amount of food pellets necessary to maintain the subject's body weight at 85-95% *ad lib* (approximately 400 rewards).

DATA ANALYSIS

The necessary data to be stored for each run of a session were 1) the frequency and duration of the presented S2 stimulus 2) the duration of S1 stimulus presentations and 3) the response. With these three values the hit-rates and reaction times for each S2 frequency presented, the number and duration of all stimuli presented in that session, and the False-Positive rate were determined. These values could be determined over the entire session, within any subset of the session, and with respect to the bin of the S2 presentation.

Five categories of responses were used for data analysis.

1) HIT: The response was made during the reward-window for S2 presentations in bins 2-5. Each S2 frequency was counted independently.

2) MISS: No response was made through the presentations of S1 or the reward window for S2 presentations in bins 2-5. Each S2 frequency was

counted independently.

3) FALSE-POSITIVE: The response was made before the reward window but after the onset of the second S1 presentation.

4) PRE FALSE-POSITIVE: The response was made before the onset of the second stimulus presentation, either S1 or S2. These runs were not used to compute the False-Positive rate.

5) CATCH: Correct hand position was maintained to the last stimulus presentation (bin 6). The animal was rewarded with a correct response, or punished with a Miss Time-out as appropriate. These runs were not included in the data analysis.

Threshold determination

The determination of threshold for any session, or subset of the session, was dependent on two parameters, the hit rate at each presented S2 and the False-Positive rate. The hit rate for a given S2 frequency was defined as:

$$H_{S2} = \#\text{ correct responses} / \#\text{ stimulus presentations}$$

The data used in this equation were pooled from runs in which the given S2 frequency was presentation in bins 2-5. To access the rate of False-Positives we calculated the rate in which no response was made to the S1 stimulus (S). This value was derived for each stimulus bin as well as the overall rate. For each bin S_n this value was derived by:

$$S_n = \#\text{presentations of S1 in bin } n \text{ with no response} / \#\text{ S1 presentations in bin } n$$

The False-Positive values of each presentation bin were always comparable

when the animal was under stimulus control. The total False-Positive rate for the session, S_t, was then derived by:

$$S_t = \#\text{ presentations of } S1_{2\text{-}5} \text{ with no response} / \#\text{ presentations of } S1_{2\text{-}5}$$

where the subscript corresponds to the bin of stimulus presentation. The overall performance rate for a given S2 frequency (P_{S2}) can then be calculated using the hit rate for that frequency and the total False-Positive rate as:

$$P_{S2} = S_t - ((1-H_{S2}) \times S_t)$$

This equation goes to H as S goes to 1 (no False-Positives) and goes to 0 as S goes to 0 (all False-Positives).

A typical performance function is shown in Fig. A3 demonstrating the effect of False-Positive rate on threshold. Part A shows data taken from a well-trained owl monkey and shows the raw performance function (solid symbols) and the corrected function (open symbols) This animal had a False-Positive rate of 8%, making a difference in threshold of only 0.14 Hz (5.6% of 2.48). Part B shows the same raw data with theoretical False-Positive rates of 5, 10, 15 and 20%. False-Positive rates above 10% result in much higher thresholds (11.7% and 16.5% of 2.48 for False-Positive rates of 15% and 20%, respectively). In addition, animals performing at a high False-Positive rate were commonly not under strict stimulus control. We excluded all data in which the overall False-Positive rate exceeded 15%.

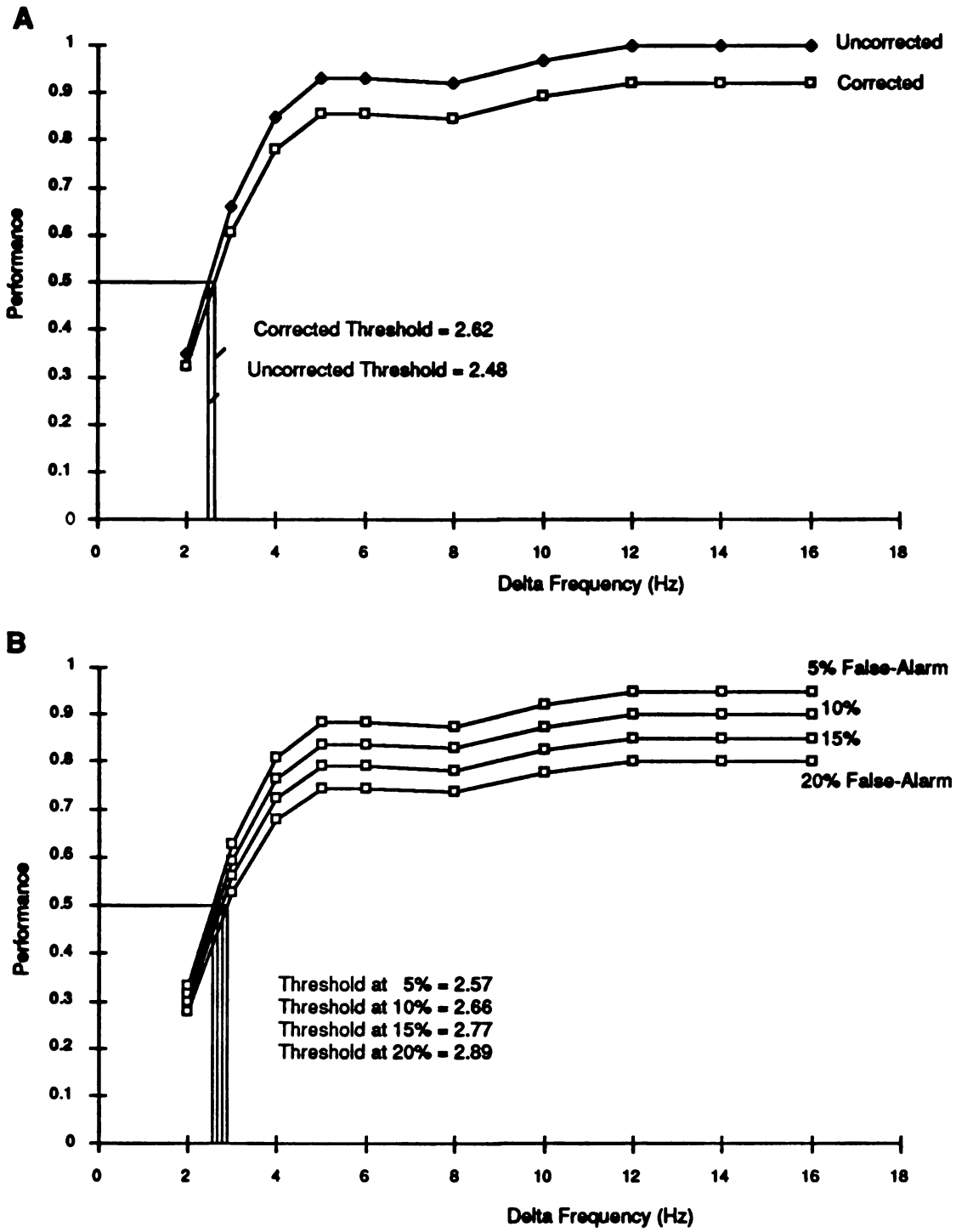

Figure A3. Psychometric functions shown corrected for different False-Positive rates. See text for details.

SHAPING

A three stage strategy was used. All hardware used was made as uniform as possible to aid in the transition between stages. Animals were trained for about two hours a day for six days a week.

Stage one

The first stage selected animals with a predisposition for the task and shaped the animal to make appropriate contact with a hand mold. A food pellet dispenser was attached to the home cage. Initial screening of owl monkeys was performed by providing 100 pellets each day in addition to the usual diet of chow biscuits. If the animal showed little or no interest in the food pellets they were eliminated from the study. *Ad lib* body weight was determined for the selected subjects. Water was freely available and chow biscuits and fruit were provided as supplements to the food pellet diet only as necessary to maintain body weight between 90-110% *ad lib* body weight.

A hand mold was attached to the outside of the home cage. Contact with any part of this mold completed a low impedance detection circuit that activated a small incandescent light and a pellet dispenser which delivered a single pellet. This free-operant apparatus was available to the animal throughout the day and care was taken to ensure the animal was receiving sufficient nutrition. After two weeks the conductive surface of the mold was restricted to three 3mm X 5mm copper foil strips placed to underlie digits 2, 3 and 4 when the hand was placed squarely on the mold. Initially contact with any one of the strips was required to receive a reward. The stringency was slowly increased until simultaneous contact with all three strips was required. When the animal could routinely receive 300-400 pellets in less than two hours, commonly within 3

weeks time, a limited hold requirement was added. The incandescent light provided feedback to the animal that the hand was in the correct position and contact had to be maintained until the pellet dispenser was activated. Breaking contact early resulted in the limited hold time being reset. The limited hold period started at 100 msec and was slowly increased over a period of several weeks, ultimately to 5 seconds.

Stage two

For the remainder of the training the animal was transported via a small opaque transport box to the testing apparatus described in detail above. The first goal of stage two was to shape the animal to contact the hand mold in an invariant way. Animals quickly adopted a stereotypic hand position which had a unique corresponding combination of contacts activated. An opening in the hand mold was created for the tactile stimulator to contact the selected skin surface. With the incandescent light providing feedback when the "correct" hand placement was achieved, the animals could be quickly trained to maintain contact for up to 3 seconds to receive a reward.

The second goal was to train the animal in a detection task following a variable hold. In the initial procedure a 40 Hz, 3mm peak-to-peak stimulus was presented following a variable hold period of 1-3 seconds. This stimulus remained on until the animal made a response. The time the stimulus was presented was recorded for each run and the average time displayed continuously. Once the mean response time fell below 2 seconds, which occurred within 3-5 sessions, the variable hold period was increased to 3-5 seconds.

Stage three

The final stage required the animal to perform the discrimination task. Following correct hand placement, a short fixed delay followed in which contact could be broken without penalty. A 5 Hz, low-amplitude stimulus was then presented for 650 msec followed by a 650 msec pause. The animal was not rewarded if contact was broken during the presentation of this stimulus (S1). The S1 was initially presented 1 or 2 times before the 40 Hz stimulus (S2) was presented and continuous until contact was broken. Once the animal could easily make this discrimination the S2 presentation time was gradually restricted, ultimately to the 650 msec used in the testing paradigm. The time window in which a response resulted in a reward was set to 800 msec. At this time a time-out was imposed following a miss. The number of S1 stimuli presented before the S2 was then gradually increased to 5, which was used in the testing protocol. A False-Positive time-out was then imposed.

Once the animal was consistently making these easy discriminations at the timing pattern used in the testing procedure, the amplitude of the S1 was increased to match that of the S2. The S1 frequency was then increased over the next several sessions to approach 20 Hz. The animal was allowed several sessions (3-10) in which it consistently made the 20Hz vs. 40Hz discrimination. At this point the animal was considered trained and was moved to the testing apparatus.

12-5045C